



UNIVERSITY OF NAIROBI

SCHOOL OF ENGINEERING

DEPARTMENT OF MECHANICAL AND MANUFACTURING ENGINEERING

Development of a Small-Scale Machine for Extraction and Brushing of Sisal Fibre

BY:

NELSON WANJALA BARASA

F56/83035/2015

A thesis submitted in partial fulfilment for the degree of Master of Science in Mechanical Engineering in the department of Mechanical and Manufacturing Engineering in the University of Nairobi

November 2020

DECLARATION

I declare that this thesis is my original work and has never been submitted to any other university for an award.



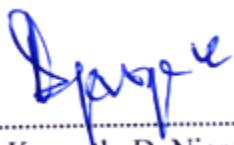
.....
Nelson W. Barasa

Reg. No: F56/83035/2015

25th November, 2020

Date

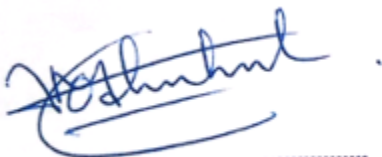
This thesis has been submitted for examination with our approval as university supervisors.



.....
Dr. Kenneth. D. Njoroge

25th November, 2020

Date



.....
Dr. Thomas M. Ochuku

25th November, 2020

Date

DEDICATION

I value the understanding and support accorded to me by my wife during the entire project period. Her prayers, financial support and concerns synergized my effort. I dedicate this work firstly, to the Almighty God and secondly, to my lovely wife and son.

ACKNOWLEDGEMENT

I would like to acknowledge a number of people that played key roles in ensuring the research work was accomplished;

Dr. Kenneth D. Njoroge and Dr. Thomas O. Mbuya, my supervisors, for their corrections, advice, guidance and fatherly support in the course of the research.

Mr. W. Mengo for linking up with the Managing Director of Rea Vipingo Sisal Estate Ltd, Mr. Neil Cuthbert, to get the Estate Sisal fibre for a comparative analysis.

Mr. Anyona, Mr. Sitati and Mr. Kigen for the technical support at Mechanical and Civil Engineering workshops and laboratories.

In conclusion, I would like to appreciate my wife, Praizy Zakaria, for her emotional, spiritual and financial support.

ANTI-PLAGIARISM STATEMENT

I am fully aware of plagiarism and I understand the policy of the University of Nairobi towards the same. It is my declaration that this research is my own original work and has never been submitted elsewhere be it for publication, examination or award of a degree. In this work, other people's works consulted are well cited in accordance with the university's requirements. In addition, I have not employed the services of any professional agencies to assist in carrying out this research. I have not permitted, and shall not permit any person to reproduce my work intentionally to pass it off as his/her own work. I comprehend that any false claim concerning this work shall lead to disciplinary action as stipulated in the University Plagiarism Policy.



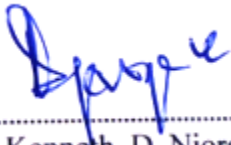
.....
Nelson W. Barasa

Reg. No: F56/83035/2015

25th November, 2020

Date

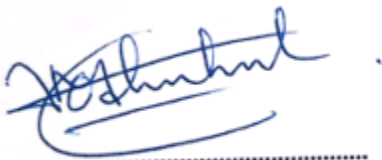
Supervisors;



.....
Dr. Kenneth. D. Njoroge

25th November, 2020

Date



.....
Dr. Thomas M. Ochuku

25th November, 2020

Date

ABSTRACT

Sisal fibre is a raw material used in the production ropes, mats, gunny bags, carpets and polymer composites. UNIDO, in 2001, revealed that there is large amount of small-scale sisal in East Africa that is inadequately exploited due to lack of appropriate decortication technology. Small-scale have for a long time relied on tedious and low yielding manual methods that only contributed less than 25% to the total Kenyan sisal fibres exports in 2003. To increase processing of hedge sisal, UNIDO recommended that appropriate small-scale decortication technology should be developed. However, the raspadors developed so far have only focus on extraction ignoring brushing that greatly improves fibre quality. Low grade fibre obtained by these machines is sold at very low prices (Kshs 17 per kg) compared to a better under grade that would be sold at Kshs 175 per kg for brushed fibres. Moreover, research has shown that environmental conditions, fibre surface modification, age and processing methods cause the variability of sisal fibre properties. Howbeit, inadequate research quantifying the variability of sisal fibre properties with processing method was found. Therefore, this project aimed at developing a raspador for extraction and brushing of sisal fibres and quantifying the effects of raspador processing variables on sisal fibre properties.

A raspador for extraction and brushing of sisal fibres was designed based on the raspador principle using Autodesk Inventor. It was fabricated and extensively tested at Mechanical Engineering Workshop. Tensile tests were conducted using Hounsfield Tensometer (type W) in accordance with the ASTM C1557 standard. The raspador achieved extraction and brushing capacities of 10.85 kg/hr and 24.64 kg/hr respectively with a design efficiency of 39%. The power consumption per sisal leaf was 1.368 kW and 1.018 kW for extraction and brushing respectively and increased with drum speed. Moreover, the increase in power due to incorporation of a brushing unit is 16%. The fibre properties highly correlate with the gap size, number of blades/brushing elements and drum speed. For instance, the properties reduced with increase in speed and number of blades/elements but increased with gap size. Furthermore, brushing improved the grade of fibres from UHDS to UG. The average σ_u , E and ϵ for fibres obtained by the raspador were 124.04 MPa, 1.48 GPa and 0.085 for extraction and 142.68 MPa, 1.78 GPa and 0.081 for brushing as compared to 236.65 MPa, 1.58 GPa and 0.09 for manually extracted fibres and 87.23 MPa, 1.48 GPa and 0.07 for estate fibre. The values obtained are

comparable to 161 MPa σ_u , 3.6 GPa E and 4.5% ϵ reported by a research on Rea Vipingo Kenyan estate sisal. The machine's tensile properties were lower than those of manual method but comparable to UG estate sisal. Optimum results were obtained at a gap size of 1.5 - 2 mm, speed of 1000 - 1200 rpm and 6 blades and a gap size of 2 - 3 mm, speed of 1000 - 1200 rpm and 3 brushing elements for extraction and brushing respectively. The total cost of the raspador is Kshs. 115,908.10. In conclusion, a farmer who manually extracts 3 kg/day of fibre earning Kshs. 150/day, will process 80 kg of brushed fibre earning Kshs. 4,588.83/day. A positive NPV was obtained implying that the raspador makes economic sense to the small-scale farmers.

TABLE OF CONTENTS

DECLARATION	ii
DEDICATION.....	ii
ACKNOWLEDGEMENT.....	iv
ANTI-PLAGIARISM STATEMENT.....	v
ABSTRACT	v
TABLE OF CONTENTS	viii
LIST OF FIGURES	xi
LIST OF TABLES	xiv
NOMENCLATURE.....	xv
ABBREVIATIONS	xvi
CHAPTER ONE: INTRODUCTION.....	1
1.1. Background.....	1
1.2. Problem statement.....	2
1.3. Objectives.....	3
1.3.1. Overall objective	3
1.3.2. Specific objectives.....	3
1.4. The justification of the study.....	3
CHAPTER TWO: LITERATURE REVIEW.....	5
2.1. Sisal.....	5
2.1.1 Sisal production in Tanzania.....	5
2.1.2 Sisal production in Kenya.....	6
2.1.3 Sisal production in Brazil	7
2.2 Processing of sisal fibre	9
2.3 Properties of sisal fibres.....	11
2.4 Economic viability of the small-scale decorticator	13
CHAPTER THREE: METHODOLOGY.....	14
3.1. Phase One: Design of the machine	14

3.1.1.	Extraction unit	14
3.1.2.	Kinematic study of the machine	15
3.1.3.	Kinetic study of the machine	20
3.1.4.	Brushing unit	21
3.1.5.	Design of the components	22
3.1.6.	Design of the belt drive	23
3.1.7.	Generation of Computer Aided Design (CAD) drawings	25
3.2.	Phase Two; Acquisition of materials, fabrication and laboratory testing	25
3.2.1.	Identification and acquisition of materials for fabrication.	25
3.2.2.	Fabrication of the components and assembly of the machine	26
3.2.3.	Laboratory testing	31
CHAPTER FOUR: DATA ANALYSIS, DISCUSSION AND RECOMMENDATIONS		37
4.1.	Machine design	37
4.1.1.	Kinematic study of the machine	37
4.1.2.	Decortication resistance	37
4.1.3.	Design power	38
4.1.4.	Design of the belt drive	40
4.1.5.	Shaft design	44
4.1.6.	Bearing selection.....	48
4.1.7.	Design of frame, belt and pulley cover	49
4.1.8.	Computer Aided Design drawings.....	50
4.2.	Obtainable speeds with taper pulleys	52
4.3.	Power consumption.....	53
4.4.	Properties of processed sisal fibres	57
4.4.1.	Properties of manually extracted sisal fibres.....	58
4.4.2.	Rea Vipingo.....	60

4.4.3.	Extracted sisal fibre.....	60
4.4.4.	Brushed fibre	76
4.4.5.	Optimized design specifications	90
4.5.	Machine cost and revenue analysis	91
4.5.1.	Machine costs	91
4.5.2.	Machine revenues for small scale farmers	93
4.6.	Recommendations.....	97
CHAPTER FIVE: CONCLUSION.....		98
REFERENCES		99
APPENDICES		104
Appendix A: Necessary data for the design of belt drive and sheaves and frame		104
Appendix B: Bill of materials		114
Appendix C: Machine design drawings.....		115
Appendix D: Sisal fibre grades		135
Appendix E: Sample laboratory data sheet for power consumption		136
Appendix F: Raw results.....		137
Appendix G: Sisal fibre prices for the 2017/2018 fiscal year [5]		151
Appendix H: Useful data for economic feasibility analysis		152

LIST OF FIGURES

Figure 1.1: Sisal plant and its scientific classification [1].....	1
Figure 1.2: Women extracting sisal fibre manually in Eastern Kenya	Error! Bookmark not defined.
Figure 2.1: Sisal production in Tanzania [9]	5
Figure 2.2: Hedge sisal in Kenya	7
Figure 2.3: Sisal fibre production in Kenya from 1999-2003 (MT) [10].....	7
Figure 2.4: World production of sisal from 1975 to 2005 (tons) [8]	8
Figure 2.5: Sisal fibre production [13].....	8
Figure 2.6: Automatic decorticators [3]	9
Figure 2.7: Methods of evaluating economic viability	13
Figure 3.1: The sisal machine design procedure.....	14
Figure 3.2: The extraction unit	15
Figure 3.3: Model of the extraction unit	16
Figure 3.4: Tips of blade P_1 at $t = 0$ and at t	17
Figure 3.5: Profiles traced by tips of blades P_1 and P_2 in a quarter turn	18
Figure 3.6: Time difference and the swept area of successive tips.....	18
Figure 3.7: Kinetic model of the machine	20
Figure 3.8: Cantilever model to determine decortication resistance.....	21
Figure 3.9: Conceptualization for brushing	22
Figure 3.10: Proposed design one	23
Figure 3.11: Proposed design two.....	23
Figure 3.12: Sketch of the intended design	24
Figure 3.13: Fabrication of the drum	26
Figure 3.14: Fabrication of side discs	27
Figure 3.15: Fabrication of the machine frame	27
Figure 3.16: Fabrication of the extraction blades	28
Figure 3.17: Fabrication of the chute	28
Figure 3.18: Drum cover	29
Figure 3.19: Bending machine and guard	29
Figure 3.20: Anvil steel bar	29

Figure 3.21: Standard parts.....	30
Figure 3.22: Harvesting hedge sisal at Kasarani Constituency	31
Figure 3.23: Manually extracted fibre.....	32
Figure 3.24: Extraction of fibres.....	33
Figure 3.25: Extracted sisal fibres	34
Figure 3.26: Brushed sisal fibres	34
Figure 3.27: Fibre dust and tow fibre.....	35
Figure 3.28: Specimens for tensile tests.....	35
Figure 3.29: Tensile testing using Hounsfield Tensometer.....	36
Figure 3.30: LV 800AT Tester	36
Figure 4.1: Extraction blade modelled as a cantilever	38
Figure 4.2: Belt tensioning	43
Figure 4.3: FBD of the drum shaft assembly.....	44
Figure 4.4: Loads acting on the shaft	45
Figure 4.5: Force and bending moment diagram.....	46
Figure 4.6: Pillow block	48
Figure 4.7: The views of the proposed machine showing the machine frame	49
Figure 4.8: Drum cover	50
Figure 4.9: CAD drawing of assembled machine.....	51
Figure 4.10: Assembled machine.....	51
Figure 4.11: Drum speeds from speed ratio	52
Figure 4.12: Variation of power consumption with gap size and speed	53
Figure 4.13: Power variation with gap sizes	55
Figure 4.14: Bar chart for power variations	55
Figure 4.15: Variation of total power with drum speed at 1 mm gap size	56
Figure 4.16: Variation of total power with drum speed at 2 mm gap size	56
Figure 4.17: Variation of total power with drum speed at 3 mm gap size	56
Figure 4.18: Fracture strain against gap size at 900 rpm and 3 blades	63
Figure 4.19: Fracture strength against gap size at 900 rpm and 3 blades	64
Figure 4.20: Young's modulus against gap size at 900 rpm and 3 blades	64
Figure 4.21: Fracture strain against gap size at 1400 rpm and 3 blades	65

Figure 4.22: Fracture strength against gap size at 1400 rpm and 3 blades.....	66
Figure 4.23: Young's Modulus against gap size at 1400 rpm and 3 blades	66
Figure 4.24: The length ratio against speed at 1 mm gap and 6 blades	67
Figure 4.25: Fracture strain against gap size at 900 rpm and 12 blades	68
Figure 4.26: Fracture strength against gap size at 900 rpm and 12 blades.....	69
Figure 4.27: Young's modulus against gap size at 900 rpm and 12 blades	69
Figure 4.28: Fracture strain against speed at 2.5 mm gap size and 12 blades	70
Figure 4.29: Fracture strength against speed at 2.5 mm gap size and 12 blades	70
Figure 4.30: Young's modulus against speed at 2.5 mm gap size and 12 blades.....	71
Figure 4.31: Variation of fracture strain with number of blades	72
Figure 4.32: Variation of fracture strength with number of blades	73
Figure 4.33: Variation of Young's modulus with number of blades	74
Figure 4.34: Fracture strain against gap size at 900 rpm and 3 elements	79
Figure 4.35: Fracture strength against gap size at 900 rpm and 3 elements.....	79
Figure 4.36: Young's modulus against gap size at 900 rpm and 3 elements	80
Figure 4.37: Fracture strain against gap size at 1400 rpm and 3 elements.....	81
Figure 4.38: Fracture strength against gap size at 1400 rpm and 3 elements.....	81
Figure 4.39: Young's modulus against gap size at 1400 rpm and 3 elements	82
Figure 4.40: Fracture strain against gap size at 900 rpm and 12 elements.....	83
Figure 4.41: Fracture strength against gap size at 900 rpm and 12 elements.....	84
Figure 4.42: Young's modulus against gap size at 900 rpm and 12 elements	84
Figure 4.43: Fracture strain against speed at 2.5 mm gap size and 12 elements	85
Figure 4.44: Fracture strength against speed at 2.5 mm gap size and 12 elements	85
Figure 4.45: Young's modulus against speed at 2.5 mm gap size and 12 elements.....	86
Figure 4.46: Variation of properties with number of elements at 1200 rpm for 1 mm and 2.5 mm gap size	87
Figure 4.47: Variation of properties with number of elements at 1400 rpm and 2.5 mm gap	88
Figure 4.48: Discount rate (Source CBK)	94

LIST OF TABLES

Table 4.1: Recommended values for K_m and K_t	47
Table 4.2: Operational conditions of the bearing	48
Table 4.3: Pillow block dimensions	49
Table 4.4: Analysis of power consumption.....	54
Table 4.5: Analysed data for manually extracted sisal fibre	58
Table 4.6: Mean values for hammer and anvil method.....	59
Table 4.7: Properties of sisal from Rea Vipingo	60
Table 4.8: The properties of sisal fibre extracted using the machine	61
Table 4.9: Mean values after extracted fibre	62
Table 4.10: The properties of sisal fibre after brushing using the machine	76
Table 4.11: Mean values after extraction of fibres	77
Table 4.12: Summary of results	90
Table 4.13: Projected cash flows for the project	95
Table 4.14: The payback period	96

NOMENCLATURE

σ – Fracture stress

σ_u – Fracture strength

ε – Fracture strain

E – Modulus of elasticity

L_R – Length ratio, the ratio of original leaf length to final average fibre length

$(D_R)_e$ – Mean decortication resistance

K_m – Combined shock and fatigue factor for bending

K_t – Combined shock and fatigue factor for torsion

P_m – Rated power

S_{stat} – Static shaft load

S_{dyn} – Dynamic shaft load

SPZ belt – SchmalProfil Z (type of V belt)

UCP205 – Metric Series Two Bolt Pillow Block

ABBREVIATIONS

AFA	Agriculture and Food Authority
ANSI	American National Standards Institute
ASALs	Arid and Semi-Arid Lands
ASME	American Society of Mechanical Engineers
ASTM	American Society for Testing and Materials
BP	Brushing Power
CAD	Computer Aided Design
CFC	Common Fund for Commodities
DC	Depreciation cost
DE	Design efficiency
DUF	Decorticated Unbrushed Fibre
EP	Extraction Power
FAO	Food and Agricultural Organization
FBD	Free Body Diagram
FEA	Finite Element Analysis
HLSRS	High Level Sisal Research Station
IC	Interest cost
IP	Idling Power
IRR	Internal Rate of Return
KSB	Kenya Sisal Board
KSGA	Kenya Sisal Growers Association
LCC	Life Cycle Cost
LSA	London Sisal Association
MT	Metric Tons
MTC	Meristematic Tissue Culture
NPV	Net Present Value
NPVR	Net Present Value Ratio
PI	Profitability Index
PP	Purchase price
R&D	Research and Development

SSUG	Sub Standard Under Grade
SV	Salvage value
TC	Total cost
TP	Total Power
UG	Under Grade
UHDS	Unwashed Hand Decorticated Sisal
UNIDO	United Nations Industrial Development Organization
VAT	Value Added Tax

CHAPTER ONE: INTRODUCTION

1.1. Background

Sisal is a succulent plant fibre named after a seaport town (Sisal) in Yucatan State, Mexico.



Kingdom:	Plantae
Division:	Magnoliophyta
Class:	Liliopsida
Order:	Asparagales
Family:	Agavaceae
Genus:	Agave
Species:	<i>A. sisalana</i>

Figure 1.1: Sisal plant and its scientific classification [1]

It is a hardy cactus plant consisting of a rosette of sword-shaped leaves, each about 1.5 to 2 metres long and grows well in a variety of warm climates, including arid and semi-arid lands (ASALs). Among the leading commercial varieties are *Agave sisalana* and *Agave fourcroydes*. Sisal plants cope with prolonged droughts and high temperatures prevalent in tropical and subtropical regions [1]. In Kenya, sisal is among the top six important cash crops including tea, coffee, pyrethrum, cotton and sugarcane.

The sisal plant has many applications and more are still under investigation. Traditionally, sisal fibre has been used to manufacture agricultural and parcelling twine, gunny bags, carpets, ropes, sacks, mats, pulp, upholstery and handicrafts. The demand for sisal worldwide has been on the increase, mainly because it is environmentally friendly unlike the synthetic fibres [2]. Large amounts of sisal fibre are consumed in the small-scale industries to produce woven bags and other types of handicrafts.

The most preferred part of the sisal plant is its strong fibre. The fibres are obtained from the plant in a process called extraction or decortication. This process must take place in not more than 5 hours after harvesting otherwise hardening of the sap and cellular tissues not only make extraction very difficult but also degrades the sisal fibres [3]. Sisal is usually grown on large-

scale in estates and small-scale as hedge sisal along farm demarcations. In sisal estates, large, sophisticated and expensive machines are used for fibre extraction, brushing and baling in factories and warehouses. This method consumes a lot of water and its discharge contributes to water pollution. No wonder, small-scale farmers in Brazil have embraced mobile field decorticators (raspadores) for fibre extraction [4]. In Kenya, most small-scale farmers extract the fibre manually in a process that is laborious and yields fibre that is poor in quality and quantity. Lack of appropriate technology hinders the expansion of small-scale sisal production in Kenya.

There is need, therefore, to develop a suitable small-scale technology for processing of sisal from small-scale farmers. Preliminary observations during site visits revealed that farmers need to incur extra cost to invest in a separate machine to brush and increase the value of sisal fibre. Alternatively, they opt to sell the unbrushed fibre to traders at low prices (mostly the case). Normally, unbrushed fibre is sold to the traders who increase its value through brushing and baling in their warehouses. This deprives the small-scale farmers of extra income. Development of a small-scale and affordable machine that can extract and brush sisal fibre geared towards increasing the value of sisal fibre is a welcome innovation in the small-scale sisal processing industry.

1.2. Problem statement

The lack of appropriate small-scale sisal fibre decortication technology is significant barrier to the development of the small-scale sisal farming in East African and perhaps the rest of the region. The farmers largely rely on manual decortication methods that are not only tedious and low yielding but also precipitates of health-related complications [1]. Furthermore, the fibres obtained are UHDS grade sold cheaply at Kshs. 17/kg [2] as compared to UG grade sold at Kshs. 175/kg [5] hence the farmers lose a considerable income. Moreover, although the properties of sisal fibres have been reported to vary with environmental conditions, surface modifications and processing methods, there is inadequate information on the quantification of the variation with processing method. This lack of information is a significant problem for utilization of sisal fibres in development of polymer composites. Therefore, this research sort to address these two problems.

1.3. Objectives

1.3.1. Overall objective

- To develop a small-scale and affordable sisal fibre extraction and brushing machine for use by small-scale farmers

1.3.2. Specific objectives

- ❖ To design a small-scale sisal fibre extraction and brushing machine
- ❖ To fabricate and test the machine to determine the performance characteristics such as quantity and quality of sisal fibres
- ❖ To determine the effects of extraction and brushing variables on the strength of sisal fibres
- ❖ To determine the best parameters for extraction and brushing of sisal fibre
- ❖ To optimize the design specifications and carry out a cost analysis of the prototype machine to establish various costs

1.4. The justification of the study

Hedge sisal and sisal from small-scale farmers is inadequately explored in East Africa due to lack of appropriate technology [6].



Figure 1.2: Women extracting sisal fibre manually in Eastern Kenya

Figure 1.2 shows a woman extracting fibre manually in Eastern Region, Kenya [2]. The manual methods used for processing are very tedious, low yielding and unhealthy as reported by Kayumba et al. [1]. They yield about 3 kg of sisal fibre per day earning about Kshs 50 [7]. In addition to poor extraction, the farmers do not brush the fibre due to lack of appropriate machine. The large and sophisticated machines used for processing the fibres in sisal estates are uneconomical and inaccessible to the small-scale farmers [7]. The lack of suitable machine is consequently a significant limitation in the expansion of the small-scale sisal industry in Kenya. There is need to develop an economical small-scale machine that can be used for extraction and brushing by small-scale farmers [6]. The machines developed so far have inadequately addressed the challenge of brushing sisal fibres. As a result, the small-scale farmers have either to incur extra costs of purchasing a brushing machine or sell the unbrushed fibre at low prices. Due to the rising demand of natural fibre worldwide and the ban on plastic bags and other plastic products, there is an opportunity for investing in this machine.

CHAPTER TWO: LITERATURE REVIEW

2.1. Sisal

The three leading nations in the production of sisal fibre as per the year ending 2018 were Brazil (120,000 tonnes), Tanzania (35,000 tonnes) and Kenya (25,000 tonnes) [8]. Brazil has emerged the first due to her increased focus on the small-scale technology. The following is a brief look at sisal production in the three countries;

2.1.1 Sisal production in Tanzania

Dr. R. Hindorf introduced sisal in East Africa in Tanganyika in 1893 during the period of Germany administration. He obtained 1000 sisal plants (*Agave sisalana*) from Yucatan out of which 62 survived the long trip and were planted in Mwera [6, 9]. Towards the end of 1898, these plants reproduced to a plant population of 63,000, enough to be propagated to a 40 ha of land [6]. In the 1950s, sisal output increased tremendously making Tanzania the world leader in sisal production Figure 2.1.

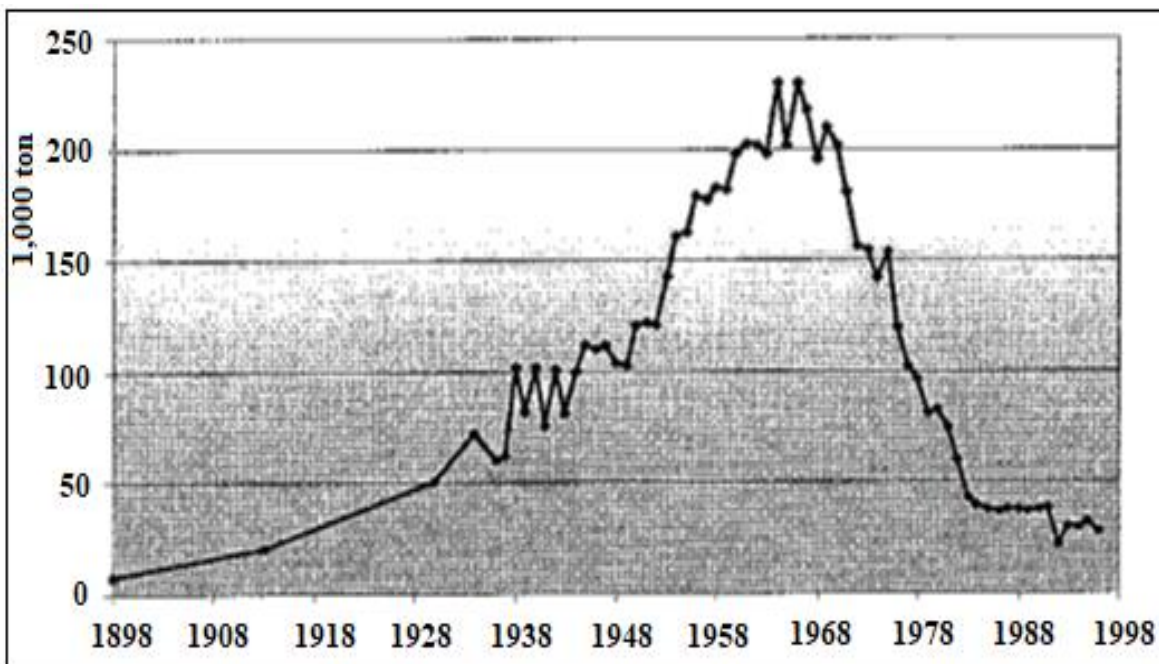


Figure 2.1: Sisal production in Tanzania [9]

Tanzania remained a world leader in production of sisal fibres until 1964 when the worldwide market of sisal fibres collapsed because of stiff competition from cheap synthetic fibres [9].

2.1.2 Sisal production in Kenya

The Agave Sisalana was introduced in Kenya in 1903 due to successful trials in neighbouring Tanzania. The first crops were planted in the coastal regions and did very well [6, 10]. Therefore, in 1907 the first sisal estate was created by Swift and Rutherford at Punda Milia, Thika [10]. In the year 1914, the demand of the Kenyan sisal had grown sharply pushing for the expansion of sisal plantations. In 1965, the sisal estates increased to 54, occupying over 120,000 ha with a production capacity of 126,000 MT per annum and employed over 20,000 people [10].

The rapid increase in demand led to the establishment of Research and Development (R&D) support services like the Thika High Level Sisal Research Station (HLSRS) in 1937 and the Juja spinning factory in 1954 [6, 10]. The station researched on better sisal varieties, agronomics, management and processing strategies establishing a strong foundation for the sisal fibre industry. The Kenya Sisal Growers Association (KSGA) ran the industry until the mid-1940s when the colonial government formed the Kenya Sisal Board (KSB) in accordance to the Sisal Industrial Act (Cap. 341) to promote the welfare of the industry. A major challenge that faced the industry was in the 1940s when the rise of synthetic fibres led to decline in production [6, 9, 10].

The discovery of new applications of natural fibres in 1990s has rejuvenated the production in the industry [10, 11]. Such new applications include use of natural fibres in interior motor panels, gypsum blocks for building and in specialty paper. Currently, the use of the fibre in geo-textiles and the ban on synthetic bags in Kenya and other neighbouring countries are increasing the sisal fibre demand [6]. Moreover, research is at an advanced stage to determine the use of sisal waste for animal feed, bio-energy generation and organic fertilizers. For instance, the first biomass plant was inaugurated in Tanzania in 2008 with a capacity of 300 kW of power per day [13].

The Kenyan sisal fibre has the highest amount of hemicellulose and lignin compared to others across the globe [10]. Most of the exported sisal fibres in Kenya comes from Sisal Estates namely; Real Vipingo, DWA Estate Ltd, Teita Estate, Mogotiyo Plantations Ltd, Tabu Plantations Ltd and Voi Sisal Estate. Because of the increasing demand for high quality fibre, there is need to also process the sisal from small-scale farmers to meet the demand. Many farmers in Kenya, for instance in the rift valley and eastern regions grow hedge sisal for demarcation that is inadequately exploited due to the lack of suitable processing technology [7, 10]. Figure 2.2 shows the unexploited hedge sisal in the rift valley and in the Eastern Province.

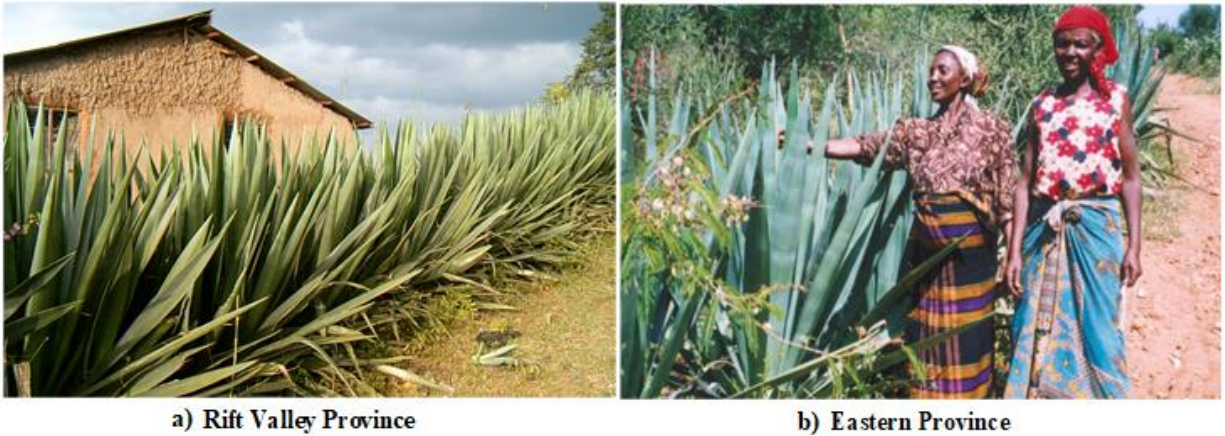


Figure 2.2: Hedge sisal in Kenya

The technologies used in estates are very expensive, inaccessible and sophisticated to small-scale farmers who resort to manual decortication [7]. UNIDO [6] recommended that appropriate small-scale technology should be developed to enable exploitation of sisal from small-scale farmers to increase its production capacity. As seen in Figure 2.3, sisal fibre from small-scale farmers contributes very little to the overall fibre production in Kenya.

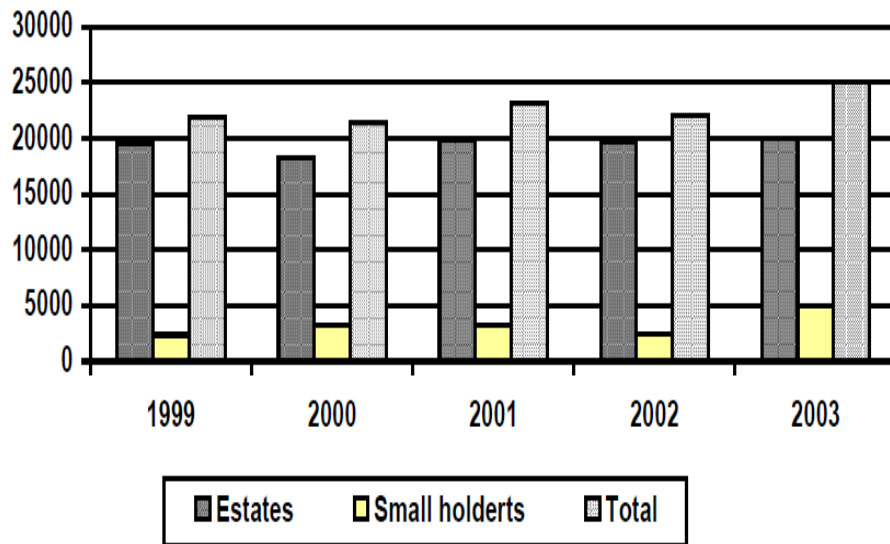


Figure 2.3: Sisal fibre production in Kenya from 1999-2003 (MT) [10]

2.1.3 Sisal production in Brazil

Brazil currently leads the world in production and exportation of sisal fibres [4, 8, 11, 12]. The sisal plants are extensively grown in the northeast region and is a major source of livelihood to at least 700,000 people [4, 12]. The Agave Sisalana, a variety grown in Kenya and Tanzania, is also grown in Brazil, but the production system in Brazil is mainly composed of small plots [4, 9]. It

extensively uses small mobile decorticators and though with a low production capacity (15 to 20 kg/h dry sisal fibre), they cumulatively produce more sisal fibres than Kenya and Tanzania (Figure 2.4 and Figure 2.5) [4].

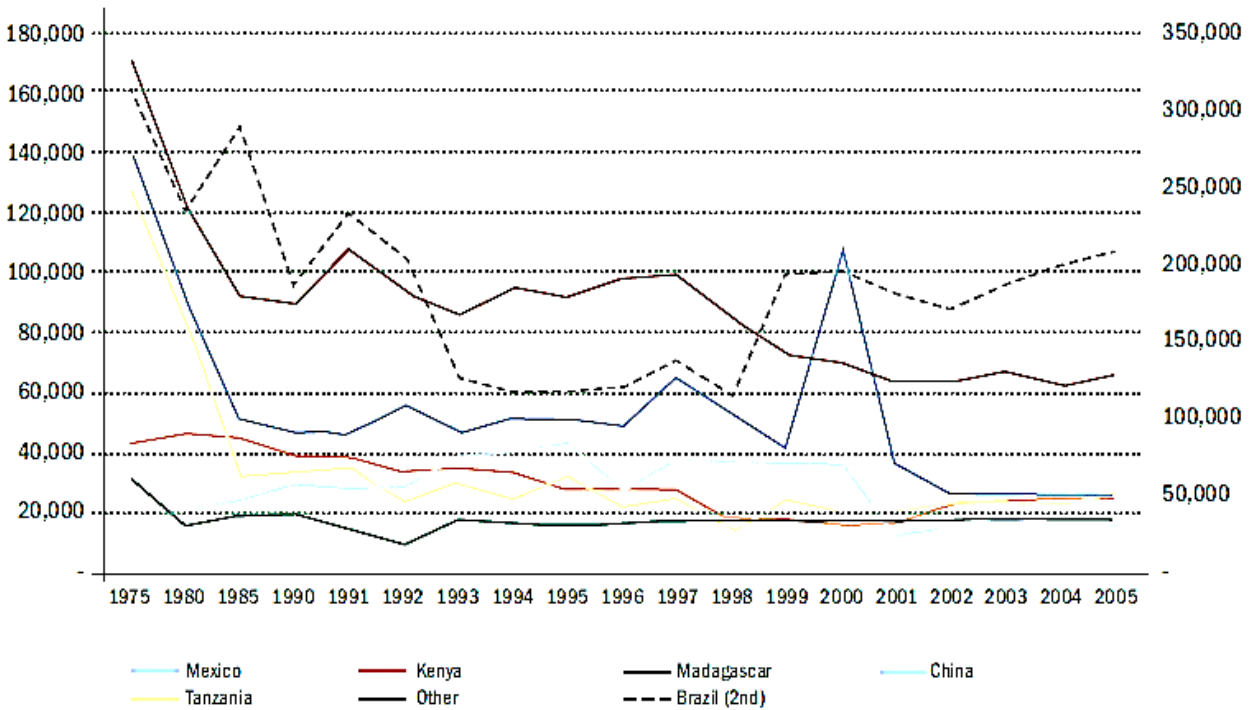


Figure 2.4: World production of sisal from 1975 to 2005 (tons) [8]

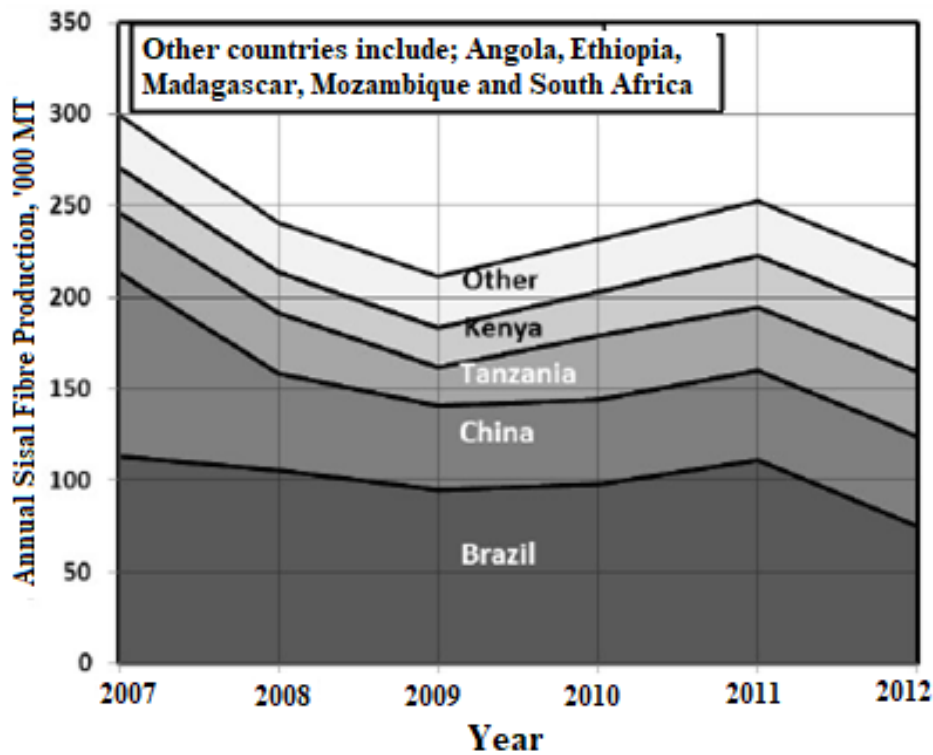


Figure 2.5: Sisal fibre production [13]

The sisal plant is the only cash crop that survives the harsh climatic conditions prevalent in the northeast region of Brazil that receives between 400 and 500 mm of rainfall all year round [4]. And although Mexico and China once provided stiff competitions for production of sisal fibres are now large consumers of the same after opting out to produce other cash crops.

2.2 Processing of sisal fibre

Sisal extraction is done using larger-scale automatic decorticators in sisal estates or raspadoras/manual methods in small-scale extraction. The large-scale extraction technologies are sophisticated and expensive to the small-scale farmers. They use large amounts of water that cause water pollution [3, 7]. Figure 2.6 depicts one of the extraction technologies used in the sisal estates consuming a lot of water.



Figure 2.6: Automatic decorticators [3]

This technology being inaccessible and uneconomical to small-scale farmers, UNIDO recommended that appropriate small-scale technology should be developed to increase the production of the sisal fibres [6]. In Brazil, for example, small-scale farmers use fully mobile field decorticators [4]. However, brushing and baling is done in the warehouses given that these machines can only extract the fibres.

For small-scale processing, there are a number of past designs of sisal fibre extraction machines that have been developed as recommended by UNIDO. For instance, Brenters [7] designed a

sisal extraction machine that encompassed a crushing unit and a decorticating unit. It was determined whether driving the machine manually was possible or not. From the results, the machine needed at least 1600 W to operate whereas a fully-grown adult could produce a maximum of 200 W on a single day [14]. It was impossible to operate the machine manually. In addition, all tests on crushing the leaves prior to decortication failed. Extraction of sisal fibre was achieved. However, extraction and brushing could not be achieved by the machine at the same time. A lot of adjustments were required before attempts on brushing could commence hence leading to waste of productive hours. Moreover, high amount of tow was also reported [15]. From the approach used and the information given, it was impossible to determine the actual machine capacity.

Kawongolo *et al.* [16] designed and fabricated a sisal fibre decortication machine for small-scale farmers in Uganda. However, the machine could only extract the sisal fibres. Moreover, the results indicated that the sisal fibre required further washing and brushing to improve quality. The machine's capacity was 12 kg/hr of dry fibre with a design efficiency of 42.9% and fibre percentage yield of 3.2% [16].

Oduori [2] also designed and fabricated a sisal decortication machine for small-scale farmers in Kenya. It was observed in this study that a speed of 1000 rpm and gap size of 2 mm led to better extraction quality [7]. However, the research did not report on the design efficiency and capacity of the machine. Moreover, the machine was limited to extraction ignoring an important process that improves fibre quality. Kanogu *et al.* [17] and Snyder *et al.* [18] remodified Oduori's [2] design. However, the two designs did not include the brushing unit. Also, the modification done by Snyder *et al.* included a vertical feed mechanism that did not yield conclusive results.

Ahmad *et al.* [19] designed and fabricated a sisal fibre extraction machine for Pakistanis. The production capacity of the decorticator was 15.94 kg/hr. The average power required to drive the machine was 3.1 kW [19]. Just as all the small-scale machines reviewed so far, the limitation of this particular machine was that it could only extract sisal fibre. No brushing was achieved nor reported in the research.

Brushing unit is characterized by the percentage fibre loss during brushing. The brushing process only polishes the surface of the fibres without breaking them. A large-scale banana brushing

machine was designed to comprise of a large rotating drum with extraction blades on its periphery [15]. Moreover, another design of a fibre combing/brushing machine used a high-speed drum with staggered steel pins on the drum; the pins accomplished both the straightening and removal of adherent particles. However, the quality of brushing achieved was quite low [15]. For small-scale machines, an average minimum output of 15 kg/hr is desirable [19]. Cantalino further recommends an output of between 15-20 kg/hr of dry fibre [4]. One of the machines achieved an output of 11.67 kg/hr [16] and another 15.94 kg/hr of dry sisal fibre [19]. Moreover, Naik *et al.* [20] reported a machine capacity of between 9-10 kg/hr.

From the review, none of the machines achieved both extraction and brushing of sisal fibres simultaneously. This implied that the sisal fibre would be sold unbrushed fetching low prices or the farmers needed to invest in a separate brushing machine. To address this gap in the small-scale technology, this research aimed at developing a machine for extraction and brushing of sisal fibre simultaneously and one that is affordable and accessible to the small-scale sisal farmers.

2.3 Properties of sisal fibres

Sisal leaf has an average mass of 1558 g, spine length of 1424.3 mm, wet and dry fibre weight of 156.6 g and 48.7 g respectively [19]. Kenyan sisal has an average length of 150 cm, width of 12 cm, thickness of 3 cm, ultimate tensile strength of 450 GN/m², Young's Modulus of elasticity 32.9 GN/m² and percentage elongation ranging between 2.8 - 29.3 % [21].

In raspador principle, sisal leaf is beaten and scrapped off by a rotating drum with blunt blades on its periphery. Washing, in many cases, depending on the quality of decortication achieved by the machine, is required before sun drying. With good decortication, the need for washing may be eliminated. After drying, brushing is done to obtain good quality fibre. Brushing removes the pieces that stick to the fibre after decortication or drying, frees individual fibre strands from one another, and removes tow (short fibres) from the hank. The brushing process straightens and polishes the curled and tangled fibre.

According to London Sisal Association (LSA) [22] (refer to Appendix D), factors that determine the quality of sisal fibre include; fibre length, colour, amount of tow and decortication defects (harshness, knots, barks, tousles and bunched ends). For instance, grade 1 sisal fibre should have a

fibre length of at least 90 cm, colour of cream-white or cream, free of decortication defects, brushed and contain no tow. Similarly, Auckland [23] proposes that the quality of sisal fibres should be judged based on the fibre length, colour, decortication defects and the presence of tow. Its usability in reinforcement of composites is dictated by its strength.

The high mechanical properties, disposability, affordability and environmental friendliness of sisal fibres have contributed to their increased utilization in reinforcement of composites [24]. However, the mechanical properties are affected by the environmental conditions and the processing techniques employed. For example, moisture content and temperature have been found to affect the strength of natural fibres [25]. The variability in the fibre properties needs to be quantified before the resultant properties of fibre reinforced composites can be predicted or otherwise determined [25].

There are past attempts to quantify the variability in properties of the natural fibres. A study on the relationship between tensile strength and gauge length of coir fibre established that there is a low correlation between the tensile strength of coir fibres with the gauge length [26]. A similar study on sisal fibres concluded that the mechanical properties of sisal fibres do not depend on the gauge lengths [27]. It was argued that the variability in the properties of natural fibres affects the strengths of fibre reinforced composites [28]. However, sisal fibre has the least variability among the natural fibres and can be classified under high performance natural fibres if well quantified [29]. Natural fibres being very irregular, optic microscope is mostly used to determine the average diameter of natural fibres [30].

The variation of tensile and fatigue strength of sisal fibres with gauge length was quantified using statistical analysis [25]. It was found that the tensile strength varied inversely with the gauge length. Moreover, the Young's Modulus of elasticity was independent of the gauge length. It was discovered that there is a high correlation between the properties of sisal fibres and the strength of fibre-reinforced composites [31]. Another research characterized the Kenyan sisal and found that it had the highest amount of hemicellulose and lignin [21]. And although the properties of sisal fibres vary with the environmental conditions and processing techniques, no research so far has quantified the variation of sisal properties with processing techniques. This research gap was addressed by this study.

2.4 Economic viability of the small-scale decorticator

Project ideas need to be subjected to a process of preliminary filtration through viability assessment [32]. An economical project should generate adequate cash flow and profits that can help the project withstand risks and uncertainties [33]. The analysis determines the extent to which an idea economically appeals to potential investors and identifies the key resources required to produce the much-anticipated service [34]. Cost and revenue analysis are required to generate the useful data required for the viability assessment. Correct facts, up to date financial data and correct assumptions should be used otherwise wrong conclusions may be arrived at just for the projects to fail in the implementation phase [33, 35]. A good cost and revenue analysis should provide an estimate of the possible amount of start-up capital needed to get the enterprise up and running [34]. Various methods are used to determine the economic viability as listed in Figure 2.7.

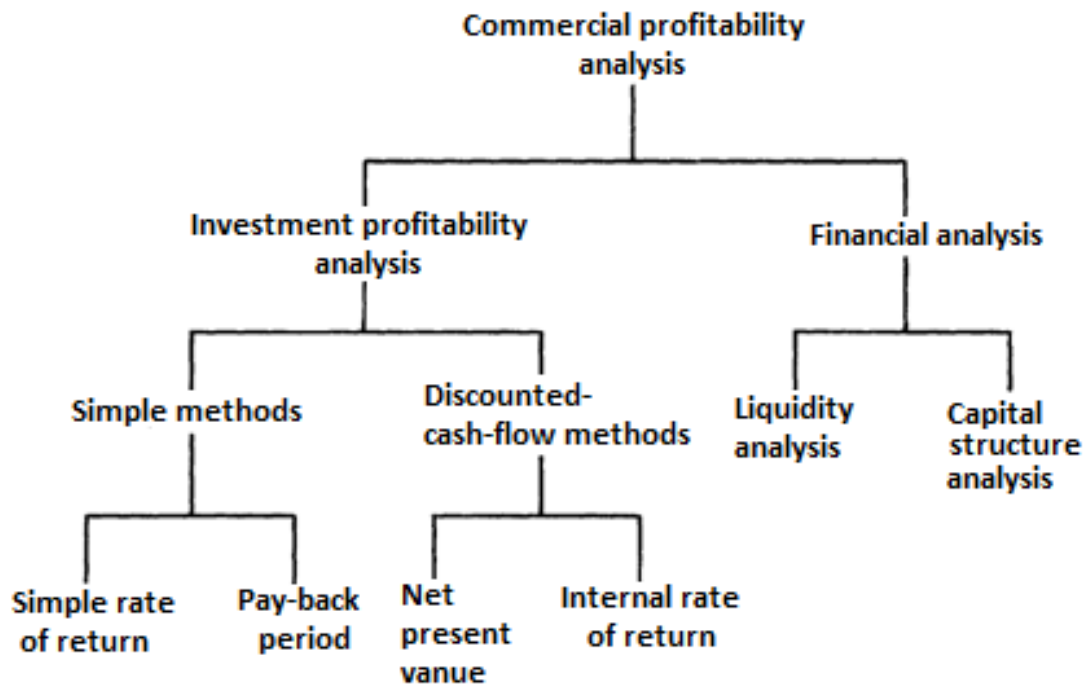


Figure 2.7: Methods of evaluating economic viability

It is recommended that at least two methods be used for evaluation of a project [36]. For a small-scale machine, its overall cost highly depends on the power source. Proper selection of this saves manufacturing cost and make it affordable to the target group [7].

CHAPTER THREE: METHODOLOGY

The methodology was simplified using the framework illustrated in Figure 3.1. In this methodology, design, fabrication and testing was preferred to finite element analysis (FEA) because it requires validation.

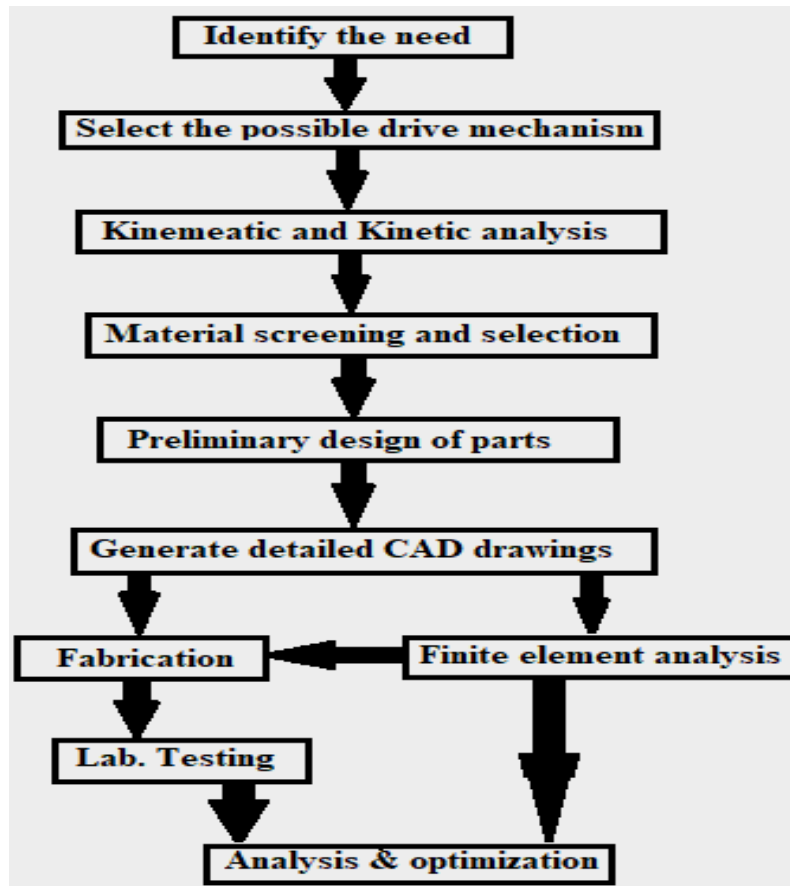


Figure 3.1: The sisal machine design procedure

This was achieved in two phases; (i) Design of the machine and (ii) Acquisition of materials, fabrication and laboratory testing.

3.1. Phase One: Design of the machine

The following two units of the machine were designed; the extraction unit and the brushing unit.

3.1.1. Extraction unit

The extraction unit responsible for decorticating sisal leaves was designed based on the fundamentals of the raspador principle (drum, beater and anvil) as illustrated in Figure 3.2. The principle was first used in Mexico and later redeveloped in Germany [6].

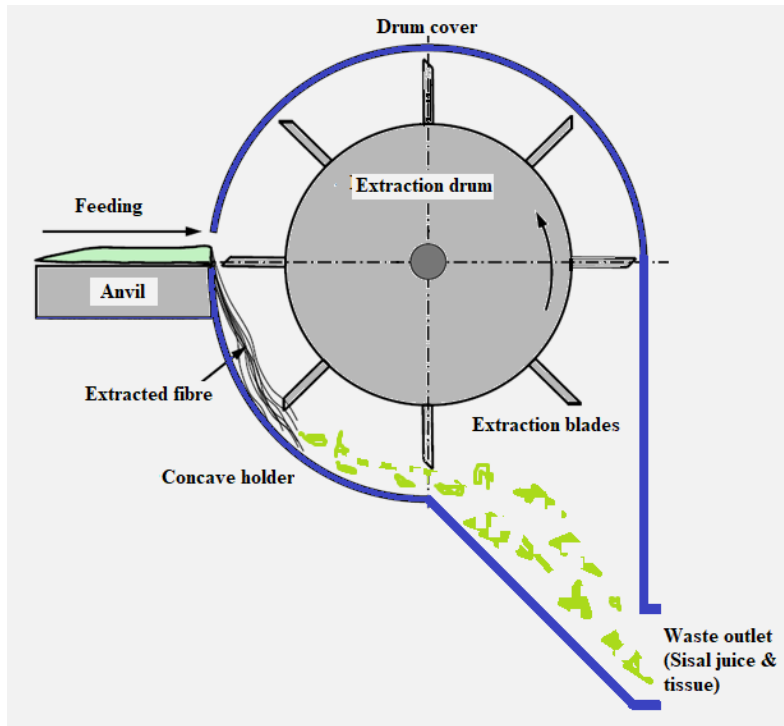


Figure 3.2: The extraction unit

The unit was designed to enable the beating and scraping of the green leafy matter from the leaf. The major functional parts designed for this unit included a cast-iron drum, extraction blades and an anvil, drum cover, frame and concave holder. The drum with radius r , and mass m , was used to inject inertia into the unit to smoothen the rotation. The inertia of the drum was given by equation (3.1).

$$\text{Inertia of the drum} = \frac{1}{2}mr^2 \dots\dots\dots (3.1)$$

where,

m – mass of the drum

r – radius of the drum

A belt-pulley mechanism was selected to drive the drum using either a motor or an engine as the power source.

3.1.2. Kinematic study of the machine

The kinematic analysis was conducted to determine the motions of the machine. For simplification, it was assumed that;

- i. The rate of feeding the leaf was uniform
- ii. The drum advanced towards the anvil at uniform speed equal to feed rate.

With these assumptions, the extraction unit was then modelled as shown in Figure 3.3.

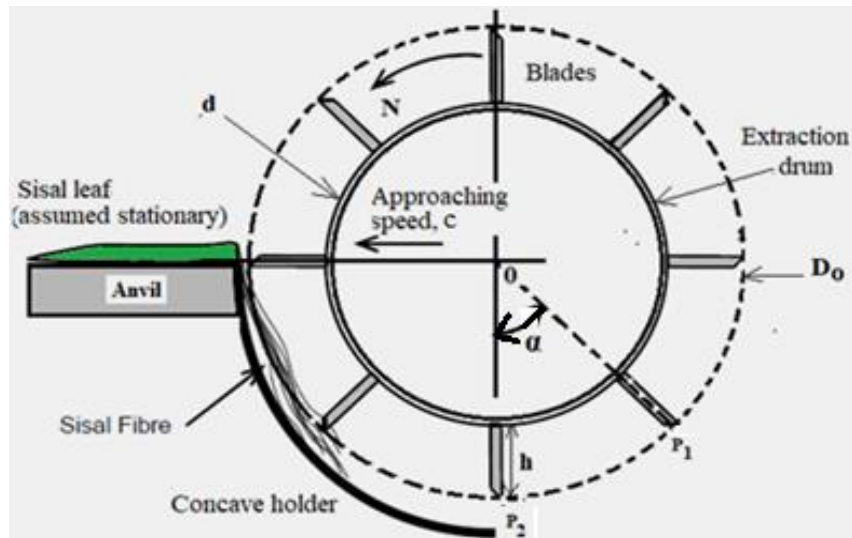


Figure 3.3: Model of the extraction unit

where;

- D_0 – the overall diameter of the extraction unit (drum plus height of blades)
- D – diameter of the extraction drum
- H – the height of the extraction blades
- 0 – the origin of reference cartesian plane (the symmetry of rotation)
- α – the angular difference between two successive blades about origin (in radians)
- n – the number of extraction blades
- c – the rate of feeding (also rate at which the drum approaches the anvil)
- G – clearance gap
- N – the rotational speed of the drum (rpm)
- ω – angular speed of the drum (rad/s)
- P_1 and P_2 – two arbitrary points at the tip of two successive blades

The number of extraction blades (n) required were determined from equation (3.2).

$$n = \begin{cases} \frac{360}{\alpha}, & \text{if } \alpha \text{ is in degrees} \\ \frac{2\pi}{\alpha}, & \text{if } \alpha \text{ is in radians} \end{cases} \dots\dots\dots (3.2)$$

Equation (3.2) was used to determined relationship between the number of extraction blades and the angle α . Figure 3.4 represents the extraction drum at time ($t = 0$) and at time, t . At time t , the tips of blades P_1 and P_2 were described by equation (3.2) and equation (3.3) [7];

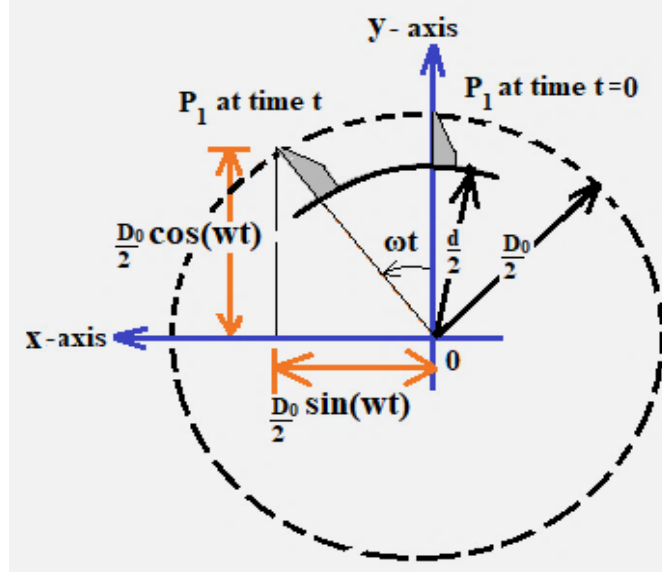


Figure 3.4: Tips of blade P_1 at $t=0$ and at t

$$X_{P_1}(t) = \begin{cases} 0, & \text{at } t = 0 \\ ct + \frac{D_0}{2} \sin(\omega t), & \text{at time } t \end{cases} \dots\dots\dots (3.3)$$

$$Y_{P_1}(t) = \begin{cases} \frac{D_0}{2}, & \text{at } t = 0 \\ \frac{D_0}{2} \cos(\omega t), & \text{at time } t \end{cases} \dots\dots\dots (3.4)$$

Equally, the tips of blade P_2 at $t = 0$ and at time t were represented as;

$$X_{P_2}(t) = \begin{cases} \frac{D_0}{2} \sin(-\alpha), & \text{at } t = 0 \\ ct + \frac{D_0}{2} \sin(\omega t - \alpha), & \text{at time } t \end{cases} \dots\dots\dots (3.5)$$

$$Y_{P_2}(t) = \begin{cases} \frac{D_0}{2} \cos\alpha, & \text{at } t = 0 \\ \frac{D_0}{2} \cos(\omega t - \alpha), & \text{at time } t \end{cases} \dots\dots\dots (3.6)$$

where;

ct - the displacement of the drum in the x-direction in time t and speed c .

$\frac{D_0}{2} \sin(\omega t)$ and $\frac{D_0}{2} \cos(\omega t)$ – the displacements of the blades in x-direction and y-direction respectively due to rotation of drum in time t .

α - the phase angle between the tips of blades P_1 and P_2 at an initial moment of time.

For convenience, R_0 and c were let to be;

$R_0 = \frac{D_0}{2}$ (the radius of the imaginary circle that touches the tips of the blades) and

$R = \frac{c}{\omega}$ (m/rads) (ratio of the linear speed to radial speed of the drum).

The set of equations were then simplified to;

$$X_{p_1}(t) = \begin{cases} 0, & \text{at } t = 0 \\ R\omega t + R_0 \sin(\omega t), & \text{at time } t \end{cases} \dots\dots\dots (3.7)$$

$$Y_{p_1}(t) = \begin{cases} R_0, & \text{at } t = 0 \\ R_0 \cos(\omega t), & \text{at time } t \end{cases} \dots\dots\dots (3.8)$$

$$X_{p_2}(t) = \begin{cases} R_0 \sin(-\alpha), & \text{at } t = 0 \\ R\omega t + R_0 \sin(\omega t - \alpha), & \text{at time } t \end{cases} \dots\dots\dots (3.9)$$

$$Y_{p_2}(t) = \begin{cases} R_0 \cos\alpha, & \text{at } t = 0 \\ R_0 \cos(\omega t - \alpha), & \text{at time } t \end{cases} \dots\dots\dots (3.10)$$

As the drum rotates, the tips of the blades usually trace out a given path. For any two successful tips, say P_1 and P_2 , the profile traced within a quarter turn is represented by Figure 3.5 [7];

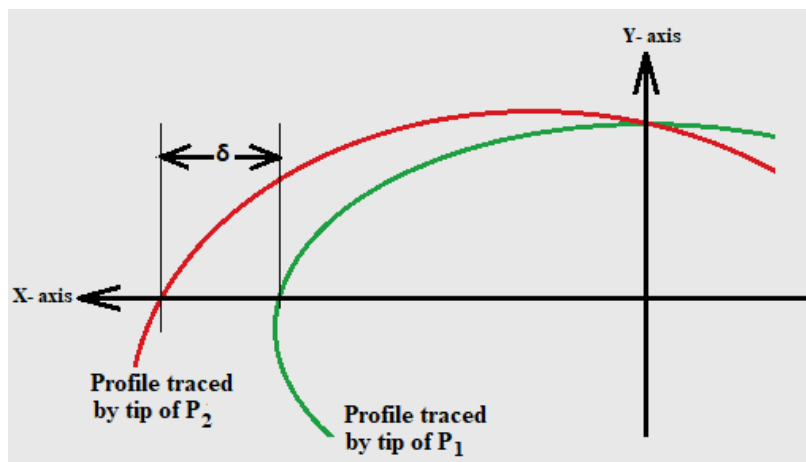


Figure 3.5: Profiles traced by tips of blades P_1 and P_2 in a quarter turn

δ an important parameter in the design of the machine, is referred to as pitch in some studies [7, 15]. In this study, it was referred to as delta (δ), the difference in the x-direction where the two successive tips strike the x-axis. It was also assumed that the tips of blades P_1 and P_2 strike the axis at t_1 and t_2 respectively (see Figure 3.6 for illustration).

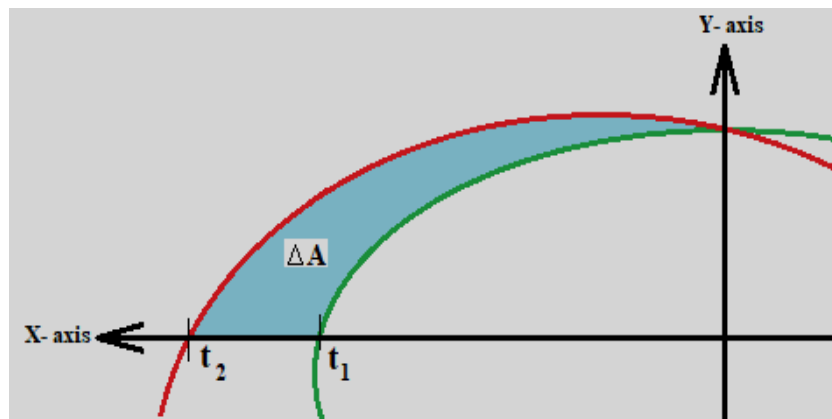


Figure 3.6: Time difference and the swept area of successive tips

The notation ΔA represented the difference in swept area by the tips P_1 and P_2 in a quarter turn and related to δ as given by equation (3.11).

$$\delta = f(\Delta A, c) \dots\dots\dots (3.11)$$

On the x-axis and at t_1 and t_2 , the displacements of the tips in the y-axis about the origin being zero, equation (3.8) and equation (3.10) were equated to zero to obtain useful relations as follows;

$$\begin{aligned} Y_{P_1}(t_1) &= R_0 \cos(\omega t_1) = 0 \\ R_0 &\neq 0 \\ \cos(\omega t_1) &= 0 \\ \omega t_1 &= \frac{\pi}{2} \dots\dots\dots (3.12) \end{aligned}$$

From equation (3.7), the value of x at t_1 was determined as follows;

$$\begin{aligned} X_{P_1}(t_1) &= R t_1 \frac{\pi}{2 t_1} + R_0 \sin\left(t_1 \frac{\pi}{2 t_1}\right) \\ &= R \frac{\pi}{2} + R_0 \sin \frac{\pi}{2} \\ &= R \frac{\pi}{2} + R_0 \dots\dots\dots (3.13) \end{aligned}$$

Equally, the tip of blade P_2 first crosses the x-axis at t_2 hence;

$$\begin{aligned} Y_{P_2}(t_2) &= R_0 \cos(\omega t_2 - \alpha) = 0 \\ \cos(\omega t_2 - \alpha) &= 0 \\ \omega t_2 &= \frac{\pi}{2} + \alpha \dots\dots\dots (3.14) \end{aligned}$$

And from equation (3.9);

$$\begin{aligned} X_{P_2}(t_2) &= R t_2 \left(\frac{\pi + 2\alpha}{2 t_2}\right) + R_0 \sin\left(\frac{\pi + 2\alpha}{2 t_2} t_2 - \alpha\right) \\ &= R \left(\frac{\pi + 2\alpha}{2}\right) + R_0 \sin\left(\frac{\pi}{2} + \alpha - \alpha\right) \\ &= \frac{R}{2}(\pi + 2\alpha) + R_0 \dots\dots\dots (3.15) \end{aligned}$$

An expression for delta (δ) was found by subtracting equation (3.13) from equation (3.15);

$$\begin{aligned} \delta &= X_{P_2}(t_2) - X_{P_1}(t_1) \\ &= \frac{R}{2}(\pi + 2\alpha) + R_0 - \left(R \frac{\pi}{2} + R_0\right) \\ &= \alpha R \end{aligned}$$

Substituting the values for c and n as earlier stated, the equation (3.16) for δ was derived.

$$\delta = \frac{2\pi}{n} \left(\frac{c}{\omega} \right) = \frac{2\pi c}{n\omega} \dots\dots\dots (3.16)$$

Equation (3.16) was further analysed to guide on selecting the number of blades/elements and speed and sizing the drum.

3.1.3. Kinetic study of the machine

The machine was modelled as shown in Figure 3.7 to analyse its kinematics. And since the forces involved in this machine are negligible and do not pose any quantifiable problem to the integrity of the structure, the kinetic analysis was conducted to determine the decortication resistance and the power required to successfully extract sisal fibres.

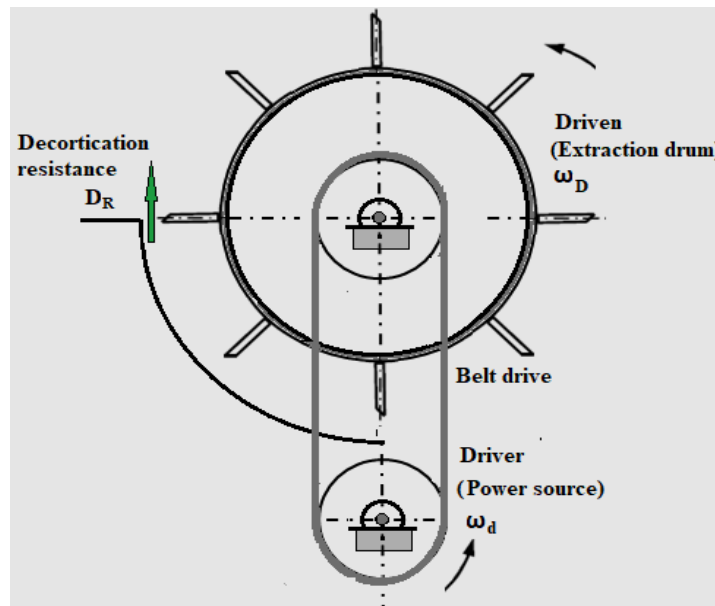


Figure 3.7: Kinetic model of the machine

Given that decortication resistance depends on the speed (ω), clearance gap (G) and time (t) and given that G and ω are constants, from time t_1 to time t_2 , the amount of energy dissipated during extraction was given by equation (3.17).

$$E = \omega R_O \int_{t_1}^{t_2} D_R(t) dt \dots\dots\dots (3.17)$$

Using the mean value theorem, the decortication resistance equation is reduced to equation (3.18).

$$(D_R)_e = \frac{1}{t_2 - t_1} \int_{t_1}^{t_2} D_R(t) dt \dots\dots\dots (3.18)$$

where;

$(D_R)_e$ - the mean decortication resistance.

Power consumption equation was derived from its definition, that is, the rate of doing work.

$$\begin{aligned}
 P &= \frac{E}{\Delta t} \dots\dots\dots (3.19) \\
 &= \frac{1}{\Delta t} \omega R_O \int_{t_1}^{t_2} D_R(t) dt \\
 &= \frac{1}{t_2 - t_1} \omega R_O \int_{t_1}^{t_2} D_R(t) dt \\
 &= (D_R)_e \omega R_O \dots\dots\dots (3.20)
 \end{aligned}$$

$(D_R)_e$ was presumed to vary with clearance and motor speed as supported by research [7].

It was determined from literature that the forces involved in extraction are very negligible compared to the strength of the fabrication materials. For brushing, it was assumed that these forces are equally negligible given that the fibres are weaker than any metal. The decortication resistance was then approximated by modelling the system as a cantilever beam (Figure 3.8) and applying Timoshenko's equations for maximum bending [37].

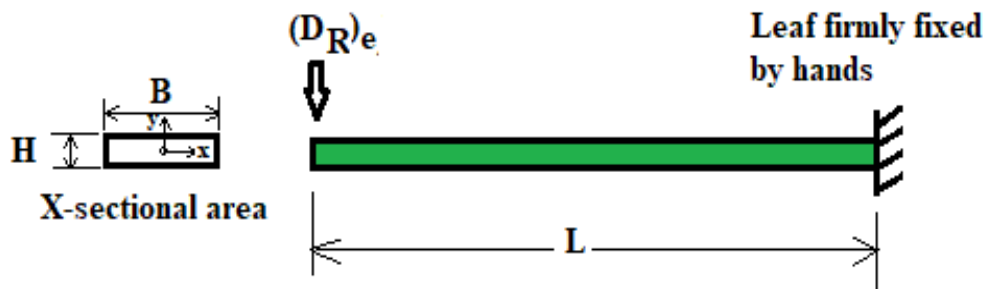


Figure 3.8: Cantilever model to determine decortication resistance

The maximum bending of a cantilever is given by equation (3.21) [38];

$$y_{max} = \frac{(D_R)_e L^3}{3EI} \dots\dots\dots (3.21)$$

3.1.4. Brushing unit

Since there was no such a principle that directly applied to the brushing unit, it was first designed based on the raspador principle for extraction. A trial and error approach were equally employed to optimize the brushing unit. The trials were done using blunter bitters, brushes and spikes. To save on power cost, the brushing unit was designed to utilize the same shaft as the extraction unit. This enabled both decortication and brushing to be carried out simultaneously. Figure 3.9 shows the brushing unit that was conceptualized.

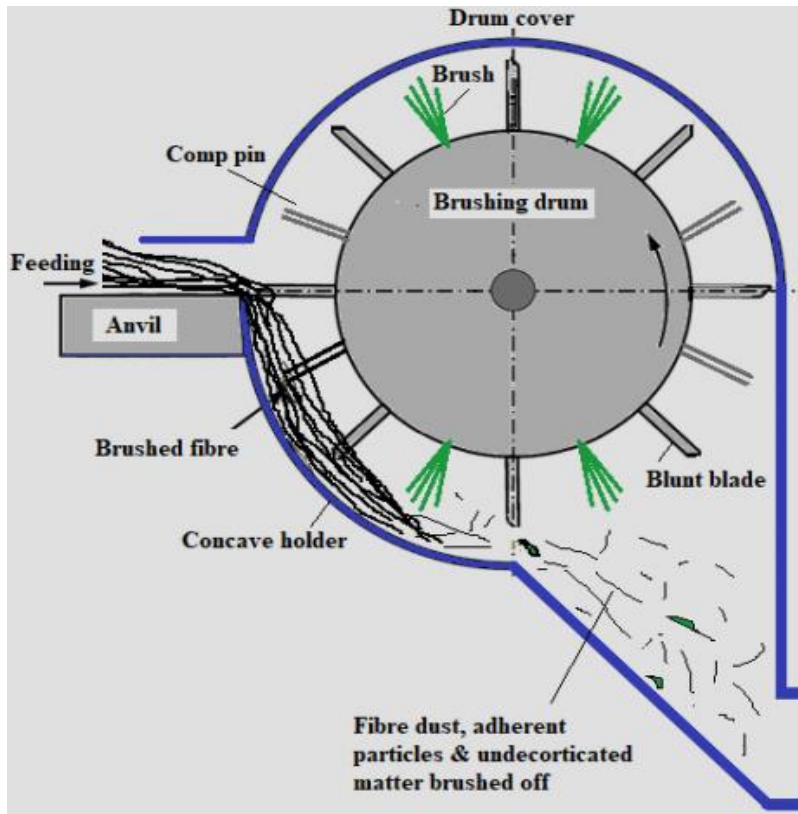


Figure 3.9: Conceptualization for brushing

A combination of both blades and wire brushes was used to achieve better brushing outputs. The steel pins were used to comb and straighten the sisal fibres. Since the extraction and brushing units were designed to share most of the core parts (drum, some of blades and shaft), the kinetic and kinematic analysis of the extraction unit were equally employed for the brushing unit due to lack of sufficient literature on the brushing. Therefore, for kinetic analysis, equation (3.16) was employed.

3.1.5. Design of the components

An iterative technique was used to design the various components of the machine. For the machine to be commercially acceptable, its dry fibre minimum output needed to be between 15 – 20 kg/hr as recommended in the literature [2]. Therefore, a minimum output of 15 kg/hr was selected for design purposes. Two designs for the two units were conceptualized based on the objective of achieving both extraction and brushing at the same time at no additional cost (Figure 3.10 and Figure 3.11).

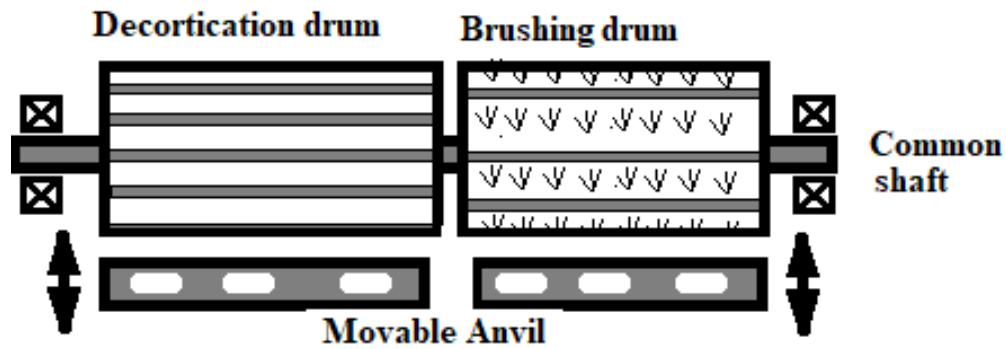


Figure 3.10: Proposed design one

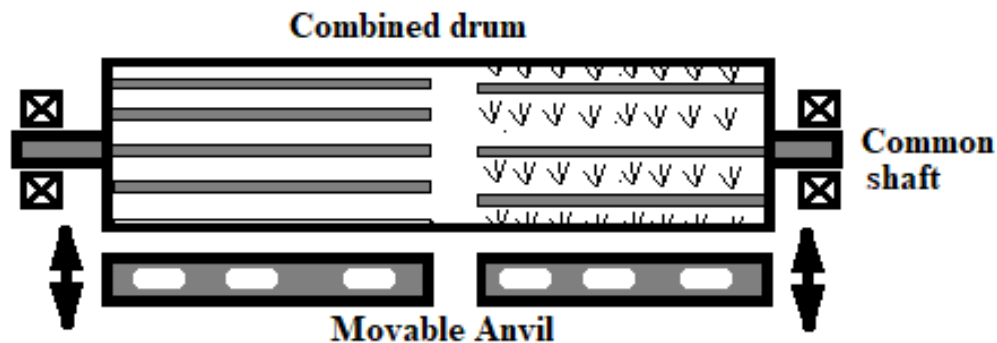


Figure 3.11: Proposed design two

To reduce the size and weight of the machine, the second design was selected. The feeding velocity (c) was then determined based on the expected output. The power required to decorticate a sisal leaf and to brush fibre from one leaf was determined. Hence, a proper prime mover was selected based on the maximum power required to operate the two units.

3.1.6. Design of the belt drive

Belt drive was selected for torque transmission from the motor/engine to the drum. The belt drive was designed using Roulunds design catalogue and in accordance with the ISO 4184 standard. A V belt was selected for the design because it is the most preferred for machine designs due to its higher power transmission capacity and negligible slip [39]. The belt length, centre distance, pulley diameters among other variables were determined.

3.1.6.1. Shaft design

To design the shaft, the forces on the shafts were determined. Figure 3.12 was modelled to show the location of the point of application of forces on the shaft.

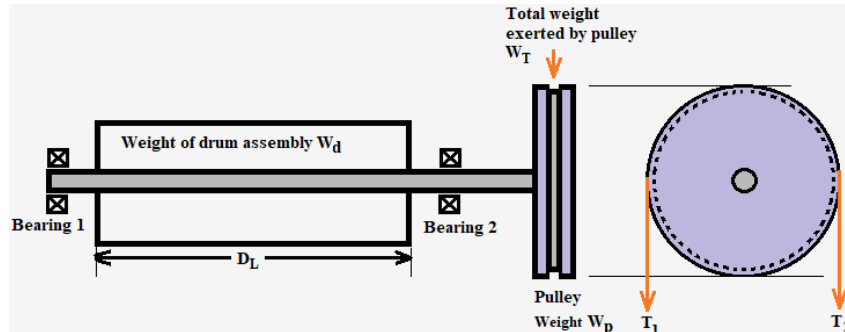


Figure 3.12: Sketch of the intended design

where;

W_p – weight of the pulley

W_T – total weight exerted on the shaft by the pulley

W_d – the weight of the drum assembly acting at the centre

T_1 and T_2 – the belt tensions on tight and slack sides respectively

The extraction/brushing drum of 273.1 mm outer diameter was selected from the ANSI/ASME B36.10 standard pipe sizes. The weight of the pulley, the weight of the drum, the total weight exerted on the shaft and the belt tensions were determined. The maximum bending moment in the shaft was determined. Thereafter, maximum shear stress theory (Guest's or Tresca's theory) and maximum normal stress theory (Rankine's theory), equation (3.22) and equation (3.23) respectively, were used to design the shaft.

Maximum shear stress theory (Guest's theory);

$$\frac{\pi}{16} * \tau_{max} * d^3 = \sqrt{(K_m * M_{max})^2 + (K_t * T)^2} \dots\dots\dots (3.22)$$

Maximum normal stress theory (Rankine's theory)

$$\frac{\pi}{32} * \sigma_b * d^3 = \frac{1}{2} \left\{ K_m * M_{max} + \sqrt{(K_m * M_{max})^2 + (K_t * T)^2} \right\} \dots\dots\dots (3.23)$$

where;

M_{max} – maximum bending moment

K_m – combined shock and fatigue factor for bending

K_t – combined shock and fatigue factor for torsion

τ_{max} – the maximum shear stress allowable

σ_b – maximum allowable normal stress for the shaft material

T – torque

3.1.6.2. Bearing selection

To select a suitable bearing, the torque, speed of the machine, dynamic shaft load and static shaft load needed to be determined first. An appropriate bearing unit was one that could withstand the dynamic and the static loads of the shaft. A UCP205 cast iron pillow block was selected because its dynamic and static shaft loads were higher than the required.

3.1.6.3. Design of machine frame and pulley/belt drive guard

The frame of the machine was designed from mild steel angle plates measuring 50 mm by 50 mm by 3 mm for two reasons; its Euler's critical buckling load (1.79 GPa) for a designed height of 598.5 mm was greater than total supported load of 742.4 N (Appendix A-14) and secondly, its 50 mm wide surface was appropriate for supporting the 80 mm wide anvil and still leave just enough gap size (50 mm) required for investigation. The dimensions of the columns and beams were sized based on the overall height and length of the machine required to minimize its weight and size and still provide a comfortable working height. The pulley/belt drive cover was designed to meet the required belt drive centre distance.

3.1.7. Generation of Computer Aided Design (CAD) drawings

Autodesk Inventor Professional 2018 was used to draft and generate the drawings of the machine making it easy to visualize and fabricate. The design specifications were used to generate the various components, the sub-assemblies and the assembly of the designed machine. CAD drawings were generated for all the components. Moreover, the views of the sub-assemblies and the overall assembly were also generated.

3.2. Phase Two; Acquisition of materials, fabrication and laboratory testing

The tasks carried out during this phase included the identification and acquisition of required materials, the fabrication of the components and the machine and lastly, the laboratory testing.

3.2.1. Identification and acquisition of materials for fabrication.

Ashby's 'traditional' method based on past experience was used for material selection [39]. The cost, availability and mechanical properties were considered in the selection of the most suitable materials for fabrication of the machine. Considering these factors, suitable materials were selected for all the components and a bill of materials generated. The materials and standard parts selected were acquired from Kens Metal Ltd in Nairobi industrial area. A standard mild

steel pipe (outer diameter 273.1 mm, thickness 6 mm and half meter length) weighing 21 kg and 12 mm thick mild steel plate (for fabrication of disc plates) were purchased at Kshs 150 per kg. Motor vehicle transmission shaft (hardened steel) was acquired from a nearby garage.

3.2.2. Fabrication of the components and assembly of the machine

A full-scale laboratory model was fabricated at Mechanical Engineering Workshop, University of Nairobi. The specific components were fabricated as follows;

3.2.2.1. Fabrication of the drum

From the design equations, it was expected that although the drum size does not affect the quality of processing, a larger drum would increase the power consumption. Therefore, the minimal available ANSI/ASME standard pipe of 273.1 mm outer diameter was used to fabricate the drum. Acetylene gas welding was used to cut the drum to a length of 420 mm leaving an allowance of 20 mm to be machined precisely on the lathe machine. The drum was then faced on the lathe machine using a four-jaw chuck to obtain the required length of 400 mm (Figure 3.13 c)).



a) Drilling on radial drill b) Indexing of fastening holes c) Facing on lathe machine

Figure 3.13: Fabrication of the drum

A radial drilling machine (Figure 3.13 a)), with the help of a dividing head, was used to drill holes on the circumference of the drum for fastening the blades and brushes. The indexing head was used to locate the exact points (Figure 3.13 b)) to be drilled on the circumference of the drum using the equation (3.24). Number of divisions was the maximum number of blades/elements to be investigated (12 in this case).

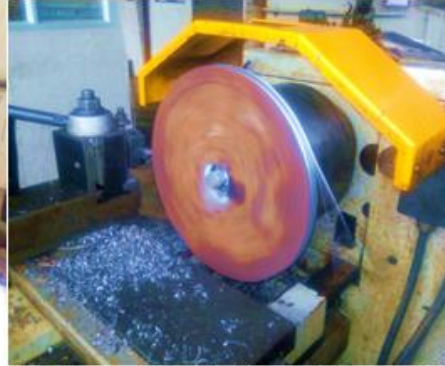
$$\begin{aligned} \text{Number of turns of crank} &= \frac{40}{\text{Number of divisions}} \dots\dots\dots (3.24) \\ &= \frac{40}{12} = 4\frac{1}{3} \end{aligned}$$

3.2.2.2. Fabrication of side discs

Acetylene gas welding was also used to flame cut the circular side discs from the 12 mm thick plate (Figure 3.14 a)).



a) Flame cutting for side discs



b) Turning the side disc on lathe machine

Figure 3.14: Fabrication of side discs

The discs were then drilled on the face and fastened together using bolts and nut for even machining on the lathe machine (Figure 3.14 b)).

3.2.2.3. Fabrication of shaft

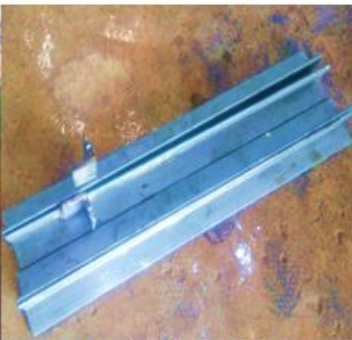
The shaft was first cut using acetylene gas welding and then machined precisely to a length of 560 mm and diameter of 25 mm using lathe machine.

3.2.2.4. Fabrication of machine frame

The frame was cut from angle bars measuring 50 mm by 50 mm by 3 mm thick using a power saw (Figure 3.15 a)). The various parts of the frame were assembled using arc welding (Figure 3.15 b) and c)).



a) Power saw and frame pieces cut using the machine



b) Welding of machine frame



c) Welded frame

Figure 3.15: Fabrication of the machine frame

3.2.2.5. Fabrication of blades

The extraction blades (Figure 3.16) were fabricated from angle bars 25 mm by 25 mm by 2 mm thick and a length of 400 mm. 12 blades were cut in bundles of six using the power saw. The holes for fasteners were drilled using the radial drilling machine and threaded using a tap.



Figure 3.16: Fabrication of the extraction blades

3.2.2.6. Fabrication of chute

The chute was fabricated from mild steel sheet 2 mm thick. The sheet was cut to respective sizes using Hydraulics Guillotine Machine. It was then bent into the required profile using a three roller-bending machine (Figure 3.17 b)).

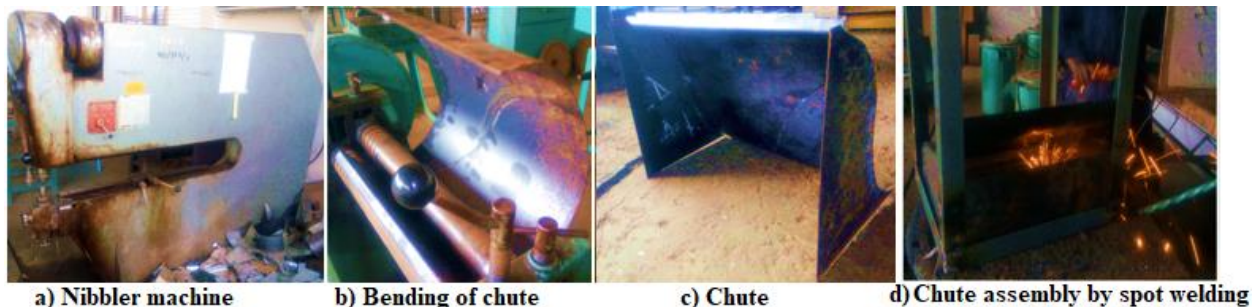


Figure 3.17: Fabrication of the chute

A nibbler machine (Figure 3.17 a)) was used to cut the side parts into the required circular profiles. Spot welding machine was used to weld the side parts of the chute and to weld the chute onto the frame (Figure 3.17 c) and d)).

3.2.2.7. Fabrication of drum cover

The drum cover (Figure 3.18) was also fabricated from the 2 mm thick mild steel sheet. Hydraulic Beam Shearer was used to cut the sheet into the required profile. It was then bent into the required profile using a three roller-bending machine. The side parts were cut using the nibbling machine to precisely shear into the required circular profile. It was then welded together using spot welding.



Figure 3.18: Drum cover

3.2.2.8. Fabrication of belt guard

2 mm sheet was marked using scribes, dividers and the profile was cut using the nibbling machine (Figure 3.19a)). The bending was done using bending machine (Figure 3.19 b)).



Figure 3.19: Bending machine and guard

3.2.2.9. Fabrication of the anvils

The extraction and brushing anvils were machined from a 20 mm by 6 mm steel bar (Figure 3.20). A power saw was used to precisely cut lengths of 150 mm and 250 mm for extraction and brushing respectively. The slots for fastening the anvils on the frame and for adjustments were machined using vertical milling machine.



Figure 3.20: Anvil steel bar

The anvils were separated to allow adjustments of the extraction and brushing gaps independently.

3.2.2.10. The standard parts used

The following standard parts (some shown in Figure 3.21) were used;

- **Fasteners;** M6, M8 and M14, ISO 4017 bolts and nuts, were used because they are most commonly used for general purpose. Moreover, they were affordable and locally available. The M6 bolts and nuts were used to fasten the blades to the drum and the drum cover to the frame. M8 bolts and nuts were used for fastening the motor/engine and the anvil to the frame. The bearings were fastened to the frame using M14 bolts and nuts.
- **Engine and motor;** a 5 HP two stroke variable speed engine and a 3 HP fixed speed (2880 rpm) motor were used because of their availability. The motor was mainly used for laboratory testing and the engine was appropriate for both laboratory and field tests.
- **Pulleys;** ISO certified tapered pulleys were used. The smaller pulley diameters were 5.5 cm, 6.5 cm, 7.5 cm and 8 cm. The larger pulley diameters were 11cm, 13 cm, 13.3 cm and 16.4 cm. A permutation of these diameters was used to obtain different speed ratios and hence drum speeds while using the electric motor. However, the speed of the engine was varied using choke and accelerator.

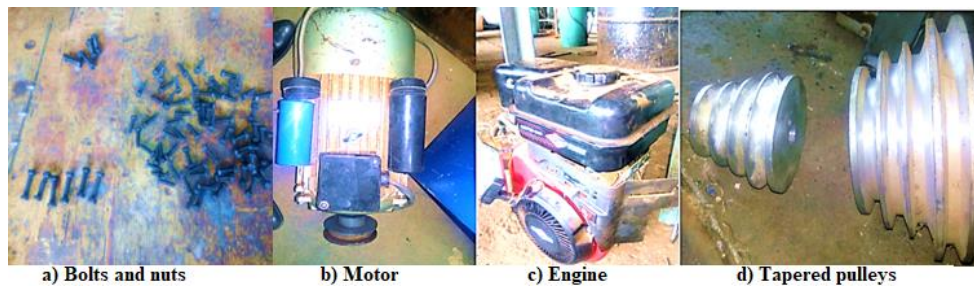


Figure 3.21: Standard parts

- **Bearing assembly;** 4 UCP205 ISO certified pillow block bearing units of bore diameter 25 mm were used because they are mounted bearing and self-aligning pillow blocks suitable for medium speeds required.
- **Belt drive;** A 3V belt of top width of 9.525 mm and depth 7.9375 mm with a belt length of 1587 mm was selected based on ISO 4184 standard of its quietness, flexibility, affordability and suitability for low torque high-speed designs [39]. Only one belt was needed to transmit the torque required.

3.2.2.11. Assembly of the machine

The blades were fastened to the holes drilled on the drum periphery using 60 M6 bolts. The two side discs were spot-welded on the drum. The shaft was carefully fitted through the central holes on the side discs leaving just enough space for fitting the bearings and pulley. The shaft was then spot-welded on the side discs. The frame sub-assembly on the other hand consisted of the frame,

chute and motor/engine plate. The chute was spot welded on the frame as per the design diagram. Spot welding was used because a 2 mm metal sheet was used to fabricate the chute. Four M8 bolts were welded on the bottom frame and two bearing fastened on them to secure the motor/engine plate.

All the necessary components were painted using a spray gun. The drum and frame assemblies were assembled to obtain an overall assembly by incorporating a number of standard parts. Respective holes for assembling the drum cover, bearing, guard and anvils were drilled using a radial drilling machine. A rectangular slot was machined on the shaft and the pulley assembled using a key. The bearings were fixed to the shaft and fastened to the frame. The engine/motor was fixed on the engine/motor plate with a vertical and horizontal movement allowance for alignment and tightening of the belt. The belt was then fixed on the pulley ensuring there was enough tension to avoid slip. The guard and drum cover were fixed on the frame using M8 bolts and nuts.

3.2.3. Laboratory testing

The machine was installed in the laboratory for extensive tests. Machine trial tests were done to ensure the machine operated as required and any vibrations arrested. Engine plate bearings were used to damp the engine vibrations. Hedge sisal was obtained from Kasarani constituency, Nairobi county (Figure 3.22). Testing was done for over a period of three months giving enough time for fibres to dry up.



Figure 3.22: Harvesting hedge sisal at Kasarani Constituency

3.2.3.1. Determination of power consumption

To determine the power consumed at various speeds, the motor was assembled on the motor plate. The pulley guard was removed and the belt connected on the various pulley diameters to vary speeds. The machine was run at 960 rpm, 1130.5 rpm, 1210 rpm, 1308 rpm, 1429 rpm and 1615 rpm. During each test for given set of parameters, the machine was run without feeding any leaf. The power consumed was read from a wattmeter (the idling power (IP)). The drum speed was read from a digital tachometer in rpm. The power consumed by the machine while decorticating a single sisal leaf was also read for six separate samples. After drying the fibre for three days, the fibre from a single leaf was also brushed and the power consumed recorded.

3.2.3.2. Extraction of fibres

The sisal leaves obtained from Kasarani Constituency, Nairobi City County Kenya was extracted using two methods for comparison purposes; manual extraction (mostly used by small-scale farmers) and the fabricated machine.

3.2.3.2.1. Manual extraction

Eighteen sisal leaves were randomly selected and extracted using hammer and anvil manual extraction method (Figure 3.23).



Figure 3.23: Manually extracted fibre

3.2.3.2.2. Machine extraction

Ten samples per given set of parameters were extracted using the fabricated machine. The sisal leaves were coded for easy traceability during subsequent tests (Figure 3.24 a)). The variables varied during machine extraction included gap size, drum speed and number of blades. Apparatus such as tachometer, electronic weighing balance, steel rule and stopwatch were required. Steel rule was used to measure the lengths of sisal leaves and fibres and to set the correct gap sizes. At a given gap size and number of blades, the machine was run at different speeds and the samples of the sisal leaves were extracted as shown in Figure 3.24 b).



Figure 3.24: Extraction of fibres

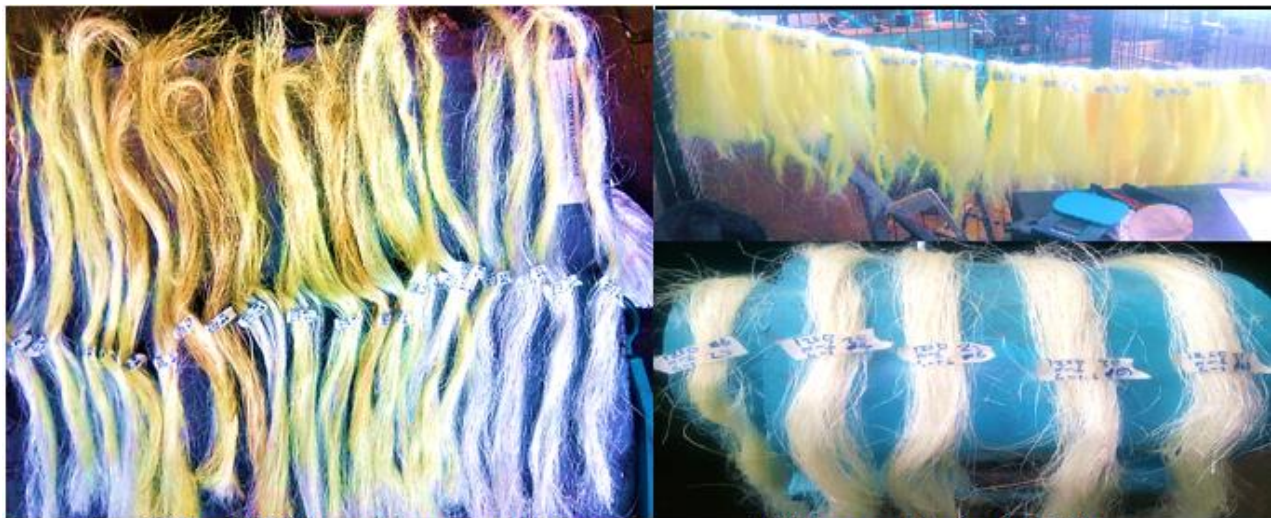
Before and after every extraction (Figure 3.25 shows the extracted sisal fibres.), the weights and lengths of the sisal leaf and its fibre were measured. The weight of the sisal fibre was taken immediately after extraction while still wet and after three days of drying. The colour of sisal fibre was also noted since it played a role in determining the grade of sisal fibre. The speeds were varied from 900 rpm to 1400 rpm. Moreover, the following gap sizes were used; 1 mm, 1.5 mm, 2 mm, 2.5 mm, 3 mm, 3.5 mm and 4 mm. The blades were equally distributed and fastened on the extraction drum. The number of blades experimented were limited to 12, 6 and 3.



Figure 3.25: Extracted sisal fibres

3.2.3.3. Brushing of sisal fibres

The sisal fibres were first dried for 3 days after extraction before brushing. Initially, the fibres were brushed using the brushing unit with similar parameters. The colour, weight and fibre lengths were recorded before and after brushing (Figure 3.26 a)).



a) Brushed fibres with varying colours

b) Cream-white brushed fibre

Figure 3.26: Brushed sisal fibres

After brushing, the amount of tow (Figure 3.27) was measured using a weighing balance. This was the small pieces of sisal fibre lost during brushing. The brushing dust was neglected in the weighing of tow. A stopwatch was used to time the amount of sisal brushed or extracted per unit

time for determination of machine capacity. The amount of fibre processed per minute was recorded. More tests were conducted using different sets of brushing elements. Figure 3.27 shows brush dust and tow fibres.

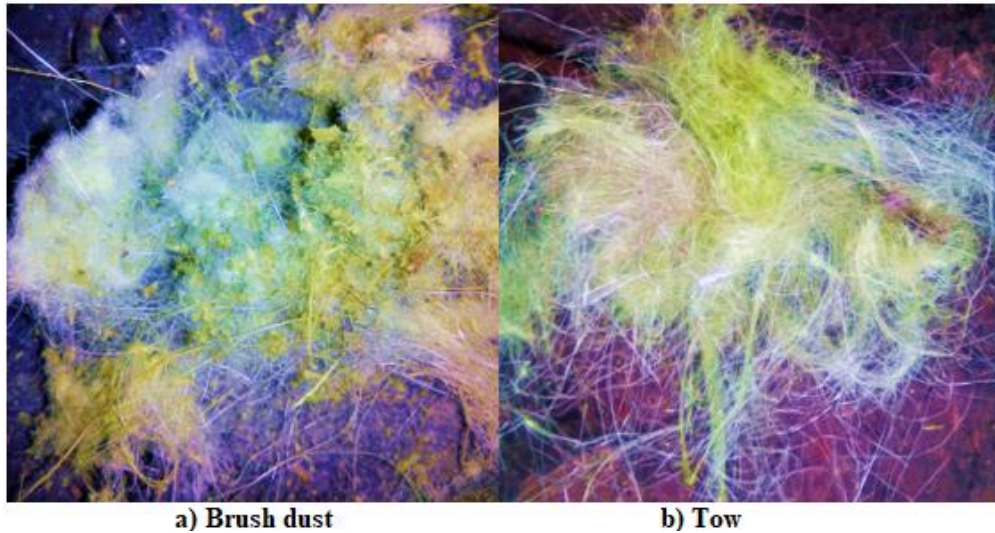


Figure 3.27: Fibre dust and tow fibre

3.2.3.4. Determination of mechanical properties of sisal fibres

The sisal fibres from hammer and anvil method, from Rea Vipingo and fibres processed by the machine were tested to determine the variations in their properties. Estate sisal fibre was obtained from Rea Vipingo with the help of Mr. Neil Cuthbert (the managing director). The tensile fibre samples were tested as per the ASTM C1557 standard [40]. The sisal fibres were dried in the oven at 30⁰ C for one hour to attain same moisture content for all samples since it affects the strength of fibres [25]. After drying, the fibres were picked at random from the bunch to a total of 40 strands and a gauge length of 140 mm cut using a paper shredder. Figure 3.28 shows specimens for tensile test.



Figure 3.28: Specimens for tensile tests

The specimens were constrained to the butt end of the sisal fibres for sound comparisons. The properties have been shown to vary with length of fibre especially from one section to another. Moreover, the properties of sisal fibre vary from one strand to another [25]. One strand is composed of untwisted single sisal fibre that can be pulled out of fibres obtained from a one sisal leaf. Therefore, to obtain average properties, more than one fibre strands from a given leaf were used. Wood paper and wood glue were used to fix the ends of the fibre strands and allowed to cure for 24 hours. 18 samples of manually extracted fibre, 22 samples of Rea Vipingo fibres and at least 160 samples from 58 leaves extracted and brushed in the laboratory were tested using the Hounsfield Tensometer (Serial No. W 5385) (Figure 3.29). From every leaf, three randomly sampled tensile test specimens were mounted and tested.

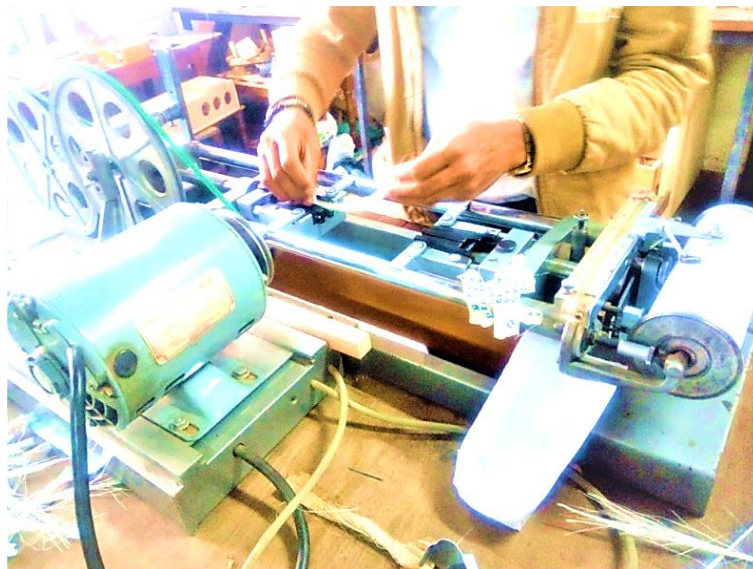
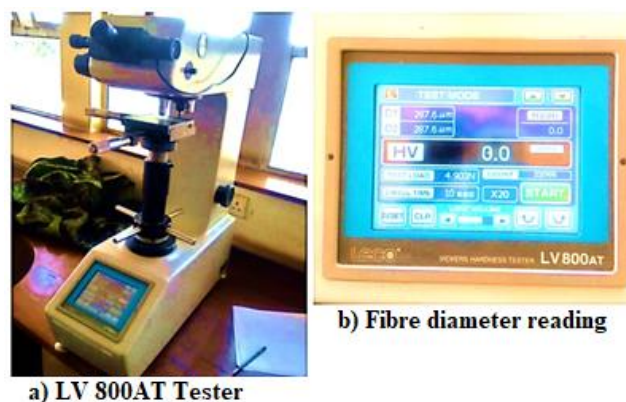


Figure 3.29: Tensile testing using Hounsfield Tensometer

The diameters of the fibre strands were determined using optic microscope and software embedded in the LV 800AT Tester (Figure 3.30).



a) LV 800AT Tester

b) Fibre diameter reading

Figure 3.30: LV 800AT Tester

CHAPTER FOUR: DATA ANALYSIS, DISCUSSION AND RECOMMENDATIONS

4.1. Machine design

4.1.1. Kinematic study of the machine

It was found that the parameter, δ , inversely varied with the quality (q) of decortication. Its value purely depended on three variables; the rate of feeding (c), the number of extraction blades (n) and the angular speed of the drum (ω).

$$\delta = f(\Delta A, c) \dots \dots \dots (4.1)$$

and since $\Delta A = f(n, \omega, c)$, therefore, it was concluded that;

$$\delta = f(n, c, \omega) \dots \dots \dots (4.2)$$

This relation implied that large δ (large swept area) results to poor extraction and brushing and increased energy wastage. On the other hand, too small δ results to too much crushing forces/blade stresses on the leaves and consequently increased amount of tow in the sisal hunk. Since none of the parameters (n,c, ω) that dictate the quality of extraction or brushing depends on the diameter of the drum, the diameter of the extraction drum was selected based on other design constraints like overall size and weight of the required machine and the power requirement. The best values of n, c and ω could only be determined from an experiment.

4.1.2. Decortication resistance

The maximum bending of the cantilever was determined from equation (3.21). The average properties of sisal from Kenya, as reported by Phologolo *et. al.* [21], were applied to determine a rough value for decortication resistance for initial design purpose. These properties include L= 150 cm, B = 12 cm, H = 3 cm and E = 32.9 GN/m².

$$I = \frac{BH^3}{12} \dots \dots \dots (4.3)$$
$$= \frac{0.12 * 0.03^3}{12} = 2.7 * 10^{-7} \text{ m}^4$$

The maximum deflection;

$$Y_{max} = \frac{H}{2} = \frac{0.03}{2} = 0.015 \text{ m}$$

And from equation (3.21);

$$(D_R)_e \approx \frac{32.9 * 10^9 * 2.7 * 10^{-7} * 3 * 0.015}{0.015^3} = 118.44 \text{ N}$$

This was the maximum extraction resistant force that could possibly be offered by a sisal leaf from Kenya on average. The maximum bending force for the mild steel extraction blade was also determined using the same approach (Figure 4.1).

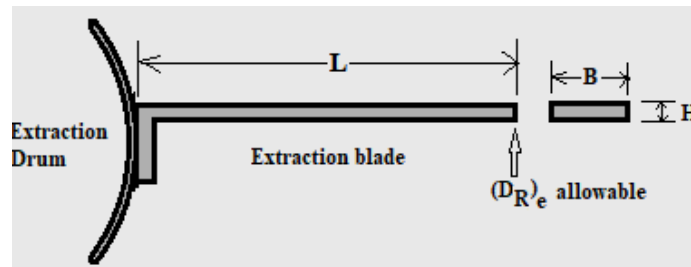


Figure 4.1: Extraction blade modelled as a cantilever

The blades were fabricated from angle bars measuring 38 mm by 38 mm by 3 mm. Therefore, the length of the blade was 38 mm and thickness of 3 mm. The width B of the blade was equivalent to the desired length of the drum, initially fixed at 400 mm. Hence;

$$I = \frac{0.4 * 0.003^3}{12} = 9.0 * 10^{-10} m^4$$

and maximum deflection and allowable blade force were;

$$y_{max} = \frac{H}{2} = \frac{0.003}{2} = 0.0015 m$$

$$(D_R)_e allowable = \frac{210 * 10^9 * 9.0 * 10^{-10} * 3 * 0.0015}{0.038^3}$$

$$= 15499.7 N$$

Given that $(D_R)_e allowable$ was greater than $(D_R)_e$, there was negligible chance that the decortication resistance would pose any danger to the integrity of the structure. Therefore, it was justified that the resistant forces offered by the sisal fibre were negligible compared to strength of mild steel and there was no need for further kinetic analysis.

4.1.3. Design power

The data from an earlier research on characterization of Kenyan sisal was used to approximate the design power. In the research, one sisal leaf had an average mass of 1558 g, total length of 1424.3 mm, wet and dry fibre weight of 156.6 g and 48.7 g respectively [19]. For this machine, the minimum output required was 15 kg/h of dry fibre. Therefore;

$$\text{Leaves per hour} = \frac{\text{Minimum output capacity (kg/hr)}}{\text{Dry weight of fibre from one leaf (kg)}} \dots\dots\dots (4.4)$$

$$= \frac{15 kg}{0.0487 kg} = 308$$

To achieve this, the machine needed to extract one leaf in 11.6 seconds. The time includes 4 seconds of inserting the leaf. This time is within the recommended range for extracting one sisal leaf using a raspador [4, 15]. Therefore, the right feeding speed was one required to decorticate one sisal leaf in 11.6 seconds and highly depends on the skill of the machine operator and gap size (G). In small-scale machines, an engine is the most expensive component that accounts for about 60% of the total cost for gasoline engine or 90% for diesel engines. Therefore, proper selection was required to keep the cost of the machine to a minimum. The design power required to decorticate a sisal leaf was determined using equation (3.20). The recommended optimum speed for good decortication according to Oduori was 1000 rpm [7] and between 1000 to 1300 rpm according to Ahmad *et al.* [19]. It was also found that the idling power in extraction accounts for about 57% of the total power [7]. Therefore, for a drum of 200 mm diameter initially selected;

$$\begin{aligned} P &= (D_R)_e \omega R_O = 148.05 * 100 * 0.1 \\ &= 1480.5 W = 1.4805 kW \end{aligned}$$

If 57% of this is used for idling, then 0.6366 kW is used for extraction. It was assumed that brushing would require the same amount of power as extraction. Therefore, the total power for extraction and brushing simultaneously was approximated as follows;

$$\begin{aligned} P_T &= \text{Idling power} + \text{extraction power} + \text{brushing power} \\ &= 1.4805 + 0.6366 = 2.117 kW \\ &= 2.84 HP \end{aligned}$$

The power required was also approximated using the data obtained by Oduori [7]. The research found that power required to decorticate one sisal leaf was 600 W plus an idling power of 800 W amounting to 1400 W [7]. In the same way, assuming that the brushing unit would require the same power as extraction unit to brush fibres from one sisal leaf, then the total power required would be;

$$\begin{aligned} P_T &= 800 + 600 * 2 \\ &= 2000 W \\ &= 2.68 HP \end{aligned}$$

From the power determined by the two approaches, it was concluded that a 3 HP internal combustion engine or motor was sufficient for the design. One advantage of this machine was that it would save on power since the idling power remains constant irrespective of whether extraction or brushing or both are being done.

4.1.4. Design of the belt drive

Belt drive was preferred to gear drive because of its quietness, flexibility, affordability and suitability for low torque high-speed designs [39]. The useful design data for belt drive was a rated power (P_m) of 3 HP (2.206 kW), a motor/engine speed (N_1) of 1500 rpm, decortication resistance of 148.05 N, a service time ranging from 8 am to 12 pm (10 hours per day) and extraction drum speed (N_2) of 1000 rpm. The following results were obtained during design of the belt drive;

a) Service factor, C_1

From Appendix A-1, for a machine that operates for 10 hours a day in the class of textile machines needs a service factor of 1.4. Hence C_1 for this machine was 1.4.

b) Belt type

$$\begin{aligned} \text{The design power } P_D &= P_M * C_1 \dots\dots\dots (4.5) \\ &= 2.206 * 1.4 \\ &= 3.089 \text{ kW} \end{aligned}$$

With a design power P_D and N_1 of 3.089 kW and 1500 rpm respectively, SPZ belt type (Appendix A-2) equivalent to 3V belt (Appendix A-5) was selected.

c) Speed ratio, G

$$\begin{aligned} G &= \frac{N_1}{N_2} \dots\dots\dots (4.6) \\ &= \frac{1500}{1000} = 1.5 \end{aligned}$$

d) Pulley datum diameter

Appendix A-3 was used to select the small pulley datum diameter. Since there was no preferred diameter in the design, 150 mm was selected for a start.

$$\begin{aligned} d_d &= 150 \text{ mm} \\ D_d &= d_d * G \dots\dots\dots (4.7) \\ &= 150 * 1.5 = 225 \text{ mm} \end{aligned}$$

The closest standard datum diameter for the large pulley diameter selected from Table 2 in Appendix A-3 was 224 mm hence $D_d = 224 \text{ mm}$. A quick check on the effect of the new standard diameter on the speed ratio was conducted.

$$G = \frac{D_p}{d_p} \dots\dots\dots (4.8)$$

where

$$D_p = D_d + 2b_d \dots\dots\dots (4.9)$$

$$d_p = d_d + 2b_d \dots\dots\dots (4.10)$$

b_d (correction factor) was obtained from Table 2a in Appendix A-6 with a 3V belt type (Program 11, equivalent to belt SPZ)

$$\begin{aligned} 2b_d &= -1.4 \\ D_p &= 224 - 1.4 = 223.6 \text{ mm} \\ d_p &= 150 - 1.4 = 148.6 \text{ mm} \\ G &= \frac{223.6}{148.6} = 1.505 \end{aligned}$$

Therefore, the deviation from the desired ratio of 1.5 was negligible.

e) Selected centre distance C_s

The centre distance was given by;

$$\begin{aligned} 0.7(d_p + D_d) \text{ mm} < C_s < 2(d_p + D_d) \dots\dots\dots (4.11) \\ 0.7(150 + 224) \text{ mm} < C_s < 2(150 + 224) \text{ mm} \\ 262 \text{ mm} < C_s < 748 \text{ mm} \end{aligned}$$

One objective of this design was to reduce the size and weight of the machine. This presented a good opportunity to achieve it by minimizing the centre distance. Therefore, C_s was fixed at 500 mm.

f) Belt length L_d (mm)

Belt length was determined using equation (4.12).

$$\begin{aligned} L_d &= 2C_s + 1.57(d_p + D_d) + \frac{(D_d - d_p)^2}{4C_s} \text{ (mm)} \dots\dots\dots (4.12) \\ &= 2 * 500 + 1.57(150 + 224) + \frac{(224 - 150)^2}{4 * 500} \\ &= 1589.9 \text{ mm} \end{aligned}$$

The closest standard datum length from Appendix A-5 was 1587 mm

g) Actual centre distance C_a (mm)

$$C_a = C_s - \frac{L_d(\text{Calculated}) - L_d(\text{Standard})}{2} \dots\dots\dots (4.13)$$

and

$$C_a(\text{Maximum}) = C_a + x \text{ (mm)} \dots\dots\dots (4.14)$$

$$C_a(\text{Minimum}) = C_a - y \text{ (mm)} \dots\dots\dots (4.15)$$

The values of x and y were determined from Appendix A-7 for a 3V belt;

$$\begin{aligned} y &= 21 \text{ mm} \\ x &= 17 \text{ mm} \end{aligned}$$

therefore;

$$C_a = 500 - \frac{1590 - 1587}{2} = 498.5 \text{ mm}$$

$$C_a(\text{Maximum}) = 515.5 \text{ (mm)}$$

$$C_a(\text{Minimum}) = 477.5 \text{ (mm)}$$

h) Belt speed V_b (m/s)

$$\begin{aligned} V_b &= \frac{d_p * N_1}{19100} \text{ (ms}^{-1}\text{)} \dots\dots\dots (4.16) \\ &= \frac{148.6 \text{ mm} * 1500 \text{ rpm}}{19100} \text{ (ms}^{-1}\text{)} \\ &= 11.67 \text{ (ms}^{-1}\text{)} \end{aligned}$$

To check if this speed was within the recommendable belt speed, Appendix A-4 was used; for a 3V belt, the maximum recommended belt speed is 42 m/s. This requirement was therefore met.

i) Deflection frequency f (Hz)

$$f = \frac{a * v * 1000}{L_d} \dots\dots\dots (4.17)$$

where;

$$a = \text{number of pulleys (2)}$$

$$v = \text{belt speed (11.67 m/s)}$$

$$L_d = \text{belt length (1587 mm)}$$

$$f = \frac{2 * 11.67 * 1000}{1587} = 14.71 \text{ Hz}$$

The maximum allowable frequency for 3V belt is 100 Hz; hence, this frequency was acceptable.

j) Power rating per belt P_N (kW)

Using data in Appendix A-9 with;

$$d_d = 150 \text{ mm}, G = 1.5, N_1 = 1500 \text{ rpm and } L_d \cong 1600 \text{ mm}$$

$$\text{For 3V belt; } P_N = 4.69 + 0.20 = 4.89 \text{ kW}$$

k) Belt length correction factor, C_2

From Appendix A-10 for belt length correction factors, for $L_d = 1587 \text{ mm}$ from 3V column, an interpolation was done to find $C_2 = 0.9986$.

l) Arc and angle of contact correction factor C_3

Were determined from Appendix A-11 using the following parameters;

$$\frac{D_d - d_d}{C} = \frac{224 - 150}{498.5} = 0.14845$$

and under wrapped V belts

$$C_3 = 0.99$$

$$\beta = 172^\circ$$

m) *The number of belts required z*

$$z = \frac{P_M * C_1}{P_N * C_2 * C_3} \dots\dots\dots (4.18)$$

$$= \frac{2.206 * 1.4}{4.89 * 0.9986 * 0.99}$$

$$= 0.65 \cong 1 \text{ belt}$$

n) *Belt tension, T_{stat} (N) per belt*

$$T_{stat} = 500 * K_1 * \frac{P_m}{zV} + K_2 * V^2 \left(\frac{N}{\text{belt}} \right) \dots\dots\dots (4.19)$$

K₁ and K₂ the tension factor and centrifugal factor were determined from Table 8 and Table 9 in Appendix A-12. For a new belt, *tension* = 1.3 * T_{stat} to compensate for initial belt tension drop during installation [41]. For machine operating at mean load;

$$\beta = 172^\circ$$

$$K_1 = 1.746$$

$$K_2 = 0.095 \text{ kg/m}$$

hence;

$$T_{stat} = 500 * 1.746 * \frac{2.206}{1 * 11.67} + 0.095 * 11.67^2 \text{ (N/belt)}$$

$$= 180 \text{ N/belt}$$

To check belt tensioning, consider Figure 4.2;

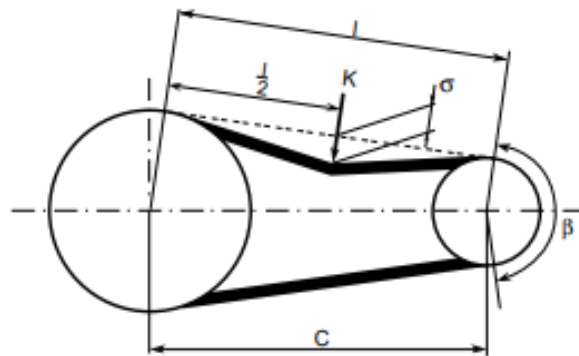


Figure 4.2: Belt tensioning

$$K = 0.06 * T_{stat} \dots\dots\dots (4.20)$$

$$= 0.06 * 180 = 10.8 \text{ N}$$

span length, l

$$l = c \sin \left(\frac{\beta}{2} \right) \text{ (mm)} \dots\dots\dots (4.21)$$

$$= 498.5 \sin \left(\frac{172}{2} \right) \text{ (mm)}$$

$$= 497 \text{ (mm)}$$

$$\begin{aligned} \text{deflection, } \sigma &= \frac{l \cdot 15}{1000} \text{ (mm)} \dots\dots\dots (4.22) \\ &= \frac{497 \cdot 15}{1000} \text{ (mm)} = 7.5 \text{ mm} \end{aligned}$$

o) Shaft load, (Static and dynamic)

$$\begin{aligned} S_{stat} &= 2 \cdot z \cdot T_{stat} \cdot \sin\left(\frac{\beta}{2}\right) \text{ (N)} \dots\dots\dots (4.23) \\ &= 2 \cdot 1 \cdot 180 \cdot \sin\left(\frac{172}{2}\right) \text{ (N)} \\ &= 359 \text{ N} \end{aligned}$$

$$\begin{aligned} S_{dyn} &= 707 \cdot \frac{P_m}{v} \cdot \sqrt{K_1^2 + 1 - (K_1^2 - 1)\cos\beta} \text{ (N)} \dots\dots\dots (4.24) \\ &= 707 \cdot \frac{2.206}{11.67} \cdot \sqrt{1.746^2 + 1 - (1.746^2 - 1)\cos 172} \text{ (N)} \\ &= 334 \text{ N} \end{aligned}$$

S_{stat} and S_{dyn} were very necessary in dimensioning the bearings and shaft.

4.1.5. Shaft design

A larger drum could imply a bigger machine that could equally increase the weight and power consumption of the machine. From the analysis, it was seen that the diameter of the drum was not a variable in the quality of decortication. Therefore, for convenience, a pipe of nominal diameter (D_N) 250 mm, internal diameter (D_I) 266.3 mm, outer diameter (D_O) 273.1 mm, weight 22.63 kg/m and length (D_L) 420 mm was selected. The frame was fabricated from 50 by 50 by 3 mm mild steel angle-bars. A shaft length (S_L) of 560 mm was selected as well. This was just enough to cater for both units; extraction unit (150 mm) and brushing unit (250 mm). For easy analysis, the drum shaft assembly was modelled as a free body diagram (FBD) (Figure 4.3);

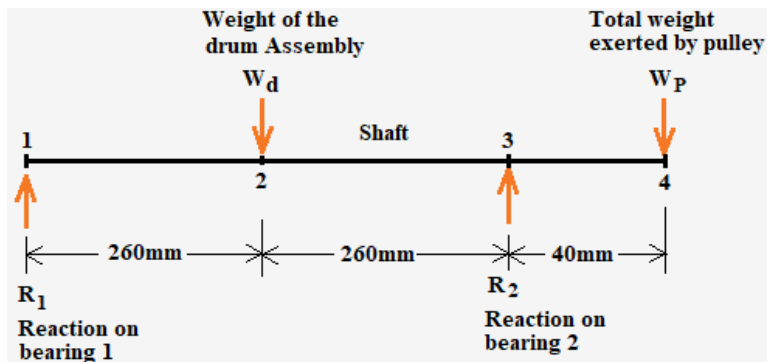


Figure 4.3: FBD of the drum shaft assembly

▪ **Weight of drum assembly**

W_d comprised of the weight of the drum assembly (extraction blades, drum and two side discs)

Weight of the drum = 22.63 kg/m * 0.42 m = 9.52 kg

The extraction blades were fabricated from angle bars measuring 38 mm by 38 mm by 3 mm with mass distributed at 1.74 kg/m. There was no preferred number of blades according to the kinematic analysis. Since the machine weight was to be minimized, the number of blades initially chosen was 14. The weight of extraction blades was estimated as;

$$= 1.74 \text{ kg/m} * 0.42 \text{ m} * 14 = 10.23 \text{ kg}$$

The side discs were to be fabricated from mild steel. With an internal diameter of 263.3 mm, thickness of 12.70 mm and using the density of mild steel of 7860 kg/m³, the weight of side discs would be;

$$= 7860 * \frac{\pi}{4} * 0.2633^2 * 0.0127 * 2 = 10.87 \text{ kg and therefore;}$$

$$W_d = 10.87 + 10.2312 + 9.5246 = 30.63 \text{ kg or}$$

$$= 30.63 * 9.81 = 300 \text{ N taking g as 9.81 N/kg}$$

The weight of the drum assembly was distributed along the length of the drum, but for simplification, it was assumed to be a point load acting at the centre of the drum.

▪ **Weight exerted by the pulley**

The weight of the pulley was approximated from the standard pulley weights. For a pulley of D_p = 223.6 mm and D_d = 224 mm the weight was 8.5 kg (W_p = 83.4 N). Therefore, the total weight was given by;

$$W_T = W_p + T_1 + T_2 \dots\dots\dots (4.25)$$

$$T_1 + T_2 = \text{dynamic or static shaft load (greater of the two)}$$

From the previous calculations, it was found that the shaft would be subjected to a static load of 359 N and a dynamic load of 334 N due to belt drive tensions. Picking the greater load for sizing the shaft;

$$W_T = 83.4 + 359 = 442.4 \text{ N}$$

The shaft was then modelled as a simply supported beam subjected to the following forces as seen in Figure 4.4;

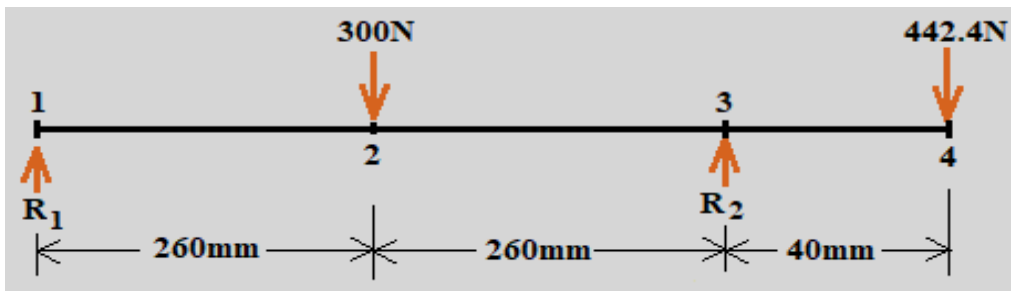


Figure 4.4: Loads acting on the shaft

Taking the equilibrium of forces on the vertical plane;

$$\sum F_v = 0$$

$$R_1 + R_2 = 300 + 442.4 = 742.4 \text{ N} \dots\dots\dots (4.26)$$

Summing moments about point 1;

$$300 * 0.26 + 442.4 * 0.56 - R_2 * 0.52 = 0$$

$$R_2 = 626.4 \text{ N}$$

$$R_1 = 116 \text{ N}$$

From Figure 4.5, the maximum bending moment would occur at the middle of the drum.

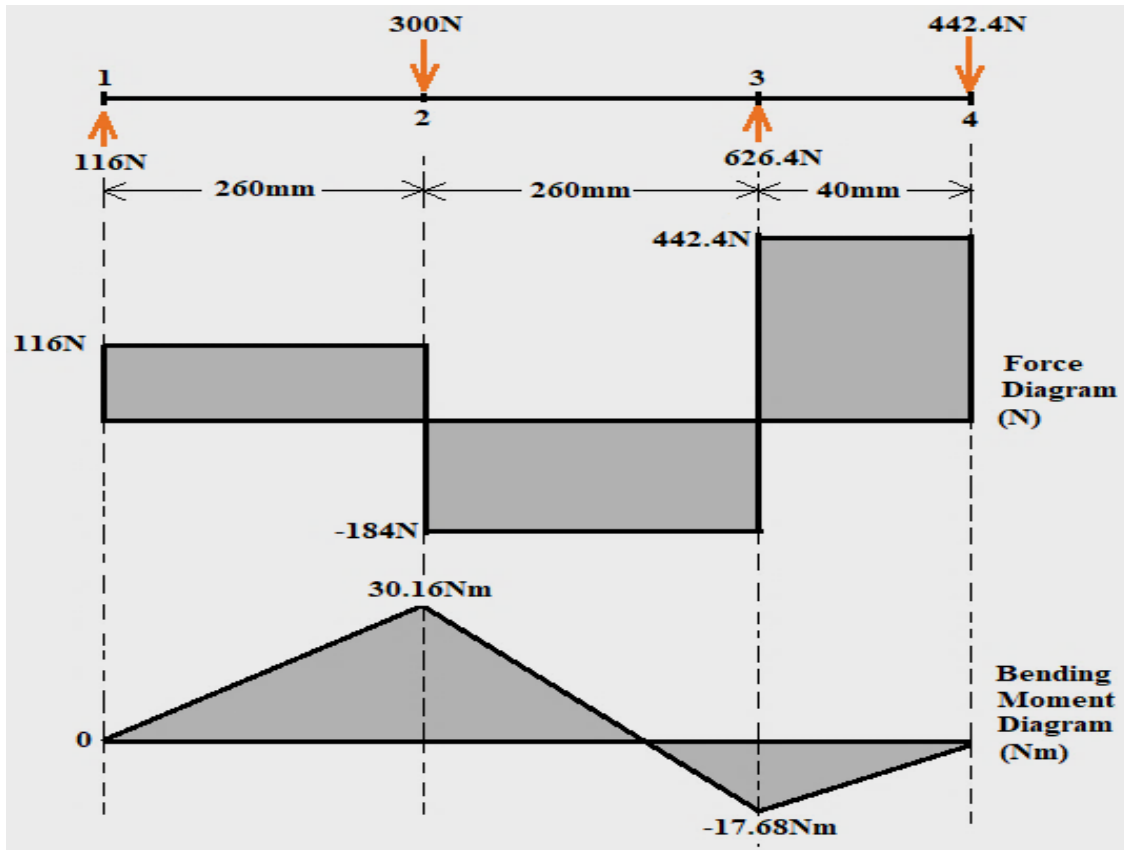


Figure 4.5: Force and bending moment diagram

The maximum bending moment, $M_{\max} = 30.16 \text{ Nm}$. The torque was determined from equation (4.27).

$$P = \frac{2\pi NT}{60} \dots\dots\dots (4.27)$$

$$T = \frac{P * 60}{2\pi N} = \frac{60 * 2206}{2 * \pi * 1000}$$

$$= 21.07 \text{ Nm}$$

The shaft was designed based on the two theories; i) maximum shear stress theory and ii) maximum normal stress theory.

i. Maximum shear stress theory

For a rotating shaft where the loads are gradually applied from Table 4.1;

$$K_m = 1.5$$

$$K_t = 1.0$$

Table 4.1: Recommended values for K_m and K_t

<i>Nature of load</i>	K_m	K_t
Stationary shafts		
a) Gradually applied load	1	1
b) Suddenly applied load	1.5 to 2.0	1.5 to 2.0
Rotating shafts		
a) Gradually applied or steady load	1.5	1
b) Suddenly applied load with minor shocks only	1.5 to 2.0	1.5 to 2.0
c) Suddenly applied load with heavy shocks	2.0 to 3.0	1.5 to 3.0

For most common shaft materials, the maximum allowable shear stress and normal stress are;

$$\tau_{max} = 56 \text{ Mpa}$$

$$\sigma_{max} = 115 \text{ Mpa}$$

and from the calculations;

$$M_{max} = 30.16 \text{ Nm}$$

$$T = 21.07 \text{ Nm}$$

Hence, from equation (3.22);

$$\frac{\pi}{16} * 56 * 10^6 * d^3 = \sqrt{(1.5 * 30.16)^2 + (1 * 21.07)^2}$$

$$d = 16.6 \text{ mm}$$

ii. Maximum normal stress theory

For the shaft not to fail, from equation (3.23);

$$\frac{\pi}{32} * 115 * 10^6 * d^3 = \frac{1}{2} \left\{ 1.5 * 30.16 + \sqrt{(1.5 * 30.16)^2 + (1 * 21.07)^2} \right\}$$

$$d = 16.15 \text{ mm}$$

From the two criteria, the shaft diameter required was 16.6 mm (picking the larger of the two). However, from the ISO standard shafts, the minimum shaft diameter available was 25 mm but for optimization of the design specifications, 20 mm shaft is recommended.

4.1.6. Bearing selection

Bearing unit was selected as dictated by the operation conditions highlighted in Table 4.2;

Table 4.2: Operational conditions of the bearing

S/No.	Condition	Value
1	The bearing radial forces (N)	116 and 626.4
2	Speed of shaft (RPM)	1000
3	Torque (Nm)	21.07
4	Operational temperature ($^{\circ}\text{C}$)	15 – 30
5	Dynamic shaft load (N)	334
6	Static shaft load (N)	359

With these conditions, UCP205 pillow block (Figure 4.6) of bore diameter 25 mm was selected. They are the most common units in rigid housings of simple designs. They have dynamic and static load limits of 14 kN and 7.85 kN respectively. These were against dynamic and static loads of 334 N and 359 N respectively required in the design.

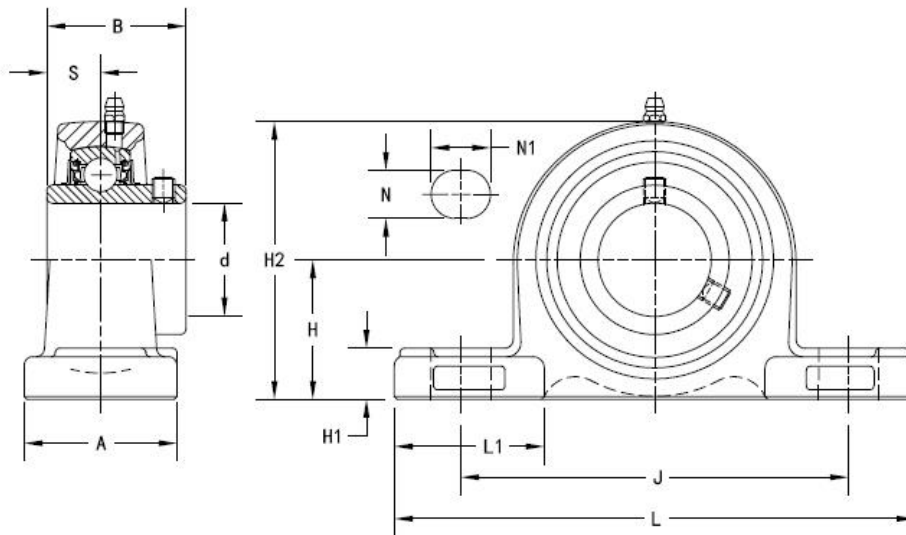


Figure 4.6: Pillow block

The UCP205 pillow blocks were suitable for all bearing units. The bearings were not subjected to any axial loads and thrust forces. Therefore, cast iron pillow blocks and steel ball bearings (25 mm by 47 mm by 12 mm) were appropriate for the design taking into consideration the cost. Dimensions of the selected pillow block bearing unit are as detailed in Table 4.3.

Table 4.3: Pillow block dimensions

Dimension	Value	Dimension	Value
Shaft size d (mm)	25	Bolt hole length N1 (mm)	18
Weight kg	0.8	Total height H2 (mm)	70
Centre height H (mm)	36.5	Dimension L1 (mm)	38
Total length L (mm)	140	Inner ring width B (mm)	34.1
Housing width A	38	Centre of bearing from end S (mm)	14.3
Bolt hole spacing J (mm)	105	Static load rating N	7,850
Bolt hole size N (mm)	13	Dynamic load rating N	14,000

4.1.7. Design of frame, belt and pulley cover

The columns and beams were sized to a height of 598.5 mm and 550 mm respectively. Length of the functional unit was 520 mm (drum housing) and the overall length L_0 was 1400 mm. The towing system contributed a length of 840 mm (Figure 4.7).

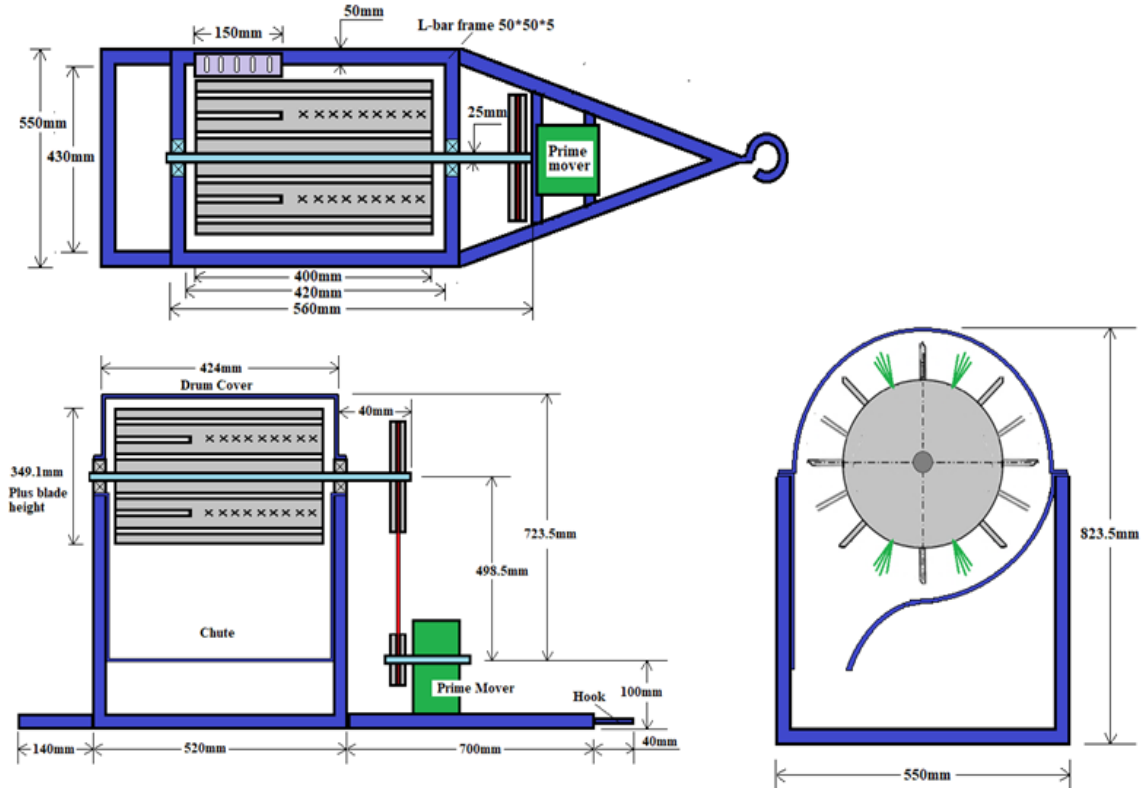


Figure 4.7: The views of the proposed machine showing the machine frame

Since the cover was not subjected to any other forces apart from its own weight, the material for fabrication was hot rolled iron sheet 2 mm thick and iron mesh to reduce its weight. The diameter of the cover was slightly larger than the diameter of the larger pulley (that is 224 mm). A diameter of 300 mm left a clearance of 38 mm from the pulley. A wire mesh of size 19 by 19 mm (3/4”) and wire diameter of 1.63 mm was appropriate for the top part of the cover (Figure 4.8).

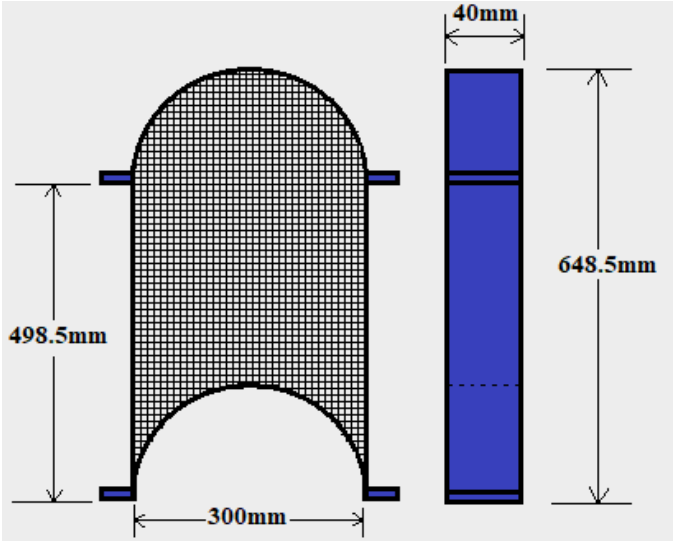


Figure 4.8: Drum cover

4.1.8. Computer Aided Design drawings

Figure 4.9 and Figure 4.10 show an isometric view of the assembled machine drawn using the software and the fabricated machine respectively. The detailed design drawings are presented in Appendix C: Machine design drawings.

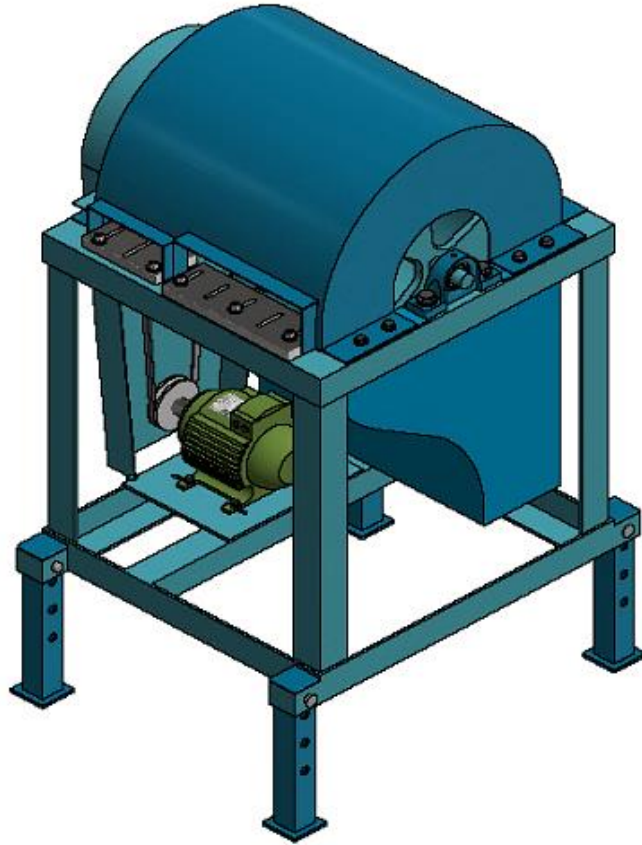


Figure 4.9: CAD drawing of assembled machine



Figure 4.10: Assembled machine

4.2. Obtainable speeds with taper pulleys

Using the tapered pulleys, it was possible to vary the speeds using a 2880 rpm fixed speed motor as shown in Figure 4.11.

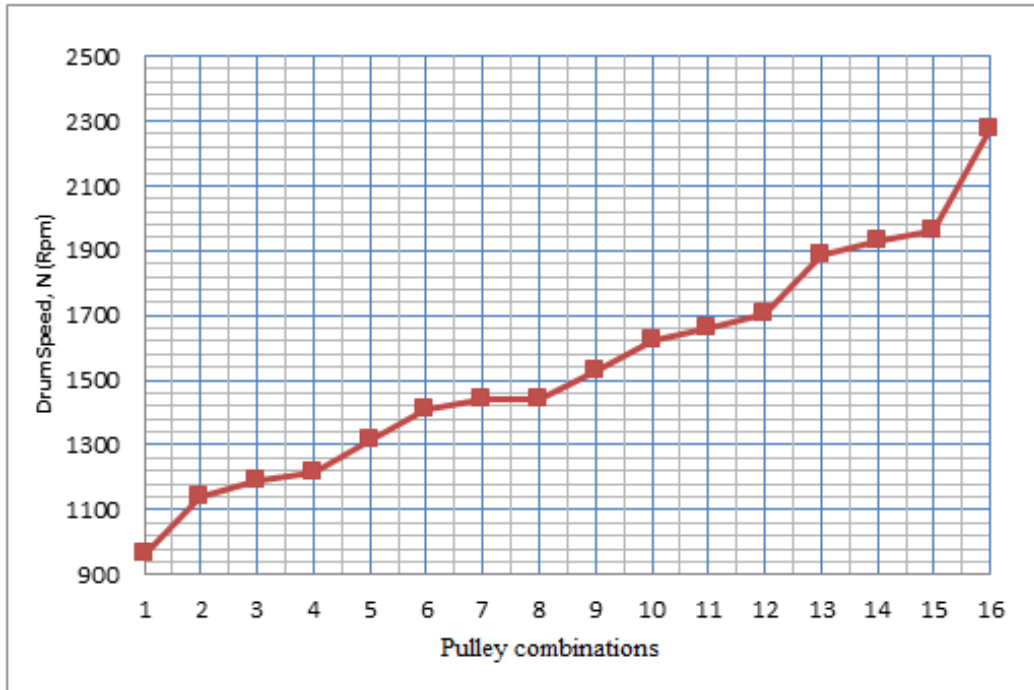


Figure 4.11: Drum speeds from speed ratio

The speeds were determined using equation (4.28);

$$\begin{aligned} \text{Speed ratio, } R &= \frac{d}{D} \dots\dots\dots (4.28) \\ &= \frac{5.5}{16.4} = 0.3354 \end{aligned}$$

$$\begin{aligned} \text{Drum speed, } N &= R * \text{Motor speed} \dots\dots\dots (4.29) \\ &= 0.3354 * 2880 = 965.9 \text{ rpm} \end{aligned}$$

The various speeds were equally determined using this approach. However, during testing, the guard needed to be removed before the pulley diameters could be exchanged. This was cumbersome. Since extensive tests were required for this study, an internal combustion engine was also used. Moreover, internal combustion engine was very suitable for field tests, typical conditions for small-scale farmers. With the engine, it was easy to smoothly vary drum speeds from 700 - 2000 rpm without disassembling the machine. The motor was only necessary for determination of power consumption.

4.3. Power consumption

Figure 4.12 shows the overall power consumption with speed at 12 blades and at different gap sizes as detailed in Table 4.4.

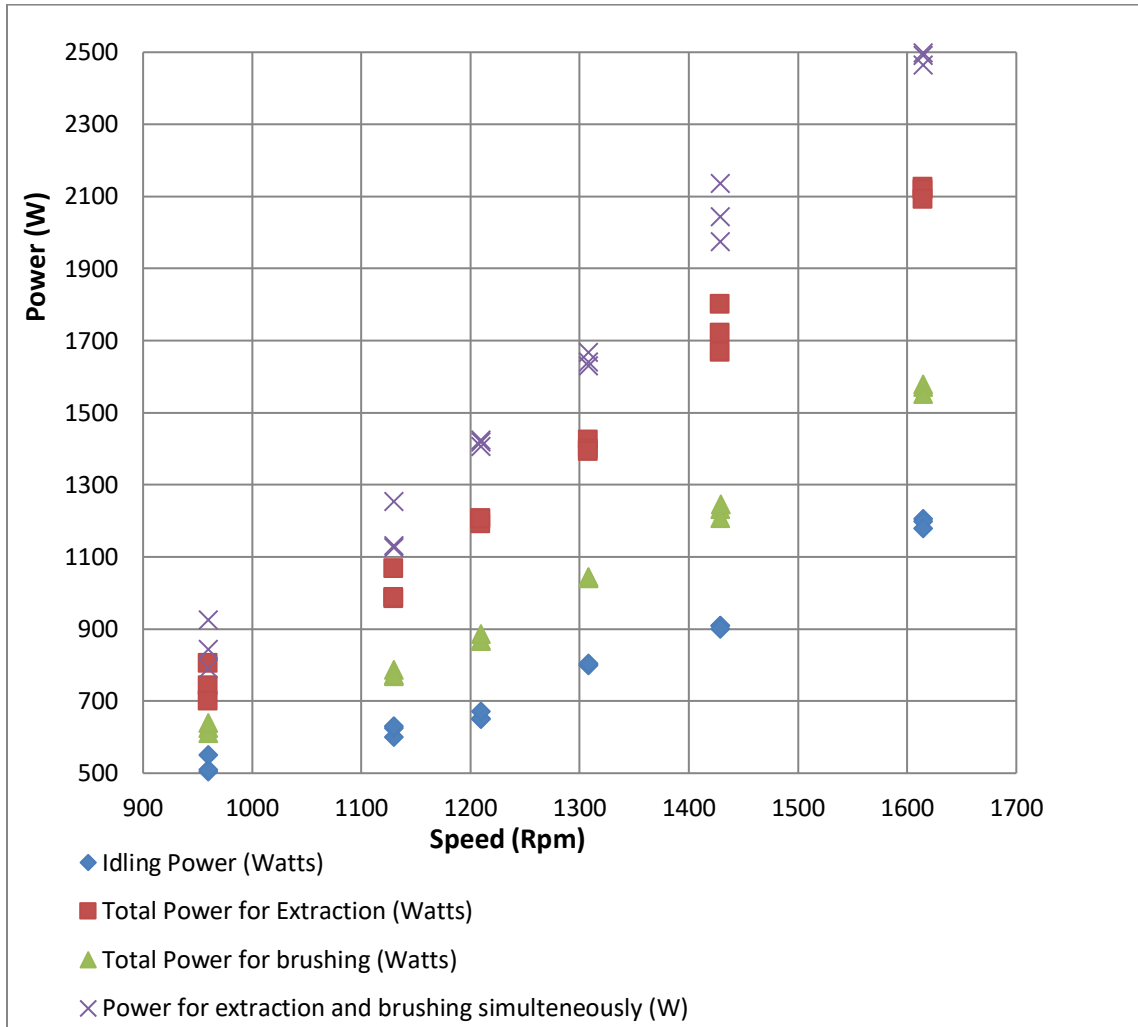


Figure 4.12: Variation of power consumption with gap size and speed

The idling power (IP) increased with speed. Since IP is undesirable, it should be as low as possible to avoid energy wastage. The extraction power (EP), brushing power (BP) and total power (TP) for extracting and brushing also increased with speed. The average EP for one leaf was 1.368 kW compared to 1.7 - 4.8 kW reported by Ahmad *et al.* [19]. Therefore, on average, this machine had a minimal power consumption.

Table 4.5: Analysis of power consumption

Drum Speed, N (rpm)	Gap Size, G (mm)	Number of blades, n	Idling Power (W)	Total Power for Extraction (W)	Total Power for brushing (W)	Power for extraction and brushing simultaneously (W)	% increase in power due to brushing unit
960	1	12	505	805	625	925	14.9
960.1	2	12	510	743	610	843	13.5
960	3	12	550	700	640	790	12.9
1130	1	12	600	1067	786.8	1253.8	17.5
1130	2	12	625	983	768.2	1126.2	14.6
1130	3	12	630	988	773.2	1131.2	14.5
1210	1	12	650	1205.5	868.6	1424.1	18.1
1210	2	12	651	1191	866.9	1406.9	18.1
1210	3	12	672	1205	885.2	1418.2	17.7
1308	1	12	799	1424.6	1042.4	1668	17.1
1308	2	12	800	1400	1040	1640	17.1
1308	3	12	805	1391.3	1043.7	1630	17.2
1429	1	12	910	1800.1	1245.9	2136	18.7
1429	2	12	910	1720	1232.8	2042.8	18.8
1429	3	12	900	1667	1206.8	1973.8	18.4
1615	1	12	1205	2125	1578.2	2498.2	17.6
1615	2	12	1198	2118	1571.2	2491.2	17.6
1615	3	12	1179.5	2091.7	1551.6	2463.8	17.8
Average			783.3	1368.1	1018.7	1603.5	16.8

The average increase in power consumed due to incorporation of a brushing unit was only 16.8%. This was a small increment compared to investing in a separate brushing machine. Utilizing an extracting unit alone, the same idling power will still be consumed. Hence it was economical and prudent to incorporate both units on the same machine. It was also found that the IP, EP and BP slightly reduce with increase in gap size as shown in Figure 4.13 and Figure 4.14.

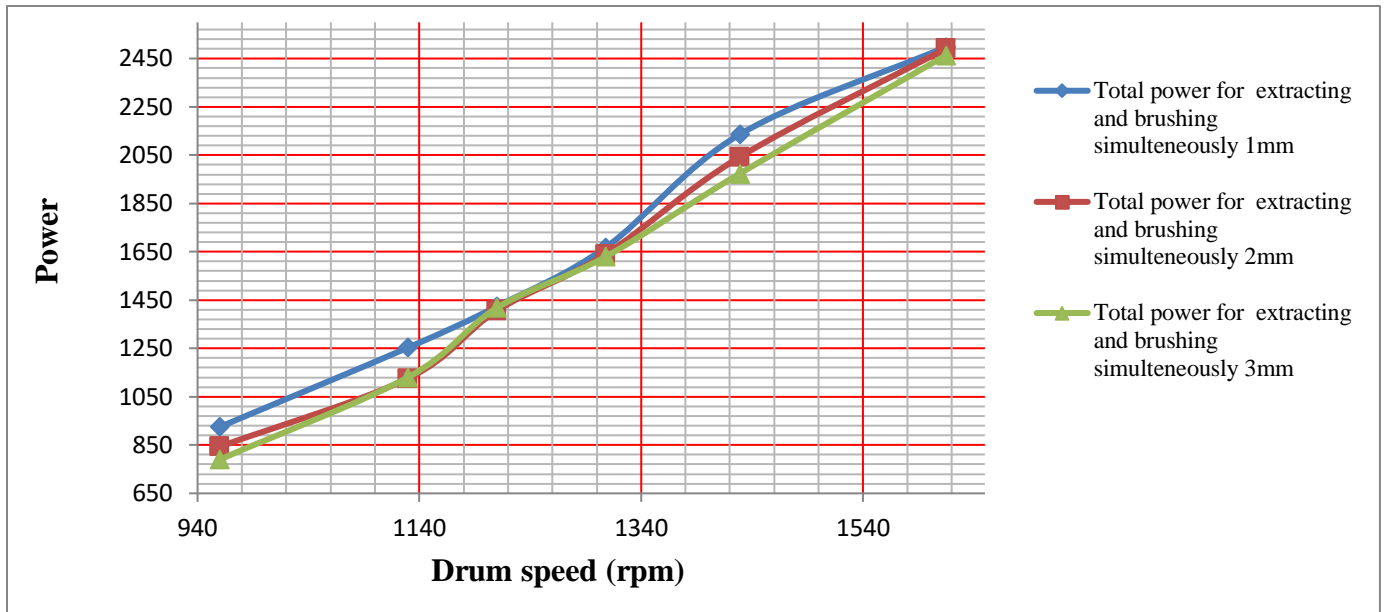


Figure 4.13: Power variation with gap sizes

This was most likely due to reduction in extraction and brushing resistances. Increase in gap size reduced the resistance force and hence the power consumed. The machine must overcome the resistance for either extraction or brushing to occur. It is interesting to note that at higher speeds, the curves tend to merge. However, from this study, it was not possible to conclude on this trend.

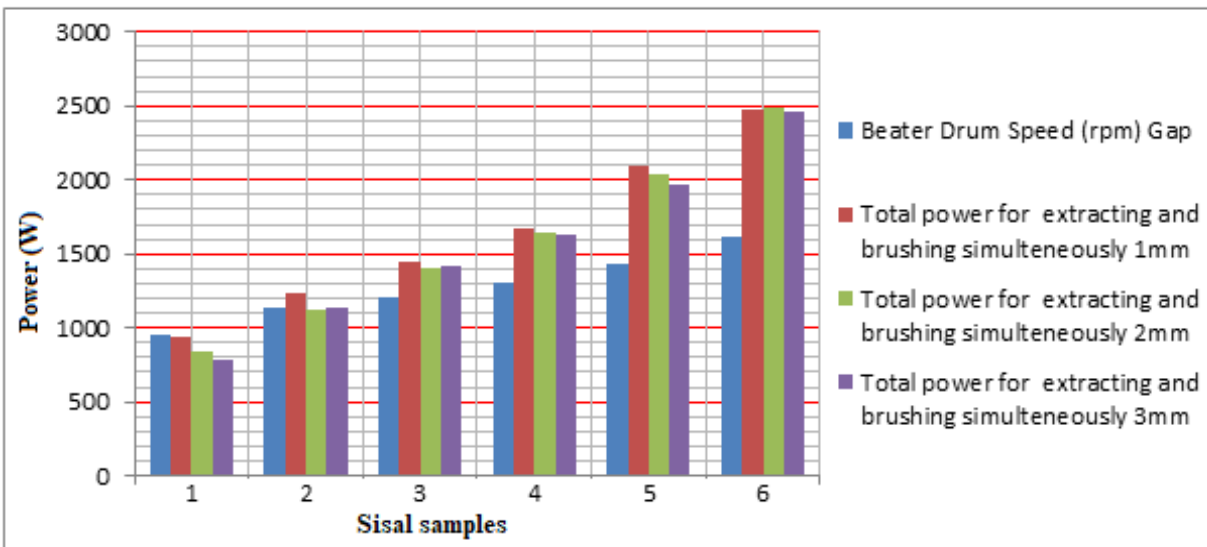


Figure 4.14: Bar chart for power variations

The correlation coefficients between the drum speed and the power consumed during extraction and brushing were determined (see Figure 4.15, Figure 4.16 and Figure 4.17).

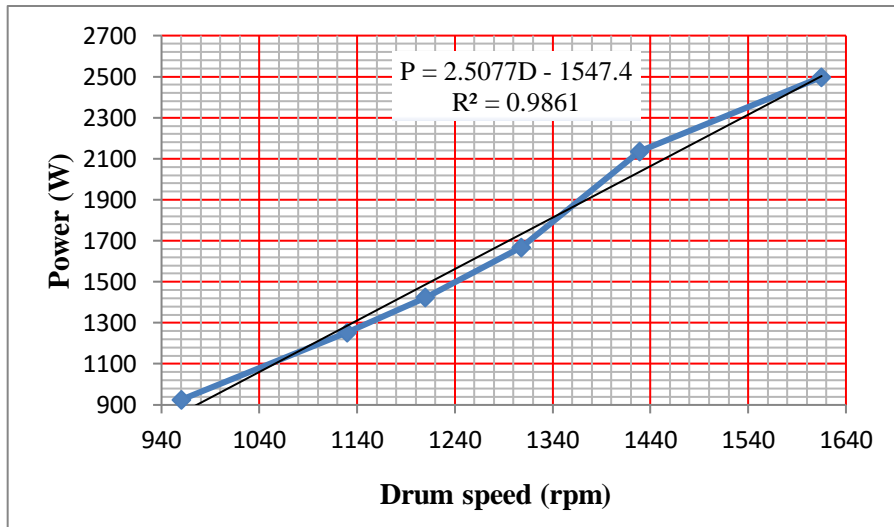


Figure 4.15: Variation of total power with drum speed at 1 mm gap size

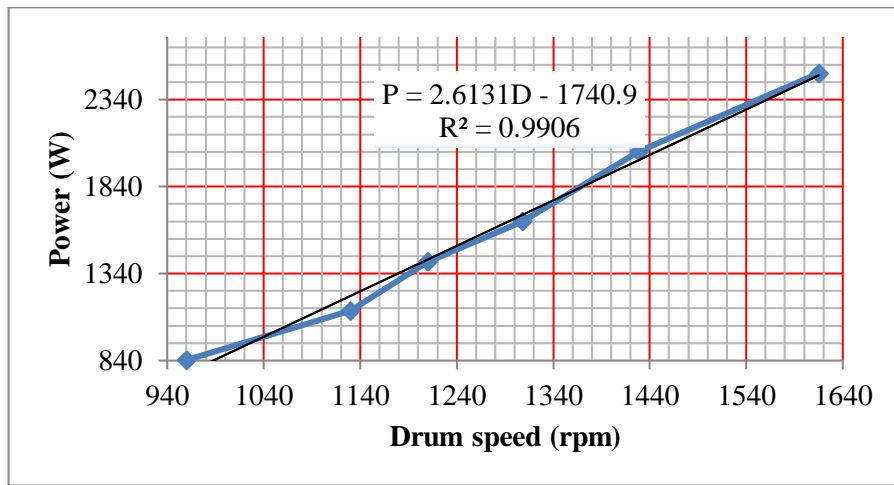


Figure 4.16: Variation of total power with drum speed at 2 mm gap size

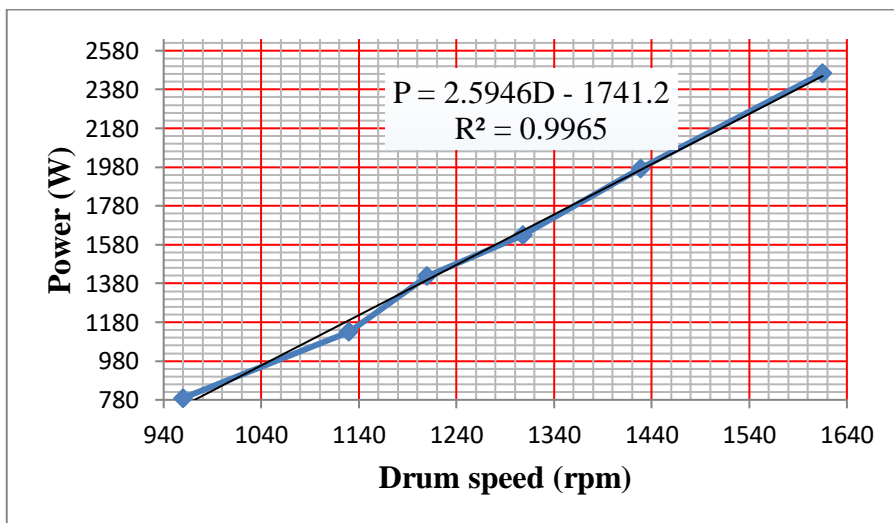


Figure 4.17: Variation of total power with drum speed at 3 mm gap size

At 1 mm gap size, the correlation coefficient was determined from the equation;

$$P = 2.5077D - 1547.4 \dots\dots\dots (4.30)$$

$$R^2 = 0.9861$$

$$Corr = \sqrt{R^2} = \sqrt{0.9861} = 0.993$$

At 2 mm gap size, the correlation coefficient was;

$$P = 2.6131D - 1740.9 \dots\dots\dots (4.31)$$

$$R^2 = 0.9906$$

$$Corr = \sqrt{R^2} = \sqrt{0.9906} = 0.995$$

At 3 mm gap size, the correlation coefficient was;

$$P = 2.5946D - 1741.2 \dots\dots\dots (4.32)$$

$$R^2 = 0.9965$$

$$Corr = \sqrt{R^2} = \sqrt{0.9965} = 0.998$$

The correlation coefficients obtained at 1 mm, 2 mm and 3 mm were 0.993, 0.995 and 0.998 respectively indicated that the power consumption at all gap sizes highly correlated to the drum speed. It was therefore necessary to maintain the optimized design speed as low as possible to minimize power consumptions.

4.4. Properties of processed sisal fibres

The important properties of sisal fibre were determined using the following equations as per the ASTM C1557 standard [40].

$$\text{Fracture strength, } \sigma_u = \frac{\text{breaking load}}{\text{cross section area}} \dots\dots\dots (4.33)$$

$$\text{Fracture strain, } \varepsilon = \frac{\text{Deformation}}{\text{Gauge length}} \dots\dots\dots (4.34)$$

$$\text{Modulus of elasticity, } E = \frac{\sigma(\varepsilon_2) - \sigma(\varepsilon_1)}{\varepsilon_2 - \varepsilon_1} \dots\dots\dots (4.35)$$

$$\text{Cross section area, } A = \frac{\pi d^2}{4} \dots\dots\dots (4.36)$$

The deformation from the Hounsfield Tensometer is given by;

$$\text{Deformation} = \frac{\text{measured elongation}}{8} \dots\dots\dots (4.37)$$

It was divided by 8 because of a magnification of x8 used. Taking sample one for instance, the maximum tensile force and elongation at fracture were 300 N and 10.7 cm respectively for 40 strands. Average diameter for manually extracted fibre strand was 275.65 μm and the gauge length was 140 mm. Therefore;

$$A = \frac{\pi(275.65*10^{-6})^2}{4} = 5.968*10^{-8} m^2$$

$$Deformation = \frac{10.7cm}{8} = 1.3375cm = 0.013375 m$$

$$\varepsilon = \frac{0.013375m}{0.14m} = 0.0955$$

$$\sigma_u = \frac{300N}{5.968*10^{-8}m^2*40} = 125.67 MPa$$

Young's Modulus of elasticity was determined by finding the gradient of the stress-strain curve within the elastic limit. The fibre being brittle, its fracture strength (σ_u) was equivalent to the maximum fracture stress (σ_{max}).

$$E = \frac{(125.67 - 0) MPa}{(0.0955 - 0)*1000} = 1.316 GPa$$

4.4.1. Properties of manually extracted sisal fibres

The mechanical properties of the sisal fibre as obtained by hammer and anvil method was analysed and presented in Table 4.6. The length ratio, or length reduction ratio, represents the ratio of fibre length to the leaf length.

Table 4.6: Analysed data for manually extracted sisal fibre

Length ratio	Fracture strength (MPa)	Fracture strain ε	Young's Modulus (GPa)	Fibre grade
0.8597	125.6263	0.0955	1.3150	UHDS
0.8326	125.6263	0.1009	1.2451	UHDS
0.8727	121.4388	0.0964	1.2594	UHDS
0.8869	127.7201	0.0946	1.3495	UHDS
0.8597	115.1575	0.0955	1.2054	UHDS
0.8688	102.5948	0.0830	1.2356	UHDS
0.8778	163.3142	0.1000	1.6331	UHDS
0.8416	134.0014	0.0804	1.6676	UHDS
0.8507	188.4395	0.0839	2.2452	UHDS
0.8416	115.1575	0.0893	1.2898	UHDS
0.8733	140.2827	0.0946	1.4822	UHDS
0.8416	144.4703	0.0946	1.5265	UHDS
0.8727	138.1889	0.0536	2.5795	UHDS
0.8545	180.0644	0.0759	2.3726	UHDS
0.8727	144.4703	0.0750	1.9263	UHDS
0.8545	125.6263	0.0982	1.2791	UHDS
0.8909	129.3951	0.0982	1.3175	UHDS
0.8727	138.1889	0.0920	1.5026	UHDS

The mean values for the sisal fibres obtained using the manual method are summarized in Table 4.7.

Table 4.7: Mean values for hammer and anvil method

Iten	Average
Leaf length (mm)	1103.1
Leaf mass (g)	556.84
Bud thickness (mm)	27.8
Tip thickness (mm)	2.7
Largest width (mm)	98.0
Wet weight (g)	35.86
Dry weight (g)	20.14
Average fibre length (mm)	951.4
Fracture strength (MPa)	136.65
Fracture strain ϵ	0.09
Length ratio	0.873
Young's Modulus (GPa)	1.58

$$\text{The average wet fibre content per sisal leaf} = \frac{35.86}{556.84} \times 100\% = 6.44\%$$

$$\text{The average dry fibre content per sisal leaf} = \frac{20.14}{556.84} \times 100\% = 3.62\%$$

Manually extracted sisal fibre had an average fracture strength, fracture strain and modulus of elasticity of 136.65 MPa, 0.09 and 1.58 GPa respectively. The fibre content as a percentage of the fresh sisal leaf was 6.44% when wet and 3.62% when dry. The average fibre length was 951.4 mm with a length reduction ratio of 0.87. Being hand decorticated, irrespective of these properties, the final sisal grade was Unwashed Hand Decorticated Sisal (UHDS) as stipulated by the London Sisal Association [22]. The fibre was unbrushed and unwashed and hence the final fibre colour was a mixture of white and brown. For this reason, small-scale farmers can only sell their fibres at relatively low prices.

4.4.2. Rea Vipingo

Sisal fibre from Rea Vipingo gave the following properties Table 4.8.

Table 4.8: Properties of sisal from Rea Vipingo

Mean fibre length (cm)	Weight (g)	Fracture strength (MPa)	Fracture strain ϵ	Young's Modulus (GPa)	Fibre grade
95	24	64.1791	0.0464	1.3823	UG
92	20	78.3202	0.0455	1.7200	UG
96	21	59.8279	0.0554	1.0808	UG
98	22	95.1808	0.0830	1.1463	UG
95	19	87.0225	0.0714	1.2183	UG
96	20	89.1980	0.0661	1.3500	UG
97	22	72.8813	0.0455	1.6005	UG
93	18	76.1446	0.0536	1.4214	UG
94	19	65.2668	0.0357	1.8275	UG
93	23	46.2307	0.0375	1.2328	UG
95	23	97.9003	0.0750	1.3053	UG
92	20	100.6197	0.0813	1.2384	UG
95	21	95.1808	0.0830	1.1463	UG
98	21.5	116.9364	0.0938	1.2473	UG
95	19	70.7057	0.0848	0.8336	UG
96	20.1	119.6559	0.0946	1.2643	UG
96.5	22	135.9726	0.1161	1.1715	UG
93	18.5	101.5262	0.0911	1.1148	UG
96	23	90.6484	0.0821	1.1035	UG
94	20	97.9003	0.0393	2.4920	UG
98	21	70.7057	0.0402	1.7598	UG
96	22	87.0225	0.0491	1.7721	UG
Average	95.16	20.87	87.23	0.07	1.38

The average properties obtained were 87.23 MPa fracture strength, 0.07 fracture strain, 1.38 GPa elastic modulus, 20.87g dry fibre weight and 951.6 mm fibre length. Rea Vipingo represented estate sisal that has been crushed, washed and brushed using automatic decorticators. The essence of testing Rea Vipingo was to compare and determine whether the fibre obtained using this technology meets the international market standards like Rea Vipingo fibre. The Rea Vipingo fibre was Under Grade (UG), the most commonly exported sisal fibre grade from Kenya [5].

4.4.3. Extracted sisal fibre

Table 4.9 detailed the effects of speed, gap size and number of blades on the quality of fibre extracted using the machine. Due to reported great variations in properties of sisal fibres, a large sample of specimens was tested and analysed.

Table 4.9: The properties of sisal fibre extracted using the machine

Speed (RPM)	Gap size (mm)	Number of blades	Length ratio	Fracture strength (MPa)	Fracture strain ϵ	Young's Modulus (GPa)	Fibre grade
900	1	12	0.650	111.967	0.085	1.313	UHDS
900	1	12	0.631	128.253	0.107	1.197	UHDS
900	1.5	12	0.897	150.646	0.088	1.716	UHDS
900	1.5	12	0.833	94.324	0.090	1.050	UHDS
900	2	12	0.939	122.417	0.083	1.474	UHDS
900	2	12	0.899	130.289	0.089	1.459	UHDS
900	2.5	12	0.932	147.253	0.060	2.460	UHDS
900	2.5	12	0.948	182.540	0.086	2.130	UHDS
1092	2.5	12	0.889	119.295	0.074	1.607	UHDS
1192	4.5	12	0.916	79.395	0.064	1.241	UHDS
1200	1	12	0.889	86.452	0.094	0.921	UHDS
1200	1.5	12	0.885	100.974	0.079	1.275	UHDS
1200	2	12	0.866	95.952	0.060	1.612	UHDS
1200	2.5	12	0.880	109.931	0.076	1.437	UHDS
1325	2.5	12	0.963	102.059	0.077	1.327	UHDS
1325	3	12	0.918	90.252	0.068	1.336	UHDS
1400	2.5	12	0.895	99.642	0.080	1.242	UHDS
1400	3	12	0.904	131.646	0.058	2.280	UHDS
900	1	6	0.974	123.163	0.093	1.326	UHDS
900	1	6	0.957	125.199	0.074	1.689	UHDS
900	1.5	6	0.886	89.573	0.065	1.384	UHDS
900	1.5	6	0.973	143.521	0.092	1.553	UHDS
1135	1	6	0.800	149.628	0.104	1.438	UHDS
1135	1	6	0.905	131.306	0.078	1.681	UHDS
1135	1.5	6	0.815	109.931	0.096	1.147	UHDS
1135	1.5	6	0.828	141.825	0.094	1.508	UHDS
1200	1	6	0.853	121.467	0.087	1.399	UHDS
1200	1	6	0.821	124.860	0.095	1.319	UHDS
1200	1.5	6	0.778	125.240	0.065	1.930	UHDS
1200	1.5	6	0.780	127.770	0.088	1.455	UHDS
1250	1	6	0.794	124.181	0.087	1.429	UHDS
1400	2	6	0.893	119.499	0.079	1.504	UHDS
1400	2	6	0.925	138.432	0.088	1.582	UHDS
1400	2	6	0.979	122.146	0.090	1.354	UHDS
1400	2.5	6	0.990	118.074	0.080	1.478	UHDS
1400	2.5	6	0.952	121.942	0.079	1.539	UHDS
900	1	3	0.991	116.038	0.109	1.067	UHDS
900	1	3	0.991	117.056	0.096	1.219	UHDS
900	1.5	3	0.986	110.949	0.113	0.986	UHDS
900	1.5	3	0.986	124.181	0.083	1.504	UHDS
900	2	3	0.972	139.449	0.096	1.457	UHDS
900	2.5	3	0.977	193.397	0.091	2.126	UHDS

1200	1	3	0.965	133.342	0.096	1.389	UHDS
1200	1	3	0.945	133.342	0.084	1.589	UHDS
1200	1.5	3	0.981	132.324	0.073	1.802	UHDS
1200	1.5	3	0.963	122.553	0.078	1.581	UHDS
1200	2	3	0.975	130.390	0.083	1.579	UHDS
1200	2.5	3	0.968	129.271	0.083	1.548	UHDS
1400	1	3	0.964	117.056	0.093	1.264	UHDS
1400	1	3	0.945	124.181	0.100	1.242	UHDS
1400	1.5	3	0.950	130.289	0.094	1.390	UHDS
1400	1.5	3	0.972	114.003	0.089	1.285	UHDS
1400	2	3	0.909	123.571	0.089	1.384	UHDS
1400	2.5	3	0.962	126.217	0.079	1.589	UHDS
1400	3	3	0.965	138.432	0.088	1.574	UHDS
1400	3	3	0.955	126.217	0.086	1.473	UHDS
1400	3.5	3	0.951	148.610	0.081	1.839	UHDS
1400	3.5	3	0.971	122.146	0.086	1.418	UHDS
Average			0.912	124.035	0.085	1.484	

Table 4.10: Mean values for extracted fibre

Item	Average
Leaf length (mm)	1135.34
Leaf mass (g)	604.09
Bud thickness (mm)	25.97
Tip thickness (mm)	2.94
Largest width (mm)	105.76
Wet weight (g)	72.14
Dry weight (g)	30.37
Average fibre length (mm)	1031.3
Fracture strength (MPa)	124.04
Fracture strain ϵ	0.085
Length ratio	0.912
Young's Modulus (GPa)	1.484

$$\text{The average fibre content (wet) per sisal leaf} = \frac{72.14}{604.09} \times 100\% = 11.94\%$$

$$\text{The average fibre content (dry) per sisal leaf} = \frac{30.37}{604.09} \times 100\% = 5.03\%$$

After extraction, the average fibre length was 1031.3 mm with a length reduction ratio (L_R) of 0.912. The average σ_u , ϵ and E were 124.04 MPa, 0.085 and 1.484 GPa respectively. The fibre content as a percentage of the fresh sisal leaf was 11.94% (wet) and 5.03% (dry). This was comparable to that obtained by Ahmad *et al* of 10.1% wet yield and 3.2% dry yield [19]. Other researches like Kawongolo *et al.* obtained 3.2% [16], Srinivasakumar *et al.* [42] obtained 3.0% and Naik *et al.* [20] recorded 3-5% all dry yields. Since the fibre was unbrushed, irrespective of the good quality in terms of strength, colour and fibre length the grade of sisal fibre was

classified under UHDS as per the London Sisal Association Standard. The colour of the fibre depended on the parameters used; it was white with green patches for low gap - high speed and green (incomplete decortication) at large gap-low speed settings. On drying, the green spots made the fibre to turn brownish leading to deterioration in fibre grade.

4.4.3.1. Three blades

For 900 rpm and a gap size of 1 mm, the extraction was incomplete with fibre mostly green in colour. The length ratio (L_R) was 0.991; high L_R indicated less amount of fibre breakage whereas a low L_R indicated an increased amount of tow and fibre breakage. The fibre σ_u was 117 MPa and E was 1.219 GPa. The poor decortication was because of reduced swept volume due to fewer blades and low speed. At 1.5 mm gap size, decortication was still incomplete, $L_R = 0.986$, $\sigma_u = 124$ MPa and $E = 1.5$ GPa. At a gap size of 2 mm, $L_R = 0.972$, $\sigma_u = 139$ MPa and $E = 1.5$ GPa and fibres were green in colour. At 2.5 mm gap, $L_R = 0.977$, $\sigma_u = 193$ MPa and $E = 2.1$ GPa. Generally, poor extraction was obtained at this set of parameters. The variation of the fibre properties with speed at 3 blades were presented by Figure 4.18, Figure 4.19 and Figure 4.20.

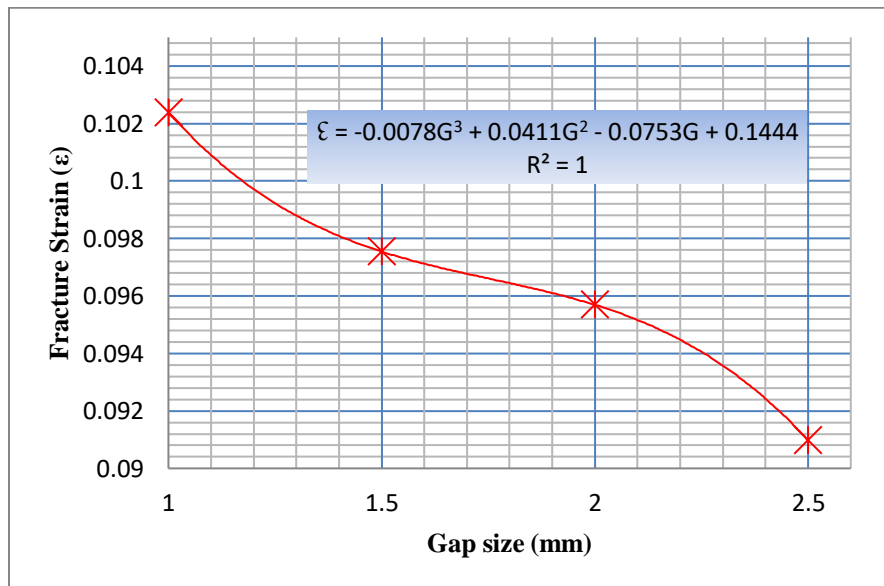


Figure 4.18: Fracture strain against gap size at 900 rpm and 3 blades

The decortication was incomplete at higher gap sizes as from 2 mm. However, as the gap size increased, the properties improved (Figure 4.19 and Figure 4.20)! When the gap increases, c also increases hence there is reduced blade stress on the fibres that would otherwise debond the cellulose microfibrils from the matrix (hemicellulose and lignin), grind the cell wall reducing crystallinity and damage the cuticle leading to stress concentrations and therefore reduce the

overall mechanical properties. The correlation coefficients between gap size and σ_u , ϵ and E were all unity implying that the tensile properties highly depend on the gap size.

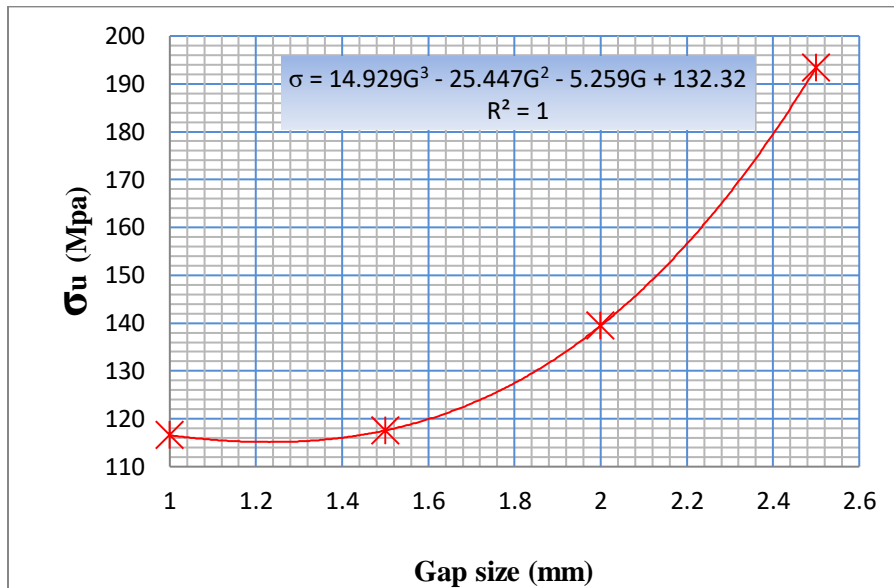


Figure 4.19: Fracture strength against gap size at 900 rpm and 3 blades

As the gap increased, there was also a slight improvement in E as shown in Figure 4.20.

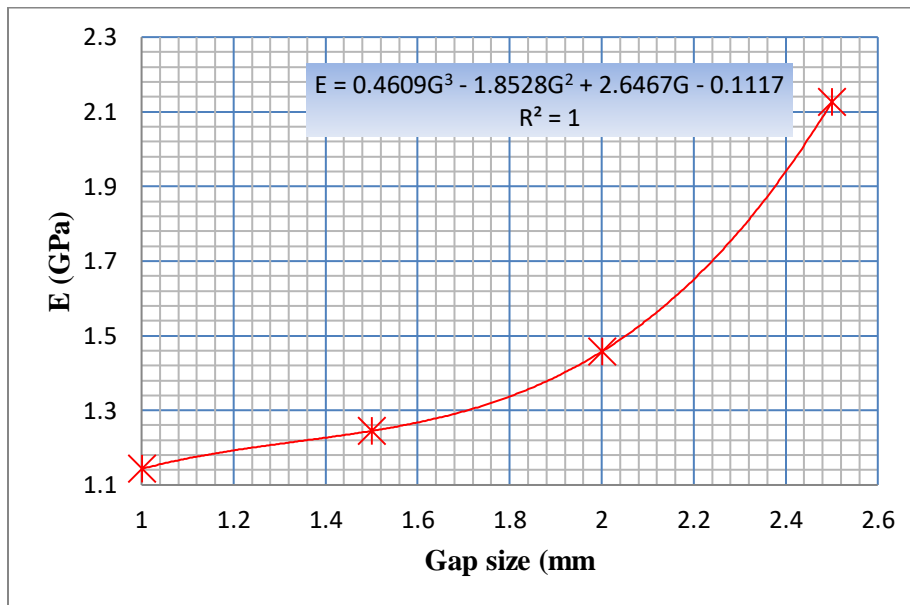


Figure 4.20: Young's modulus against gap size at 900 rpm and 3 blades

For a speed of 1200 rpm and gap size of 1 mm, $L_R = 0.965$, $\sigma = 133$ MPa and $E = 1.589$ GPa and the fibres were white with green tip end in colour. At a gap of 1.5 mm, $L_R = 0.981$, $\sigma_u = 132$ MPa and $E = 1.8$ GPa and white with green tip end fibres were obtained. At 2 mm gap, $L_R = 0.975$, $\sigma_u = 130$ MPa and $E = 1.579$ GPa and green with white butt end fibres were obtained. At 2.5 mm

gap, $L_R = 0.968$, $\sigma_u = 129$ MPa and $E = 1.548$ GPa with green fibres (incomplete decortication). At these parameters, the length ratios were pretty high indicating that the breakage of sisal fibres was very low. Generally, there was slight improvement in extraction quality. The mechanical properties of the fibres also improved with increase in gap size.

For 1400 rpm and 1 mm gap, $L_R = 0.964$, $\sigma_u = 124$ MPa and $E = 1.264$ GPa and white with green tip end fibres were obtained. At 1.5 mm gap, $L_R = 0.972$, $\sigma_u = 130.3$ MPa and $E = 1.390$ GPa and the fibres were white with green tip end in colour. At 2 mm gap, $L_R = 0.909$, $\sigma_u = 123.6$ MPa and $E = 1.384$ GPa and fibres were green with white butt end. At 2.5 mm gap, $L_R = 0.962$, $\sigma_u = 126.2$ MPa and $E = 1.589$ GPa with green- white fibres. At 3 mm gap, $L_R = 0.965$, $\sigma_u = 138.4$ MPa and $E = 1.574$ GPa with green fibres. At 3.5 mm gap, $L_R = 0.971$, $\sigma_u = 148.6$ MPa and $E = 1.84$ GPa with green fibres. The length ratios increased with gap size. Better decortication was obtained at this speed. However, the quality deteriorated with increase in gap size.

The properties at higher speed 1400 rpm varied similarly but the values were slightly lower than those at 900 rpm for the same gap sizes. This was because of the increased swept volume per unit time at high speeds (the fibres were beaten and scrapped more times at 1400 rpm than at 900 rpm).

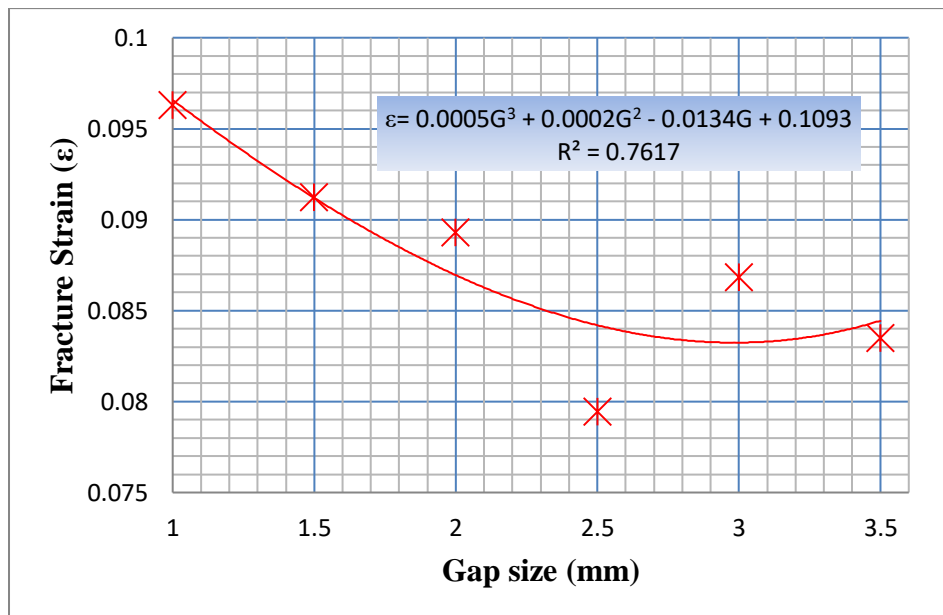


Figure 4.21: Fracture strain against gap size at 1400 rpm and 3 blades

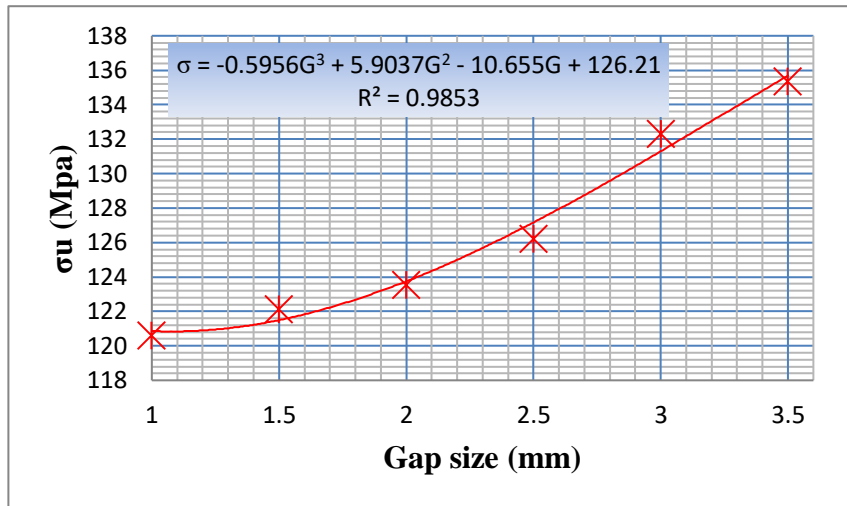


Figure 4.22: Fracture strength against gap size at 1400 rpm and 3 blades

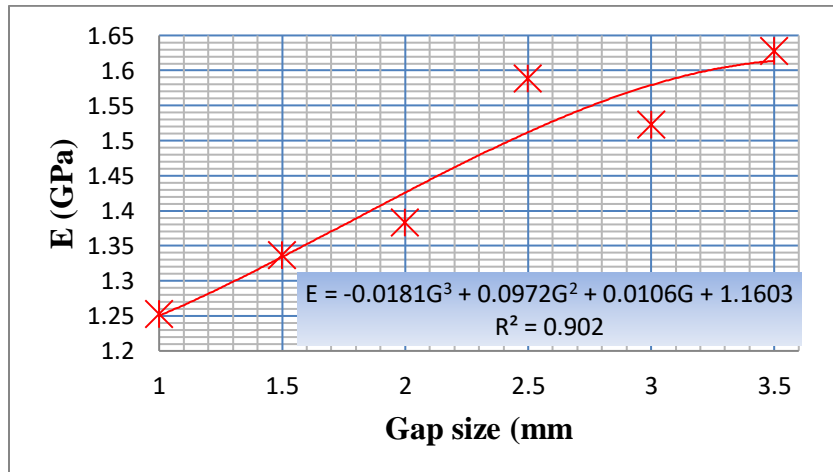


Figure 4.23: Young's Modulus against gap size at 1400 rpm and 3 blades

With 3 blades, the extraction results were generally poor. Increase in gap size, increased the clearance (and c) for the sisal leaf to slip away from being beaten by the blades. Extraction improved with speed (better results were obtained at 1400 rpm compared to 900 rpm). This was because at higher speeds, the number of times the beater blades beat the sisal leaf increased increasing the stresses on the fibres. Consequently, the swept area (the amount of material removed per second) also increased improving the colour of fibres but slightly weakening the strength of the fibres because the fibre cuticle is damaged introducing stress concentrations, microfibrils are debonded from the hemicellulose-lignin matrix and crystallinity is reduced due to grinding of cell walls. The fibre properties in terms of length ratio, σ_u and E were good though but the overall decortication was incomplete (fibres were dominantly green in colour).

4.4.3.2. Six blades

For 900 rpm and 1 mm gap size, $L_R = 0.974$, $\sigma_u = 125$ MPa and $E = 1.689$ GPa and the fibres were white with green tip ends. At 1.5 mm gap, $L_R = 0.886$, $\sigma_u = 143.5$ MPa and $E = 1.533$ GPa and white with green tip end fibres were also obtained. For 1135 rpm; at 1 mm gap, $L_R = 0.905$, $\sigma_u = 149.6$ MPa and $E = 1.681$ GPa and white at butt section with green tip end fibres. At 1.5 mm gap, $L_R = 0.815$, $\sigma_u = 141.8$ MPa and $E = 1.508$ GPa and white butt end and green tip end fibres were obtained.

For 1200 rpm and 1 mm gap, $L_R = 0.821$, $\sigma_u = 124.9$ MPa and $E = 1.399$ GPa and fibres were white in colour. At 1.5 mm gap, $L_R = 0.778$, $\sigma_u = 125.2$ MPa and $E = 1.93$ and extracted fibre were white in colour. For 1250 rpm; at 1 mm gap, $L_R = 0.794$, $\sigma_u = 124.1$ MPa and $E = 1.429$ GPa with white fibres.

1400 rpm and at 2 mm gap, $L_R = 0.893$, $\sigma_u = 138.4$ MPa and $E = 1.582$ GPa and white with some green tip end fibres were obtained. At 2.5 mm gap, $L_R = 0.99$, $\sigma_u = 121.9$ MPa and $E = 1.539$ GPa and fibres were white with green tip end. The length ratio at 6 blades reduced slightly with increase in speed (see Figure 4.24) with a very high correlation coefficient of 0.993. L_R is an important parameter with a direct implication on the overall lengths of the fibres. It is a rationalized variable for comparison purposes. The findings in Figure 4.24 meant that as speed increased, more fibres were broken due to cutting of the cuticle reducing the mean fibre length and quality.

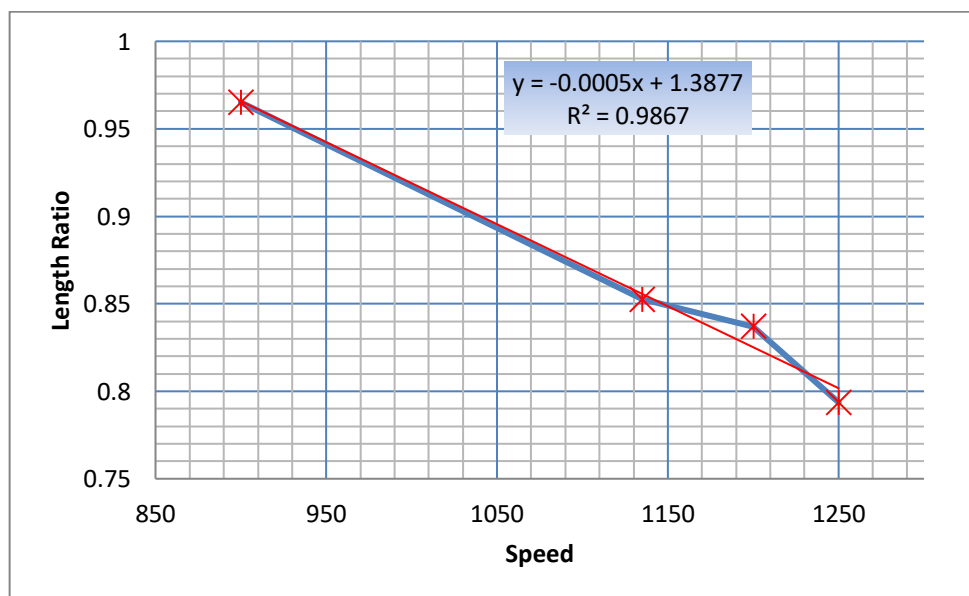


Figure 4.24: The length ratio against speed at 1 mm gap and 6 blades

The L_R was higher at 900 rpm than at 1400 rpm and slightly lower compared to those obtained at 3 blades. This was due to the breaking of sisal fibres at higher speeds due to increased blade stresses. Moreover, the increase in number of blades increased the number of interactions between blades and fibres. Better decortication quality was achieved at around 1200 rpm. However, this quality needed brushing to improve it further.

4.4.3.3. Twelve blades

At a speed of 900 rpm and 1 mm gap size, $L_R = 0.650$, $\sigma_u = 128$ MPa and $E = 1.313$ GPa and the fibres were white with green tip. At 1.5 mm gap, $L_R = 0.897$, $\sigma_u = 150.6$ MPa and $E = 1.716$ GPa and fibres were white with green tip end in colour. At 2 mm gap, $L_R = 0.939$, $\sigma_u = 130.3$ MPa and $E = 1.46$ GPa and fibres were green with white butt end. At 2.5 mm gap, $L_R = 0.948$, $\sigma_u = 182.5$ MPa and $E = 2.489$ GPa with green fibres. Equally it was noticed that L_R , σ_u and E increased with gap size (Figure 4.26 and Figure 4.27) because of reduced cuticle damage, blade stresses and cell wall grinding at higher gap sizes. The properties were generally poorer at 12 blades than at 3 or 6 blades because of the increased blade stresses that debond the microfibrils from the matrix, damages the cuticle and grind the cell wall hence reducing the average L_R , σ_u and E .

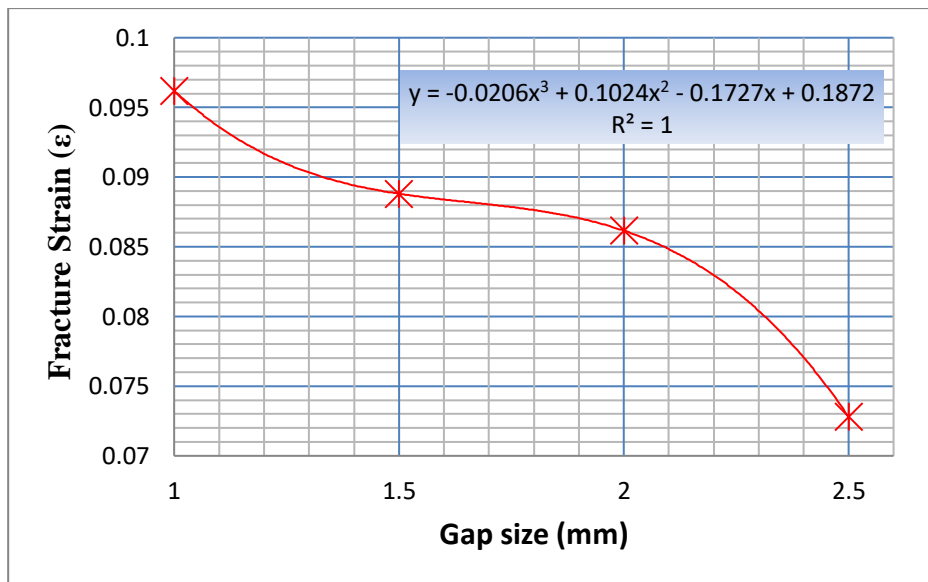


Figure 4.25: Fracture strain against gap size at 900 rpm and 12 blades

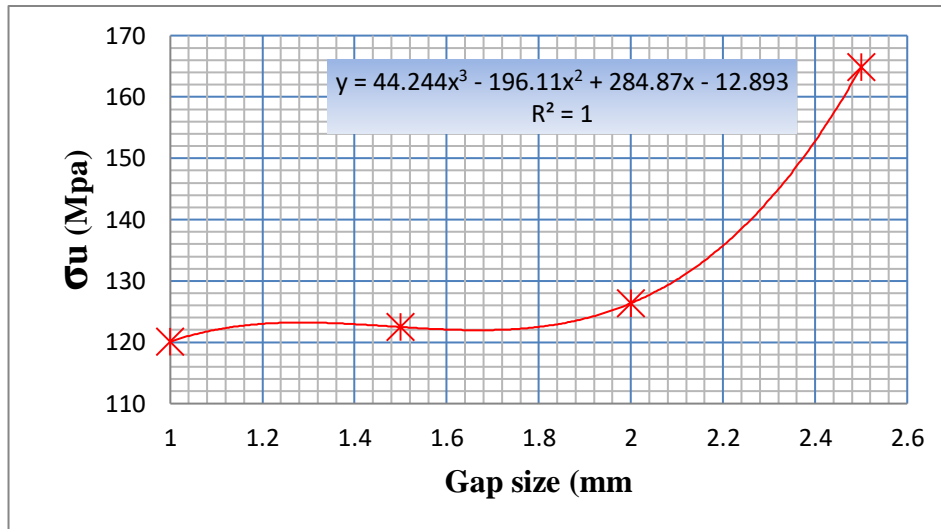


Figure 4.26: Fracture strength against gap size at 900 rpm and 12 blades

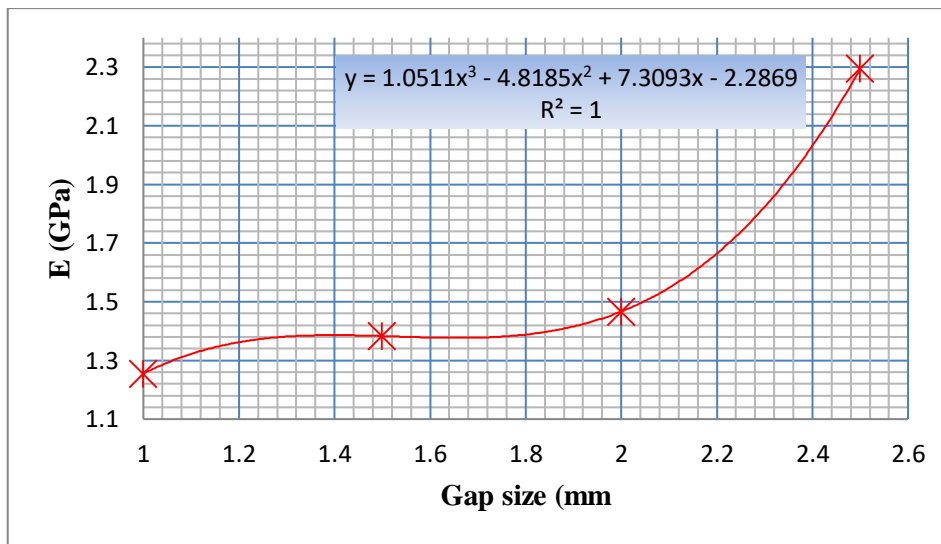


Figure 4.27: Young's modulus against gap size at 900 rpm and 12 blades

At 1200 rpm and 1 mm gap, $L_R = 0.889$, $\sigma_u = 86.45$ MPa and $E = 0.921$ GPa and white with green tip end fibres. At 1.5 mm gap, $L_R = 0.885$, $\sigma_u = 100.9$ MPa and $E = 1.2750$ GPa and white with green tip end fibres. At 2 mm gap, $L_R = 0.866$, $\sigma_u = 95$ MPa and $E = 1.61$ GPa and fibres were white with green tip. At 2.5 mm gap, $L_R = 0.88$, $\sigma_u = 109.9$ MPa and $E = 1.44$ GPa with green fibres. The properties varied with gap size following trends similar to those at 900 rpm. However, there were better extraction qualities at 1200 rpm than at 900 rpm.

At 1400 rpm and 2.5 mm gap, $L_R = 0.895$, $\sigma_u = 99.6$ MPa and $E = 1.24$ GPa and white with green tip end fibres. At 3 mm gap, $L_R = 0.904$, $\sigma_u = 131.6$ MPa and $E = 2.28$ GPa and white with some green tip end. It was noted that at lower gaps 1 mm, 1.5 mm and 2 mm, the length ratios were

very low indicating a high fibre breakage. At 1400 rpm, 12 blades and low gap, the fibres were equally subjected to higher blade stresses.

4.4.3.4. Variation of properties with speed

The properties of the sisal fibres also varied with speed at constant gap sizes and blades. It was noted that as speed increased, the fracture stress and modulus of elasticity reduced slightly (Figure 4.29 and Figure 4.30). There was a slight increase in fracture strain with speed (Figure 4.28).

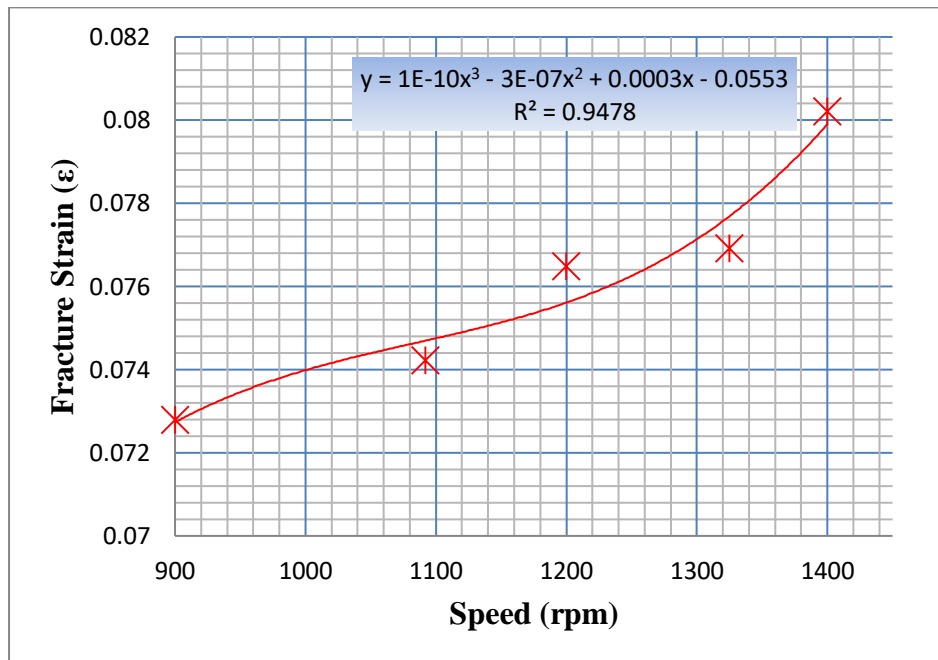


Figure 4.28: Fracture strain against speed at 2.5 mm gap size and 12 blades

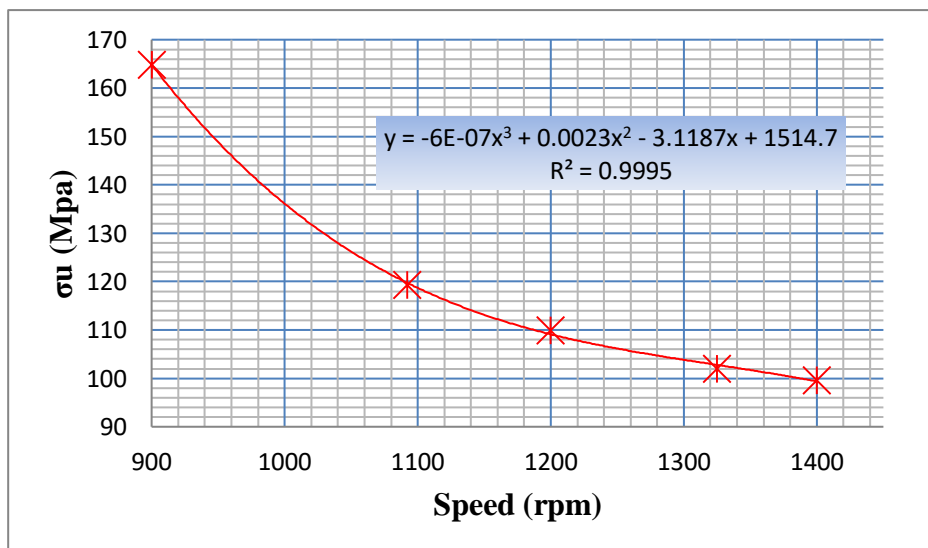


Figure 4.29: Fracture strength against speed at 2.5 mm gap size and 12 blades

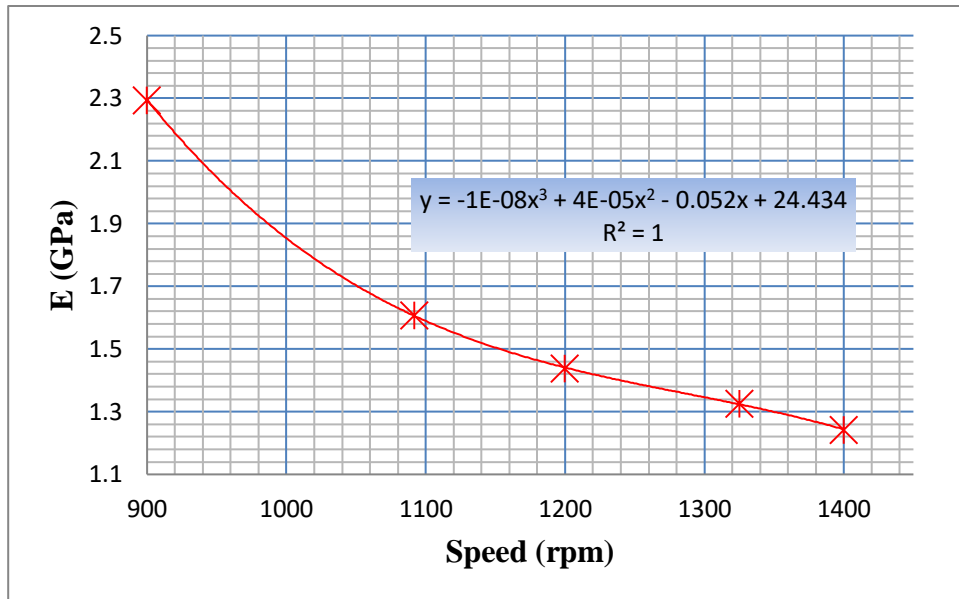
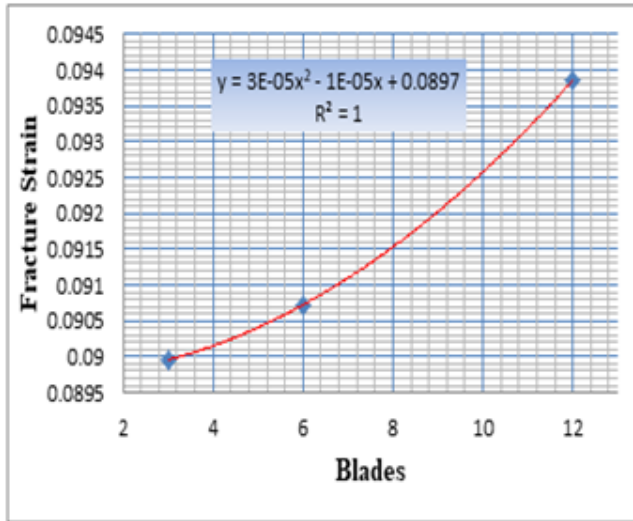


Figure 4.30: Young's modulus against speed at 2.5 mm gap size and 12 blades

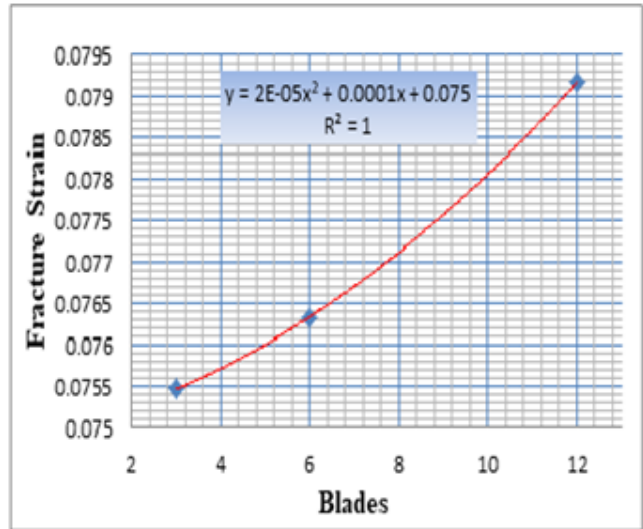
The correlation coefficients between ϵ , σ_u and E and speed were 0.97, 0.99 and 1 respectively. These suggested that the properties are highly influenced by the drum speed. There was therefore need to reconsider the design speed based on this finding. Increase in speed increased the number of interactions between the blades and the sisal leaf per unit time hence increasing the blade stresses known for debonding the microfibrils from the matrix, damaging the cuticle causing stress concentrations and grinding the cell walls reducing crystallinity and tensile properties at large.

4.4.3.5. Variation of properties with the number of blades at constant gap size and speed

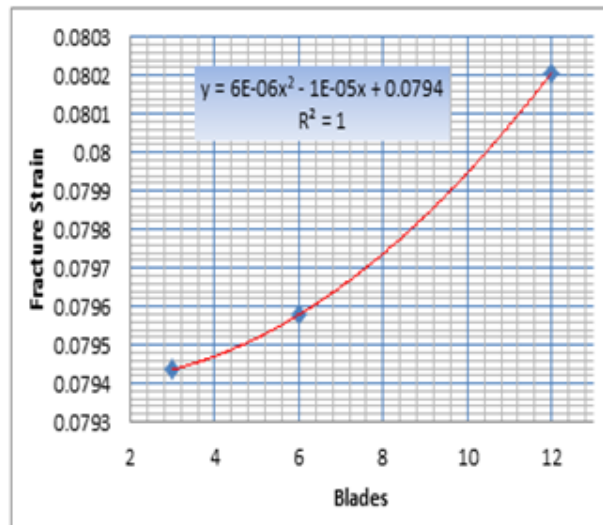
The number of blades also had an influence on the properties of the fibres. The effect can be clearly seen in Figure 4.31, Figure 4.32 and Figure 4.33. Stress and elastic modulus reduced with increase in number of blades. Strain, on the other hand, increased slightly with number of blades.



a) 1200 rpm and 1 mm gap size

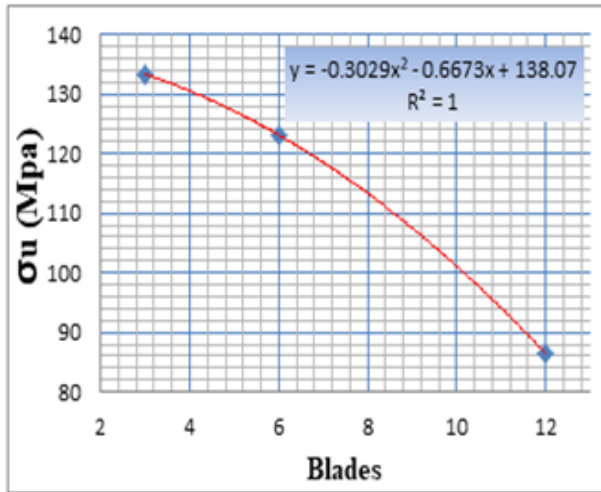


b) 1200 rpm and 1.5 mm gap size

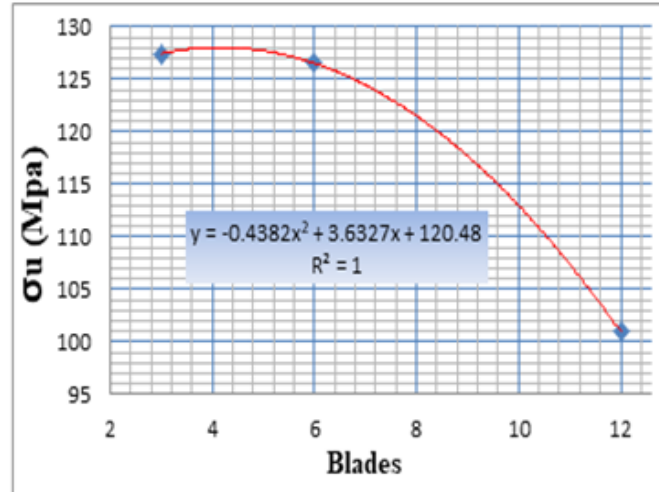


c) 1400 rpm and 2.5 mm gap size

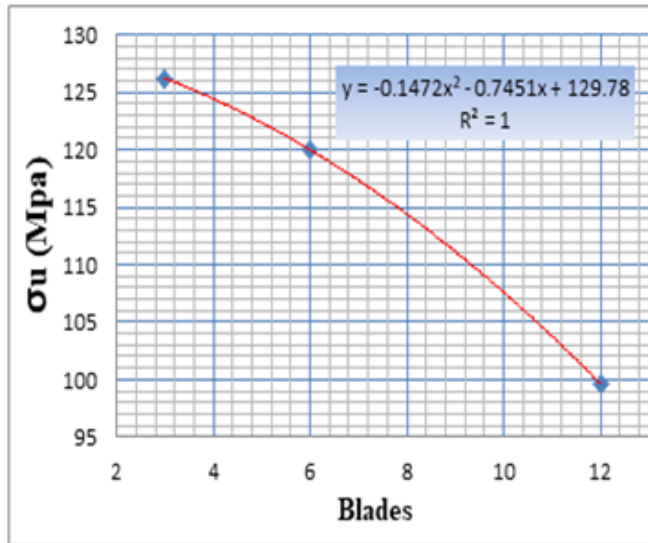
Figure 4.31: Variation of fracture strain with number of blades



a) 1200 rpm and 1 mm gap size



b) 1200 rpm and 1.5 mm gap size



c) 1400 rpm and 2.5 mm gap size

Figure 4.32: Variation of fracture strength with number of blades

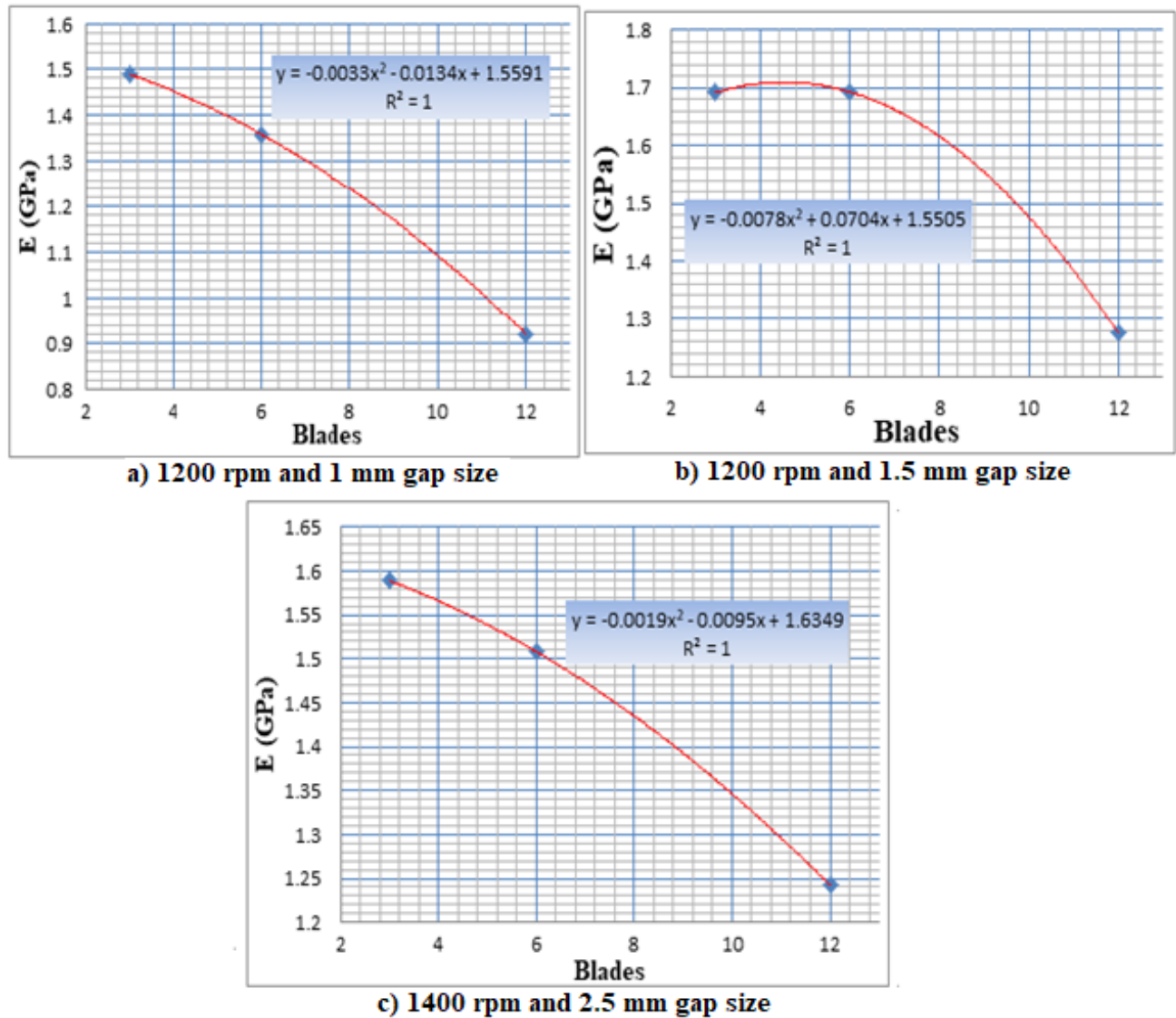


Figure 4.33: Variation of Young's modulus with number of blades

The correlation coefficient between the properties with the number of blades was one for all the cases. Therefore, it was observed that the properties of extracted sisal fibre were highly dependent on the number of blades. The fibre σ_u and E reduced whereas ϵ increased with number of blades. This was because decortication pitch inversely related to the number of blades. As earlier noted, pitch also inversely related to the amount of materials removed every time a blade interacts with the leaf. Therefore, as the blades increase, the high blade stresses debond the microfibrils from the matrix, damage the cuticle introducing stress concentrations and grind the cell walls reducing crystallinity that eventually reduce the mechanical properties.

At 12 blades, extraction results were better in terms of colour but had the poorest mechanical properties than at 3 and 6 blades. Moreover, it was very difficult to feed sisal leaves at 12 blades. The machine did blow the sisal leaf away from beater blades instead of sacking into the blades. With 12 blades and especially at high speeds, the presence of blades at the feeding gap is continuous allowing no room for sisal leaf to be fed hence increasing the resistance. At 3 blades, mechanical properties, in general, were the best. However, the extraction in most cases was incomplete as evidenced by the green fibres. 6 blades yielded results that were better in terms of properties and completeness in extraction. There was some green colour especially at tip end that could be removed with subsequent operation (brushing). Therefore, more tests were done at 6 blades for extraction to yield conclusive data. From these tests, at 900 rpm, most fibres were green due to incomplete decortication. Better results were achieved above 1000 rpm for gaps below 2 mm. Gaps more than 2 mm only yielded better results at 1300 rpm and above.

4.4.3.6. Machine extraction capacity

The total weight of fibres extracted in 10 minutes was 3631.3 g while still wet and 1807.1 g on drying. On average 363.13 g, wet fibre and 180.71 g dry fibres were extracted every minute. The machine extraction capacity per hour was therefore determined as follows;

$$\begin{aligned} \text{Wet fibres} &= \frac{3631.3}{10} \times 60 = 21787.8 \text{ g/hr} \\ &= 21.7878 \text{ kg/hr} \\ \text{Dry fibres} &= \frac{1807.1}{10} \times 60 = 10842.6 \text{ g/hr} \\ &= 10.842 \text{ kg/hr} \end{aligned}$$

$$\begin{aligned} \text{Design efficiency (DE)} &= \frac{\text{Actual capacity}}{\text{Design capacity}} \times 100\% \dots\dots\dots (4.38) \\ &= \frac{10.842}{15} \times 100 = 70\% \end{aligned}$$

The design efficiency was 39% compared to 43% obtained by Kawongolo *et al.* [16] if a design capacity of 28 kg/hr was used otherwise 70% with design capacity of 15 kg/hr. This was still good enough given that this machine was able to extract and brush at the same time whereas that of Kawongolo *et al.* [16] could only extract. The capacity of the machine was 10.84 kg/hr compared to Kawongolo *et al.* [16] of 12 kg/hr, Tanveer *et al.* [19] of 15.94 kg/hr, Naik *et al.* [20] of 9-10 kg/hr and Cantalino *et al.* [4] of 15 - 20 kg/hr. The extraction capacity achieved was still comparable to those achieved by other researchers given the machine simultaneously extracted and brushed sisal fibres.

4.4.4. Brushed fibre

The analysed results obtained during brushing are given in Table 4.11. A large sample size was used due to the reported variations in sisal fibre properties. Some of the laboratory data sheets have been appended.

Table 4.11: The properties of sisal fibre after brushing using the machine

Speed (RPM)	Gap size (mm)	Number of elements	Length ratio	Fracture strength (MPa)	Fracture strain ϵ	Young's Modulus (GPa)	Fibre grade
900	1.0	12	0.7677	167.4390	0.0830	2.0165	UG
900	1.0	12	0.7857	146.4040	0.0848	1.7260	UG
900	1.5	12	0.9615	157.3422	0.0592	2.6566	UG
900	1.5	12	0.9714	171.6461	0.0729	2.3540	UG
900	2.0	12	0.9907	153.6400	0.0923	1.6653	SSUG
900	2.0	12	0.9813	144.3846	0.0744	1.9405	SSUG
900	2.5	12	0.9817	144.7212	0.0964	1.5008	SSUG
900	2.5	12	0.9545	218.7646	0.0961	2.2757	SSUG
1325	2.5	12	0.8952	165.2514	0.0768	2.1521	SSUG
1325	3.0	12	0.9406	129.5759	0.0866	1.4961	SSUG
1192	3.0	12	1.0000	117.7963	0.0878	1.3417	SSUG
1192	4.5	12	0.9541	169.1723	0.0896	1.8884	SSUG
1200	1.0	12	0.9135	128.0614	0.0821	1.5590	UG
1200	1.5	12	0.9519	140.5142	0.0595	2.3606	UG
1200	2.0	12	0.9453	96.7613	0.0789	1.2269	UG
1200	2.5	12	0.8835	114.7673	0.0899	1.2769	UG
1400	2.5	12	0.9412	144.2163	0.0964	1.4956	SSUG
1400	3.0	12	0.9806	106.8581	0.0777	1.3756	SSUG
900	1.0	6	0.9009	173.3289	0.1057	1.6405	SSUG
900	1.0	6	0.9182	179.2187	0.0842	2.1278	SSUG
900	1.5	6	0.8899	198.5709	0.0786	2.5273	SSUG
900	1.5	6	0.8624	134.6244	0.0815	1.6509	SSUG
1135	1.0	6	0.9300	161.5492	0.0756	2.1370	UG
1135	1.0	6	0.9048	120.3205	0.0851	1.4136	UG
1135	1.5	6	0.9623	124.0227	0.0688	1.8040	UG
1135	1.5	6	0.9717	163.2320	0.0696	2.3438	UG
1200	1.0	6	0.9583	110.2237	0.0631	1.7469	UG
1200	1.0	6	0.9792	139.1679	0.1006	1.3834	UG
1200	1.5	6	0.9796	135.4658	0.0670	2.0230	UG
1200	1.5	6	0.9798	167.4390	0.0833	2.0093	UG
1250	1.0	6	0.9200	158.1836	0.0979	1.6155	UG
1400	2.0	6	0.8300	132.5209	0.0679	1.9529	SSUG
1400	2.0	6	0.8687	177.9566	0.0777	2.2909	SSUG
1400	2.0	6	0.8737	90.8714	0.0634	1.4335	UG
1400	2.5	6	0.9293	89.3569	0.0674	1.3256	SSUG
1400	2.5	6	0.9000	123.6861	0.0799	1.5478	SSUG
900	1.0	3	0.8991	126.3365	0.0772	1.6358	SSUG
900	1.0	3	0.9151	112.3272	0.0813	1.3825	SSUG
900	1.5	3	0.9260	120.0260	0.0754	1.5909	SSUG
900	1.5	3	0.9358	121.1619	0.0871	1.3918	SSUG
900	2.0	3	0.9709	153.9766	0.1004	1.5329	SSUG

900	2.5	3	0.9439	166.5976	0.1012	1.6464	SSUG
1200	1.0	3	0.9485	95.9199	0.0558	1.7189	UG
1200	1.0	3	0.9320	112.3272	0.0585	1.9207	UG
1200	1.5	3	0.8846	163.5686	0.0897	1.8229	UG
1200	1.5	3	0.9417	145.1419	0.1004	1.4450	UG
1200	2.0	3	0.9244	147.6661	0.0817	1.8075	SSUG
1200	2.5	3	0.9720	175.4324	0.0906	1.9358	SSUG
1400	1.0	3	0.8224	132.5209	0.0893	1.4842	SSUG
1400	1.0	3	0.8846	165.3355	0.0871	1.8992	SSUG
1400	1.5	3	0.9038	141.3556	0.0933	1.5150	SSUG
1400	1.5	3	0.8932	147.6661	0.0746	1.9807	UG
1400	2.0	3	0.9700	147.6661	0.0884	1.6706	SSUG
1400	2.5	3	0.9900	148.1709	0.0750	1.9756	SSUG
1400	3.0	3	0.7431	117.3756	0.0768	1.5286	UG
1400	3.0	3	0.8411	169.1218	0.0790	2.1403	UG
1400	3.5	3	0.8491	166.5976	0.0839	1.9850	UG
1400	3.5	3	0.8922	102.2304	0.0598	1.7089	UG
Average			0.9197	142.6824	0.0812	1.7759	

The average L_R , σ_u , E and ε after subsection to more brushing forces were 0.9197, 142.682 MPa, 1.776 GPa and 0.0812 respectively.

Table 4.12: Mean values after extraction of fibres

Item	Average
Leaf length (mm)	1135.34
Leaf mass (g)	604.09
Bud thickness (mm)	25.97
Tip thickness (mm)	2.94
Largest width (mm)	105.76
Overall weight (g)	20.65
Average fibre length (mm)	955.2
Fracture strength (MPa)	142.68
Fracture strain ε	0.0812
Length ratio L_R	0.920
Young's modulus (GPa)	1.776

The average fibre content per sisal leaf after brushing = $\frac{30.37}{604.09} \times 100\% = 3.42\%$

It was noted that the properties of brushed fibres at every set of parameters were better than the unbrushed fibre. For instance, σ_u , E and ε for brushed fibre were 142.68 MPa, 1.776 GPa and 0.0812 respectively against 124.04 MPa, 1.484 GPa and 0.085 respectively for unbrushed fibre.

These values are comparable to 161 MPa σ_u , 3.6 GPa E and 4.5% ϵ found by Kithiia *et al.* [43]. However, the σ_u is less than 410 MPa obtained by Phologolo *et al.* [21] given that they used a single strand that gives higher values than bundles [43]. Furthermore, this research used butt-end portion that possess the least properties hence slightly less than the values found by Kithiia *et al.* [43] and Phologolo *et al.* [21] for fibres from Kenya. In general, the low figures reported as compared to sisal fibres from across the world is because of high amount of lignin and hemicellulose in Kenyan sisal fibers that reduce the mechanical properties [21].

The improvement in properties due to brushing was attributed to, as noted from the research, removal of curled fibres, weak fibres, unextracted pieces and other foreign materials that attach to fibres hunk during drying. The decorticated pieces make the sisal fibres more brittle therefore reducing the overall strength. Brushing also reduces the effective diameter of fibres by removing more materials. As another research found out, fibres with smaller diameters have better properties than larger fibres [44]. The larger the diameters, the higher the chance of finding a larger flaw in the fibre hence the weaker the fibre. Moreover, brushing realigns the microfibrils reducing the microfibrillar angle hence strengthening the fibre. The L_R after brushing was still quite high although less than that obtained after extraction. An average fibre length of 955.2 mm was still quite high above the UG grade requirement by the London Sisal Association. Better fibre quality was also achieved during brushing. The colour of fibres was pure white for good brushing or white with brown spots (due to green colour sustained after extraction) for poor brushing. The sisal grades obtained were UG and Sub Standard Under Grade (SSUG) depending on the properties of the fibre.

4.4.4.1. Three elements

For 900 rpm and a gap size of 1 mm, $L_R = 0.79$, $\sigma_u = 167$ MPa and $E = 1.72$ GPa. The colour of fibre was pure white and its grade was UG. At 1.5 mm gap size, $L_R = 0.96$, $\sigma_u = 171.6$ MPa and $E = 2.09$ GPa and fibre colour was pure white (UG grade). At 2 mm gap, $L_R = 0.98$, $\sigma_u = 165$ MPa and $E = 2.36$ GPa and fibres were white with brownish spots (SSUG grade). At 2.5 mm gap size, $L_R = 0.98$, $\sigma_u = 164$ MPa and $E = 2.94$ GPa and fibres were white with brownish spots (SSUG grade). At 1 mm, the L_R was low due to breakage of fibres. The fibre grade was UG since

the fibres met the required length and colour for this grade according to London Fibre Association [22]. The L_R , σ_u and E increased with gap size because the beating forces reduced hence the microfibrils are not debonded from the matrix, the fibre cuticle is not damaged to introduce stress concentrations and crystallinity is also not reduced. However, the increase in σ_u and E was not perpetual but remained constant beyond a gap size of 2 mm. The correlation coefficients between gap size and σ , ϵ and E were all unity implying that the mechanical properties are highly dependent on the gap size.

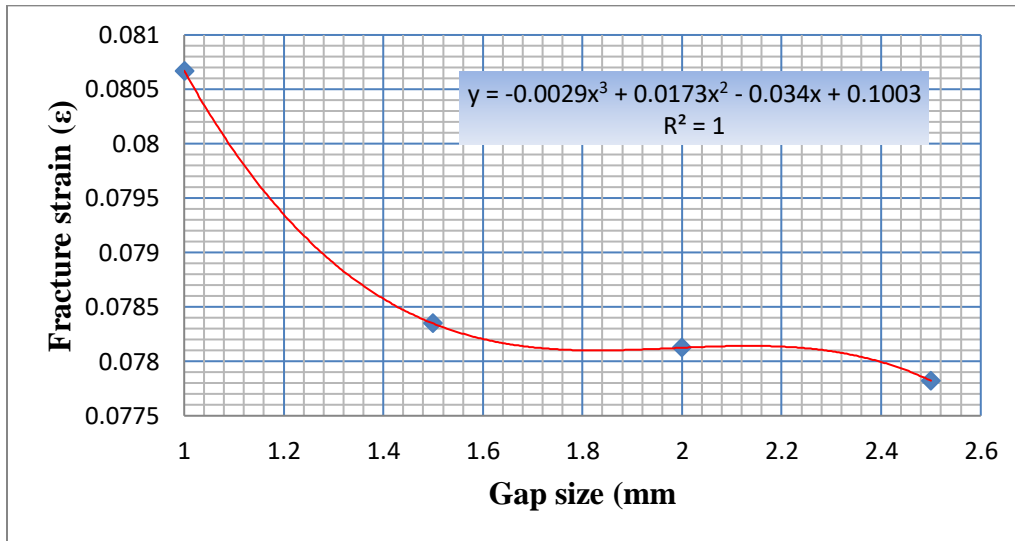


Figure 4.34: Fracture strain against gap size at 900 rpm and 3 elements

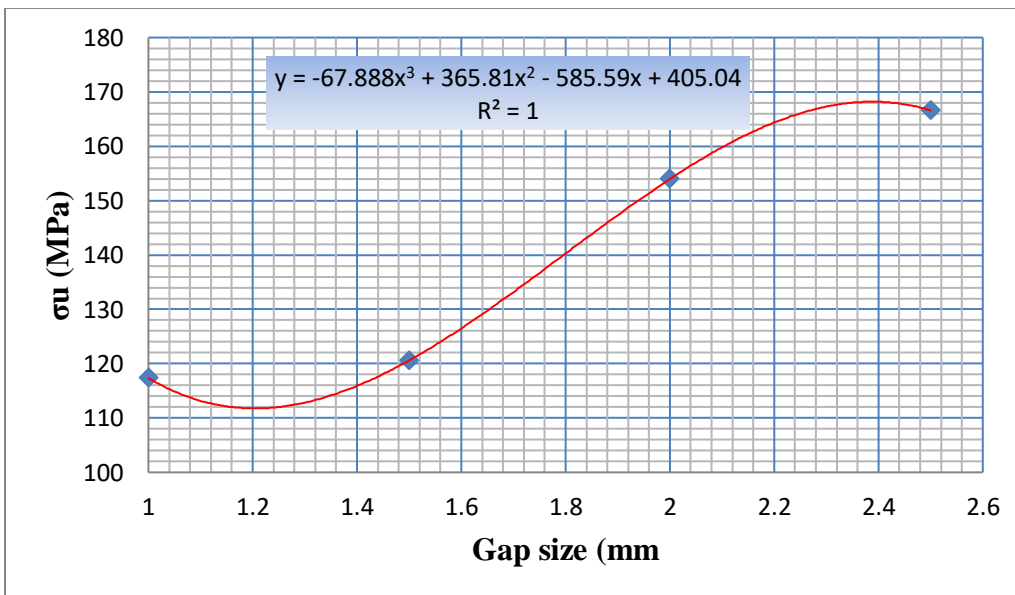


Figure 4.35: Fracture strength against gap size at 900 rpm and 3 elements

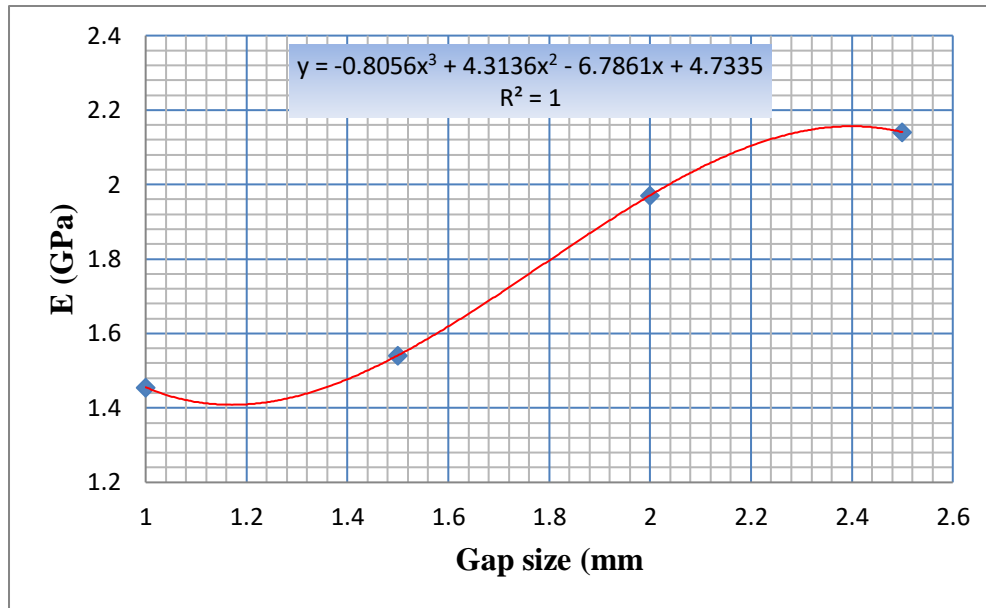


Figure 4.36: Young's modulus against gap size at 900 rpm and 3 elements

For 1200 rpm and a gap size of 1 mm, $L_R = 0.93$, $\sigma_u = 132$ MPa and $E = 2.27$ GPa. The colour of fibre was pure white and its grade was UG; at 1.5 mm gap size, $L_R = 0.88$, $\sigma_u = 145$ MPa and $E = 1.651$ GPa and fibres were pure white in colour (UG grade). At 2 mm gap, $L_R = 0.92$, $\sigma_u = 147$ MPa and $E = 1.806$ GPa and fibres were white with brownish spots (SSUG grade). At 2.5 mm gap, $L_R = 0.97$, $\sigma_u = 175$ MPa and $E = 1.94$ GPa and fibres were white with brownish spots (SSUG grade). As gap increased, L_R increased as well because of less fibre breakage at higher gaps. σ_u and E also increased with gap size due to less brushing resistance. As the gap increased, beating forces also reduced hence the fibres were not weakened due to cuticle damage or debonding of the microfibrils from the matrix. The properties at 1200 rpm were generally less compared to those at 900 rpm except for the colour of fibres that was better at 1200 rpm.

Properties at 1400 rpm and a gap size of 1 mm, $L_R = 0.88$, $\sigma_u = 137.3$ MPa and $E = 1.48$ GPa. The colour of fibre was pure white and its grade was SSUG due to reduced fibre length; at 1.5 mm gap size, $L_R = 0.89$, $\sigma_u = 141$ MPa and $E = 1.52$ GPa, pure white fibres but short fibres (SSUG grade). At 2 mm gap, $L_R = 0.97$, $\sigma_u = 147.7$ MPa and $E = 1.79$ GPa and fibres were pure white (UG grade). At 2.5 mm gap, $L_R = 0.99$, $\sigma_u = 148.2$ MPa and $E = 1.83$ GPa and fibres were pure white (UG grade). For 3 mm gap, $L_R = 0.84$, $\sigma_u = 169$ MPa and $E = 2.14$ GPa and fibres were pure white (UG grade). However, for 3.5 mm gap $L_R = 0.89$, $\sigma_u = 166$ MPa and $E = 2.78$ GPa and fibres were pure white (UG grade). As gap increased L_R increased as well leading to

less fibre breakage. Mechanical properties (stress and modulus) also increased with gap just like at 900 rpm and 1200 rpm.

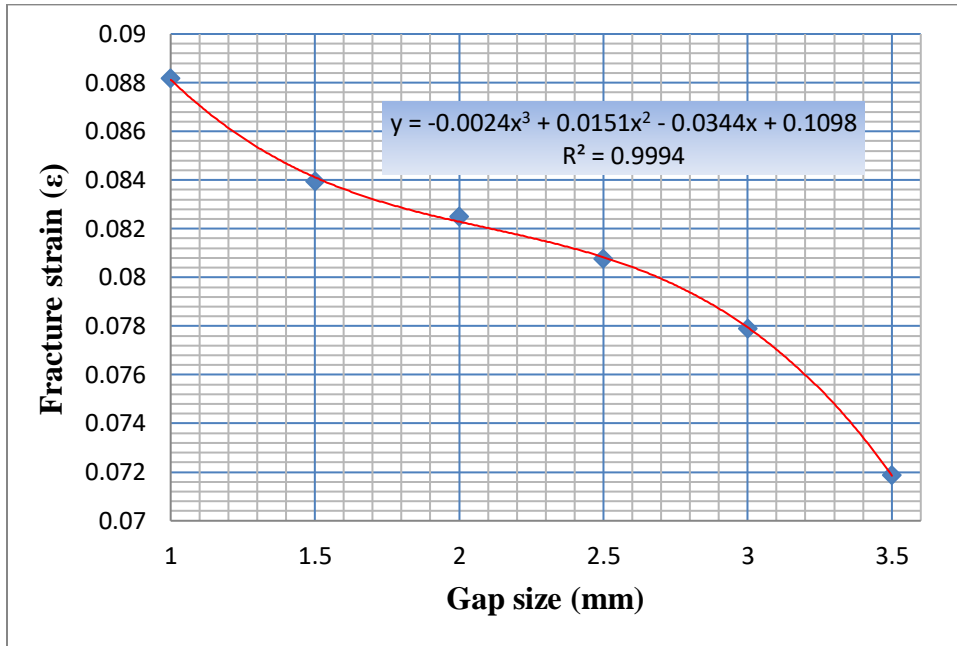


Figure 4.37: Fracture strain against gap size at 1400 rpm and 3 elements

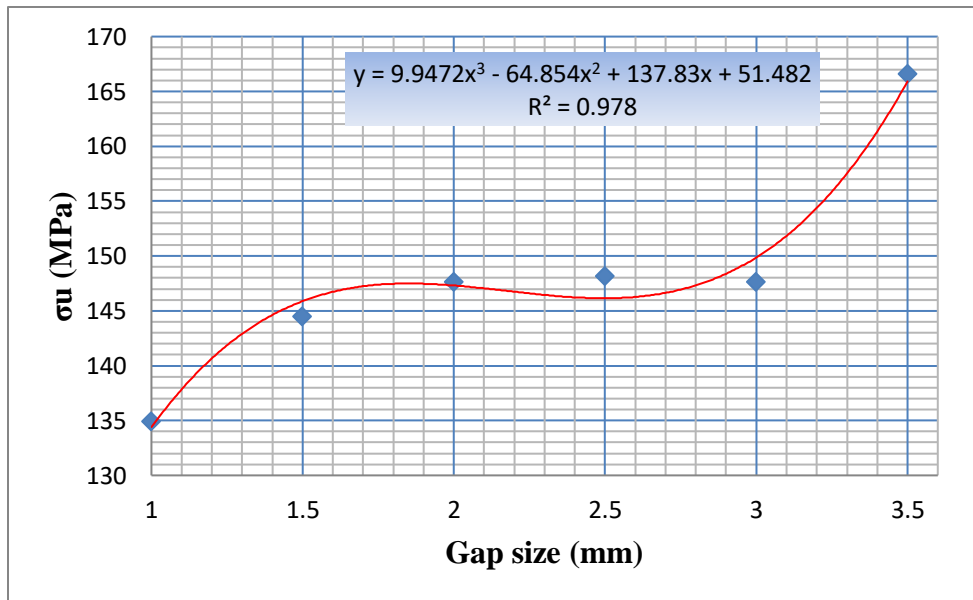


Figure 4.38: Fracture strength against gap size at 1400 rpm and 3 elements

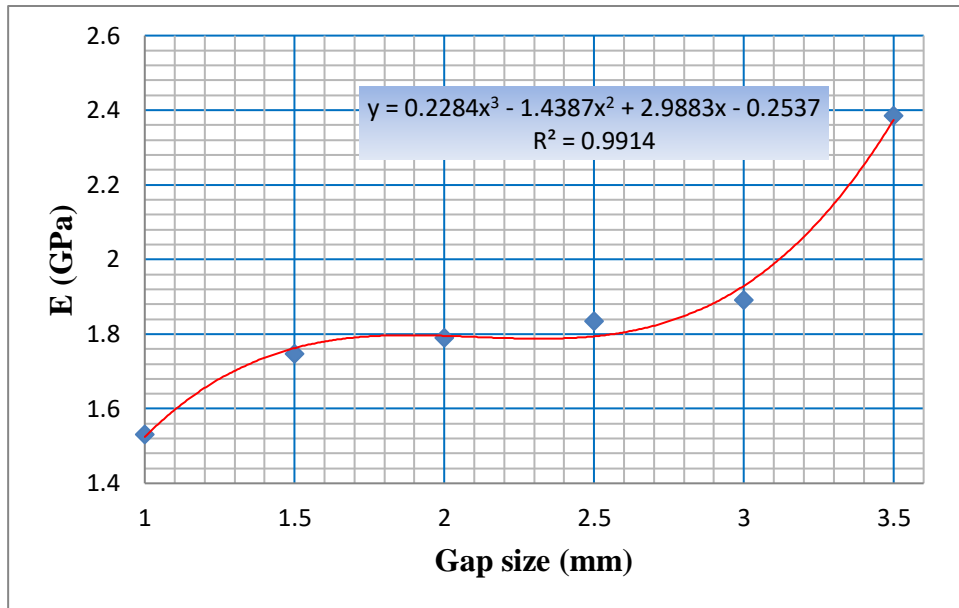


Figure 4.39: Young's modulus against gap size at 1400 rpm and 3 elements

4.4.4.2. Six elements

The properties at 900 rpm and the various gap sizes were; at a gap of 1 mm, $L_R = 0.90$, $\sigma_u = 179$ MPa and $E = 2.12$ GPa and the colour of fibre was white-brown (SSUG grade); at 1.5 mm gap size, $L_R = 0.88$, $\sigma_u = 198$ MPa and $E = 2.52$ GPa and white-brown fibres (SSUG grade). The grade of fibre was SSUG because of brown colour of fibres caused by poorly decorticated fibres that turned brown on brushing.

For a speed of 1200 rpm and a gap size of 1 mm, $L_R = 0.95$, $\sigma_u = 139$ MPa and $E = 1.38$ GPa and the colour of fibre was pure white (UG grade). At 1.5 mm gap size, $L_R = 0.97$, $\sigma_u = 167$ MPa and $E = 1.98$ GPa with pure white fibres (UG grade). The colour of fibre was to the recommended standard at 1200 rpm.

For a speed of 1400 rpm and; a gap size of 2 mm, $L_R = 0.87$, $\sigma_u = 177$ MPa and $E = 2.29$ GPa. The colour of fibre was white-brown and its grade was SSUG; at 2.5 mm gap size, $L_R = 0.92$, $\sigma_u = 146$ MPa and $E = 1.86$ GPa and fibres were white-brown in colour (SSUG grade). However, conclusive results were not yielded at this point and more results on fibre length, colour and grade were conducted.

4.4.4.3. Twelve elements

For 900 rpm and; a gap size of 1 mm, $L_R = 0.78$, $\sigma_u = 167.4$ MPa and $E = 1.7$ GP and the fibres were pure white in colour (UG grade); at 1.5 mm gap size, $L_R = 0.96$, $\sigma_u = 171.6$ MPa and $E = 2.0$ GPa and pure white fibres (UG grade). At 2 mm gap, $L_R = 0.98$, $\sigma_u = 165$ MPa and $E = 2.1$ GPa and fibres were white with brownish spots (SSUG grade). At 2.5 mm gap, $L_R = 0.98$, $\sigma_u = 218$ MPa and $E = 2.9$ GPa and fibres' colour was white with brown spots (SSUG grade). At gap size of 1 mm and 1.5 mm, the grade of sisal was UG grade due to quality brushing. Similarly, the properties improved with gap size and weakened with speed.

For 1200 rpm and; a gap size of 1 mm, $L_R = 0.91$, $\sigma_u = 128$ MPa and $E = 1.5$ GP and fibre's colour was pure white (UG grade); at 1.5 mm gap, $L_R = 0.95$, $\sigma_u = 140$ MPa and $E = 1.52$ GPa, pure white fibres (UG grade); at 2 mm gap, $L_R = 0.94$, $\sigma_u = 96.7$ MPa and $E = 1.22$ GPa and fibres were pure white (UG grade); at 2.5 mm gap, $L_R = 0.88$, $\sigma_u = 114$ MPa and $E = 1.27$ GPa and fibres were pure white (UG grade).

Brushing at 1400 rpm led to massive fibre breakage at gap sizes below 2 mm. At 2.5 mm gap, $L_R = 0.94$, $\sigma_u = 144$ MPa and $E = 1.49$ GPa. The colour of fibre was white-brown (SSUG grade); at 3 mm gap size, $L_R = 0.98$, $\sigma_u = 106$ MPa and $E = 1.37$ GPa and fibre was white-brown in colour (SSUG grade).

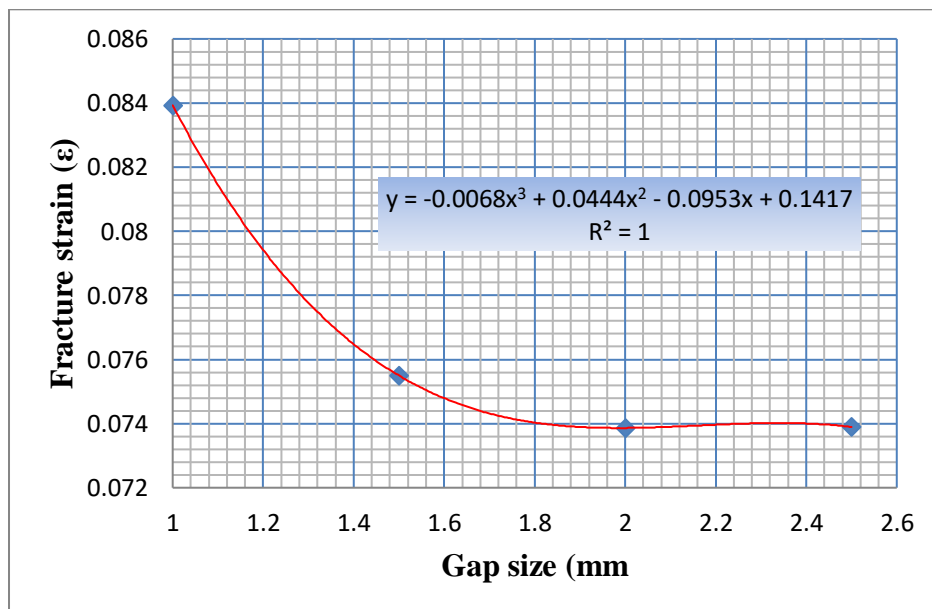


Figure 4.40: Fracture strain against gap size at 900 rpm and 12 elements

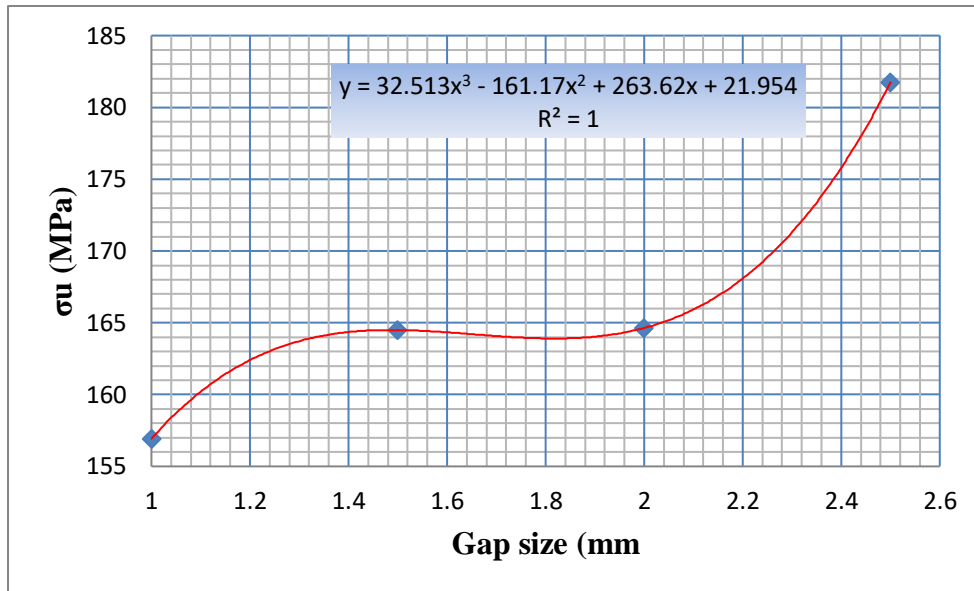


Figure 4.41: Fracture strength against gap size at 900 rpm and 12 elements

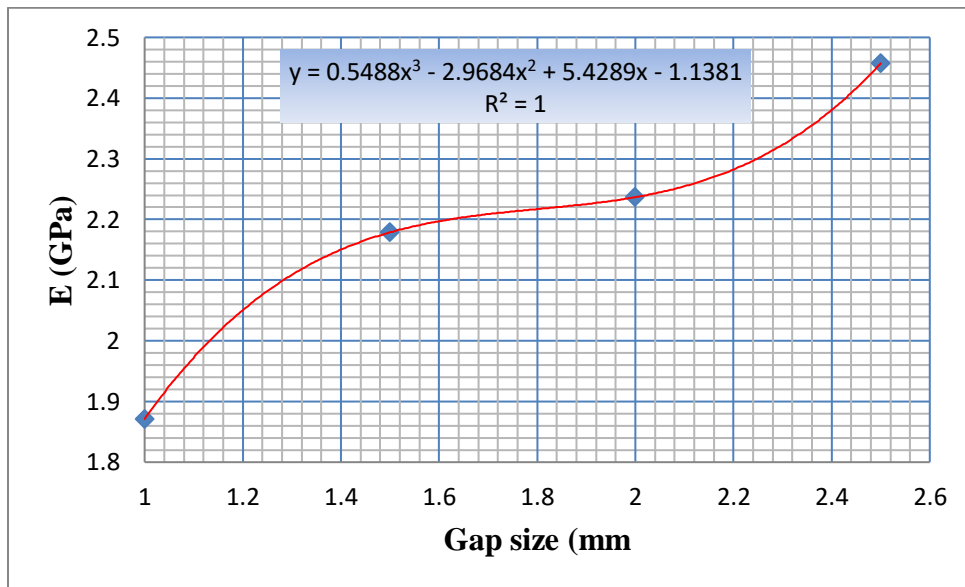


Figure 4.42: Young's modulus against gap size at 900 rpm and 12 elements

in general, brushing at 3 elements gave fibres with better properties. The colour was however brownish especially at low speeds and high gaps. Fibre breakages were too high at 12 elements and low gaps. Moreover, it was difficult to brush with 12 elements because the machine blew fibres away instead of sucking in. Sucking effect was especially good at 3 elements and partly at 6 elements. Therefore, 3 elements, gaps below 2 mm and speeds between 1000 to 1200 rpm were recommended for better brushing quality. Addition of more brushing elements like staggered pins further improved brushing quality (reduces microfibrillar angle).

4.4.4.4. Variation of properties with speed

The properties of the brushed fibres also varied with speed at constant gap sizes and number of brushing elements. The σ_u and E reduced with speeds whereas the ϵ increased slightly with speed.

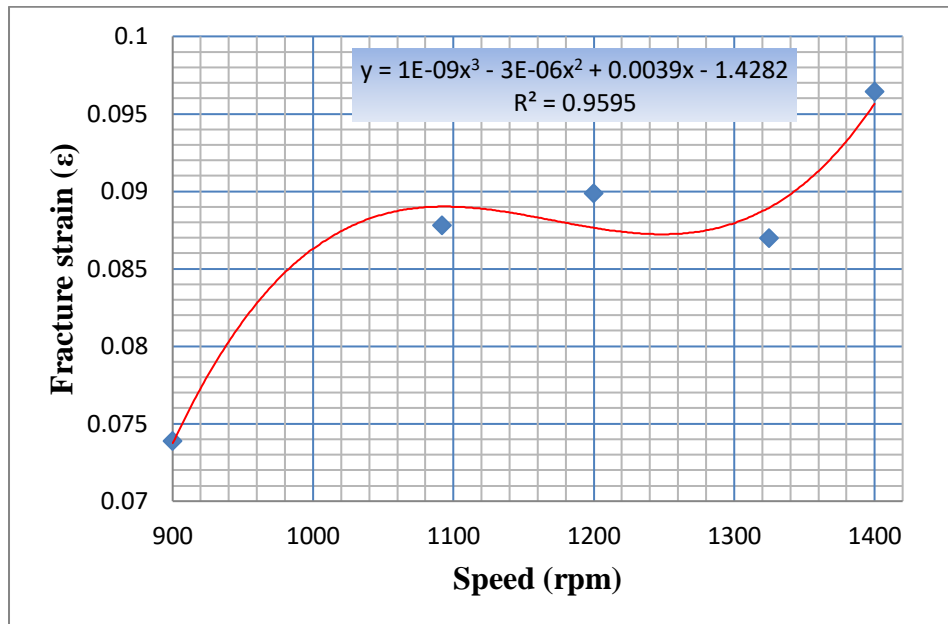


Figure 4.43: Fracture strain against speed at 2.5 mm gap size and 12 elements

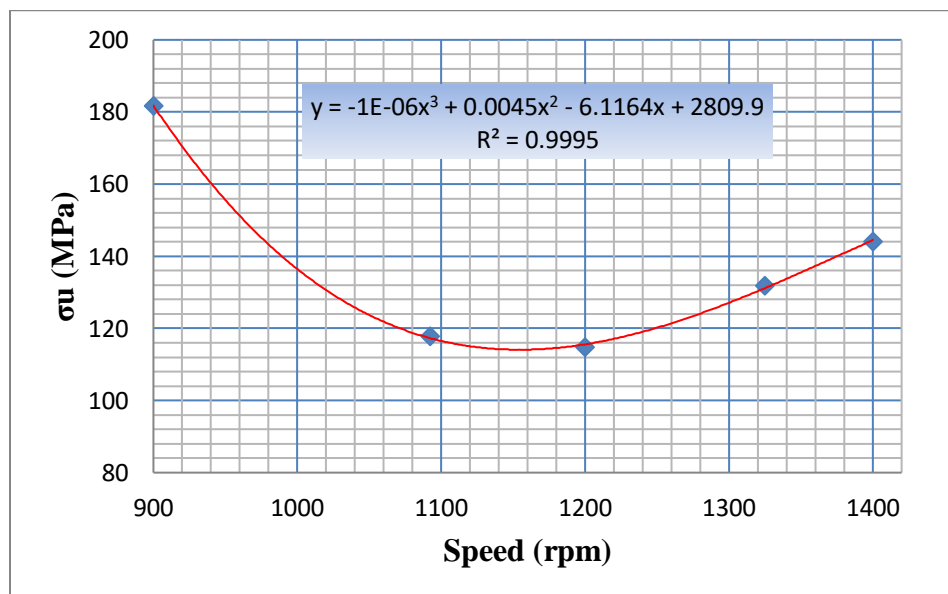


Figure 4.44: Fracture strength against speed at 2.5 mm gap size and 12 elements

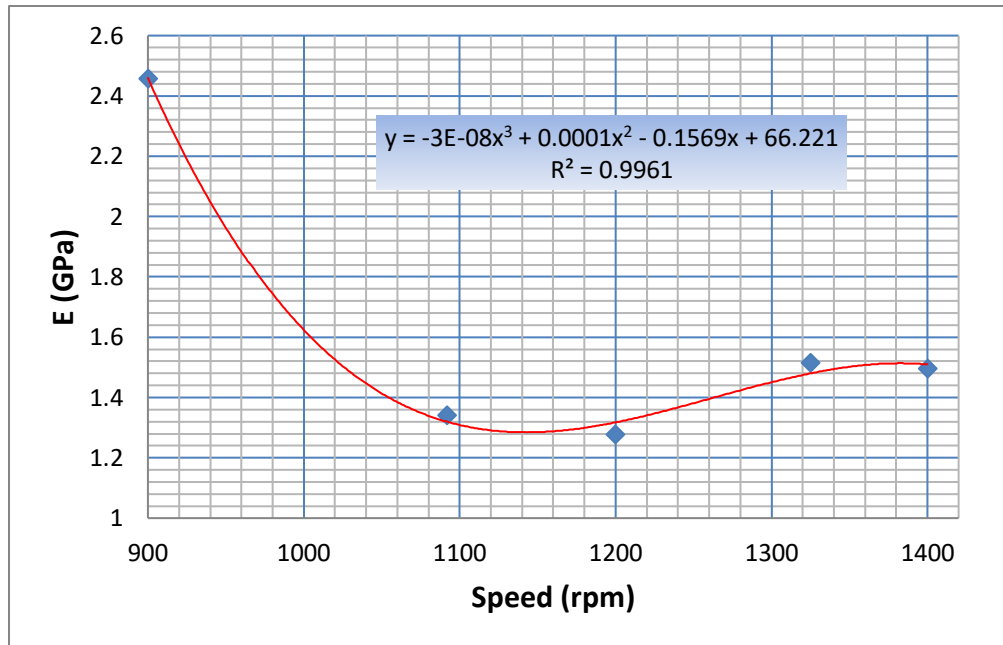


Figure 4.45: Young's modulus against speed at 2.5 mm gap size and 12 elements

The correlation coefficients between ϵ , σ_u and E and speeds were 0.9595, 0.9995 and 0.9961 respectively. These were very high implying that the brushing speed had a significant influence on the mechanical properties of brushed fibres. Therefore, more experiments were conducted to determine the lowest possible brushing speed.

4.4.4.5. Variation of properties with brushing elements at constant gap size and speed

The number of brushing elements also influenced the properties of sisal fibres. σ_u and E reduced with increase in number of brushing elements. ϵ , on the other hand, increased slightly with the number of elements (see Figure 4.46 and Figure 4.47).

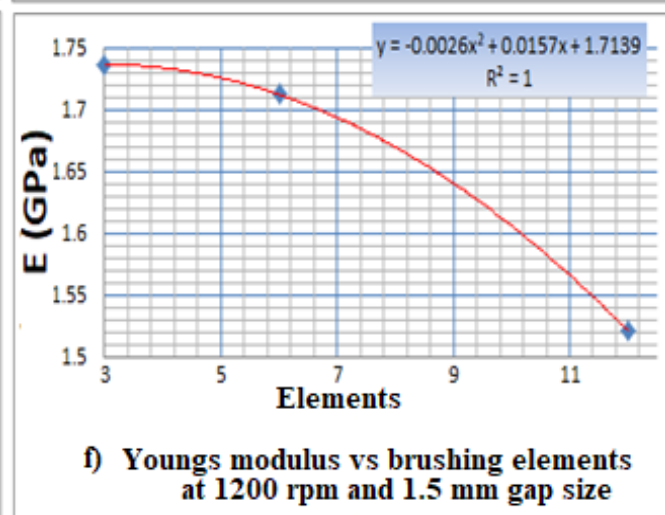
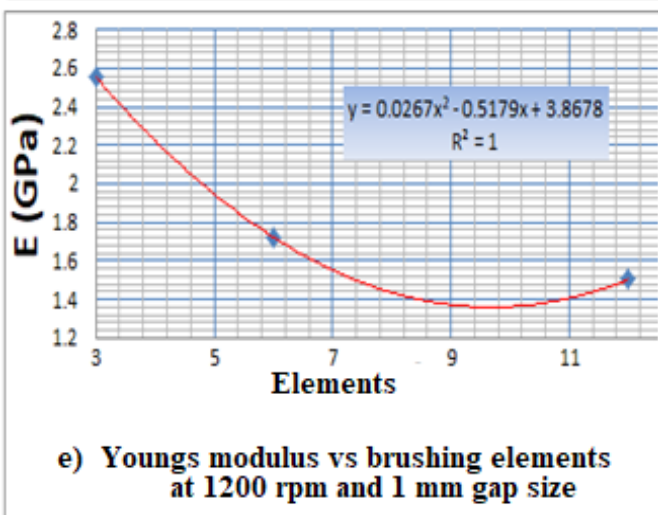
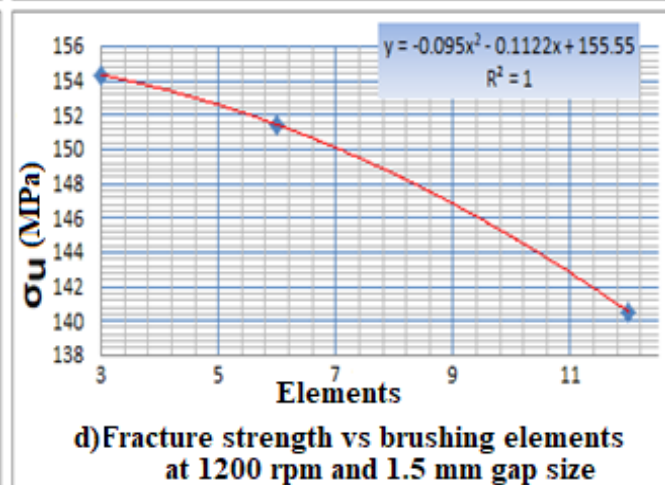
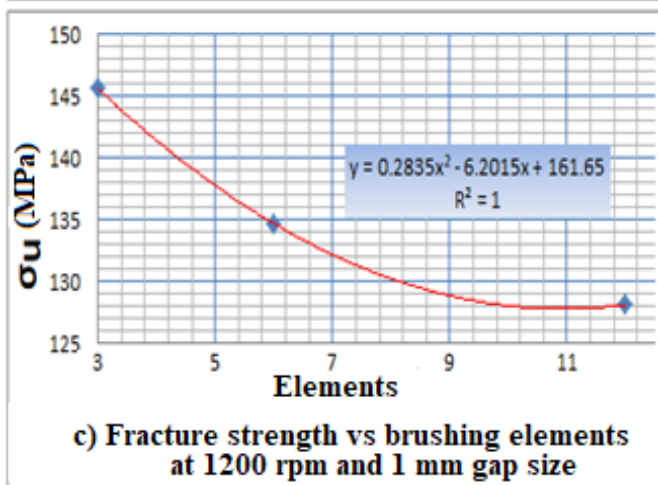
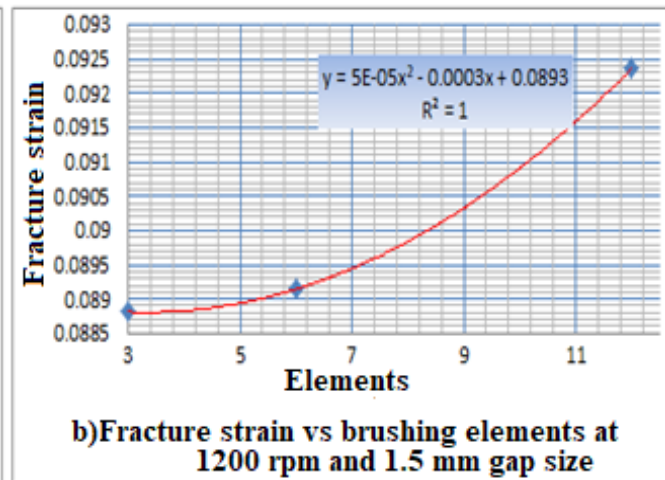
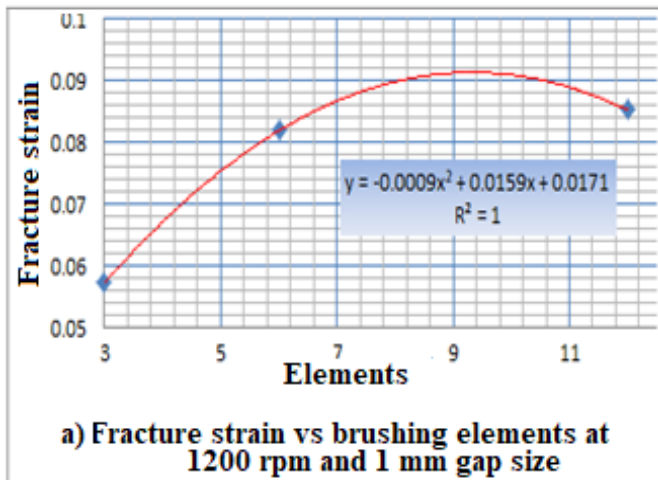


Figure 4.46: Variation of properties with number of elements at 1200 rpm for 1 mm and 2.5 mm gap size

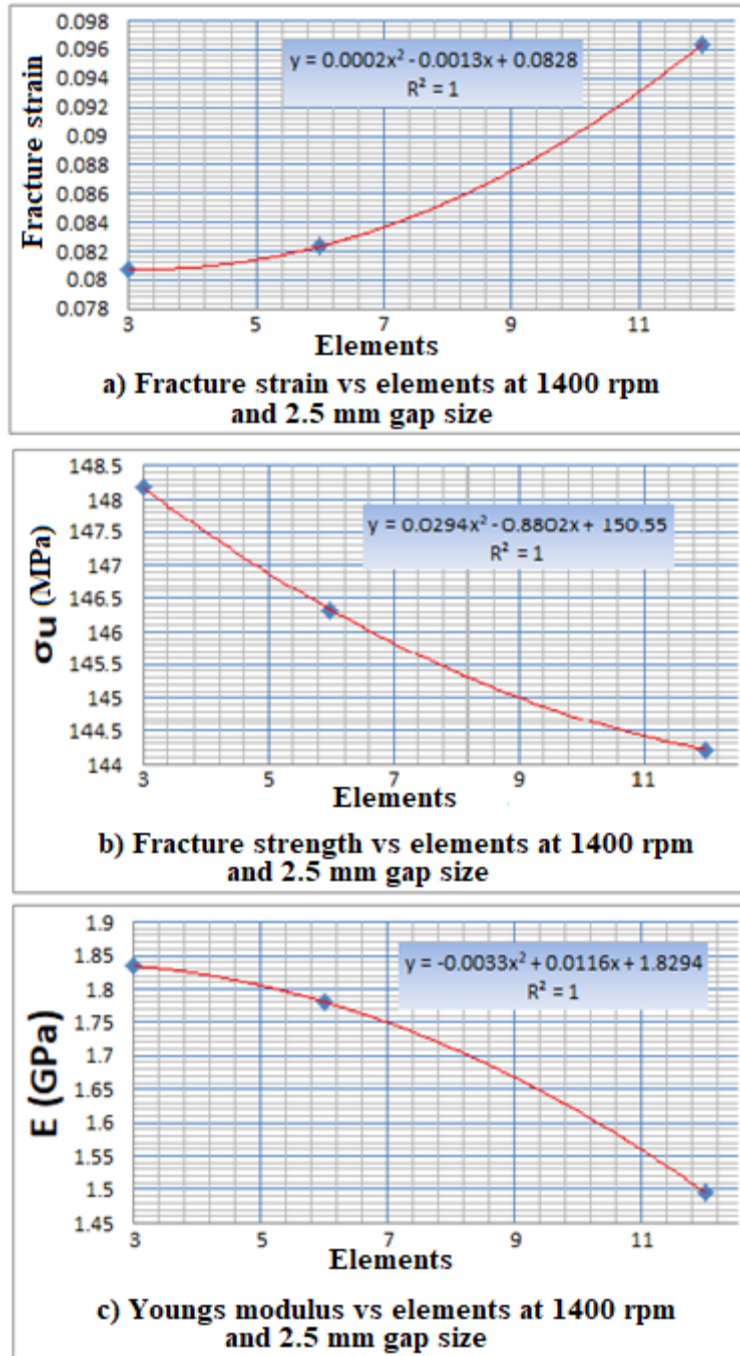


Figure 4.47: Variation of properties with number of elements at 1400 rpm and 2.5 mm gap

The correlation coefficient between the properties with the number of elements was also one for all cases. Therefore, it was observed that the properties of extracted sisal fibre were highly dependent on the number of elements. The σ_u and E of the brushed fibres reduced while ϵ increased slightly with number of elements. This was because decortication pitch is inversely related to the number of elements. When brushing pitch reduced the amount of materials brushed

every time a brushing element interacts with the fibre increased hence the fibres are subjected to higher stresses that reduce its mechanical property by debonding the microfibrils from the matrix, damaging the cuticle and reducing crystallinity.

Brushing at 12 elements was hampered by the blowing away of fibres. The machine could not suck in the fibres. This effect increased with increase in speed. Equally, the average fibre length was the lowest at 12 elements because of more fibre breakage. The mechanical properties were the poorest at 12 blades. There were many interactions between the fibres and the brushing elements that led to excessive grinding of fibres reducing crystallinity and tensile properties of the fibres. The quantity of fibres brushed per unit time was very low due to resistance offered by the machine. Brushing at 6 elements yielded averaged properties between 12 and 3 elements. The blowing away of fibres reduced and the fibre breakage was lower than at 12 elements. The colour of the brushed fibre was either pure white or white-brown depending on the gap size.

4.4.4.6. Machine brushing capacity

The machine was able to brush 1807.1g of dry fibre in 4 minutes and 24 seconds. The machine brushing capacity per hour was therefore determined as follows;

$$\text{Brushing Capacity} = \frac{1807.1}{4.4} \times 60 = 24,642.27 \text{ g/hr}$$

This capacity implied that all the sisal fibres extracted in 2 hours could be brushed comfortably in one hour. There was still room to brush more fibres per hour. The gap size could be adjusted to allow more fibres to be brushed per unit time. If a larger bunch of sisal fibre was to be brushed, then the gap size was increased accordingly to avoid curling and breaking of fibres. A research by Brenters that partly experimented on brushing did not report on the brushing capacity [15]. One advantage of this machine compared to Brenters [15] design was the fact that it made it possible to extract and brush sisal fibres simultaneously. Moreover, this design was very flexible given that both units could perform both roles if the right elements were mounted. To increase extraction capacity, the two units could perform extraction allowing two users at the same time by simply fitting two units with brushing elements. As it was also noticed, the thickness of the sisal leaf reduced towards the tail end and hence for a given gap size, the tail end was always poorly extracted. As a remedy, this machine was designed in such a way that the clearance reduced uniformly to allow tail end to be extracted at a lower gap. A summary of the results obtained can be seen in Table 4.13. The manually extracted fibres had superior properties

compared with Rea Vipingo or machine fibres. This was because in manual extraction, fibres are subjected to lesser extraction forces and the fibres are not brushed. Being estate sisal, Rea Vipingo fibres had the least properties. Therefore, in terms of properties, the fibres obtained by this machine were within the required international standard because they were comparable in quality to Rea Vipingo estate fibre.

Table 4.13: Summary of results

Variable	Manual	Rea Vipingo	Unbrushed fibre	Brushed fibre
Fracture strength, σ_u (MPa)	236.65	87.23	124.04	142.68
Elastic Modulus, E (GPa)	1.58	1.38	1.48	1.78
Fracture strain, ϵ	0.09	0.07	0.085	0.081
Fibre length, L (mm)	951.4	951.6	1031.3	955.2
Length ratio, L_R	0.89	-	0.912	0.9197
% Fibre yield (Wet)	6.44	-	11.94	-
% Fibre yield (Dry)	3.62	-	5.03	3.42
Fibre grade	UHDS	UG	UHDS	UG & above
Fibre weight/leaf (g)	20.14	20.87	30.37	20.65
Capacity (kg/hr)	0.375	-	10.8452	24.642
Power consumption (kW)	-	-	1.368	1.018
Fibre diameter (μm)	275.65	241.87	279.55	251.03

4.4.5. Optimized design specifications

From the results, it was observed that both power consumption and quality of processing increase with speed. However, the results obtained from other variables such as fibre length, colour and tensile properties, the optimum design specifications determined are; 6 (38*38*3 mm blade) extraction blades, 3 brushing elements (38*38*3 mm blades with 25 mm comping pins), drum speed of 1000 rpm, gap size of 1.5-2 mm for extraction and 2-3 mm for brushing, a prime mover with power rating of 3 HP, 20 mm diameter ISO standard shaft and ANSI/ASME 273.1 mm standard drum. The machine frame should be fabricated from 50*50*3 mm angle bars leaving just enough allowance for adjustment of gap sizes. The optimized design specifications will help in reducing the overall size, weight and cost of the machine.

4.5. Machine cost and revenue analysis

4.5.1. Machine costs

The machine costs were classified into fixed costs and operation costs. The fixed costs included costs that do not change with time or quantity whereas operation costs change with the number of products produced [45]. In this design, the following costs were considered and determined;

4.5.1.1. Fixed costs/ownership costs;

Cost of the machine; this was the total cost of purchasing the machine for a small-scale farmer. It was the total cost of fabricating the machine and the profit due to the manufacturer. The total costs for fabricating a field model of the machine were Kshs. 52,699.00 according to the costs of materials used (refer to Appendix B). It was assumed that if 50% of the fabrication cost accounts for manufacturer's net profit, income tax (charged at 20% of taxable income for a new listed company [46]) and other logistical costs and a 16% Value Added Tax (VAT), then the total production cost of the machine would be Kshs. 87,480.34.

Depreciation cost; the value of any machine deteriorates with time. The depreciation cost of this machine was estimated using the Pflueger's approach. equation (4.39).

$$\text{Depreciation cost (DC)} = \frac{\text{purchase price (PP)} - \text{Salvage value (SV)}}{\text{Useful life (n)}} \dots\dots\dots (4.39)$$

For farm machineries, a useful life of between 6 to 8 years is usually used [45]. The salvage value was determined using equation (4.40).

$$SV = PP(1 - i)^n \dots\dots\dots (4.40)$$

where *i* was the rate of depreciation.

A good approximation for depreciation rate is the interest offered by commercial banks [9]. This rate was 12.39% as of July 2019 [47].

$$SV = 87,480.34 \left(1 - \frac{12.39}{100}\right)^8 = \text{Kshs. } 30,362.67$$

Therefore, the depreciation cost for the machine was;

$$DC = \frac{87,480.34 - 30,362.67}{8} = \text{Kshs. } 7,139.71$$

Interest cost; Pflueger recommends that any investment in farm machinery needs capital and capital cost should be considered whether buying through a credit facility or not [45]. The interest cost for a machine was approximated using equation (4.41).

$$\text{Interest Cost (IC)} = \left(\frac{PP-SV}{2}\right) \times \text{rate of interest} \dots\dots\dots (4.41)$$

$$IC = \left(\frac{87,480.34 - 30,362.67}{2}\right) \times \frac{12.39}{100} = \text{Kshs. } 3,538.44$$

Insurance cost; it has been recommended that this cost should to be approximated at 2% of the cost of acquiring the machine [45].

$$\text{Insurance} = \frac{2}{100} \times 87,480.34 = \text{Kshs. } 1,749.61$$

Since the machine could easily be assembled and disassembled, its transportation and installation costs were approximated to be Kshs. 16,000. Therefore, the initial investment cost in this technology for the small-scale farmers would be Kshs. 115,908.10. This is also the total expense during project year 0 (see Table 4.14).

4.5.1.2. Operational costs

These are the costs incurred by the farmer while using the machine to process the sisal fibres. These included;

- **Labour;** the machine required at least three people to fully optimize it. Two of them were to handle the extraction and brushing and other one to deal with drying and transportation of sisal fibres. Therefore, it was assumed in the field four people would be needed to handle the operations. As of November 2019, the minimum wage for casual labourer in Kenya was Kshs. 13,572 per month [48]. For four operators, the labour cost per month would be Kshs. 54,288.
- **Raw materials;** the raw materials required are hedge sisal. Usually, sisal is grown on the hedges of farms and requires minimal tendering. However, for the sake of arriving at a better conclusion, it was assumed the costs would be incurred in hiring a casual labourer for cutting and tendering the hedge sisal. UNIDO’s research on small-scale sisal farming in Tanzania and Kenya found that on average the small farms are 2 ha, out of which 0.14 ha are under sisal on the edges of the farms [49]. The study came up with a *metre* (3300 sisal leaves) as a measure of amount of sisal for payment purposes. Moreover, it was established that there are 32.25 metres of sisal per ha [49]. In this study, the dry fibre production capacity of the machine was 10.845 kg/hr and the average weight of dry fibre from one sisal leaf was 30.37 g. This meant that the machine requires 2857 leaves per day (8 hours). Consequently, the machine would process 0.805 ha of sisal in 6 farms per month. It was estimated that one

casual worker is capable of working on two farms per month. Therefore, for 3 workers required per month, the total cost was Kshs. 40,716. This kind of farms are common in the rift valley and eastern regions (Figure 2.2). as an earlier research found [2].

- **Fuel and lubrication cost;** the fuel consumption per hour determined during laboratory testing to be 0.3 litres per hour. For a normal workday from 8 am to 5 pm with a one-hour lunch break, the total machine hours would be 8. As of 18th November 2019, the price of gasoline in Nairobi was Kshs. 112.68 per liter. Therefore, the total cost of fuel per day was;

$$\text{Fuel cost} = 0.3 \times 8 \times 112.68 = \text{Kshs. } 270.43/\text{day}$$

Lubrication cost for power machineries is approximated at 15% of the costs on fuel [45].

$$\text{Lubrication cost} = \frac{15}{100} \times 270.43 = \text{Kshs. } 40.56/\text{day}$$

- **Maintenance and repair;** for machines with a useful life of less than 5 years, the repair costs are approximated at 3% of the purchase price (PP) and a 5% is applied to machines that have replaceable components [45]. Brenters used 10% for a useful life of 14 years for a comparable technology in Tanzania [15]. A 10% of the PP for this machine was applied since it had replaceable parts and a useful life beyond 5 years.

$$\text{Repair and maintenance cost} = \frac{10}{100} \times 73,778.60 = \text{Kshs. } 7,377.86 \text{ per year}$$

The total operational costs amounted to Kshs. 903,819.22 per year.

4.5.2. Machine revenues for small scale farmers

The capacity of the machine was 10.84 kg/hr of dry fibre. This fibre would be conveniently brushed to UG or higher grades in at most one hour. Based on a past research on small-scale technology, it was noted that some working days will be needed for repair, maintenance and moving around the farms to minimize transportation of sisal leaves over longer distances [15]. Based on data from Tanzania on land subdivisions, which is not very much different from Kenya, it was established that it would take approximately 1 year to process sisal from 47 farms [15, 49]. It was recommended to spare 2 days each month for repair and maintenance. Assuming also that a farmer needs one day to move the machine from one farm to the other, then 47 days per year would be utilized for moving the machine.

If working for 6 days a week and taking into consideration days used for repairs, maintenance and moving around, the days spent processing the fibre per year would be 217. The last report

The discount rate averaged 15% since 3rd of October 2012. For the year 2019, for instance, the rate was 15% for all months. Based on this trend, it was assumed that this rate would still average 15% during the whole project useful life. NPV and IRR methods were used to determine the feasibility of the investment in technology.

$$NPV = \sum_{t=0}^n Q_t(1+r)^{-t} - \sum_{t=0}^n C_t(1+r)^{-t} \dots\dots\dots (4.42)$$

where,

Q_t = annual revenues

C_t = annual costs

t = year

r = discount rate

n = number of project yer as

Table 4.14: Projected cash flows for the project

Project Year	Cash inflow (Q _t) (Kshs.)	Cash outflow (C _t) (Kshs.)	Q _t (1+r) ^{-t}	C _t (1+r) ^{-t}	Q _t (1+r) ^{-t} - C _t (1+r) ^{-t}
0	0	115,908.10	0.00	115,908.1	-115,908.10
1	1,651,978.97	1,238,910.69	1,436,503.45	1,077,313.6	359,189.81
2	1,651,978.97	1,238,910.69	1,249,133.44	936,794.47	312,338.96
3	1,651,978.97	1,238,910.69	1,086,202.99	814,603.89	271,599.10
4	1,651,978.97	1,238,910.69	944,524.34	708,351.21	236,173.13
5	1,651,978.97	1,238,910.69	821,325.51	615,957.57	205,367.94
6	1,651,978.97	1,238,910.69	714,196.10	535,615.28	178,580.82
7	1,651,978.97	1,238,910.69	621,040.08	465,752.42	155,287.67
8	1,651,978.97	1,238,910.69	540,034.86	405,002.1	135,032.75

NPV	1,737,662.08
------------	---------------------

Since the NPV for the project was greater than 0, it implied that this investment made economic sense. Equally, the IRR was more than 100%, way above a recommended of 15%. Using the

payback method, it was determined how long it would take the project to recover the money invested through net cash earnings using equation (4.43) [33, 51];

$$I = \sum_{t=0}^P [F_t - D_t] \dots\dots\dots (4.43)$$

where;

I = the sum of initial investment

P = payback duration

F_t = yearly net profits during year t

D_t = yearly depreciation during year t

$F_t - D_t$ = the net cash returns in year t

Table 4.15: The payback period

Project Year	Net Profit (Ft)	Depreciation (Dt)	Ft-Dt	(Ft-Dt) cumulative
0	-115,908.10	0	-115908	-115908
1	413,068.28	6,021.45	407046.8	291138.7
2	413,068.28	6,021.45	407046.8	698185.6
3	413,068.28	6,021.45	407046.8	1105232
4	413,068.28	6,021.45	407046.8	1512279
5	413,068.28	6,021.45	407046.8	1919326
6	413,068.28	6,021.45	407046.8	2326373
7	413,068.28	6,021.45	407046.8	2733420
8	413,068.28	6,021.45	407046.8	3140467

The payback period was 1 year. Therefore, a farmer or group of farmers who invest in this machine will get back the investment in one year’s time. A net of Kshs. 291,138.70 in first year was more than the investment cost of Kshs. 115,908.10. The project was therefore deemed to be viable to the small-scale farmer.

4.6. Recommendations

- i) Because of financial challenge, the number of blades experimented were limited to 3, 6 and 12. There was a huge jump from 6 to 12 blades, meaning a lot of information remains undiscovered in between. It is recommended that more tests should be conducted at different blades to precisely optimise the number of blades required.
- ii) The study only assessed the economic viability of the machine from a perspective of the small-scale farmers due to financial and time constraints. It is strongly recommended that a thorough economic viability should also be conducted to establish if the project makes economic sense to the manufacturer of the machines.
- iii) The study recommends that further studies should be conducted to determine whether it is possible to incorporate a detachable spinning unit on the machine to further increase the income of the farmers through value addition.
- iv) The study also recommends that a detailed structural analysis should be conducted to determine the dynamic and static loads on the machine frame and the processing loads on the fibre to aid in further optimizing the frame and drum of the raspador. This can be aided through the application of finite element analysis.

CHAPTER FIVE: CONCLUSION

A small-scale machine for extraction and brushing sisal fibres was designed, fabricated and tested. The extraction and brushing capacities of the machine are 10.84 kg/hr and 24.64 kg/hr respectively. The power consumed varies with the processing speed and increases by 16% due to addition of a brushing unit. The quality of processing varies with gap size, speed and number of blades/elements. The tensile properties of extracted and brushed sisal fibres strongly correlate with the drum speed, gap size and number of blades/brushing elements. The best parameters for extraction and brushing of sisal fibres are 6 blades, 1000 - 1200 rpm drum speed and 1.5 - 2 mm gap size and 3 brushing elements, 1000 - 1200 rpm drum speed and between 2 - 3 mm gap size respectively. The optimized specifications to reduce the size, weight and cost of the raspador are 6 blades, 3 brushing elements, drum speed 1000 rpm, gap size of 1.5-2 mm for extraction and 2-3 mm for brushing, 3 HP power source, 273.1 mm outer diameter ASME standard drum and 20 mm ISO shaft. Brushing greatly improved the properties of processed fibres and are comparable to properties of estate fibre. Although the tensile properties of manually extracted fibre are higher than the raspador's or estate's fibre, its grade is the lowest due to lack of brushing. The total cost of the machine is Kshs. 115,908.10 and makes economic sense to the small-scale farmers because of a positive NPV obtained. Finally, this research has contributed to the body of knowledge with regard to development of small-scale decortication technology and quantification of the effects of processing methods on properties of natural fibres.

REFERENCES

- [1] V. A. Kayumba, M. Bratveit, Y. Mashalla, and B. E. Moen, 'Acute Respiratory Symptoms among Sisal workers in Tanzania', *Occupational Medicine*, vol. 57, no. 4, pp. 290–293, 2007, doi: 10.1093/occmed/kqm004.
- [2] M. F. Oduori, 'Development and Laboratory Testing of a Full-scale Raspador Decorticator', University of Nairobi, Nairobi, Kenya, 2002.
- [3] R. W. Githire, 'An Economic Analysis of the Kenyan Sisal Industry', MSc, University of Nairobi, 1987.
- [4] A. Cantalino, E. Torres, and M. Silva, 'Sustainability of Sisal Cultivation in Brazil Using Co-Products and Wastes', *Journal of Agriculture Science*, vol. 7, no. 7, pp. 64–74, 2015, doi: 10.5539/jas.v7n7p64.
- [5] AFA, 'Sisal Market Analysis Report', Fibre Crops Directorate, Nairobi, Kenya, 2018.
- [6] UNIDO, *Past Research Results and Present Production Practices in East Africa*. Viena: UNIDO, 2001 [Online]. Available: www.common-fund.org. [Accessed: 01-May-2018]
- [7] M. F. Oduori, 'Design and Experimental Data on Sisal Decorticator Laboratory Model Machine', University of Nairobi, 2016.
- [8] FAO, 'Future Fibres', *Sisal*, 2016. [Online]. Available: <http://www.fao.org/economic/futurefibres/fibres/sisal/en/>. [Accessed: 20-Jul-2016]
- [9] J. Brenters, 'Design and Financial Assessment of Small-Scale Sisal Decortication Technology in Tanzania in Technology and Development Studies', MSc, Eindhoven University of Technology, 2000.
- [10] EPZ, 'Kenya's Sisal Industry 2005 Report', Export Processing Zones Authority, Nairobi, 2005.
- [11] W. G. Clasen, 'Sisal Market Report: November 2015 - April 2016', WGC (Natural Fibres Worldwide), 2016 [Online]. Available: www.wgc.de. [Accessed: 07-Sep-2016]
- [12] TIPS, 'Fibre', Australian Agency for International Development (AUSAID), 2015.
- [13] FAO, 'International Year of Fibres', Food and Agriculture Organization, Rome, Italy, C2007/15, 2009 [Online]. Available: www.naturalfibres2009.org
- [14] G. J. Van and H. Toussaint, 'Biomechanics: Classical Mechanics Applied to Human Movement', Vrije University, Amsterdam, 1994.

- [15] J. Brenters, 'Design and Financial Assessment of Small-Scale Sisal Decortication Technology in Tanzania', MSc, Eindhoven University of Technology, 2000.
- [16] J. B. Kawongolo, J. Sentong-Kibalama, and L. Brown, 'Design of a Decorticator for Small Scale Sisal Processing in Uganda', Chicago, USA, 2002.
- [17] H. M. Kanogu, A. V. Osore, and J. K. Kiguru, 'Development of a Sisal Decortication for Small Holder Farmers/Traders: Redesign, Fabrication and Field Testing', University of Nairobi, Nairobi, 2011.
- [18] B. J. Snyder, J. Bussard, J. Dolak, and T. Weister, 'A Portable Sisal Decorticator for Kenyan Farmers', *International Journal for Science Learning in Engineering*, vol. 2, no. 1, pp. 92–116, 2006.
- [19] T. Ahmad, H. S. Mahmood, Z. Ali, M. A. Khan, and S. Zia, 'Design and Development of a Portable Sisal Decorticator', *Pakistan Journal of Agricultural Research*, vol. 30, no. 3, pp. 209–217, 2017.
- [20] K. Naik, R. P. Swamy, and P. Naik, 'Design and Fabrication of Areca Fiber Extraction Machine', *International Journal of Emerging Technology and Advanced Engineering*, vol. 4, no. 7, 2014.
- [21] T. Phologolo, C. Yu, J. I. Mwasiagi, N. Muya, and Z. F. Li, 'Production and Characterization of Kenyan Sisal', *Asian Journal of Textile*, vol. 2, no. 2, pp. 17–25, 2012, doi: 10.3923/ajtl.2012.17.25.
- [22] 'The London Sisal Association', 2016. [Online]. Available: <http://www.londonsisalassociation.org/>. [Accessed: 14-Nov-2016]
- [23] A. Abera Betelie *et al.*, 'Mechanical Properties of Sisal-epoxy Composites as Functions of Fiber-to-epoxy ratio', *AIMS Materials Science*, vol. 6, no. 6, pp. 985–996, 2019, doi: 10.3934/matensci.2019.6.985.
- [24] P. K. Sahoo, P. K. Rana, N. D. Sarkar, A. Sahoo, and S. K. Swain, 'Characterization and Properties of Chemically Modified Corchorus Capsularis Jute Fiber via Pulping and Grafting', *Journal of Polymer Science*, vol. 41, no. 17, pp. 2696–2703, Sep. 2003, doi: 10.1002/pola.10813.
- [25] M. R. Abir, S. M. Kashif, and A. Razzak, 'Tensile and Statistical Analysis of Sisal Fibres for Natural Fibre Composite Manufacture', *AMR*, vol. 1115, pp. 349–352, 2015, doi: 10.4028/www.scientific.net/AMR.1115.349.

- [26] N. Jain, M. Banerjee, and S. Sanyal, 'Effect of Fiber Length Variations on Properties of Coir Fiber Reinforced Cement-Albumen Composite (CFRCC)', *IIUM Engineering Journal*, vol. 12, 2012.
- [27] F. A. Silva, N. Chawla, and R. D. Filho, 'Tensile Behavior of High Performance Natural (sisal) Fibers', *Composites Science and Technology*, vol. 68, pp. 3438–3443, 2008.
- [28] S. M. Kashif, S. M. Ibrahim, A. M. Razzak, and M. Azram, 'Study of the Effect of Different Curing Setups on Mechanical Properties of Low-cost Composite Structures', in *ICMAAE*, 2013, pp. 2–4.
- [29] M. E. Fidelis, T. V. Pereira, O. Gomes, F. de A. Silva, and R. D. Filho, 'The Effect of Fiber Morphology on the Tensile Strength of Natural Fibers', *Journal of Materials Research and Technology*, vol. 2, pp. 149–157, 2013, doi: 10.1016/j.jmrt.2013.02.003.
- [30] A. Belaadi, A. Bezazi, M. Bourchak, and F. Scarpa, 'Tensile Static and Fatigue Behavior of Sisal Fibers', *Materials and Design*, vol. 46, pp. 76–83, 2013.
- [31] S. M. Mutuli, T. J. Bessell, and E. S. J. Talitwala, 'The Potential of Sisal as a Reinforcing Fibre in Cement Base Materials.', *African journal of science and technology (ANST)*, vol. 1, no. 1, pp. 5–16, 1982.
- [32] D. S. Clifton and D. E. Fyffe, *Project Feasibility Analysis: A Guide to Profitable New Ventures*. New York: John Wiley & Sons Inc, 1977.
- [33] P. Katimuneetorn, 'Feasibility Study for Information Systems Projects', University of Missouri- St. Louis, Fall 2008 [Online]. Available: http://en.wikipedia.org/wiki/Systems_Development_Life_Cycle. [Accessed: 14-Nov-2016]
- [34] N. Garret, N. Tasharra, and Nguyen, 'Conducting a Feasibility Analysis and Crafting a Winning Business Plan'. 27-Feb-2012.
- [35] R. Overton, *Feasibility Studies Made Simple*. Boat Harbour, Australia: Martin Books, 2007.
- [36] R. Sascha, 'The Net Present Value Rule in Comparison to the Payback and Internal Rate of Return Methods'. 02-Oct-2008.
- [37] B. U. Oreko, S. Okiy, E. Emagbetere, and M. Okwu, 'Design and Development of Plantain Fibre Extraction Machine', *Nigerian Journal of Technology (NIJOTECH)*, vol. 37, no. 2, pp. 397–406, 2018.
- [38] R. S. Khurmi, *Strength of Materials: (mechanics of solids): (SI units)*, 23rd ed. New Delhi: S. Chand & Co., 2007.

- [39] J. Shigley, C. Mischke, and T. Brown, *Standard Handbook of Machine Design*, 3rd ed. Pennsylvania: McGraw Hill Professional, 2004.
- [40] ASTM, ‘ASTM C1557 - 14: Standard Test Method for Tensile Strength and Young’s Modulus of Fibres’. ASTM International, 2018.
- [41] F. Roulunds, ‘Design Manual; The Quality Choice for any Transmission’, Denmark, 2004.
- [42] P. Srinivasakumar, M. J. Nandan, U. C. Kiran, and K. P. Rao, ‘Sisal and its Potential for Creating Innovative Employment Opportunities and Economic Prospects’, *Journal of Mechanical and Civil Engineering (IOSR-JMCE)*, vol. 8, no. 6, pp. 1–8, Oct. 2013.
- [43] M. W. Kithiia, M. D. Munyasi, and M. S. Mutuli, ‘Strength Properties of Surface Modified Kenyan Sisal Fibres’, *Journal of Natural Fibers*, pp. 1–11, 2020, doi: 10.1080/15440478.2020.1807446.
- [44] W. P. Inacio, F. P. D. Lopes, and S. N. Monteiro, ‘Diameter Dependence of Tensile Strength by Weibull Analysis: Part III sisal fiber’, *Matéria (Rio de Janeiro)*, vol. 15, no. 2, pp. 124–130, 2010, doi: 10.1590/S1517-70762010000200006.
- [45] B. Pflueger, ‘How to Calculate Machinery Ownership and Operating Costs’, presented at the Extension Circulars. Paper 485, 2005 [Online]. Available: http://openprairie.sdstate.edu/extension_circ/485
- [46] EY, ‘Manufacturing Sector in Kenya’. 2018 [Online]. Available: https://www.google.com/url?sa=t&source=web&rct=j&url=https://www.ey.com/Publication/vwLUAssets/EY-taxation-in-the-manufacturing-sector-in-kenya/%24FILE/EY-taxation-in-the-manufacturing-sector-in-kenya.pdf&ved=2ahUKEwiis5L5lftPAhVQCxoKHU7FDgEQFjACegQIAhAB&usg=AOvVaw054MEr__0A6DSkmpqhmlpC. [Accessed: 18-Feb-2020]
- [47] ‘Kenya Bank Lending Rate | 2019 | Data | Chart | Calendar | Forecast | News’, 2019. [Online]. Available: <https://tradingeconomics.com/kenya/bank-lending-rate>. [Accessed: 19-Nov-2019]
- [48] ‘Trading Economics | 20 Million Indicators from 196 Countries’, 2019. [Online]. Available: <https://tradingeconomics.com/>. [Accessed: 19-Nov-2019]
- [49] G. O. Seng’enge, ‘A Study on Existing and Previously Aborted Smallholder Farming Systems for Sisal -both Cash Crop and Hedge-Sisal- used by Farmers in Tanzania and Kenya’, UNIDO, Mara, Tanzania, 1998.

- [50] CBK, 'Discount Window | Central Bank of Kenya', 2019. [Online]. Available: <https://www.centralbank.go.ke/rates/discount-window/>. [Accessed: 21-Nov-2019]
- [51] UNIDO, *Manual for Evaluation of Industrial Projects / prepared Jointly by the United Nations Industrial Development Organization and the Industrial Development Centre for Arab States. - Version details*. UNIDO PUBLICATION, 1987 [Online]. Available: <http://trove.nla.gov.au/version/21559129>. [Accessed: 14-Nov-2016]

APPENDICES

Appendix A: Necessary data for the design of belt drive and sheaves and frame

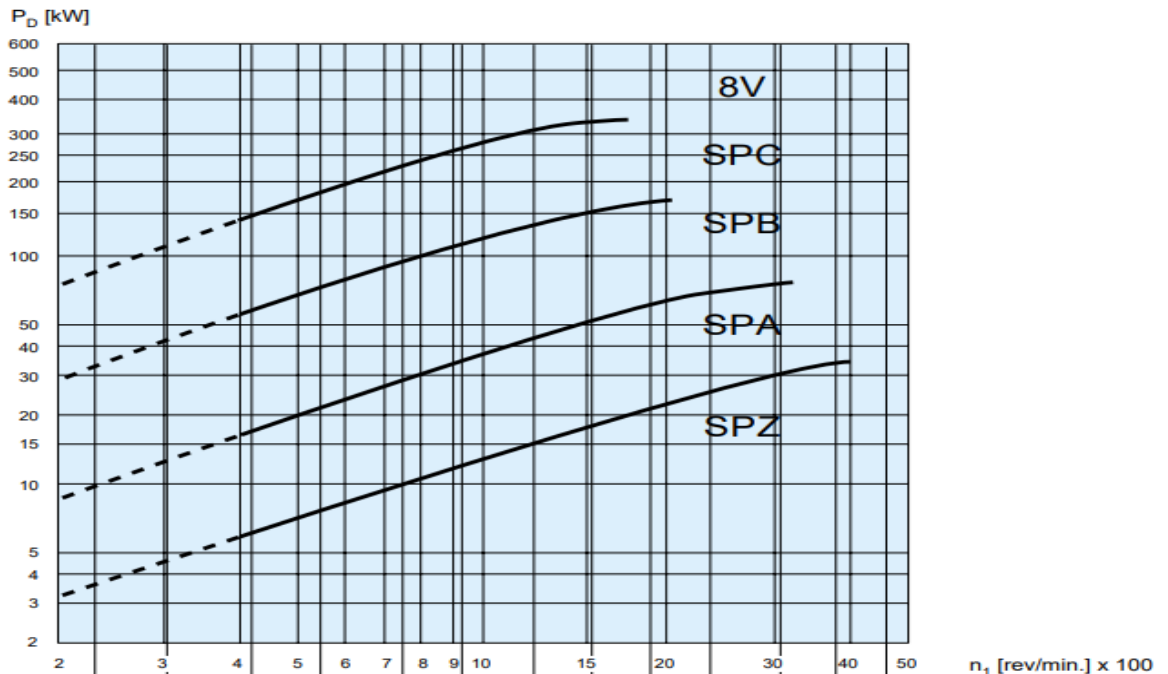
A-1: Service factor

Table 1, Service factor c_1

Driven unit	Driving unit / Motor					
	AC motors, single- and three-phase with star-delta start. DC shunt-wound motors. Multiple cylinder internal combustion engines.			AC motors, single- and three-phase, series wound, slip-ring motors with direct start. DC motors, series and compound wound. Single cylinder internal combustion engines.		
	Number of operating hours per 24 hours			Number of operating hours per 24 hours		
	Up to 10	Over 10 to 16	Over 16	Up to 10	Over 10 to 16	Over 16
Agitators for liquids. Small centrifugal blowers. Fans up to 7.5 kW. Light-duty conveyors.	1.0	1.1	1.2	1.1	1.2	1.3
Belt conveyors for sand, grain, etc. Dough mixers. Fans over 7.5 kW. Generators. Washing machines. Machine tools. Punching, pressing and shearing machines. Printing machines. Positive displacement rotary pumps. Vibrating and rotary screens.	1.1	1.2	1.3	1.2	1.3	1.4
Brick-making machinery. Bucket elevator. Piston compressors. Screw conveyors. Hammer mills. Hollanders. Piston pumps. Positive displacement blowers. Crushers. Woodworking machinery. Textile machinery.	1.2	1.3	1.4	1.4	1.5	1.6
Gyratory and jaw-roll crushers. Mills (ball/rod). Hoists (heavy loads). Rolling mills, calenders etc. for the rubber and plastics industries.	1.3	1.4	1.5	1.5	1.6	1.8

A-2: Selection of belt Section

Diagramme 2, Program 11, ROFLEX narrow V-belts



A-3: Minimum Pulley diameter

Table 2, Standard diameters [mm]

Classical V-belt sections	Z ZX 10 10X	A AX 13 13X	B BX 17 17X		20	C CX 22 22X	25	D 32	E 40
Narrow V-belt sections	SPZ XPZ	SPA XPA	SPB XPB	S19		SPC XPC			
Datum- diameter [mm]	40 50 56	50							
	63 71 80	63 71 80	80						
	90 100 112	90 100 112	100 112						
	125 132	118 125 132	125						
	140 150 160	140 150 160	140 150 160		140 160	140 160			
	180 200	180 190 200	180 190 200	180 190 200	180 200	180 190 200			
	224	224 236	224 236	212 224	224	212 224 236	224		
	250 280 300	250 280 300	250 280 300	250 280	250 280	250 280 300	250 280	280	
	315 355 400	315 355 400	315 355 400	315 355 400	315 355 400	315 355 400	315 355 400	315 355 400	
	450 500 560	450 500 560	450 500 560	450 500 560	450 500 560	450 500 560	450 500 560	450 500 560	450 500 560
	630	630	600 630	630	630	600 630	630	600 630	600 630 670
	800	710 800	710 750 800	710 800	710 800	710 750 800	710 800	710 750 800	710 800
		1000	900 1000 1120	900 1000 1120	900 1000 1120	900 1000 1120	900 1000 1120	900 1000 1120	900 1000 1120
			1250	1250 1400	1250 1400	1250 1400	1250 1400	1250 1400 1500	1250 1400 1500
				1600 1800 2000	1600 1800 2000	1600 1800 2000	1600 1800 2000	1600 1800 2000	1600 1800 2000

A-4: Recommended maximum belt speed

Section designation	Section dimension $W \times T$ [mm] -	Datum width W_d [mm]	Datum belt length $L_d \Rightarrow L_d^-$ [mm]	Datum belt length $L_d \Rightarrow L_d^+$ [mm]	Outside belt length $L_o \Rightarrow L_o^+$ [mm]	Effective belt length $L_e \Rightarrow L_e^-$ [mm]	Inside belt length $L_i \Rightarrow L_i^-$ [mm]	Inside belt length $L_i \Rightarrow L_i^+$ [mm]	Min. pulley datum-diameter d_d [mm]	Recom. max. deflection-diameter d_g [mm]	Max. deflection freq. f [Hz]	Weight [kg/m] -
---------------------	---------------------------------------	------------------------	--	--	--	--	---	---	---------------------------------------	--	--------------------------------	-----------------

ROFLEX RE-X NARROW V-BELTS ISO 4184, BS 3790, DIN 7753/1

PROGRAMME 10

XPZ	9,7 × 8	8,5		13				50	50	120	0,065
XPA	12,7 × 9	11		18			63	0,105			
XPB	16,3 × 13	14		22			100	0,190			
XPC	22 × 18	19		30			160	0,325			

ROFLEX NARROW V-BELTS ISO 4184, BS 3790, DIN 7753/1, RMA-MPTA IP-22

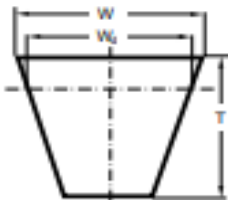
PROGRAMME

SPZ	9,7 × 8	8,5	37	13	37	63		42	100	0,065
SPA	12,7 × 10	11	45	18	45	90				0,115
SPB	16,3 × 13	14	60	22	60	140				0,200
SPC	22 × 18	19	83	30	83	224				0,350
S19	18,6 × 15	16	69	25	69	180				0,275
3V/9N	9 × 8		4		4		67			
6V/15N	15 × 13		11		11		180			
8V/25N	25 × 23		16		16		315			0,520

ROFLEX-X NARROW V-BELTS ISO 4184, BS 3790, DIN 7753/1

PROGRAMME 12

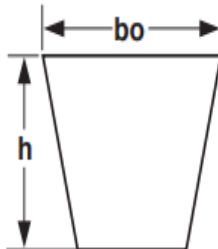
XPZ	9,7 × 8	8,5		13				50	50	120	0,060
XPA	12,7 × 9	11		18			63	0,100			
XPB	16,3 × 13	14		22			100	0,180			
XPC	22 × 18	19		30			160	0,320			



A-5: Standard belt lengths

Standard Belt Sizes

Narrow V-Belts for DIN7753 / ISO4184



Section	bo (mm)	h (mm)
SPZ (SPZX)	9.7	8.0
SPA (SPAX)	12.7	10.0
SPB (SPBX)	16.3	13.0
SPC (SPCX)	22.0	18.0

Belt indication

SPZ 1000

Cross Section

Datum length(mm)

Table 1-7

SPZ(SPZX)-Section				SPA(SPAX)-Section				SPB(SPBX)-Section				SPC(SPCX)-Section	
Datum length Ld(mm)	Outer length La(mm)	Datum length Ld(mm)	Outer length La(mm)	Datum length Ld(mm)	Outer length La(mm)	Datum length Ld(mm)	Outer length La(mm)	Datum length Ld(mm)	Outer length La(mm)	Datum length Ld(mm)	Outer length La(mm)	Datum length Ld(mm)	Outer length La(mm)
487	500	1520	1533	732	750	2132	2150	1250	1272	4620	4642	2000	2030
512	525	1537	1550	742	760	2182	2200	1320	1342	4720	4742	2120	2150
562	575	1562	1575	757	775	2232	2250	1340	1362	4750	4772	2360	2390
587	600	1587	1600	782	800	2240	2258	1400	1422	4820	4842	2500	2530
612	625	1600	1613	800	818	2307	2325	1410	1432	4870	4892	3100	3130
630	643	1612	1625	807	825	2360	2378	1500	1522	5000	5022	3150	3180
637	650	1637	1650	832	850	2432	2450	1510	1532	5070	5092	3200	3230
662	675	1662	1675	850	868	2482	2500	1590	1612	5300	5322	3220	3250
670	683	1687	1700	857	875	2500	2518	1600	1622	5380	5402	3320	3350
687	700	1700	1713	882	900	2607	2625	1690	1712	5500	5522	3350	3380
710	723	1737	1750	900	918	2650	2668	1700	1722	5600	5622	3375	3405
722	735	1762	1775	907	925	2800	2818	1750	1772	5680	5702	3420	3450
737	750	1787	1800	932	950	3000	3018	1800	1822	5800	5822	3430	3460
750	763	1800	1813	950	968	3082	3100	1850	1872	5990	6012	3450	3480
760	773	1812	1825	957	975	3132	3150	1900	1922	6000	6022	3500	3530
762	775	1837	1850	967	985	3150	3168	1950	1972	6300	6322	3520	3550

1
Properties



PULLEY DIAMETERS, standard

The recommended minimum pulley diameter is listed in the power rating table for belt programmes 10, 11 and 12.

When converting the belt section according to the RMA/MPTA standard into SP and XP, then:

3V/9N ≈ SPZ 5V/15N ≈ SPB
3VX ≈ XPZ 5VX ≈ XPB

For further information, please refer to the US standard RMA/MPTA IP-22.

A-6: Correction supplement 2b_d

Table 2a Correction supplement 2b_d [mm]

Pitch-diameter calculation:

Pitch-diameter d_p = datum-diameter d_d + 2b_d [mm]

Programme	V-belt section								
	Z ZX 10 10X SPZ XPZ	A AX 13 13X SPA XPA	B BX 17 17X SPB XPB	S19	20	C CX 22 22X SPC XPC	25	D 32	E 40
10, 12, 16, 17	0	1.7	3.2			5.5			
11	-1.4	0	0	1.8		2.5			
15	1.2	2.8	1.2		2.4	4.8	3.4	4.8	3.2

A-7: Adjustment factors for centre distance (x and y adjustments)

Finding y and x adjustment factors for determining actual centre distance C_a

Table 4 ROFLEX V-belts programmes 10, 11, 12, 15, 16, 17.

Datum belt length L _d [mm]	Minimum adjustment y [mm]											Minimum take-up x [mm]
	SPZ XPZ 3V A/13 AX 13X	SPA XPA	SPB XPB 5V 20	SPC XPC	Z/10 ZX 10X	B/17 BX 17X	C/22 CX 22X	25 S19	D/32	E/40	8V	All sections
≤ 670	16	19			13	20						10
> 670 - 1000	18	21			14	21	27					10
> 1000 - 1320	19	22	27		16	23	29				43	13
> 1320 - 1662	21	24	29		18	25	30				44	17
> 1662 - 2240	24	27	32	39	21	28	33	36	41		47	22
> 2240 - 3000	28	31	35	43	24	31	37	40	45		51	30
> 3000 - 3550	30	33	38	46	27	34	40	43	48		54	36
> 3550 - 4500	35	38	43	51	32	39	44	48	52	62	59	45
> 4500 - 5600	41	44	48	56	37	44	50	53	58	67	64	56
> 5600 - 6700	46		54	62		50	55	59	63	73	70	67
> 6700 - 8500	55		63	71		59	64	68	72	82	79	85
> 8500 - 10000			70	78		66	72	75	80	89	86	100
> 10000 - 11800			79	87		75	81	84	89	98	95	118
> 11800 - 13500			88	96		84	89	93	97	107		135
> 13500 - 15000			95	103		91	97	103	105	114		150
> 15000 - 16100			101	109		97	102	106	110	120		160

A-8: Standard sheaves widths

USEFUL INFORMATION


TABLE 8: STANDARD NUMBER OF GROOVES AVAILABLE FROM STOCK

Section	Number of grooves
A	1, 2
AB	1, 2, 3, 4, 5, 6, 7, 8, 10
C	1, 2, 3, 4, 5, 6, 7, 8, 9, 10, 12
D	3, 4, 5, 6, 8, 10, 12
3V	1, 2, 3, 4, 5, 6, 8, 10
5V	2, 3, 4, 5, 6, 7, 8, 9, 10
8V	4, 5, 6, 8, 10, 12

TABLE 9: STANDARD SHEAVE FACE WIDTHS (in inches)

	1	2	3	4	5	6	7	8	9	10	11	12	Distance between 2 grooves
A	0.75	1.375	2	2.625	3.25	3.875	4.5	5.125	5.75	6.375	7	7.625	0.63
B	*1	1.75	2.5	3.25	4	4.75	5.5	6.25	7	7.75	8.5	9.25	0.75
C	1.375	2.375	3.375	4.375	5.375	6.375	7.375	8.375	9.375	10.375	11.375	12.375	1
D	1.75	3.187	4.625	6.062	7.5	8.937	10.375	11.813	13.25	14.688	16.125	17.563	1.44
3V	*0.812	1.093	1.5	1.906	2.312	2.718	3.125	3.531	3.937	4.344	4.75	5.156	0.41
5V	1	1.687	2.375	3.062	3.75	4.437	5.125	5.812	6.5	7.187	7.875	8.562	0.69
8V	1.5	2.625	3.75	4.875	6	7.125	8.25	9.375	10.5	11.625	12.75	13.875	1.125

*B: 7/8 up to 7.15 O.D. and 1 in. thereafter
 *3V: 11/16 up to 10.6 O.D. and 13/16 in. thereafter

 Non standard products

A-9: Power ratings per belt

POWER RATINGS

optibelt SK PROFILE SPZ, 3V/9N, 3V/9J

NOMINAL POWER RATING P_N [kW]

FOR $\beta = 180^\circ$ AND $L_d = 1600$ mm



Table 41

Pulleys	v [m/s]	n_k [min ⁻¹]	Datum diameter of small pulley d_{sk} [mm]																Additional power [kW] per belt for speed ratio λ		
			63	71	80	85	90	95	100	112	125	132	140	150	160	180	200	to 1.01	to 1.06	to 1.27 > 1.57	
5	700	0.50	0.68	0.88	1.00	1.11	1.22	1.33	1.60	1.88	2.03	2.20	2.42	2.63	3.05	3.47	0.01	0.06	0.09	0.11	
	950	0.63	0.87	1.14	1.29	1.44	1.59	1.74	2.08	2.46	2.66	2.89	3.17	3.45	4.00	4.54	0.01	0.09	0.12	0.15	
	1450	0.87	1.23	1.62	1.84	2.06	2.27	2.49	3.00	3.54	3.83	4.16	4.56	4.96	5.75	6.51	0.02	0.13	0.19	0.23	
	2850	1.38	2.03	2.74	3.13	3.52	3.90	4.27	5.15	6.07	6.55	7.08	7.72	8.34	9.50	10.55	0.04	0.26	0.37	0.46	
	100	0.10	0.13	0.16	0.18	0.20	0.22	0.24	0.28	0.33	0.35	0.38	0.42	0.45	0.52	0.59	0.00	0.01	0.01	0.02	
	200	0.18	0.24	0.30	0.34	0.37	0.41	0.44	0.52	0.61	0.66	0.71	0.78	0.85	0.98	1.12	0.00	0.02	0.03	0.03	
	300	0.25	0.33	0.43	0.48	0.53	0.58	0.63	0.75	0.88	0.95	1.03	1.13	1.23	1.42	1.62	0.00	0.03	0.04	0.05	
	400	0.32	0.43	0.55	0.62	0.68	0.75	0.81	0.97	1.14	1.23	1.34	1.47	1.59	1.85	2.10	0.01	0.04	0.05	0.06	
	500	0.38	0.51	0.66	0.75	0.83	0.91	0.99	1.19	1.39	1.51	1.63	1.79	1.95	2.26	2.57	0.01	0.05	0.07	0.08	
	600	0.44	0.60	0.78	0.87	0.97	1.07	1.16	1.39	1.64	1.77	1.92	2.11	2.29	2.66	3.02	0.01	0.06	0.08	0.10	
	700	0.50	0.68	0.88	1.00	1.11	1.22	1.33	1.60	1.88	2.03	2.20	2.42	2.63	3.05	3.47	0.01	0.06	0.09	0.11	
	800	0.55	0.76	0.99	1.12	1.24	1.37	1.50	1.79	2.12	2.29	2.48	2.72	2.96	3.44	3.91	0.01	0.07	0.11	0.13	
	900	0.61	0.84	1.09	1.24	1.38	1.52	1.66	1.99	2.35	2.54	2.75	3.02	3.29	3.81	4.33	0.01	0.08	0.12	0.15	
	1000	0.66	0.91	1.19	1.35	1.51	1.66	1.81	2.18	2.57	2.78	3.02	3.31	3.61	4.18	4.75	0.01	0.09	0.13	0.16	
	1100	0.71	0.98	1.29	1.46	1.63	1.80	1.97	2.37	2.79	3.02	3.28	3.60	3.92	4.54	5.16	0.02	0.10	0.14	0.18	
	1200	0.76	1.06	1.39	1.57	1.76	1.94	2.12	2.55	3.01	3.26	3.54	3.88	4.22	4.90	5.56	0.02	0.11	0.16	0.19	
	1300	0.80	1.12	1.48	1.68	1.88	2.07	2.27	2.73	3.23	3.49	3.79	4.16	4.52	5.24	5.95	0.02	0.12	0.17	0.21	
	1400	0.85	1.19	1.58	1.79	2.00	2.21	2.42	2.91	3.44	3.72	4.04	4.43	4.82	5.58	6.32	0.02	0.13	0.18	0.23	
	1500	0.89	1.26	1.67	1.89	2.12	2.34	2.56	3.08	3.64	3.94	4.28	4.69	5.11	5.91	6.69	0.02	0.14	0.20	0.24	
	1600	0.93	1.32	1.76	2.00	2.23	2.47	2.70	3.26	3.85	4.16	4.52	4.95	5.39	6.23	7.05	0.02	0.15	0.21	0.26	
	1700	0.98	1.39	1.85	2.10	2.35	2.59	2.84	3.42	4.05	4.38	4.75	5.21	5.66	6.55	7.40	0.02	0.16	0.22	0.27	
1800	1.02	1.45	1.93	2.20	2.46	2.72	2.98	3.59	4.24	4.59	4.98	5.46	5.93	6.85	7.74	0.03	0.17	0.24	0.29		
1900	1.06	1.51	2.02	2.29	2.57	2.84	3.11	3.75	4.43	4.80	5.20	5.70	6.19	7.15	8.07	0.03	0.18	0.25	0.31		
2000	1.10	1.57	2.10	2.39	2.68	2.96	3.24	3.91	4.62	5.00	5.42	5.94	6.45	7.44	8.38	0.03	0.19	0.26	0.32		
2100	1.13	1.63	2.18	2.48	2.78	3.08	3.37	4.07	4.81	5.20	5.64	6.17	6.70	7.72	8.68	0.03	0.19	0.28	0.34		
2200	1.17	1.69	2.26	2.58	2.89	3.20	3.50	4.22	4.99	5.39	5.84	6.40	6.94	7.99	8.98	0.03	0.20	0.29	0.35		
2300	1.20	1.74	2.34	2.67	2.99	3.31	3.63	4.38	5.17	5.58	6.05	6.62	7.18	8.25	9.26	0.03	0.21	0.30	0.37		
2400	1.24	1.80	2.42	2.75	3.09	3.42	3.75	4.52	5.34	5.77	6.25	6.84	7.41	8.50	9.52	0.03	0.22	0.32	0.39		

A-10: Belt length correction factor C_2

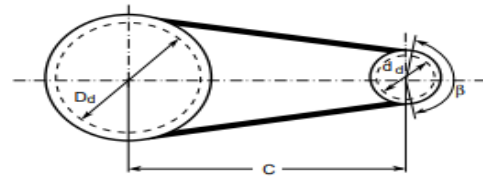
Table 6 Belt length correction factor c_2

C_2	Narrow V-belts						Classical V-belts							
	SPZ XPZ 3V 3VX	SPA XPA	SPB XPB 5V 5VX	SPC XPC	S19	8V	Z/10 ZX 10X	A/13 AX 13X	B/17 BX 17X	20	C/22 CX 22X	25	D/32	E/40
0.80	465	551	915	1.453	1.622	1.653	297	666	875	1.216	1.448	1.735	2.320	2.578
0.81	496	695	977	1.551	1.241	1.765	312	700	920	1.279	1.523	1.824	2.440	2.712
0.82	529	741	1.042	1.655	1.324	1.883	328	736	967	1.345	1.601	1.918	2.565	2.851
0.83	565	791	1.112	1.765	1.412	2.008	345	774	1.017	1.414	1.683	2.016	2.697	2.997
0.84	602	843	1.185	1.881	1.505	2.141	362	813	1.069	1.486	1.769	2.119	2.834	3.150
0.85	642	898	1.263	2.005	1.604	2.282	381	854	1.123	1.561	1.859	2.227	2.978	3.310
0.86	684	957	1.346	2.136	1.709	2.431	400	897	1.179	1.640	1.953	2.339	3.128	3.477
0.87	728	1.019	1.433	2.275	1.820	2.589	420	943	1.239	1.722	2.051	2.457	3.286	3.652
0.88	775	1.085	1.526	2.422	1.938	2.756	441	990	1.301	1.809	2.154	2.580	3.450	3.835
0.89	825	1.155	1.624	2.577	2.062	2.933	463	1.039	1.366	1.899	2.261	2.708	3.622	4.026
0.90	877	1.228	1.727	2.742	2.194	3.120	486	1.091	1.433	1.993	2.373	2.842	3.802	4.225
0.91	933	1.306	1.837	2.916	2.333	3.319	510	1.144	1.504	2.091	2.490	2.983	3.989	4.434
0.92	992	1.389	1.953	3.100	2.480	3.528	535	1.201	1.578	2.194	2.613	3.129	4.185	4.652
0.93	1.054	1.476	2.075	3.295	2.636	3.749	561	1.260	1.655	2.302	2.741	3.283	4.390	4.880
0.94	1.120	1.568	2.205	3.500	2.800	3.984	589	1.321	1.735	2.414	2.874	3.443	4.604	5.118
0.95	1.190	1.666	2.342	3.718	2.974	4.231	617	1.385	1.820	2.581	3.014	3.610	4.828	5.366
0.96	1.263	1.768	2.487	3.947	3.158	4.492	647	1.452	1.908	2.653	3.159	3.784	5.061	5.625
0.97	1.341	1.877	2.639	4.190	3.352	4.768	678	1.522	2.000	2.781	3.311	3.966	5.304	5.895
0.98	1.423	1.992	2.801	4.445	3.555	5.069	711	1.595	2.095	2.914	3.470	4.156	5.558	6.178
0.99	1.509	2.112	2.971	4.715	3.772	5.366	745	1.671	2.195	3.053	3.635	4.354	5.823	6.473
1.00	1.600	2.240	3.150	5.000	4.000	5.690	780	1.750	2.300	3.198	3.808	4.561	6.100	6.780
1.01	1.695	2.375	3.339	5.300	4.240	6.032	817	1.833	2.409	3.349	3.956	4.777	6.368	7.101
1.02	1.797	2.516	3.539	5.617	4.494	6.392	855	1.919	2.522	3.507	4.176	5.002	6.689	7.435
1.03	1.904	2.666	3.749	5.951	4.761	6.772	895	2.009	2.640	3.671	4.372	5.236	7.003	7.783
1.04	2.017	2.823	3.971	6.302	5.042	7.172	937	2.103	2.764	3.843	4.576	5.481	7.330	8.147
1.05	2.135	2.989	4.204	6.673	5.338	7.594	981	2.201	2.892	4.021	4.788	5.735	7.671	8.526
1.06	2.260	3.164	4.450	7.063	5.651	8.038	1.026	2.302	3.026	4.208	5.010	6.001	8.026	8.920
1.07	2.392	3.348	4.709	7.474	5.979	8.505	1.074	2.409	3.166	4.402	5.241	6.278	8.396	9.332
1.08	2.530	3.542	4.981	7.907	6.325	8.998	1.123	2.519	3.311	4.604	5.482	6.566	8.781	9.760
1.09	2.676	3.746	5.268	8.362	6.689	9.516	1.174	2.634	3.452	4.814	5.732	6.866	9.183	10.206
1.10	2.829	3.961	5.570	8.841	7.073	10.061	1.228	2.754	3.620	5.033	5.994	7.179	9.601	10.671
1.11	2.990	4.186	5.887	9.344		10.634	1.283	2.879	3.784	5.262	6.265	7.504	10.036	11.155
1.12	3.160	4.424	6.221	9.874		11.237	1.341	3.009	3.955	5.499	6.548	7.843	10.490	11.659
1.13	3.338	4.673	6.572	10.431		11.871	1.402	3.145	4.133	5.747	6.843	8.196	10.962	12.184
1.14	3.525	4.935	6.940	11.016		12.537	1.464	3.286	4.318	6.004	7.150	8.563	11.483	12.730
1.15	3.722	5.211	7.328	11.632		13.237	1.530	3.432	4.511	6.272	7.469	8.945	11.964	13.298
1.16	3.929	5.500	7.735	12.278		13.972	1.598	3.585	4.711	6.551	7.801	9.343	12.496	13.889
1.17	4.146		8.163	12.957		14.745	1.669	3.744	4.920	6.841	8.146	9.757	13.049	14.504
1.18	4.374		8.612	13.669		15.556	1.742	3.909	5.137	7.143	8.505	10.187	13.624	15.143
1.19	4.614		9.083	14.417		16.407	1.819	4.080	5.363	7.456	8.879	10.634	14.223	15.808
1.20	4.865		9.578	15.203			1.898	4.259	5.597	7.783	9.267	11.100	14.845	16.500
1.21	5.129		10.097	16.027			1.981	4.444	5.841	8.122	9.671	11.583	15.492	
1.22	5.405		10.641	15.551			2.067	4.667	6.095	6.474	10.091	12.035	15.164	
1.23	5.695		11.213				2.155	4.838	6.358	6.841	10.527	12.609	15.863	
1.24	6.000		11.812				2.249	5.046	6.632	7.221	10.980	13.152		

A-11: Arc of contact correction factor C_3

ARC OF CONTACT CORRECTION FACTOR c_3 , POINT 12

The V-belt power rating P_N [kW/belt] is based on a 180° arc of contact. If the arc of contact is smaller, the power transmission capability is reduced and P_N is adjusted by multiplying the read table value by factor c_3 .



Correction factor c_3 is listed in table 7

- for wrapped V-belts, programmes 11, 15.
- for raw-edge V-belts, programmes 10, 12, 16, 17.

D_d = Datum-diameter of larger V-belt pulley [mm]

d_d = Datum-diameter of smaller V-belt pulley [mm]

β = Arc of contact on smaller V-belt pulley [$^\circ$]

For those drives in which effective-diameters D_e/d_e [mm] are used, these values must be used in the calculations.

Table 7, Arc of contact correction factor c_3 .

$\frac{D_d - d_d}{C}$	0.00	0.10	0.20	0.30	0.40	0.50	0.60	0.70	0.80	0.90	1.00	1.10	1.20	1.30	1.40	1.50
Angle β [$^\circ$]	180	174	169	163	157	151	145	139	133	127	120	113	106	99	91	83
c_3 , wrapped	1.00	0.99	0.99	0.98	0.98	0.97	0.96	0.95	0.94	0.92	0.91	0.89	0.87	0.85	0.82	0.78
c_3 , raw-edge	1.00	1.00	0.99	0.99	0.99	0.98	0.98	0.97	0.97	0.96	0.95	0.94	0.92	0.90	0.88	0.85

A-12: Tension and centrifugal force factors K_1 and K_2

Table 8 Tension factor k_1

Arc of contact β [$^\circ$]	Programmes 10, 12, 16, 17			Programmes 11, 15, 20, 23		
	Operating conditions			Operating conditions		
	Light drives Constant load k_1	Mean load k_1	Heavy drives Shock load k_1	Light drives Constant load k_1	Mean load k_1	Heavy drives Shock load k_1
180	1.50	1.73	2.03	1.50	1.73	2.03
175	1.51	1.73	2.03	1.51	1.74	2.04
170	1.51	1.74	2.04	1.52	1.75	2.06
165	1.52	1.75	2.05	1.54	1.77	2.08
160	1.53	1.75	2.06	1.55	1.79	2.10
155	1.53	1.76	2.07	1.57	1.80	2.12
150	1.54	1.77	2.08	1.59	1.83	2.14
145	1.55	1.79	2.10	1.61	1.85	2.17
140	1.57	1.80	2.12	1.63	1.88	2.20
135	1.58	1.82	2.13	1.66	1.90	2.24
130	1.60	1.84	2.16	1.68	1.94	2.27
125	1.62	1.86	2.18	1.72	1.97	2.32
120	1.64	1.88	2.21	1.75	2.01	2.36
115	1.66	1.91	2.24	1.79	2.06	2.42
110	1.69	1.94	2.28	1.83	2.11	2.48
105	1.72	1.98	2.32	1.88	2.17	2.54
100	1.75	2.02	2.37	1.94	2.23	2.62
95	1.80	2.07	2.43	2.00	2.30	2.70
90	1.85	2.12	2.49	2.08	2.39	2.80

Table 9 Factor for centrifugal force k_2 [kg/m]

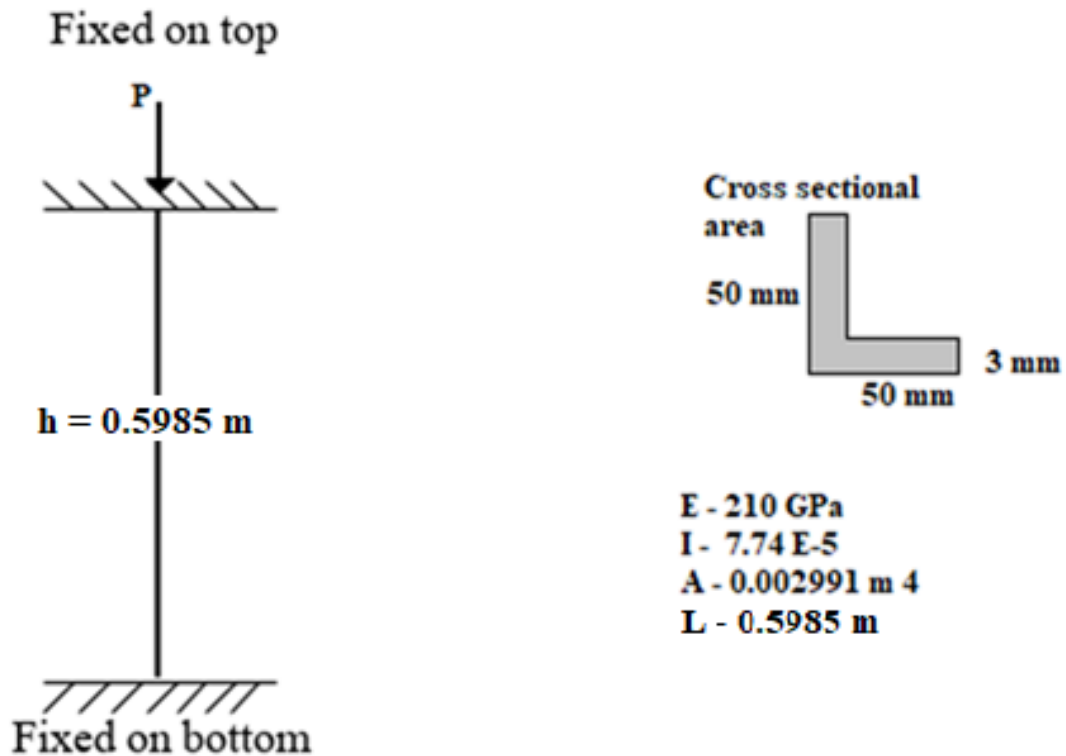
Programme	Belt section									
	XPZ	XPA	XPB	XPC	SPZ	SPA	SPB	S19	SPC	8V
10	0.065	0.105	0.190	0.325						
11					0.065	0.115	0.200	0.275	0.350	0.520
12	0.060	0.100	0.180	0.320						
	ZX/10X	AX/13X	BX/17X	CX/22X						
16	0.055	0.080	0.165	0.250						
17	0.060	0.090	0.180	0.255						
	Z/10	A/13	B/17	20	C/22	25	32	D/32	E/40	
15	0.058	0.104	0.172	0.239	0.282	0.366		0.591	0.958	
20		0.104	0.172	0.239	0.282	0.366	0.519	0.591		
	HA/A	HB/B	HC/C	HD/D	3V/9J	5V/15J	8V/25J			
23	0.154	0.237	0.406	0.750	0.095	0.250	0.637			

A-13: 3V Standard pulley weights

1 Groove

Outside Diameter	Pitch Diameter	Type	Bush	Bore		F	E	L	M	Weight kg	Designation
				Min	Max						
2,65	2,60	B-1	1108	3/8	1 1/8	1 1/16	7/32	7/8	13/32	0,75	PHP 1-3V265TB
2,80	2,75	B-1	1108	3/8	1 1/8	1 1/16	7/32	7/8	13/32	0,85	PHP 1-3V280TB
3,00	2,95	B-1	1108	3/8	1 1/8	1 1/16	7/32	7/8	13/32	1,00	PHP 1-3V300TB
3,15	3,10	B-1	1108	3/8	1 1/8	1 1/16	7/32	7/8	13/32	1,00	PHP 1-3V315TB
3,35	3,30	B-1	1610	1/2	1 5/8	1 1/16	3/32	1	13/32	1,10	PHP 1-3V335TB
3,65	3,60	B-1	1610	1/2	1 5/8	1 1/16	3/32	1	13/32	1,30	PHP 1-3V365TB
4,12	4,07	B-1	1610	1/2	1 5/8	1 1/16	3/32	1	13/32	2,00	PHP 1-3V412TB
4,50	4,45	B-1	1610	1/2	1 5/8	1 1/16	3/32	1	13/32	2,30	PHP 1-3V450TB
4,75	4,70	B-1	1610	1/2	1 5/8	1 1/16	3/32	1	13/32	2,60	PHP 1-3V475TB
5,00	4,95	B-1	1610	1/2	1 5/8	1 1/16	3/32	1	13/32	2,90	PHP 1-3V500TB
5,30	5,25	B-1	1610	1/2	1 5/8	1 1/16	3/32	1	13/32	3,30	PHP 1-3V530TB
5,60	5,55	B-1	1610	1/2	1 5/8	1 1/16	3/32	1	13/32	3,70	PHP 1-3V560TB
6,00	5,95	B-1	1610	1/2	1 5/8	1 1/16	3/32	1	13/32	4,20	PHP 1-3V600TB
6,50	6,45	B-1	1610	1/2	1 5/8	1 1/16	3/32	1	13/32	5,00	PHP 1-3V650TB
6,90	6,85	B-1	1610	1/2	1 5/8	1 1/16	3/32	1	13/32	5,60	PHP 1-3V690TB
8,00	7,95	C-2	2517	3/4	2 1/2	1 1/16	0	1 3/4	13/32	8,50	PHP 1-3V800TB
10,60	10,55	C-2	2517	3/4	2 1/2	1 1/16	0	1 3/4	13/32	14,00	PHP 1-3V1060TB
14,00	13,95	C-3	2517	3/4	2 1/2	1 1/16	0	1 3/4	13/32	20,00	PHP 1-3V1400TB
19,00	18,95	C-3	3020	1 1/4	3	1 1/16	0	2	13/32	26,00	PHP 1-3V1900TB

A-14: Design and selection of the frame



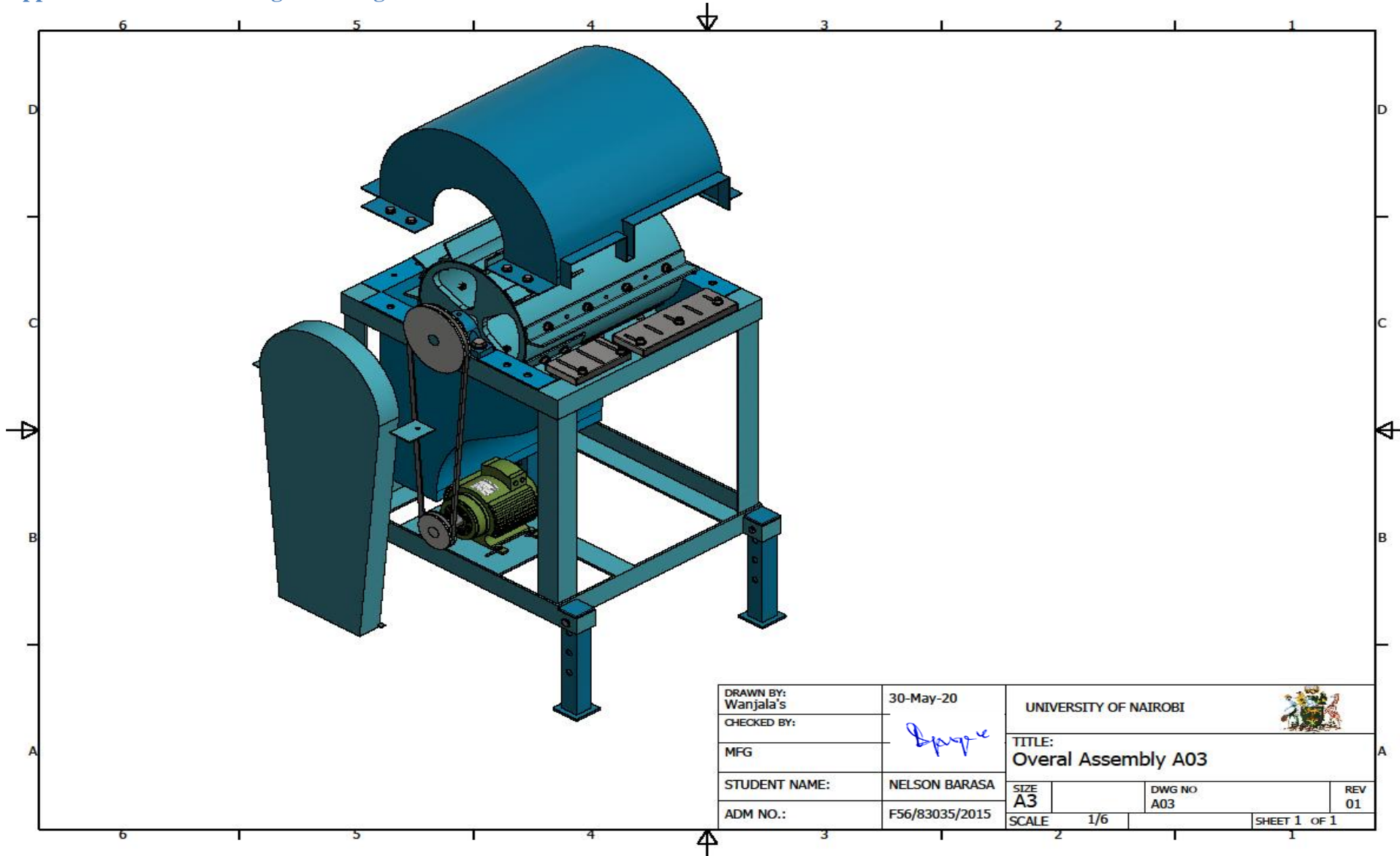
$$r = \sqrt{\frac{I}{A}} = \text{radius of gyration}$$

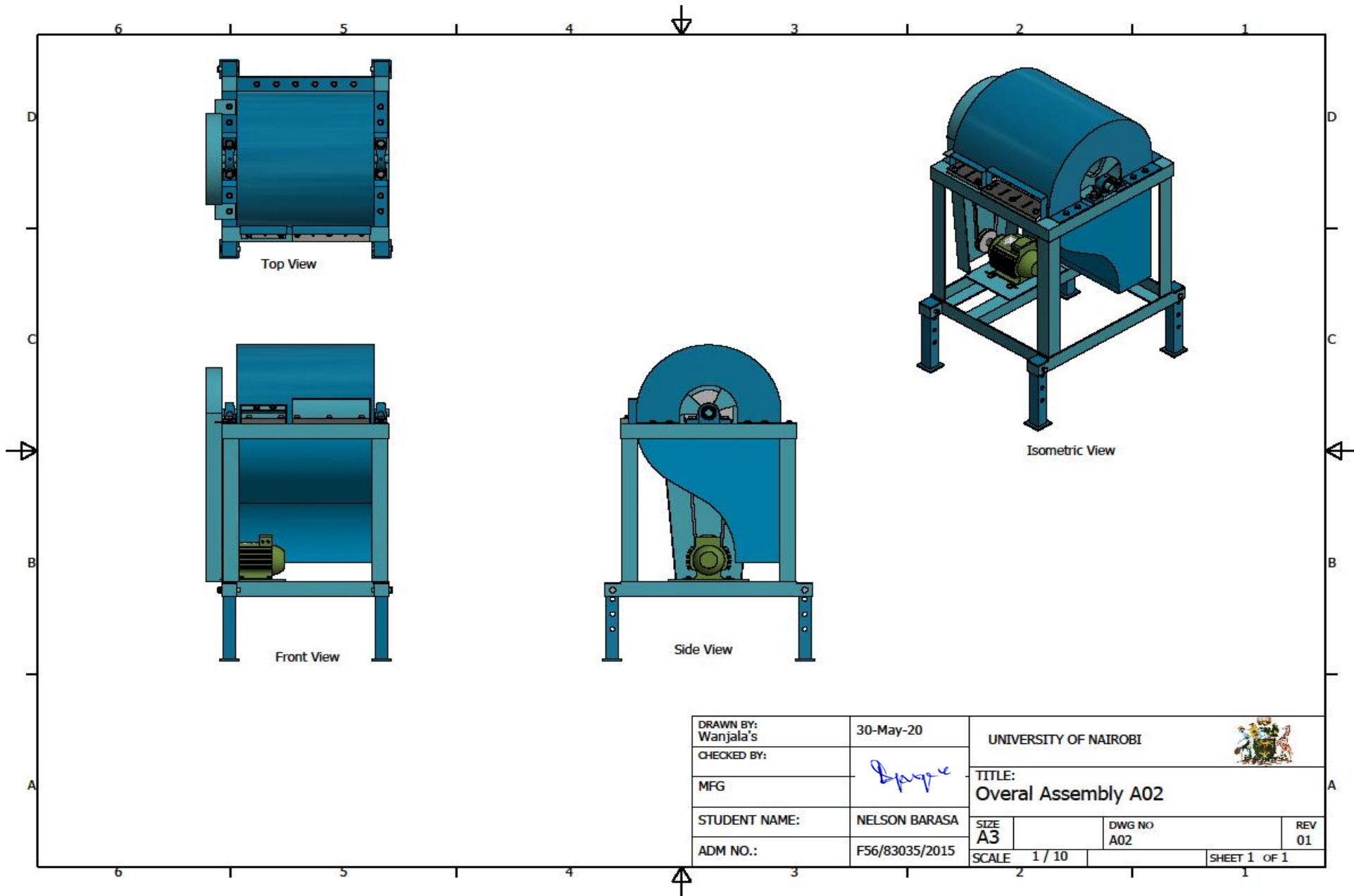
$$P_{cr} = \frac{\pi^2 EA}{\left(0.5L/r\right)^2} = 1.792 \text{ GPa}$$

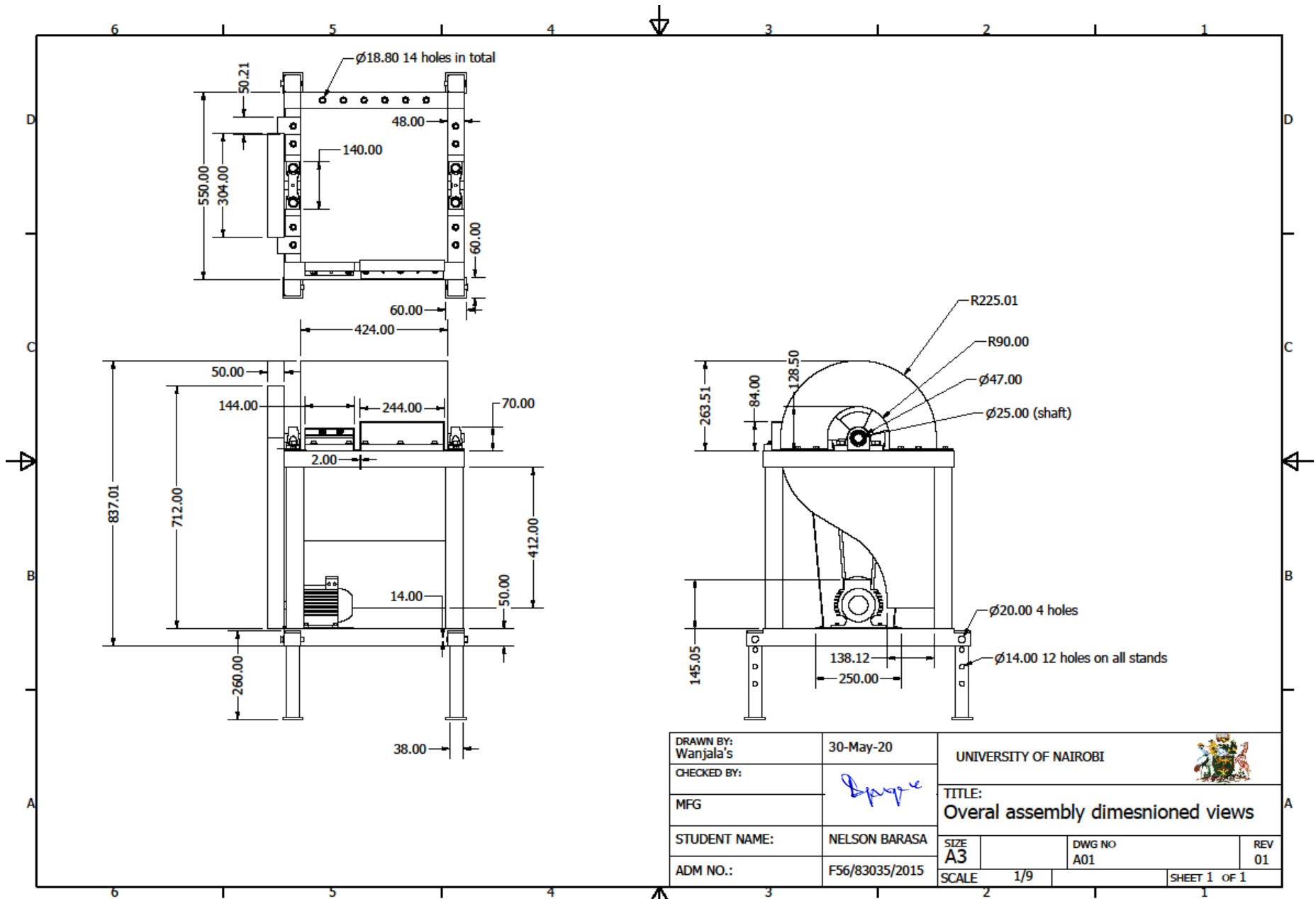
Appendix B: Bill of materials


S/n	Item	Quantity	Specifications	Appro. Cost (Kshs)
1	Extraction drum (ED)	1	Circular hollow steel section, 273.1 mm diameter, length 655 mm and 3 mm thickness	3,100
2	Extraction blades (EB)	10	L-bar of 25*25*2 mm and 5.06 m long	1,000
3	ED side discs	2	Circular steel bars 263.3 mm external diameter, 25 mm internal diameter and 12.7 mm in length	1,000
4	Frame	1	Mild steel L-bars of 50*50*3 mm and 5.17 long.	2,450
5	Anvil	2	Cast iron rectangular bar ,170 mm by 80 mm by 25 mm with the top filleted edges of 2 mm	1,250
6	BD protective cover	1	Hot rolled iron sheet, 2 mm thickness developed as per design drawings.	1,500
7	Pulley & belt protective cover	1	Hot rolled iron sheet, 2 mm thickness. developed as per design drawings.	1,200
8	Pulley	2	Tapered Pulley, made from aluminium alloy (smaller pulley measuring 5.5 cm, 6.5cm, 7.5 cm and 8 cm and larger pulley measuring 11 cm, 13 cm, 13.3 cm and 16.4 in diameter)	1,400
9	Belt	1	One 3V rubber belt	650
10	Chute	1	Hot rolled iron sheet, 2mm thickness developed as per design drawings.	800
11	Bearing & pillow blocks	2	25 mm bore diameter UCP205 Cast iron pillow block and steel ball bearing 25*47*12 mm	1600
12	IC Engine/motor	1	Approximately 5.5 horse power I.C engine.	24,000
13	Brushes		Pins and emery cloth	800
14	Bolts & nuts	84	4 M14, 20 M8 and 60 M6 bolts and nuts	1,000
15	Wheels and accessories	1	For field model, to make the machine mobile	10,949
Total				52,699

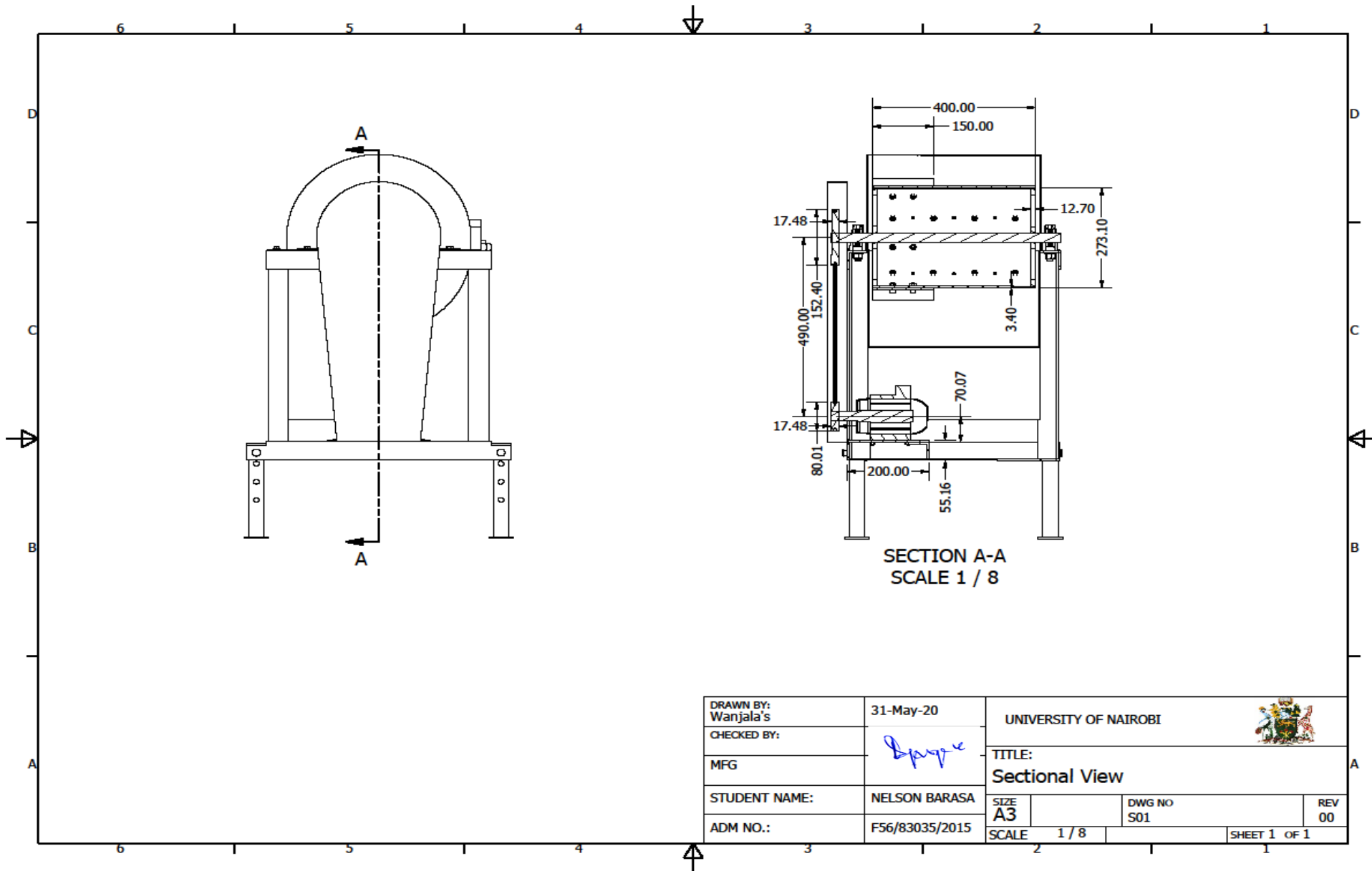
Appendix C: Machine design drawings

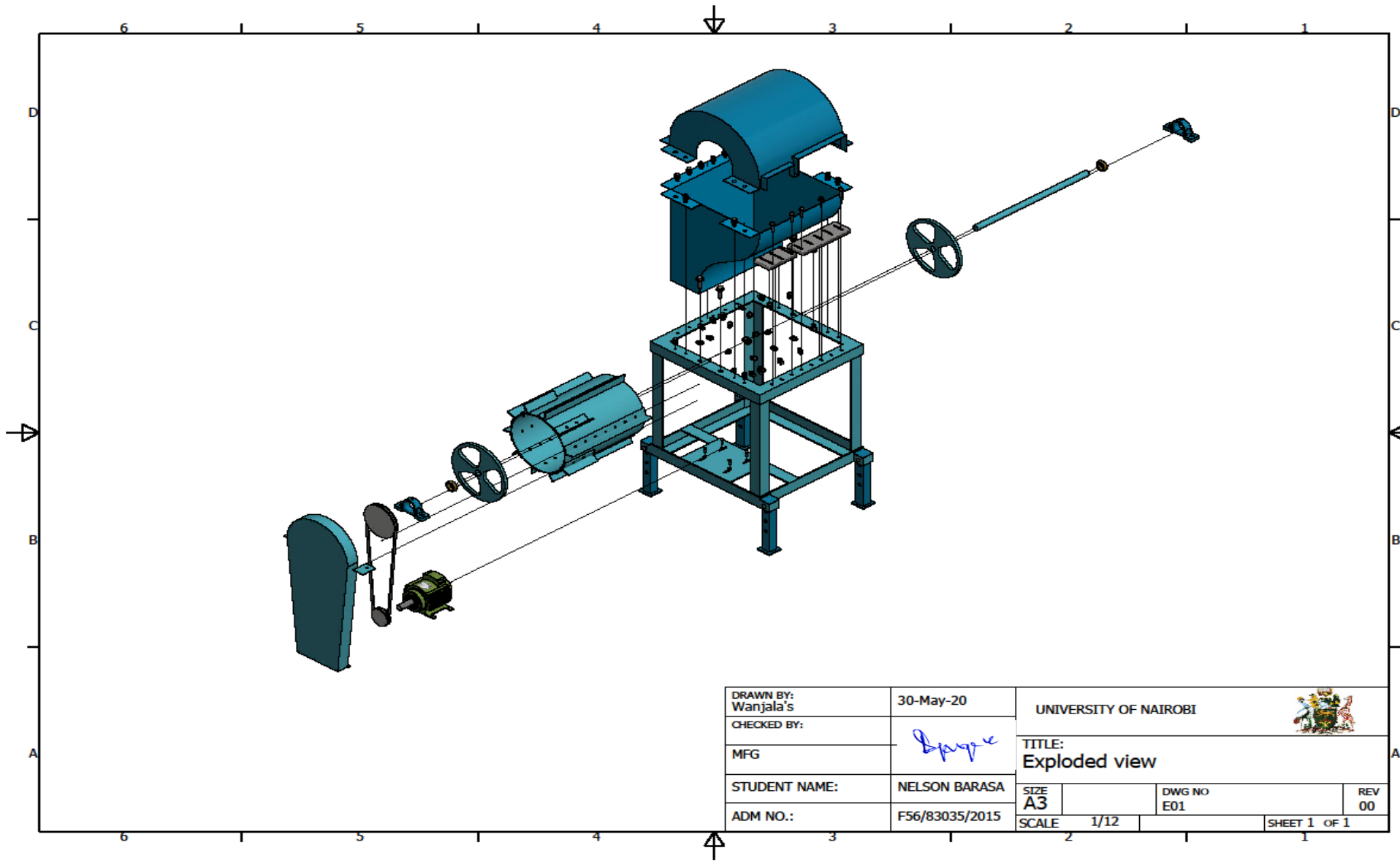


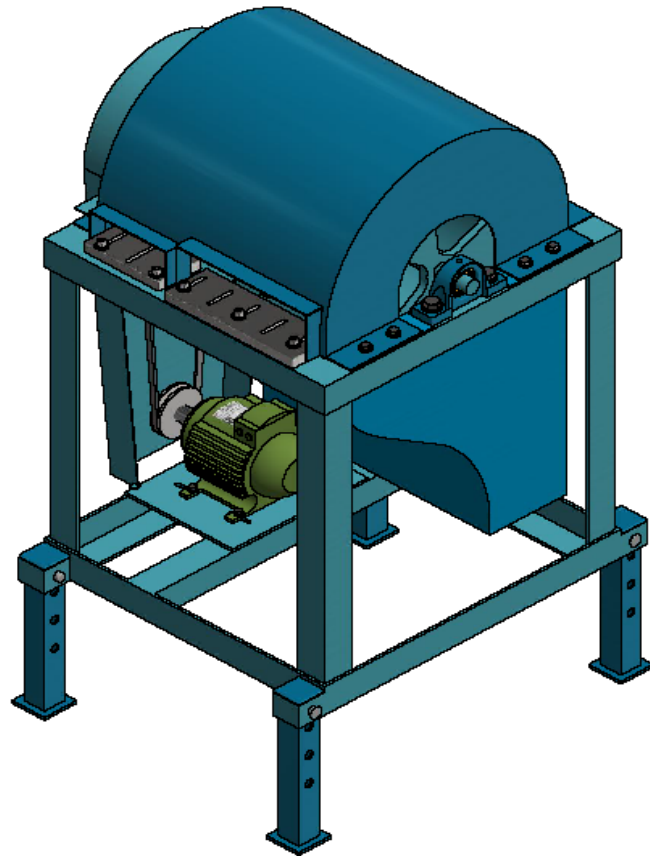





DRAWN BY: Wanjala's	30-May-20	UNIVERSITY OF NAIROBI		
CHECKED BY:	<i>Spige</i>	 TITLE: Overall assembly dimensioned views		
MFG				
STUDENT NAME:	NELSON BARASA	SIZE A3	DWG NO A01	REV 01
ADM NO.:	F56/83035/2015	SCALE 1/9	SHEET 1 OF 1	

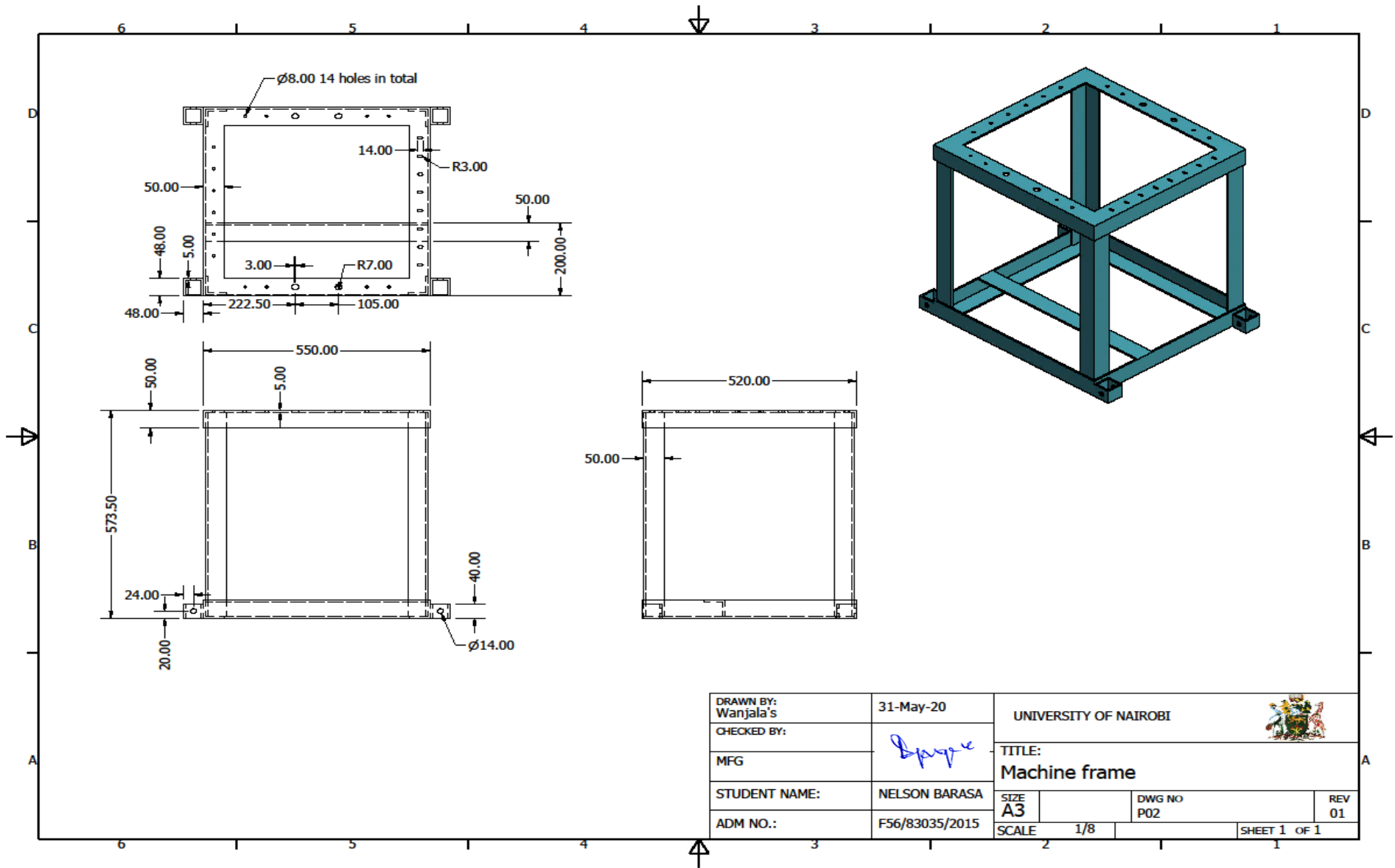


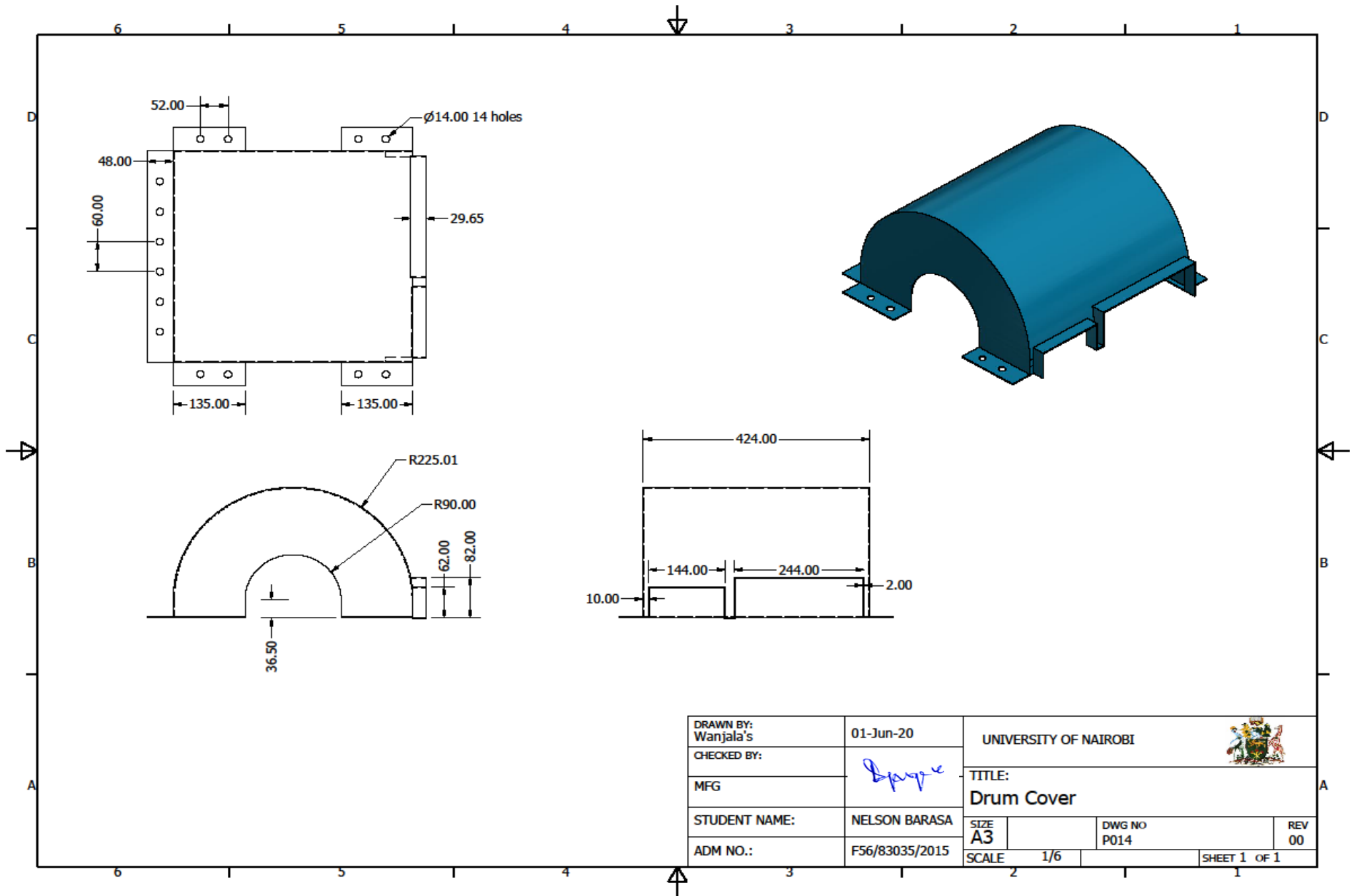


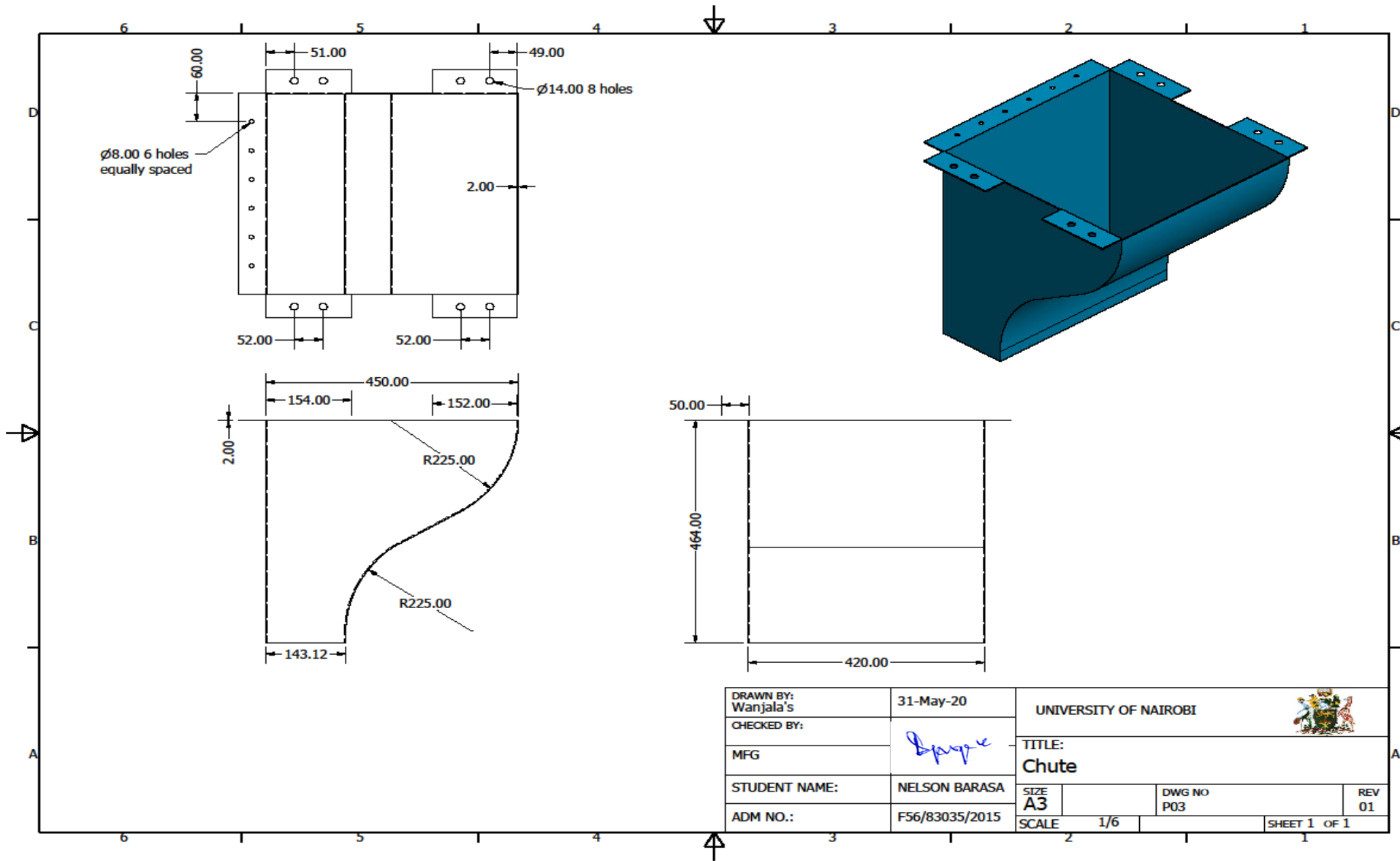



PARTS LIST			
ITEM	QTY	PART NUMBER	DESCRIPTION
1	1	Bottom Part	
2	2	Pillow block	
4	1	Chute	
5	1	Motor plate	
6	2	Ball bearing assembly	
7	1	Drum	
8	2	Drum Side disc	
9	1	Shaft	
10	4	Stand	
11	1	Drum Cover	
12	1	Anvil for extraction	
13	1	Anvil for brushing	
14	4	Stand pin	
15	8	ANSI B18.22M - 14 N	Metric Plain Washers
16	4	ANSI B18.2.3.5M - M14 x 2 x 45	Hex Bolt
17	4	ANSI B 18.2.4.1 M - M14 x 2	Hex Nut
18	98	ANSI B18.22M - 8 N	Metric Plain Washers
19	14	ANSI B18.2.3.5M - M8 x 1.25 x 25	Hex Bolt
20	49	ANSI B 18.2.4.1 M - M8 x 1.25	Hex Nut
21	30	ANSI B18.3.1M - M8x1.25 x 20	*Varies*
22	5	ANSI B18.3.1M - M8x1.25 x 40	Broached Socket Head Cap Screw - Metric
23	1	Pulley guard	
24	1	Motor	
28	1	V-Belt	
29	1	Grooved Pulley1	
30	1	Grooved Pulley2	
31	8	ANSI B18.22M - 6 N	Metric Plain Washers
32	4	ANSI B18.2.3.5M - M6 x 1 x 20	Hex Bolt
33	4	ANSI B 18.2.4.1 M - M6 x 1	Hex Nut

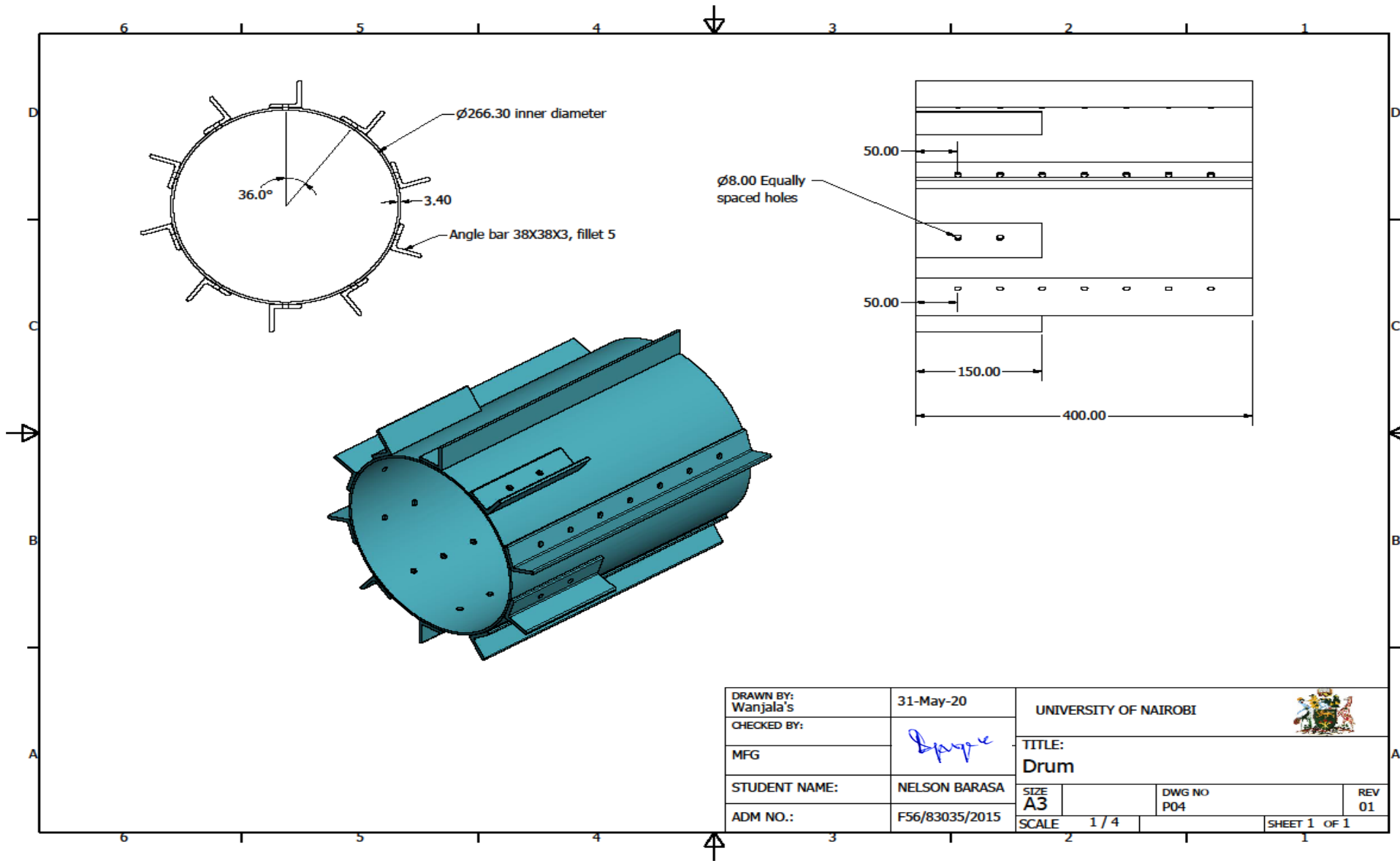
DRAWN BY: Wanjala's	30-May-20	UNIVERSITY OF NAIROBI			
CHECKED BY:	<i>Barasa</i>	TITLE: Part list			
MFG		SIZE A3	DWG NO A04	REV 01	
STUDENT NAME:	NELSON BARASA	SCALE	1 / 6	SHEET 1 OF 1	
ADM NO.:	F56/83035/2015				

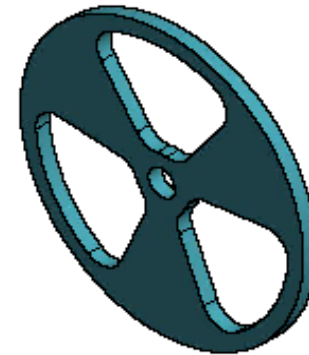
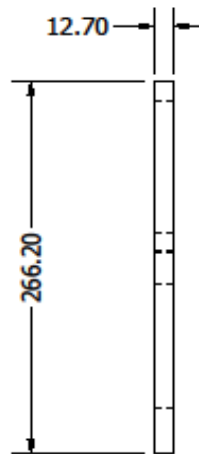
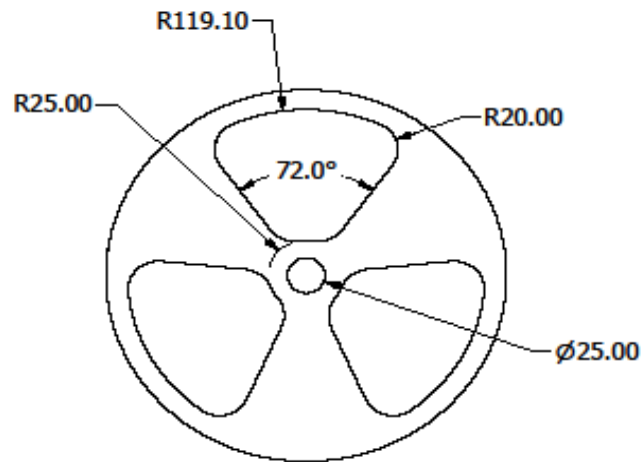






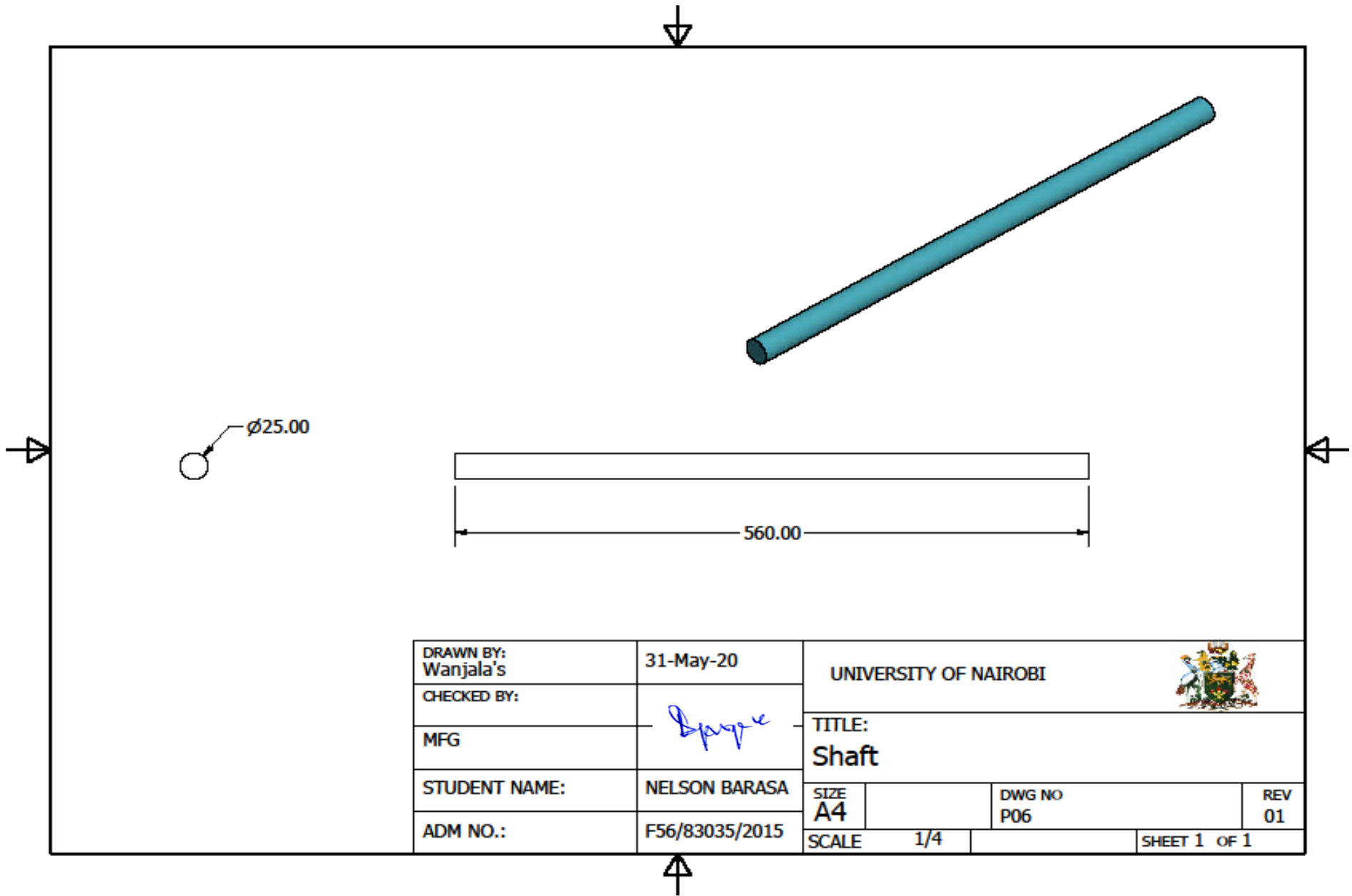



DRAWN BY: Wanjala's	31-May-20	UNIVERSITY OF NAIROBI		
CHECKED BY:	<i>Spige</i>			
MFG		TITLE: Chute		
STUDENT NAME:	NELSON BARASA	SIZE A3	DWG NO P03	REV 01
ADM NO.:	F56/83035/2015	SCALE 1/6	SHEET 1 OF 1	

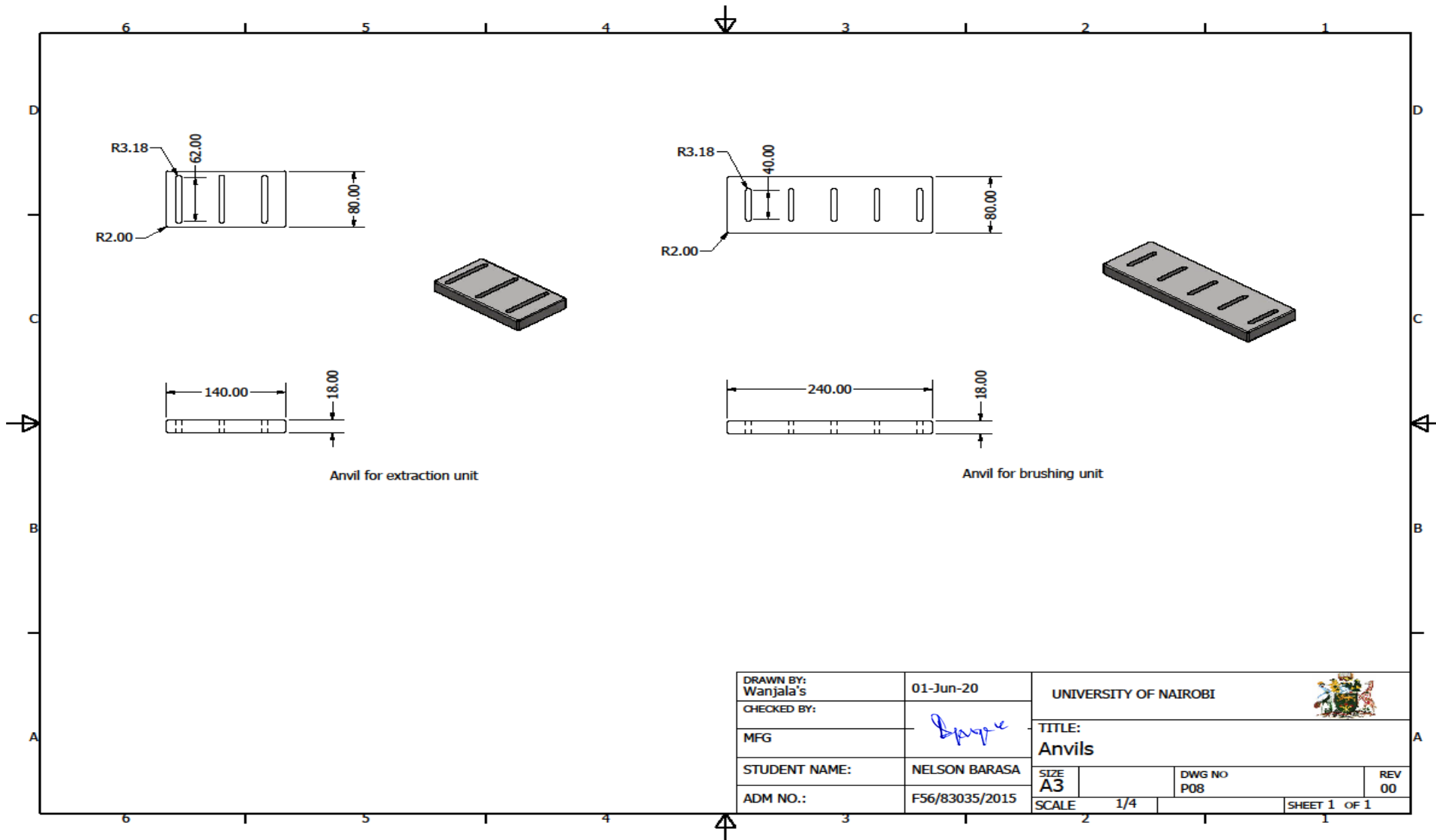





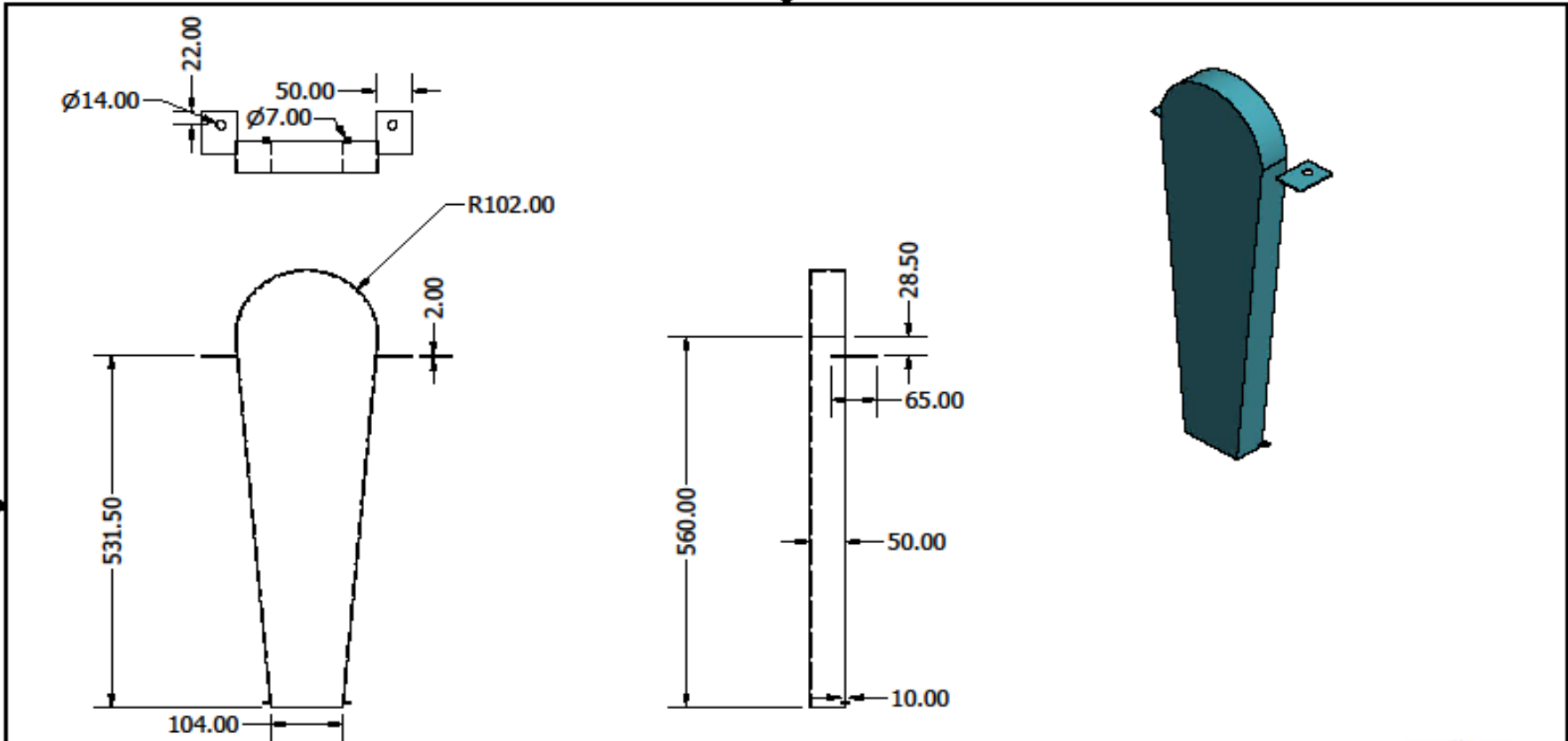
DRAWN BY: Wanjala's	31-May-20	UNIVERSITY OF NAIROBI		
CHECKED BY:		TITLE: Drum Side disc		
MFG		SIZE A4	DWG NO P05	REV 01
STUDENT NAME:	NELSON BARASA	SCALE 1 / 4	SHEET 1 OF 1	
ADM NO.:	F56/83035/2015			




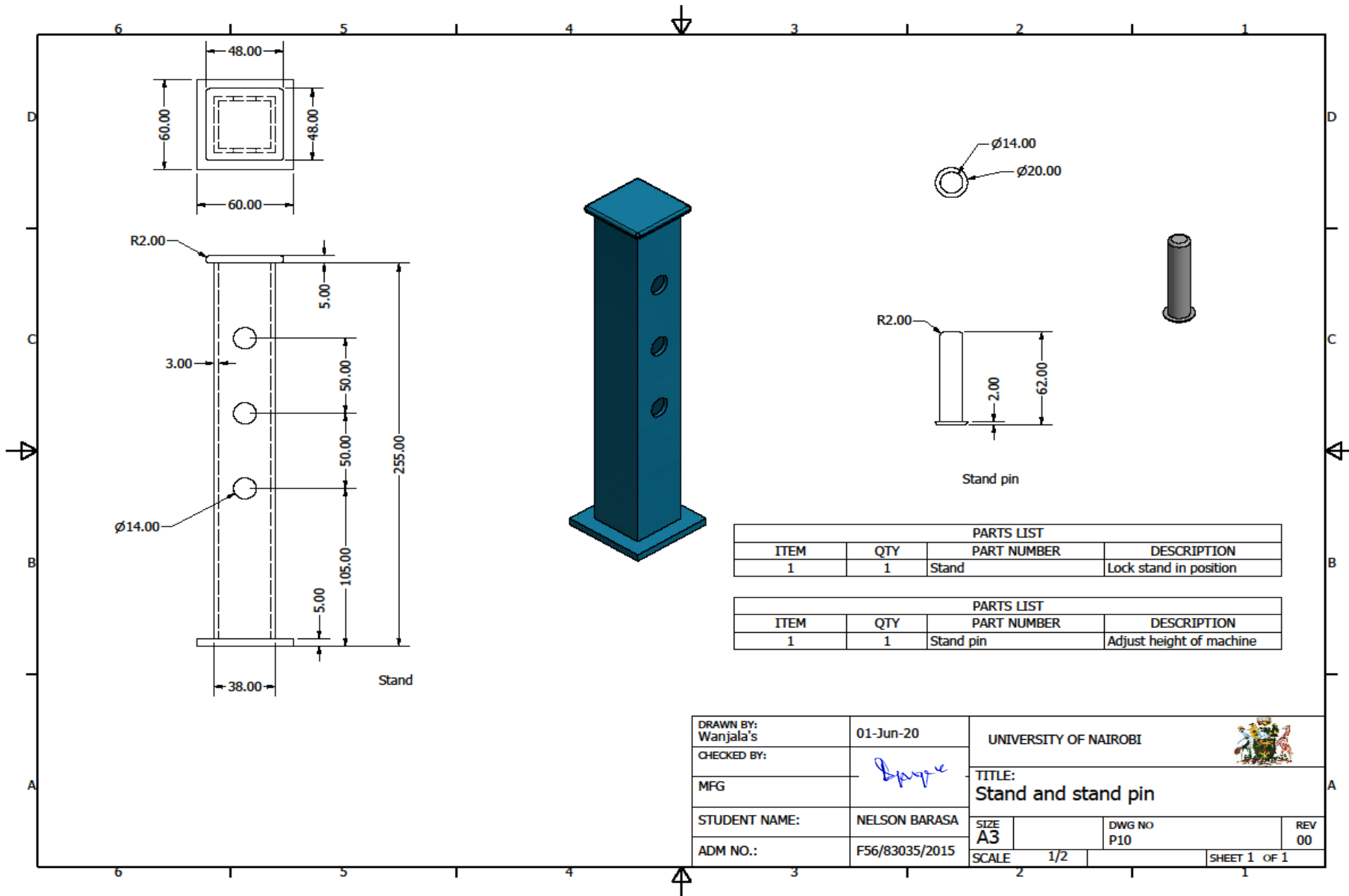
DRAWN BY: Wanjala's	31-May-20	UNIVERSITY OF NAIROBI			
CHECKED BY:	<i>Spape</i>	TITLE: Shaft			
MFG		SIZE A4	DWG NO P06	REV 01	
STUDENT NAME:	NELSON BARASA	SCALE	1/4	SHEET 1 OF 1	
ADM NO.:	F56/83035/2015				



DRAWN BY: Wanjala's	01-Jun-20	UNIVERSITY OF NAIROBI		
CHECKED BY:	<i>Spayce</i>			
MFG		TITLE: Anvils		
STUDENT NAME:	NELSON BARASA	SIZE A3	DWG NO P08	REV 00
ADM NO.:	F56/83035/2015	SCALE 1/4	SHEET 1 OF 1	




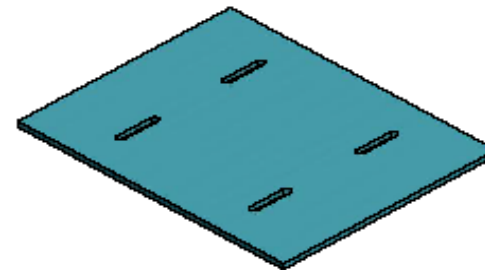
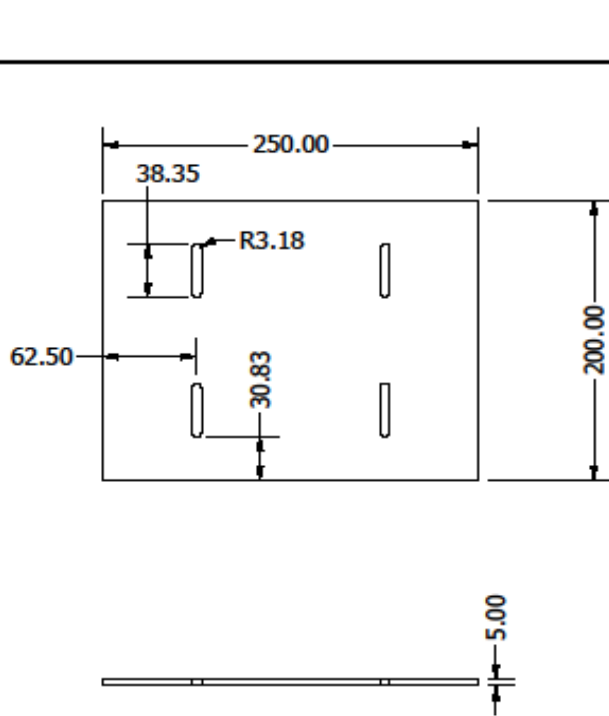
DRAWN BY: Wanjala's	31-May-20	UNIVERSITY OF NAIROBI			
CHECKED BY:	<i>Barasa</i>	TITLE: Pulley and belt guard			
MFG		SIZE A4	DWG NO P07	REV 01	
STUDENT NAME:	NELSON BARASA	SCALE	1/8	SHEET 1 OF 1	
ADM NO.:	F56/83035/2015				




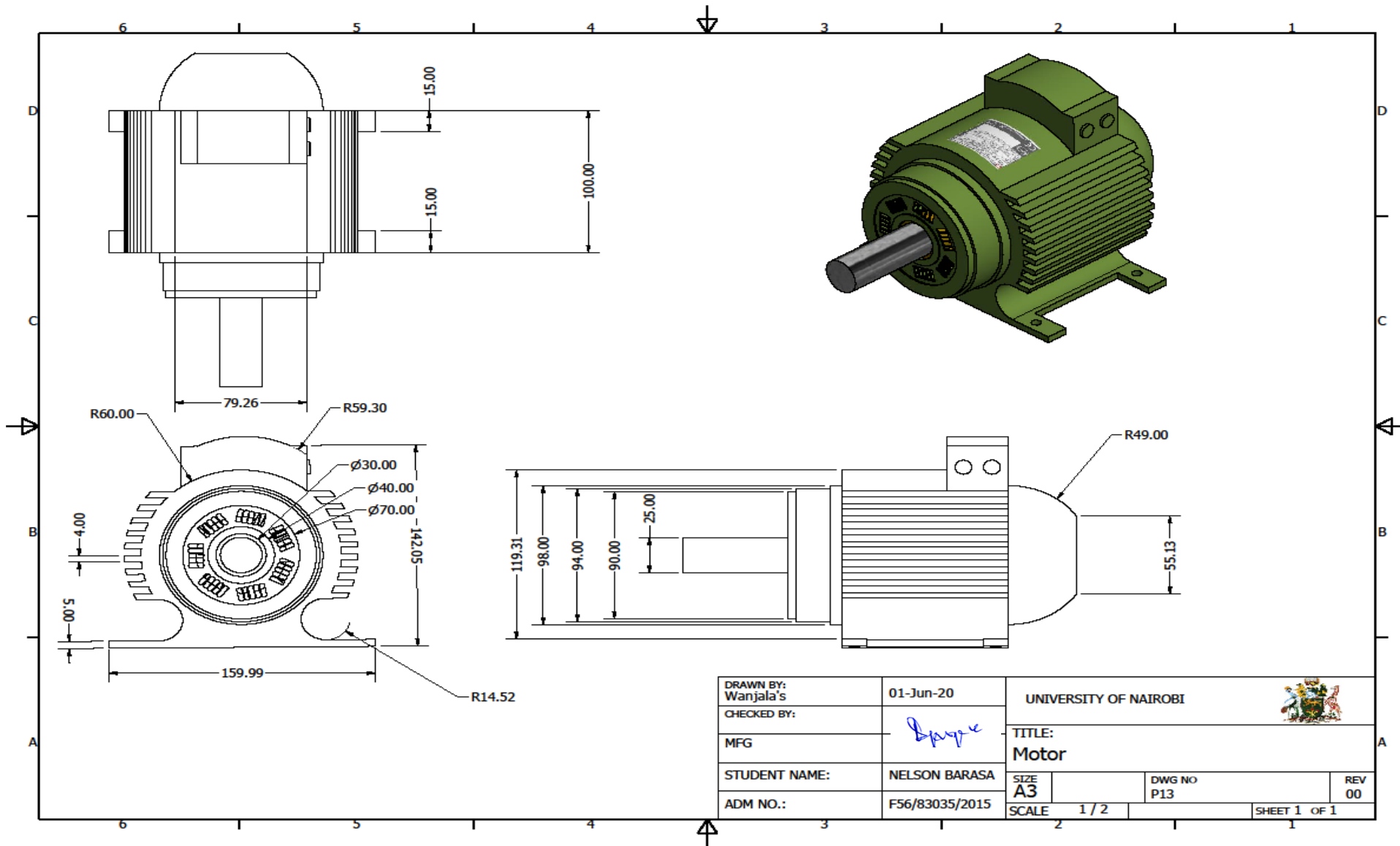
PARTS LIST			
ITEM	QTY	PART NUMBER	DESCRIPTION
1	1	Stand	Lock stand in position

PARTS LIST			
ITEM	QTY	PART NUMBER	DESCRIPTION
1	1	Stand pin	Adjust height of machine

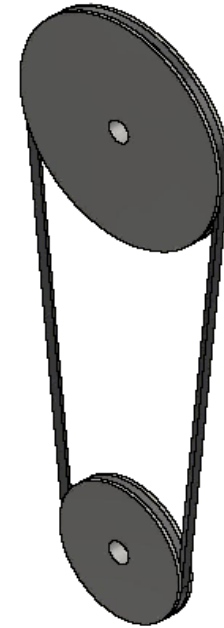
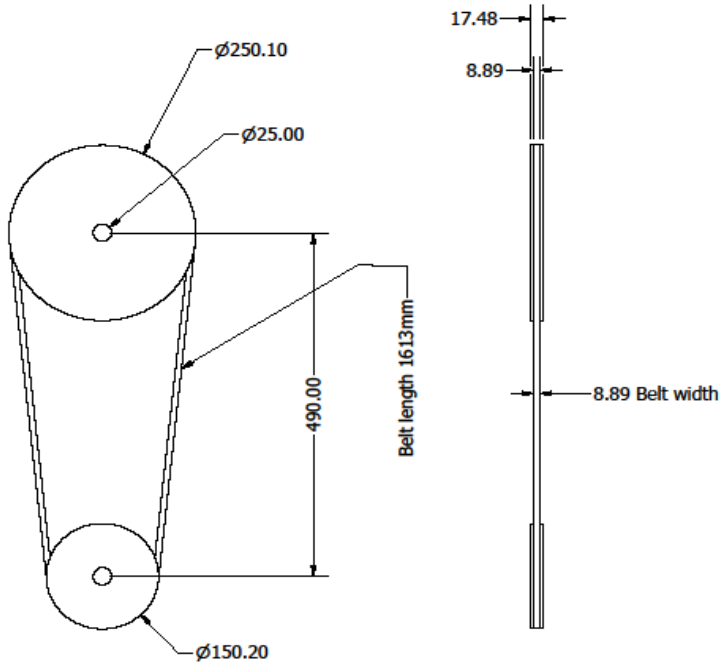
DRAWN BY: Wanjala's	01-Jun-20	UNIVERSITY OF NAIROBI		
CHECKED BY:	<i>Barasa</i>			
MFG		TITLE: Stand and stand pin		
STUDENT NAME:	NELSON BARASA	SIZE A3	DWG NO P10	REV 00
ADM NO.:	F56/83035/2015	SCALE 1/2	SHEET 1 OF 1	




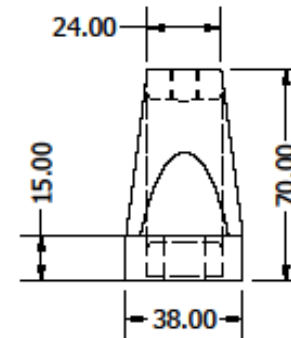
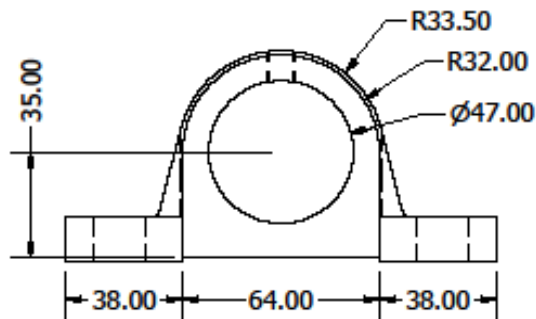
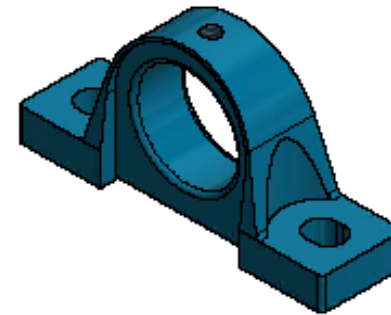
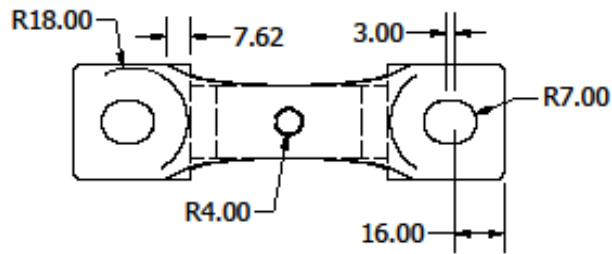
DRAWN BY: Wanjala's	31-May-20	UNIVERSITY OF NAIROBI			
CHECKED BY:	<i>Barasa</i>	TITLE: Motor plate			
MFG		SIZE A4	DWG NO P08	REV 01	
STUDENT NAME:	NELSON BARASA	SCALE 1 / 4	SHEET 1 OF 1		
ADM NO.:	F56/83035/2015				




PARTS LIST			
ITEM	QTY	PART NUMBER	DESCRIPTION
1	1	V-Belt	Rubber belt
2	1	Grooved Pulley1	Larger
3	1	Grooved Pulley2	Smaller



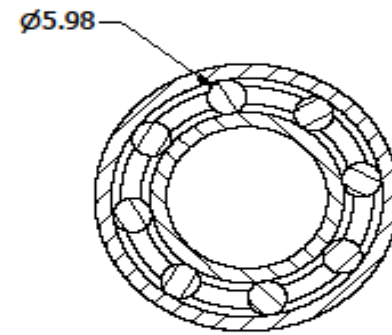
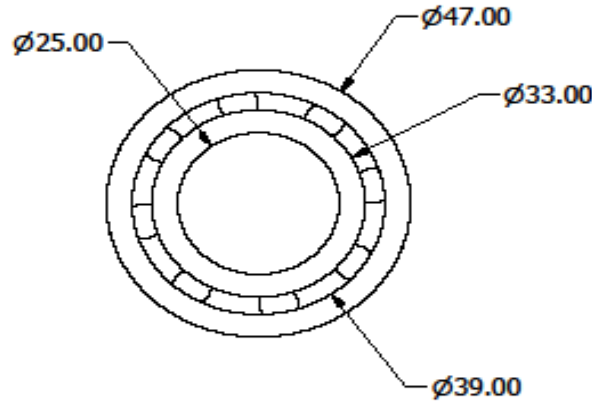
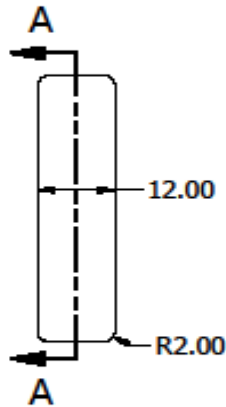
DRAWN BY: Wanjala's	31-May-20	UNIVERSITY OF NAIROBI			
CHECKED BY:	<i>Barasa</i>	TITLE: V-Belt transmission			
MFG		SIZE A3	DWG NO P01	REV 01	
STUDENT NAME:	NELSON BARASA	SCALE	1 / 6	SHEET 1 OF 1	
ADM NO.:	F56/83035/2015				




DRAWN BY: Wanjala's	01-Jun-20	UNIVERSITY OF NAIROBI		
CHECKED BY:	<i>Barasa</i>	TITLE: Pillow block		
MFG		SIZE A4	DWG NO P12	REV 00
STUDENT NAME:	NELSON BARASA	SCALE 1/2		SHEET 1 OF 1
ADM NO.:	F56/83035/2015			



PARTS LIST			
ITEM	QTY	PART NUMBER	DESCRIPTION
1	1		Outer ring for bearing
2	1		Inner ring for bearing
3	8		Ball



SECTION A-A
SCALE 1 : 1

DRAWN BY: Wanjala's	01-Jun-20	UNIVERSITY OF NAIROBI		
CHECKED BY:	<i>Barasa</i>	TITLE: Ball bearing assembly		
MFG		SIZE A4	DWG NO P011	REV 00
STUDENT NAME:	NELSON BARASA	SCALE 1 : 1		SHEET 1 OF 1
ADM NO.:	F56/83035/2015			

Appendix D: Sisal fibre grades



Welcome to

THE LONDON SISAL ASSOCIATION (Established 1953)

East African Sisal Fibre Grades

GRADE 1

Length of fibre should be from 90cm (3 feet) upwards. Colour of fibre should be creamy white to cream. It should be free from defective decortication and be properly brushed. Free of undecorticated barks, harshness, knots, tousled and bunched ends. It should be free of tows.

GRADE 2

Length of fibre should be from 75cm (2.5 feet) to 89cm. Colour of fibre should be creamy white to cream. It should be free of defective decortication and be properly brushed. Free of undecorticated barks, harshness, knots, tousled and bunched ends. It should also be free of tows.

GRADE 3L

Length of fibre should be from 90cm (3 feet) upwards. Colour of fibre should be a mixture of whitish and yellowish. It should be free of defective decortication and be properly brushed. Free of undecorticated barks, harshness, knots, tousled and bunched ends. It should also be free of tows.

GRADE 3 (or 3S)

Length of fibre should be from 60cm (2 feet) to 89cm. Colour of fibre should be a mixture of whitish and yellowish. It should be free of defective decortication and be properly brushed. Free of undecorticated barks, harshness, knots, tousled and bunched ends. It should also be free of tows.

GRADE UG

Length of fibre should be from 60cm (2 feet) upwards. Colour of fibre may be brownish and spotted due to damaged leaf or greenish due to insufficient water during decortication. Black coloured fibre is not allowed in this grade because this shows that it is in the process of rotting (or rotten). Moreover, fibre should be properly brushed, free of undecorticated barks, harshness, knots, tousled and bunched ends. It should also be free of tows.

GRADE S.S.U.G. (SUB STANDARD UNDER GRADE)

This is the fibre that does not conform to standard UG grade but can be exported as line fibre. Length of fibre should not be less than 60cm (2 feet). Colour of fibre may vary from yellowish to more dark and blemished.

GRADE TOW NO.1

This is fibre which has been cut and thrown behind the brushing machines during the process of brushing. Colour of fibre should be creamy white to cream. It should be free of undecorticated barks, knots, dusts and sweepings and should not contain fibre of other mentioned grades.

GRADE TOW NO.2

This is fibre which has been cut and thrown behind the brushing machines during the process of brushing. Colour of fibre may be brownish, spotted, yellowish or greenish. Black coloured fibre is not allowed in this grade because this shows that it is in the process of rotting (or rotten). Moreover, fibre should be free of undecorticated barks, knots, dusts and sweepings and should not contain fibre of other mentioned grades.

UNCARDED FLUME TOW

It should be uniform in colour of creamy white to light brown. Devoid of undecorticated strips of sisal leaf, rotten fibre and foreign materials. It should be properly dried with a moisture content similar to other grades. Dust content not to exceed 15% when extracted by hand. The bales should be pressed to standard size weighing 200kgs per bale.

CARDED FLUME TOW

It should be the same as uncarded flume tow except the total dust content not to exceed 10%.

UHDS

Unwashed hand decorticated sisal, non Estate produced fibre

Appendix E: Sample laboratory data sheet for power consumption

Laboratory Data sheet					
When: 10/09/2019(E) 13/09/2019(B)		Where: Mechanical Workshop UoN			By: Mr. Barasa & Mr. Anyona
No. of blades: 12		Gap size: 1 mm			Idling power: 505 W
S/No.	Extraction		Brushing		Observations
	Tachometer reading (RPM)	Wattmeter reading (W)	Tachometer reading (RPM)	Wattmeter reading (W)	
1	960	810	960	629	Extraction; White with some green tip end Brushing; white with brownish tip end
2	960.1	800	960	622	Extraction; White with some green tip end Brushing; white with some brownish tip end
3	960	804	960	624	Extraction; White with some green tip end Brushing; white with some brownish tip end
4	960	799	960.2	620.5	Extraction; White with some green tip end Brushing; white with some brownish tip end
5	960	806.5	960	626.9	Extraction; White with some green tip end Brushing; white with some brownish tip end
6	960	812.5	960	628.1	Extraction; White with some green tip end Brushing; white with some brownish tip end
Ave.	960.0	805.3	960.0	625.08	

Appendix F: Raw results

F-1: Attainable drum speeds

Smaller Pulley, d (cm)	Larger Pulley D (cm)	Speed Ratio	Motor Speed, n (RPM)	Drum Speed, N (RPM)
5.5	16.4	0.3354	2880	965.9
	13.3	0.4135	2880	1191.0
	13	0.4231	2880	1218.5
	11	0.5000	2880	1440.0
6.5	16.4	0.3963	2880	1141.5
	13.3	0.4887	2880	1407.5
	13	0.5000	2880	1440.0
	11	0.5909	2880	1701.8
7.5	16.4	0.4573	2880	1317.1
	13.3	0.5639	2880	1624.1
	13	0.5769	2880	1661.5
	11	0.6818	2880	1963.6
8.7	16.4	0.5305	2880	1527.8
	13.3	0.6541	2880	1883.9
	13	0.6692	2880	1927.4
	11	0.7909	2880	2277.8

F-2: Power consumption

Drum speed N (rpm)	Gap Size, G (mm)	Number of blades n	Idling Power (W)	Total Power for extraction (W)	Total Power for brushing (W)
960.0	1	12	505	805.3	625.1
960.1	2	12	510	743.0	610.0
960.0	3	12	550	700.0	640.0
1130.0	1	12	600	1067.0	786.8
1130.0	2	12	625	983.0	768.2
1130.0	3	12	630	988.0	773.2
1210.0	1	12	650	1205.5	868.6
1210.0	2	12	651	1191.0	866.9
1210.0	3	12	672	1205.0	885.2
1308.0	1	12	799	1424.6	1042.4
1308.0	2	12	800	1400.0	1040.0
1308.0	3	12	805	1391.3	1043.7
1429.0	1	12	910	1800.1	1245.9
1429.0	2	12	910	1720.0	1232.8
1429.0	3	12	900	1667.0	1206.8
1615.1	1	12	1205	2125.0	1578.2
1615.1	2	12	1198	2118.0	1571.2
1615.1	3	12	1179	2091.7	1551.6

F-3: Extraction results for anvil and hammer method

Sisal leaf variables						Extraction variables					
S/No	Length (cm)	Weight (g)	Bud thickness (cm)	Tip thickness (cm)	Largest width (cm)	Wet Weight (g)	Dry Weight (g)	Colour	Mean fibre length (cm)	Max. Tensile Force (N)	Elongation (cm)
1	110.5	581	3	0.25	9.4	37	20	White with brown	95	300.00	10.70
2	110.5	582	3	0.25	9.3	36	19	White with brown	92	300.00	11.30
3	110	581	2.4	0.3	10.4	40	21	White with brown	96	290.00	10.80
4	110.4	581.5	3	0.3	9.5	38	21	White with brown	98	305.00	10.60
5	110	581	3	0.25	9.4	37	20	White with brown	95	275.00	10.70
6	110.8	582	2.4	0.3	9.4	36	19.5	White with brown	96	245.00	9.30
7	109.5	539.1	3	0.3	9.5	31	20	White with brown	97	390.00	11.20
8	110.5	539	2.5	0.25	9.5	32	21	White with brown	93	320.00	9.00
9	110.5	539.2	3	0.25	9.5	31.5	20	White with brown	94	450.00	9.40
10	110.5	540	3	0.3	9.5	31	19.5	White with brown	93	275.00	10.00
11	110	541	2.6	0.3	9.5	31	18	White with brown	96.5	335.00	10.60
12	108	538	3	0.25	9.5	31	20	White with brown	93	345.00	10.60
13	109	549.5	2.4	0.3	10.4	40	21	White with brown	96	330.00	6.00
14	111	550.2	2.5	0.3	10.4	39	20	White with brown	94	430.00	8.50
15	111.5	549	2.4	0.25	10.3	40	21	White with brown	96	345.00	8.40
16	110	550	2.6	0.3	10	38	20	White with brown	94	300.00	11.00
17	110.5	550.1	2.4	0.3	10.4	37	20.5	White with brown	98	309.00	11.00
18	110	548.9	2.4	0.29	10.5	40	21	White with brown	96	330.00	10.30

F-4: Results for Rea Vipingo fibres

Crushed, washed and brushed							
S/No.	Weight (g)	Colour	Mean fibre length (cm)	Maximum Tensile Force (N)	Elongation (cm)	Fibre Grade	No. of strands
1	24	White	95	118	5.2	UG	40
2	20	White	92	144	5.1	UG	40
3	21	White	96	110	6.2	UG	40
4	22	White	98	175	9.3	UG	40
5	19	White	95	160	8.0	UG	40
6	20	White	96	164	7.4	UG	40
7	22	White	97	134	5.1	UG	40
8	18	White	93	140	6.0	UG	40
9	19	White	94	120	4.0	UG	40
10	23	White	93	85	4.2	UG	40
11	23	White	95	180	8.4	UG	40
12	20	White	92	185	9.1	UG	40
13	21	White	95	175	9.3	UG	40
14	21.5	White	98	430	10.5	UG	80
15	19	White	95	260	9.5	UG	80
16	20.1	White	96	440	10.6	UG	80
17	22	White	96.5	375	13	UG	60
18	18.5	White	93	280	10.2	UG	60
19	23	White	96	250	9.2	UG	60
20	20	White	94	90	4.4	UG	20
21	21	White	98	65	4.5	UG	20
22	22	White	96	80	5.5	UG	20

F-5: The maximum tensile force and elongation of sisal fibres using the Hounsfield Tensometer

S/No.	Extraction								Brushing							
	Max Force (N)				Elongation (cm)				Max Force (N)				Elongation (cm)			
Sample	1	2	3	Mean	1	2	3	Mean	1	2	3	Mean	1	2	3	Mean
1	195	202	240	212.33	7.1	7.3	7	7.13	256	250	255	253.67	8.7	9.3	9.6	9.20
2	279	230	235	248.00	9.1	8.8	8.7	8.87	320	255	260	278.33	8.3	5.5	6.2	6.67
3	272	230	205	235.67	6.5	6.8	6.7	6.67	205	175	195	191.67	9.1	8.9	8.5	8.83
4	235	310	265	270.00	8.6	8.4	8.7	8.57	230	200	252	227.33	10.5	9.2	10.5	10.07
5	325	315	280	306.67	6.5	10.3	6.3	7.70	272	295	290	285.67	10.5	11	10.9	10.80
6	360	345	265	323.33	6.1	6.3	7	6.47	250	200	185	211.67	8.4	9.2	8.5	8.70
7	210	285	280	258.33	10.7	10.4	10.9	10.67	210	215	275	233.33	9.8	9.9	9.8	9.83
8	180	210	195	195.00	7.1	7	7.4	7.17	360.3	325	320	335.10	9.4	10.5	10.2	10.03
9	195	327	230	250.67	7	8	7.7	7.57	257	360	365	327.33	8.7	8.5	8.6	8.60
10	240	190	235	221.67	7.8	8	6.9	7.57	265	250	255	256.67	10.5	10	8.6	9.70
11	260	290		275.00	9.3	9.8		9.55	300	365	330	331.67	9.2	9.4	9.3	9.30
12	290	340		315.00	12.2	11.8		12.00	280	280	310	290.00	9.6	9.5	9.4	9.50
13	425	330	355	370.00	10.2	9.6	9.7	9.83	325	295	315	311.67	6.4	6.3	7.2	6.63
14	235	205	255	231.67	7.2	5.4	6.8	6.47	305	340	375	340.00	8	8.2	8.3	8.17
15	305	285	312	300.67	9.7	9.2	9	9.30	293	285	335	304.33	10.5	10.2	10.3	10.33
16	250	400	310	320.00	9.8	10.3	9.9	10.00	340	245	273	286.00	7.7	7.8	9.5	8.33
17	350	385	350	361.67	9	9.2	9.1	9.10	355	305	200	286.67	10.7	10.8	10.9	10.80
18	470	420	455	448.33	9.5	10.5	9.3	10.53	455	410	435	433.33	10.7	11.2	10.4	10.77
19	235	370		302.50	10.3	10.5		10.40	290	340	400	343.33	11.6	10.5	13.4	11.83
20	270	345		307.50	7.6	9		8.30	345	355	365	355.00	9.5	9.7	9.1	9.43
21	210	230		220.00	7.2	7.3		7.25	435	485	260	393.33	10	7	9.4	8.80
22	310	395		352.50	10.3	10.4		10.35	240	295	265	266.67	6.5	10.5	10.4	9.13
23	375	360		367.50	11.8	11.5		11.65	340	430	190	320.00	10	10.4	5	8.47
24	300	345		322.50	8.3	9.2		8.75	280	225	210	238.33	8.1	10.2	10.3	9.53
25	225	335	250	270.00	11	10.6	10.6	10.73	232	235	270	245.67	7	7.9	8.2	7.70
26	395	335	315	348.33	10.4	10.7	10.5	10.53	390	265	315	323.33	7.3	7	9.1	7.80
27	300	295	300	298.33	8	9.2	7.8	8.33	195	225	235	218.33	7.3	6.5	7.4	7.07
28	330	265	325	306.67	10.6	10.5	10.7	10.60	325	260	242	275.67	11.4	11	11.4	11.27
29	350	330	310	330.00	7.6	7.7	6.5	7.27	230	300	275	268.33	7.6	7.5	7.4	7.50
30	340	320	350	336.67	9.9	9.8	9.8	9.83	405	390	200	331.67	10	11	7	9.33

31	325	230	360	305.00	9.8	8.5	10.9	9.73	340	280	320	313.33	10.5	11.2	11.2	10.97
32	292	295		293.50	8.3	9.5		8.90	300	225		262.50	7.7	7.5		7.60
33	410	270		340.00	9.8	9.8		9.80	350	355		352.50	8.9	8.5		8.70
34	275	325		300.00	10.4	9.8		10.10	180	180		180.00	7	7.2		7.10
35	310	270		290.00	9	8.9		8.95	176	178		177.00	7	8.1		7.55
36	299	300		299.50	7.9	8		7.95	250	240		245.00	8.9	9		8.95
37	365	320		342.50	10.7	11.5		11.10	365	245		305.00	11.2	11.3		11.25
38	480	470		475.00	12	14.2		13.10	395	275	320	330.00	12.5	10.3	11.2	11.33
39	320	320.5		320.25	9	9.5		9.25	280	305		292.50	7.8	10.5		9.15
40	395	240		317.50	9.1	9.6		9.35	400	295		347.50	11	9.3		10.15
41	315	292		303.50	10	9.5		9.75	330	255		292.50	10.3	9.5		9.90
42	280	320		300.00	9.8	9.9		9.85	315	272		293.50	8.3	8.5		8.40
43	300	305		302.50	8.4	9		8.70	250	250.5		250.25	8.2	9.1		8.65
44	270	305		287.50	8.5	8.4		8.45	230	215		222.50	8.9	9.3		9.10
45	335	210		272.50	12.5	12.7		12.60	240	235.5		237.75	8.7	8.2		8.45
46	310	300		305.00	9	9.5		9.25	235	245		240.00	9	10.5		9.75
47	380	275		327.50	10.7	10.8		10.75	210	170		190.00	7.2	5.3		6.25
48	375	280		327.50	9.3	9.5		9.40	230	215		222.50	6.4	6.7		6.55
49	375	275		325.00	9.5	9.3		9.40	328	320		324.00	10.2	9.9		10.05
50	345	257		301.00	12.2	9.5		10.85	305	270		287.50	11.5	11		11.25
51	310	265		287.50	8	8.3		8.15	320	205		262.50	11	9		10.00
52	340	270		305.00	8.9	8.7		8.80	360	295		327.50	9.5	10		9.75
53	350	320		335.00	10.3	11		10.65	310	250		280.00	10.5	10.4		10.45
54	400	260		330.00	10	10.3		10.15	335	250		292.50	8.5	8.2		8.35
55	385	295		340.00	9.8	9.9		9.85	220	245		232.50	8.2	9		8.60
56	355	265		310.00	9.5	9.7		9.60	405	265		335.00	9	8.7		8.85
57	355	375		365.00	9	9.1		9.05	390	270		330.00	9.8	9		9.40
58	300	265		282.50	9.4	9.9		9.65	165	240		202.50	6.3	7.1		6.70

F-6: Results for extraction tests

S/No	Sisal leaf parameters					Extraction								
	Length (cm)	Weight (g)	Bud thickness (cm)	Tip thickness (cm)	Largest width (cm)	Speed (RPM)	Gap size (mm)	No.of blades	Weight (wet) (g)	Weight (dry) (g)	Colour	Mean fibre length (cm)	Max. Tensile Force (N)	Elongation (cm)
1	117	702	2.8	0.25	10.3	900	1	12	37	22	White, tip end green	76	275.00	9.55
2	122	803	2.8	0.3	10	900	1	12	56	30	White, tip end green	77	315.00	12.00
3	116	607	2.5	0.3	10.8	900	1.5	12	56	28	White, tip end green	104	370.00	9.83
4	126	713	2.7	0.3	10.4	900	1.5	12	62	34	White, tip end green	105	231.67	6.47
5	114	571	2.5	0.3	12	900	2	12	118	39	Green, some white	107	300.67	9.30
6	119	635	2.5	0.3	10	900	2	12	115	40	Green, some white	107	320.00	10.00
7	117	611	3	0.35	10.3	900	2.5	12	176	49	Green	109	361.67	10.20
8	116	647	2.4	0.25	11.1	900	2.5	12	232	59	Green	110	448.33	10.53
9	112.5	541	3	0.3	9.6	1092	2.5	12	78	31	Green, some white	100	292.50	10.67
10	119	627	3	0.3	11.6	1192	4.5	12	155	43	Green	109	195.00	7.17
11	117	633	2.5	0.5	11.8	1200	1	12	59	29.7	White, tip end green	104	212.33	7.13
12	117.5	532	2.6	0.4	11.6	1200	1.5	12	61	29	White, tip end green	104	248.00	8.87
13	116	697	2.5	0.45	13	1200	2	12	69	31	White, tip end green	100.5	235.67	6.67
14	117	630	2.5	0.35	12	1200	2.5	12	70	31	White, tip end green	103	270.00	8.57
15	109	558	2.5	0.4	11.9	1325	2.5	12	65	29	White, tip end green	105	250.67	7.57
16	110	532	2.5	0.4	11	1325	3	12	84	38	White, tip end green	101	221.67	7.57
17	114	597	2.5	0.3	11.5	1400	2.5	12	70	38	White, tip end green	102	306.67	7.70
18	114	568	2.5	0.3	10.5	1400	3	12	69	35	White, tip end green	103	323.33	6.47
19	114	571	2.7	0.3	11.2	900	1	6	81	34	Green, some white	111	302.50	10.40
20	115	635	2.9	0.25	11.8	900	1	6	68	31	Green, some white	110	307.50	8.30
21	123	762	2.9	0.2	12	900	1.5	6	66	30	Green, some white	109	220.00	7.25
22	112	592	2.4	0.25	11	900	1.5	6	109	38	Green	109	352.50	10.35
23	125	746	2.8	0.3	10	1135	1	6	61	32	White, tip end green	100	367.50	11.65
24	116	630	2.4	0.3	11.6	1135	1	6	55	27	White, tip end green	105	322.50	8.75
25	130	607	2.8	0.2	11	1135	1.5	6	52	27	White, tip end green	106	270.00	10.73
26	128	756	2.7	0.2	12	1135	1.5	6	62	37	White, tip end green	106	348.33	10.53
27	112.5	620	2.5	0.2	11.6	1200	1	6	51	27	White	96	298.33	8.33

28	117	534	2.5	0.2	10	1200	1	6	42	24	White	96	306.67	10.60
29	126	550	2.5	0.2	8.5	1200	1.5	6	53	31	White	98	330.00	7.27
30	127	731	2.8	0.3	9.9	1200	1.5	6	70	33	White, tip end green	99	336.67	9.83
31	126	720	2.7	0.25	9.5	1250	1	6	61	32	White	100	305.00	9.73
32	112	560	2.4	0.3	12	1400	2	6	48	24	White, tip end green	100	293.50	8.90
33	107	507	2.5	0.3	10.8	1400	2	6	46	21	White, tip end green	99	340.00	9.80
34	97	530	2.5	0.2	9.2	1400	2	6	42	21	White, tip end green	95	300.00	10.10
35	100	606	2.6	0.25	9	1400	2.5	6	44	25	White, tip end green	99	290.00	8.95
36	105	512	1.9	0.3	10.2	1400	2.5	6	38	21	White, tip end green	100	299.50	7.95
37	110	590	2.5	0.3	11.2	900	1	3	92	33	Green	109	302.50	8.70
38	107	505	2.1	0.35	10.6	900	1	3	64	25	Green	106	287.50	8.45
39	109.5	640	3.1	0.4	10.8	900	1.5	3	112	39	Green	108	272.50	12.60
40	110.5	561	2.5	0.25	8.9	900	1.5	3	99	34	Green	109	305.00	9.25
41	106	578	2.5	0.3	10.3	900	2	3	106	38	Green	103	342.50	11.10
42	109.5	590	2.7	0.3	10.1	900	2.5	3	101	35	Green	107	475.00	13.10
43	100.5	467	2.2	0.35	9.5	1200	1	3	40	16	White, tip end green	97	327.50	10.75
44	109	526	2.5	0.2	9.5	1200	1	3	40	20	White, tip end green	103	327.50	9.40
45	106	503	2.2	0.2	9.5	1200	1.5	3	41	19	White, tip end green	104	325.00	9.40
46	107	580	2.5	0.3	9.5	1200	1.5	3	59	26	White, tip end green	103	301.00	10.85
47	122	651	2.3	0.3	9.4	1200	2	3	82	36	Green	119	320.25	9.25
48	110.5	591	2.5	0.3	8.2	1200	2.5	3	94	34	Green	107	317.50	9.35
49	111	583	2.5	0.25	10.3	1400	1	3	39	20	White, tip end green	107	287.50	8.15
50	110	632	3	0.25	10	1400	1	3	49	23	White, tip end green	104	305.00	8.80
51	109.5	611	2.7	0.3	10.9	1400	1.5	3	46	23	White, tip end green	104	335.00	10.65
52	106	531	2.5	0.35	10	1400	1.5	3	40	20	White, tip end green	103	330.00	10.15
53	110	652	3	0.3	10.5	1400	2	3	50	24	Green, some white	100	303.50	9.75
54	104	500	2.3	0.3	10	1400	2.5	3	46	20	Green, some white	100	300.00	9.85
55	113	645	3.1	0.31	10	1400	3	3	80	29	Green	109	340.00	9.85
56	112	602	2.5	0.3	11.5	1400	3	3	74	28	Green	107	310.00	9.60
57	111.5	607	2.6	0.3	11	1400	3.5	3	104	35	Green	106	365.00	9.05
58	105	519	3	0.3	11	1400	3.5	3	45	34	Green	102	282.50	9.65

F-7: Results for brushing tests

S/No.	Before brushing			After brushing							
	Weight (dry) (g)	Colour	Mean fibre length (cm)	Speed (rpm)	Gap size (mm)	No. of elements	Weight (g)	Colour	Mean fibre length (cm)	Maximum Tensile Force (N)	Elongation (cm)
1	22	White, some green	99	900	1	12	17	White	76	331.67	9.30
2	30	White, some green	98	900	1	12	24	White	77	290.00	9.50
3	28	White, some green	104	900	1.5	12	23	White	100	311.67	6.63
4	34	White, some green	105	900	1.5	12	26	White	102	340.00	8.17
5	39	Greenish white	107	900	2	12	26	White, some brown	106	304.33	10.33
6	40	Greenish white	107	900	2	12	25	White, some brown	105	286.00	8.33
7	49	Green	109	900	2.5	12	32	White, some brown	107	286.67	10.80
8	59	Green	110	900	2.5	12	32	White, some brown	105	433.33	10.77
9	29	White, some green	105	1325	2.5	12	27	White, some brown	94	327.33	8.60
10	38	White, some green	101	1325	3	12	31	White, some brown	95	256.67	9.70
11	31	Greenish white	100	1192	3	12	22	White, some brown	100	233.33	9.83
12	43	Green	109	1192	4.5	12	31	White, some brown	104	335.10	10.03
13	29.7	White, some green	104	1200	1	12	23.5	White	95	253.67	9.20
14	29	White, some green	104	1200	1.5	12	19	White	99	278.33	6.67
15	31	White, some green	100.5	1200	2	12	19	White	95	191.67	8.83
16	31	White, some green	103	1200	2.5	12	18	White	91	227.33	10.07
17	38	White, some green	102	1400	2.5	12	17	White, some brown	96	285.67	10.80
18	35	White, some green	103	1400	3	12	22	White, some brown	101	211.67	8.70
19	34	Greenish white	111	900	1	6	23	White, some brown	100	343.33	11.83
20	31	Greenish white	110	900	1	6	25	White, some brown	101	355.00	9.43
21	30	Greenish white	109	900	1.5	6	24	White, some brown	97	393.33	8.80
22	38	Green	109	900	1.5	6	24	White, some brown	94	266.67	9.13
23	32	White, some green	100	1135	1	6	22	White	93	320.00	8.47
24	27	White, some green	105	1135	1	6	22	White	95	238.33	9.53
25	27	White, some green	106	1135	1.5	6	31	White	102	245.67	7.70
26	37	White, some green	106	1135	1.5	6	28	White	103	323.33	7.80
27	27	White	96	1200	1	6	20	White	92	218.33	7.07
28	24	White	96	1200	1	6	20	White	94	275.67	11.27
29	31	White	98	1200	1.5	6	24	White	96	268.33	7.50
30	33	White, some green	99	1200	1.5	6	26	White	97	331.67	9.33
31	32	White	100	1250	1	6	23	White	92	313.33	10.97
32	24	White, some green	100	1400	2	6	12	White, some brown	83	262.50	7.60
33	21	White, some green	99	1400	2	6	14	White, some brown	86	352.50	8.70
34	21	White, some green	95	1400	2	6	12	White	83	180.00	7.10
35	25	White, some green	99	1400	2.5	6	17	White, some brown	92	177.00	7.55

36	21	White, some green	100	1400	2.5	6	14	White, some brown	90	245.00	8.95
37	33	Green	109	900	1	3	20	White, some brown	98	250.25	8.65
38	25	Green	106	900	1	3	15	White, some brown	97	222.50	9.10
39	39	Green	108	900	1.5	3	20	White, some brown	100	237.75	8.45
40	34	Green	109	900	1.5	3	23	White, some brown	102	240.00	9.75
41	38	Green	103	900	2	3	27	White, some brown	100	305.00	11.25
42	35	Green	107	900	2.5	3	25	White, some brown	101	330.00	11.33
43	16	White, some green	97	1200	1	3	13	White	92	190.00	6.25
44	20	White, some green	103	1200	1	3	11	White	96	222.50	6.55
45	19	White, some green	104	1200	1.5	3	13	White	92	324.00	10.05
46	26	White, some green	103	1200	1.5	3	18	White	97	287.50	11.25
47	36	Green	119	1200	2	3	24	White, some brown	110	292.50	9.15
48	34	Green	107	1200	2.5	3	22	Brown White	104	347.50	10.15
49	20	White, some green	107	1400	1	3	14	Cream White	88	262.50	10.00
50	23	White, some green	104	1400	1	3	19	Cream White	92	327.50	9.75
51	23	White, some green	104	1400	1.5	3	17	Cream White	94	280.00	10.45
52	20	White, some green	103	1400	1.5	3	14	White	92	292.50	8.35
53	24	Greenish white	100	1400	2	3	17	White, some brown	97	292.50	9.90
54	20	Greenish white	100	1400	2.5	3	13	White, some brown	99	293.50	8.40
55	29	Green	109	1400	3	3	12	White	81	232.50	8.60
56	28	Green	107	1400	3	3	17	White	90	335.00	8.85
57	35	Green	106	1400	3.5	3	16	White	90	330.00	9.40
58	34	Green	102	1400	3.5	3	12	White	91	202.50	6.70

F-8: Extraction and brushing results at 6 blades for optimisation

S/No.	Sisal leaf parameters			Speed (rpm)	Gap size (mm)	No. of blade s/elements	Extraction				Brushing			Final Sisal Grade
	Length (cm)	Weight (g)	Bud thickness (cm)				Weight (wet) (g)	Weight (dry) (g)	Colour	Mean fibre length (cm)	Weight (g)	Colour	Mean fibre length (cm)	
1	111	648	3	900	1	6	61	31	Greenish white	108	23	White	96	UG
2	101	471	2.5	900	1	6	53	25	Greenish white	96	20	White	96	UG
3	104	503	2.6	900	1	6	49	25	White, some green tip	100	21	White with brown	97	SSUG
4	103	502	2.9	900	1.5	6	67	29	Greenish white	100	23	White	96	UG
5	97	476	2.4	900	1.5	6	71	29	Green	95	28	White	89	UG
6	99	419	2.1	900	1.5	6	57	28	Green	94	18	White	89	UG
7	96	426	2.4	900	2	6	94	38	Green	91	18	White with brown	80	SSUG
8	111	604	2.6	900	2	6	75	33	Green	108	24	White with brown	96	SSUG
9	90	430	1.8	900	2	6	91	34	Green	88	11	White with brown	79	SSUG
10	93	401	1.8	1000	1	6	38	19	Greenish white	90	10	White with brown	86	SSUG
11	90	474	2.3	1000	1	6	55	27	White, some green tip	88	20	White	95	UG
12	99	449	2.3	1000	1	6	48	27	White, some green tip	94	18	White	95	UG
13	100	477	2.5	1000	1.5	6	66	30	White, some green tip	97	23	White	90	UG
14	108	673	3.1	1000	1.5	6	85	38	White, some green tip	104	23	White	94	UG
15	99	488	2.5	1000	1.5	6	68	30	White, some green tip	94	22	White	90	UG
16	100	686	3	1000	2	6	87	38	White, some green tip	108	28	White	90	UG
17	98	478	2.3	1000	2	6	88	34	White, some green tip	96	19	White	89	UG
18	102	572	2.5	1000	2	6	61	29	White, some green tip	97	23	White	90	UG
19	110	726	3	1200	1	6	41	23	White, some green tip	96	18	White	84	UG
20	96	449	2.3	1200	1	6	42	22	White, some green tip	90	18	White	88	UG
21	106	629	3	1200	1	6	46	27	White, some green tip	93	20	White	90	UG
22	100	481	2.2	1200	1.5	6	44	27	White, some green tip	97	15	White	87	UG
23	109	686	3	1200	1.5	6	59	30	White, some green tip	100	18	White	89	UG
24	109	551	2.5	1200	1.5	6	47	24	White, some green tip	102	18	White	87	UG
25	111	663	3	1200	2	6	60	31	White, some green tip	105	23	White	86	UG
26	109	619	2.9	1200	2	6	56	27	White, some green tip	100	16	White	80	UG
27	102	505	2.5	1400	1	6	40	24	White, some green tip	95	16	White	88	UG
28	109	662	3	1400	1	6	47	27	White, some green tip	100	16	White	81	UG
29	99	453	2	1400	1	6	37	21	White, some green tip	90	10	White	79	UG
30	109	677	2.8	1400	1.5	6	56	29	White, some green tip	101	11	White	84	UG
31	109	619	2.5	1400	1.5	6	57	29	White, some green tip	103	17	White	85	UG
32	99	422	1.8	1400	1.5	6	42	24	White, some green tip	90	15	White	81	UG
33	89	388	1.7	1400	2	6	44	20	White, some green tip	84	17	White	80	UG
34	109	681	2.6	1400	2	6	54	29	White, some green tip	101	18	White	80	UG

F-9: Brushing results at 3 and 6 blades for optimisation of brushing unit

S/No.	Before brushing			Brushing						Final Sisal Grade
	Weight before brushing (g)	Average fibre length (cm)	Colour	Speed (RPM)	Gap size (mm)	Number of elements	Weight (g)	Average fibre length (cm)	Colour	
1	77	102	White, some green spots	900	1	3	46	99	White, some brown spots	SSUG
2	64	103	White, some green spots	1000	1	3	51	96	White, some brown spots	SSUG
3	71	100	White, some green spots	1200	1	3	28	89	Clean White	UG
4	79	94	White, some green spots	1400	1	3	21	80	Clean White	UG
5	76	94	White, some green spots	900	1.5	3	64	93	White, some brown spots	SSUG
6	99	107	White, some green spots	1000	1.5	3	86	98	White, some brown spots	SSUG
7	103	110	White, some green spots	1200	1.5	3	78	101	Clean White	UG
8	77	100	White, some green spots	1400	1.5	3	55	91	Clean White	UG
9	176	104	White, some green spots	900	2	3	154	102	Clean White	UG
10	139	99	White, some green spots	1000	2	3	118	98	Clean White	UG
11	150	98	White, some green spots	1200	2	3	114	96	Clean White	UG
12	132	105	White, some green spots	1400	2	3	104	92	Clean White	UG
13	98	105	White, some green spots	900	1	6	77	100	White, few brown spots	UG
14	98	105	White, some green spots	1000	1	6	71	99	Clean White	UG
15	67	98	White, some green spots	1200	1	6	40	90	Clean White	UG
16	67	98	White, some green spots	1400	1	6	27	80	Clean White	UG
17	66	75	White, some green spots	900	1.5	6	60	71	Clean White	UG
18	68	81	White, some green spots	1000	1.5	6	71	73	Clean White	UG

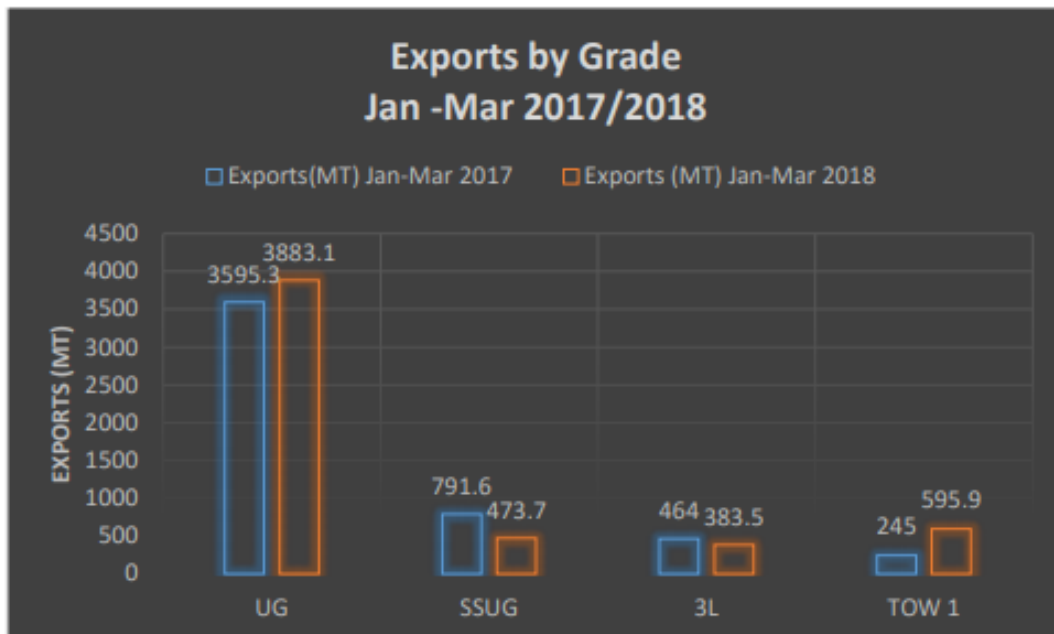
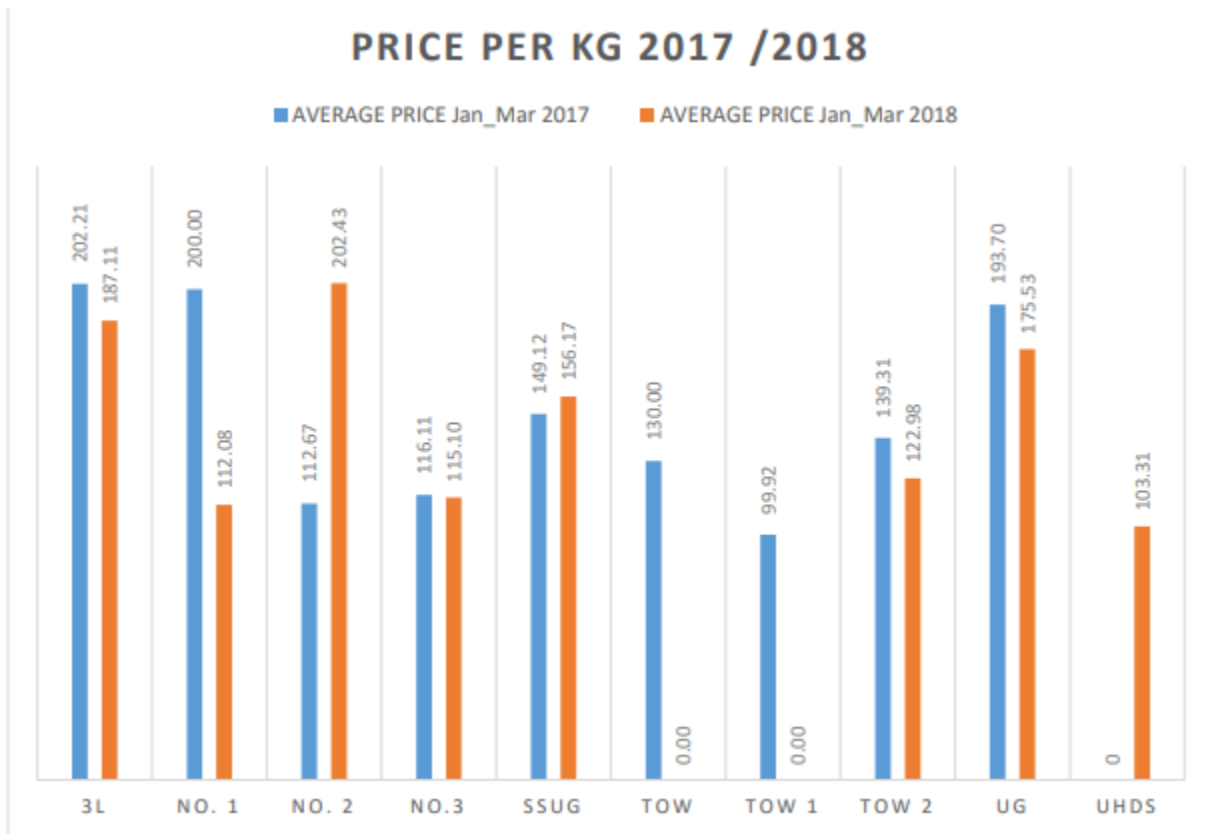
F-10: Fibre diameters as determined by the LV 800AT Tester

S/No.	Manual Decortication (µm)	Real Vipingo (µm)	Fibre from tested machine	
			Unbrushed (µm)	Brushed (µm)
1	273.5	244.6	281.4	252.4
2	281	248.6	285	255.7
3	262.6	247.2	293	248.6
4	273	244	287.6	249.7
5	267.8	244.2	286	254.1
6	278.8	237.1	283.3	249.1
7	271.4	239.3	276.5	259.9
8	271.6	245.2	288.5	250.5
9	292	240.6	270.5	251.5
10	277.7	249.3	274.7	253.1
11	275	231.8	268.5	250.6
12	274	241.1	292	244.2
13	287	238.9	287	247
14	282.3	231.9	269.3	249.3
15	287	242.1	279.4	257.6
16	274.7	231	275.8	250.1
17	272.8	250.1	282.3	253.2
18	268.5	250.1	268.4	250
19	276.5	247.5	281	256.6
20	268.4	233.6	277.3	247.5
21	273.1	241	263.6	241.3
Average	275.65	241.87	279.55	251.05

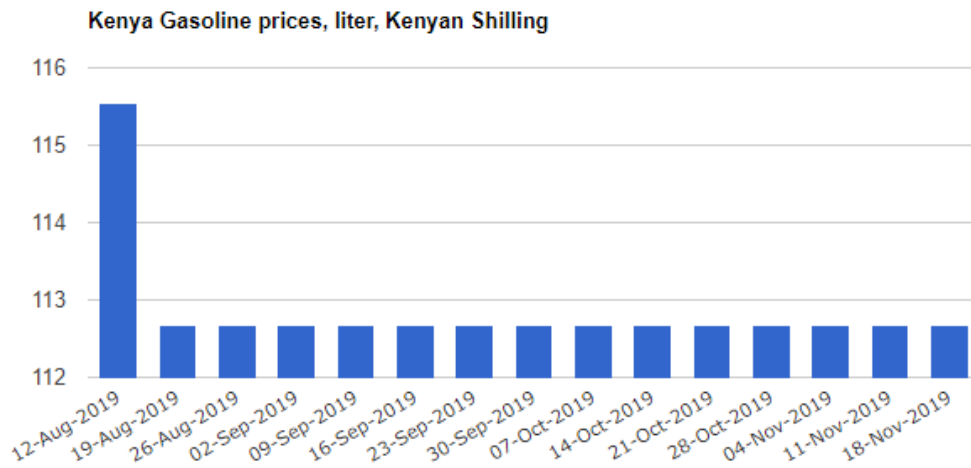
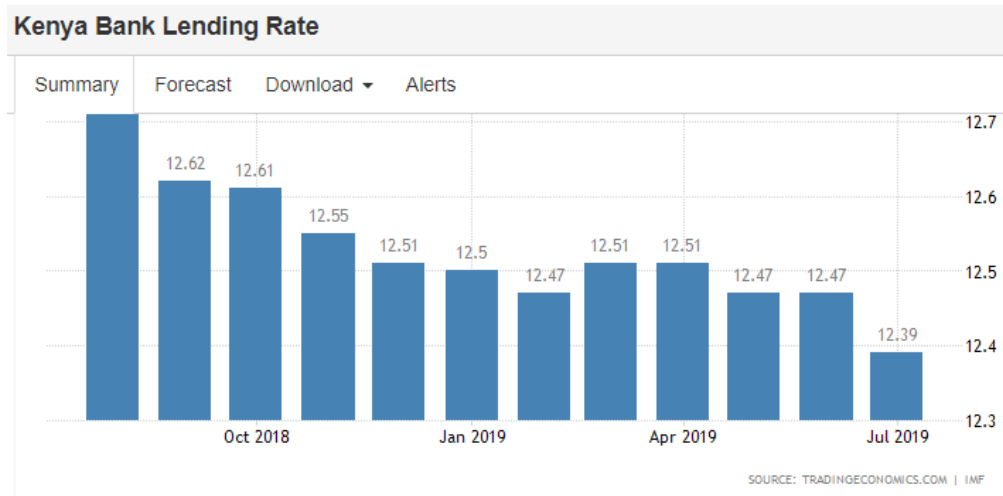
F-11: Machine processing capacity

Time (min)	Weight per unit time (g)		Cumulative weight (g)		Brushing (g)
	Wet	Dry	Wet	Dry	
1	325.4	163.5	325.4	163.5	341
2	350	178.3	675.4	341.8	703
3	386	194	1061.4	535.8	1047
4	340	168.1	1401.4	703.9	1413
5	299	150.9	1700.4	854.8	1807
6	384	193	2084.4	1047.8	
7	398	200	2482.4	1247.8	
8	387	165.4	2869.4	1413.2	
9	366	195.3	3235.4	1608.5	
10	395.9	198.6	3631.3	1807.1	

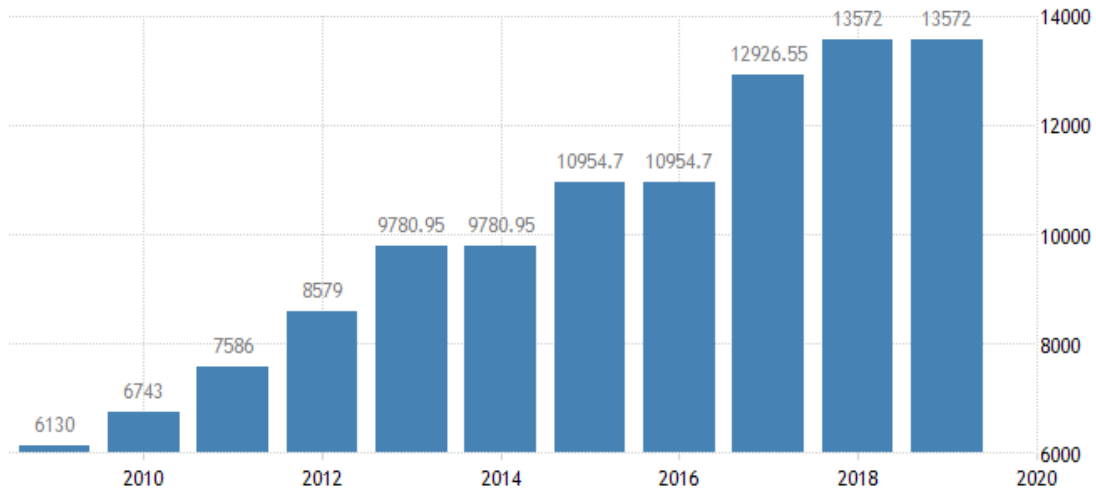
Appendix G: Sisal fibre prices for the 2017/2018 fiscal year [5]



Appendix H: Useful data for economic feasibility analysis



The Kenyan minimum wages



<https://tradingeconomics.com/kenya/minimum-wages>